THÈSE

En vue de l'obtention des

DOCTORATS DE L'UNIVERSITÉ DE TOULOUSE et DE L' UNIVERSITÉ BABEŞ-BOLYAI dans le cadre d'une procédure de co-tutelle

Délivrés par *l'Université Toulouse III Paul Sabatier et l'Université Babeş-Bolyai*
Discipline ou spécialité : *Chimie Moléculaire*

Présentée et soutenue par *Lucian-Cristian Pop*
Le *12 novembre 2010*

Titre : N,N'- and N,O-chelated pnictogenium cations (P, As, Sb) and germylenes: syntheses, structural studies and reactivity
Pnictogénium cations (P, As, Sb) et germylènes à ligands N,N' et N,O-chélatants: synthèse, étude structurale et réactivité

JURY

M. P. L. Fabre, *Professeur à l'Université de Toulouse III, Toulouse, Président*
M. I. Mangalagiu, *Professeur à l'Université Al.I.Cuza, Iaşi, Rapporteur*
M. J. Moreau, *Professeur à l'Université de Montpellier, Montpellier, Rapporteur*
M. M. Dărăbanţu, *Professeur à l'Université Babeş-Bolyai, Cluj-Napoca, Examinateur*
Mme. L. Silaghi-Dumitrescu, *Professeur à l'Université Babeş-Bolyai, Cluj-Napoca, Directrice de thèse*
Mme. A. Castel, *Chargée de Recherche au C.N.R.S., Toulouse, Directrice de thèse*

Ecole doctorale : *Sciences de la Matière*
Unité de recherche : *Laboratoire Hétérochimie Fondamentale et Appliquée UMR-CNRS 5069, Université Paul Sabatier, Bat 2R1 - 118 route de Narbonne - 31062 Toulouse cedex 9, Faculty of Chemistry and Chemical Engineering, Babeş-Bolyai University, 1, Kogalniceanu Str, 400084, Cluj-Napoca, Romania*

Directeur(s) de Thèse *:* *Mme. L. Silaghi-Dumitrescu, Mme. A. Castel*

“Nothing in life is to be feared. It is only to be understood.”
“Be less curious about people and more curious about ideas.”

Marie Skłodowska Curie - Polish - French physicist and chemist

“Science knows no country, because knowledge belongs to humanity, and is the torch which illuminates the world.”

Louis Pasteur - French chemist and microbiologist

“The difficulty lies, not in the new ideas, but in escaping the old ones, which ramify, for those brought up as most of us have been, into every corner of our minds.”

John Maynard Keynes - British economist

“Peace is our gift to each other.”

Elie Wiesel – Romanian-born Jewish-American Nobel Peace Prize laureate

Acknowledgements

Firstly, I owe my deepest gratitude to the "Facultatea de Chimie şi Inginerie Chimică, Cluj-Napoca, România" and to the "Laboratoire d'Hétérochimie Fondamentale et Appliquée, Toulouse, France" (LHFA), for giving me the opportunity to improve my knowledge, skills and abilities in the areas of Chemistry of Materials, which lead to the broadening and improvement of my set of tools and techniques.

I would like to begin by thanking to M. Ionel Mangalagiu, Professor at "Al. I. Cuza" University, Iaşi, and M. Joël Moreau, Professor at "Ecole Nationale Supérieure de Chimie de Montpellier", Montpellier who brought together the comments and recommendations on this work as rapporteurs.

A special thanks also goes to M. Mircea Dărăbanțu, Professor at "Babeş-Bolyai", Cluj-Napoca, University and M. Paul-Louis Fabre, Professor at "l'Université de Toulouse III", Toulouse, for their participation in the jury.

I am very grateful to my supervisors, Prof. Dr. Luminţa Silaghi – Dumitrescu and Dr. Annie Castel, for there continuous support, patient guidance, advice (particularly so when exploring new ideas) and encouragement over the past three years and for giving me the opportunity to work in an international and multicultural laboratory. There positive outlook and confidence in my research inspired me and gave me confidence. I have been extremely lucky to have two supervisors who cared so much about my work, and who responded to my questions and queries so promptly.

I must express my gratitude to Monsieur Dr. Jean Escudie who gave me helpful advices during my stay in Toulouse, told me about the Musee D'Orsay from Paris, and kindly and carefully reviewed my Ph.D. thesis. Your help, support and valuable advice were amazing, thank you.

I would like to thank Monsieur Dr. Henri Ranaivonjatovo for making the lab a pleasant place to work in, who provided a much needed form of escape from my studies and of course let's not forget the "salsa nights" that we spend together.

I must thank Prof. Dr. Evamarie Hey-Hawkins from Institute of Inorganic Chemistry Faculty of Chemistry and Mineralogy University of Leipzig, Germany, for allowing me the opportunity to work in the laboratories of Institute of Inorganic Chemistry where I first came into contact with the arsenic.

I am grateful to Nathalie Saffron, Heinz Gornitzka and Sonia Ladeira for there keen interest and patience in obtaining those beautiful X-ray structures.

I would also like to thank Prof. Dr. Ioan Silaghi – Dumitrescu from Facultatea de Chimie şi Inginerie Chimică, Romania, Dr. Jean-Marc Sotiropoulos from Université de Pau & des Pays de l'Adour, France and Dr. Desmond Mac-Leod from Pontificia Universidad Católica de Chile, for the DFT calculations.

My sincere gratitude goes to the lab technicians, Pierre, Olivier and Isabelle**,** for keeping the lab running. Thank you Madame Marie Josée Pedussault and Madame Maryse Béziat for being there for me. A thank also goes to Christian Pradel for mass-spectral work.

Amongst those whom made my stay in Toulouse much more pleasant are: Nadia, Fatima, Dimitri and Raluca. Thanks Dumitru for coming in and hanging with me in the lab in the weekends or when I had a really late night at LHFA.

On the Romanian side of the project, I would like to thank the staff of the Faculty of Chemistry and Chemical Engineering, Ms. Castelia, Ms. Luiza, M. Tamás and Ms. Lena. Thanks also go to my colleagues and friends for their priceless support Ana-Maria, Emese, Larisa, Laci, Mihai, Iani, Imola, Agota, Tibor, Iudit, Ioana, Márta and last but not least Dan.

A massive thank you goes to my parents Rodica and Tiberiu and my brother Paul. I would not be the person I am, or where I am today without your constant love and support.

Finally, thanks to my friends on both countries who helped me in ways unknown to them.

Table of contents

Introduction générale/General introduction

Introduction générale

De manière similaire au développement extraordinaire de la chimie des carbènes, la chimie des phosphénium cations (analogues phosphorés des carbènes) a connu un essor important aussi bien en raison des enjeux fondamentaux qu'au niveau des applications. Toutefois malgré des avancées significatives, ces phosphénium cations restent des espèces très réactives dont la stabilisation est toujours d'actualité. Leur stabilité dépend essentiellement de la délocalisation de la charge positive soit en utilisant des hétéroatomes (N, S) soit en incluant l'élément du groupe 15 dans un système π-conjugué. Parmi les nombreuses structures qui ont été étudiées, les structures analogues des carbènes d'Arduengo qui présentent deux liaisons E_{15}–N covalentes et l'élément du groupe 15 inclus dans un cycle à 5 chaînons sont les plus nombreuses. Plus récemment, les premières tentatives de stabilisation par complexation intramoléculaire ont été décrites dans la littérature. Les auteurs ont utilisé principalement des ligands N,N'-chélatants présentant un groupement imino et amino comme les amidinates et les β-dicétiminates. C'est cette dernière approche que nous avons choisie avec comme ligand le fragment aminotroponiminate ou amonotroponate qui offre en plus la possibilité de délocalisation électronique sur un système π-conjugué.

Le premier chapitre décrit la mise au point des synthèses de ces nouveaux pnictogénium cations (phosphénium, arsénium et stibénium). Deux voies sont envisagées: une réaction de substitution nucléophile par l'aminolithien correspondant et une réaction de déshydrochloration en présence d'une base. Une étude physicochimique approfondie (RMN multinoyaux, spectrométrie de masse) de toutes ces espèces ainsi que la détermination de leurs structures par diffraction des rayons X seront effectuées. Des études théoriques viendront en complément pour la détermination de leurs structures électroniques et en particulier pour la position du doublet libre de ces pnictogenium cations.

Dans le deuxième chapitre, nous présenterons divers tests de réactivité comme des réactions d'échange de contre-ions avec des triflates et des réactions d'oxydation avec le DMSO, le soufre et le sélénium. Nous tenterons également des réactions de cycloaddition avec différents dienes et hétérodiènes (*o*-quinone). Il serait également intéressant d'évaluer le

pouvoir σ-donneur du doublet libre de ces espèces dans des réactions de complexation avec des métaux de transition.

Le troisième chapitre portera sur la synthèse et la caractérisation de bis(pnictogenium) cations pontés avec une extension aux composés divalents du germanium. Nous essayerons d'évaluer l'influence de la nature du ligand (N,N- ou N,O-chélatant) et de la longueur du pont carboné sur la stabilisation de ces nouvelles espèces. L'étude de leur réactivité et en particulier celles des bis-germylènes sera menée en parallèle avec celle des monogermylènes correspondants. Pour cela, nous envisageons des réactions d'oxydation, de cycloaddition et de complexation.

General introduction

Similarly to the extraordinary development of the chemistry of carbenes, the chemistry of phosphenium cations (phosphorus analogues of carbenes) has received considerable attention both for academic and industry research. Despite the advances in this particularly field, the stabilization of these highly reactive phosphenium cations is still relevant. Their stability depends mainly on the delocalization of the positive charge either by using heteroatoms (N, S) or by including a group 15 element in the π-conjugated system. Among the many structures studied, these analogues of Arduengo's carbenes which have two covalent bonds E_{15}-N (E_{15} = P, As, Sb) with a group 15 element included in a 5-membered ring are the most numerous. More recently, the first attempts of stabilization of such species by intramolecular complexation have been described in the literature: the authors used mainly N, N'-chelating ligands having imino and amino groups such as amidinate and β-diketiminates. We have chosen this latter approach with the ligand aminotroponiminate or aminotroponate that offers the possibility of electron delocalization on π-conjugated systems.

The first chapter describes the syntheses of these new pnictogenium cations (phosphenium, arsenium and stibenium). Two pathways are considered: a nucleophilic substitution reaction by an aminolithiated derivative or a base-induced dehydrohalogenation coupling reaction. Detailed physicochemical data (multinuclear NMR, mass spectrometry) and X-ray structural studies of all these species are presented. Theoretical studies will complement the determination of their electronic structures and in particular the position of the lone pair of these pnictogenium cations.

In the second chapter, we present various tests of reactivity such as the reactions of ion-exchange with triflates and oxidation reactions with DMSO, sulfur and selenium. We also describe attempts of cycloaddition reactions with various dienes and heterodienes (*o*-quinone). It also appears interesting to evaluate the σ-donor ability of this species having a lone pair in complexation reactions with transition metals.

The third chapter focuses on the synthesis and characterization of bridged bis(pnictogenium) cations with an extension to divalent germanium compounds. We try to evaluate the influence of the ligand (N,N- or N,O-chelating) nature and the length of the methylene bridge on the stabilization of these new species. The study of their reactivity and in particular those of bis-germylene (oxidation, cycloaddition and complexation reactions) will be conducted in parallel with that of the corresponding monogermylenes.

General Data and Instrumentation

All reactions and manipulations were done under an atmosphere of purified argon using standard Schlenk techniques (high-vacuum-line techniques) or inside of a Saffron Scientific glove-box unless otherwise stated. Glassware was oven-dried at 105 °C overnight. Solvents were dried and distilled according to standard procedures and degassed prior to use. THF was dried and freshly distilled from sodium benzophenone ketyl. Also, for determination of water content in solvent an automatic titrator was used (Schott TitroLine KF trace - coulometric water determination according to Karl Fischer).

NMR spectra were recorded with the following spectrometers: ^{1}H, Bruker Avance II 300 (300.13 MHz), Bruker Avance 400 (400.13 MHz) and Bruker Avance 500 (500.13 MHz); ^{13}C, Bruker Avance II 300 (75.47 MHz) and Bruker Avance 500 (100.61 MHz) (reference TMS); ^{31}P, Bruker Avance II 300 (121.49 MHz) (reference H_3PO_4); ^{19}F, Bruker Avance 300 (282 MHz) (reference $CFCl_3$); ^{77}Se, Bruker Avance 400 (76 MHz) (reference Me_2Se); ^{7}Li, Bruker Avance 400 (155 MHz) (reference LiCl in D_2O). ^{1}H and ^{13}C NMR assignments of compounds **6a** and **6b** were obtained by COSY (^{1}H-^{1}H), HSQC (^{1}H - ^{13}C) and HMBC (^{1}H - ^{13}C) experiments.

IR spectra were recorded on a VARIAN 640-IR FT-IR spectrometer. Mass spectra were measured with a Hewlett-Packard HP 5989A in the electron impact mode (70 eV).

Melting points were measured on a Leitz microscope or Electrothermal apparatus (capillary).

Elemental analyses were done by the Centre de Microanalyse de l'Ecole Nationale Supérieure des Ingénieurs en Arts Chimiques Et Technologiques.

Abbreviations and symbols

Me	Methyl
Et	Ethyl
*i*Pr	*iso*-Propil
*n*Bu	*normal*-Butyl
*i*Bu	*iso*-Butyl
*t*Bu	*tert*-Butyl
Ph	Phenyl
Ts	Tosyl
OTf	Trifluoromethanesulfonate
DMSO	Dimethylsulfoxide
DMF	Dimethylformamide
Dipp	1,3-diisopropylbenzene
Mesnacnac	
THF	Tetrahydrofurane
COD	1,5-cyclooctadiene
CpH	Cyclopentadiene

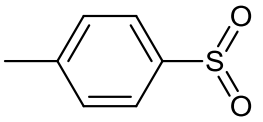

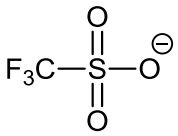

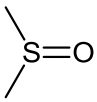

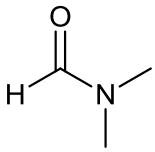

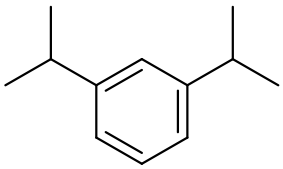

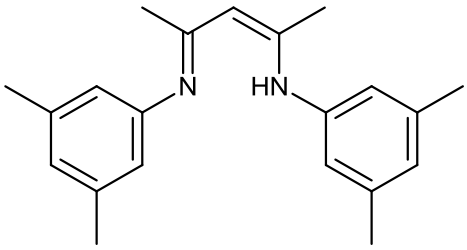

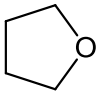

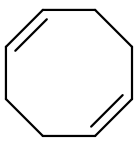

Cp*H	1,2,3,4,5-Pentamethylcyclopentadiene

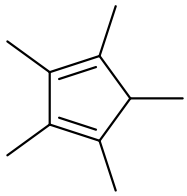

IR	Infrared
MS	Mass Spectrometry
EI	Electron Ionisation (Impact)
CI	Chemical Ionisation
HRMS	High Resolution Mass Specrometry
NMR	Nuclear Magnetic Resonance
HMBC	Heteronuclear Multiple Bond Correlation
HMQC	Heteronuclear Multiple Quantum Coherence
DFT	Density Functional Theory

CHAPTER I

Pnictogenium cations: syntheses and spectroscopic studies

RESUME

Après un bref rappel bibliographique sur les espèces di-coordinnés cationiques du groupe 15 (phosphénium, arsénium et stibénium), ce chapitre décrit un nouveau type de stabilisation par des substituants N-chélatants présentant des groupements amino et imino/ou cétone. Notre choix s'est porté sur les groupements aminotroponiminate et aminotroponate qui offrent en plus la possibilité de conjugaison avec un système π-délocalisé.

Deux voies de synthèse ont été utilisées à partir du trichloropnictogène (ECl_3, E = P, As, Sb):

- une réaction de déshydrochloration en présence d'une amine
- une réaction de substitution nucléophile par le composé aminolithié.

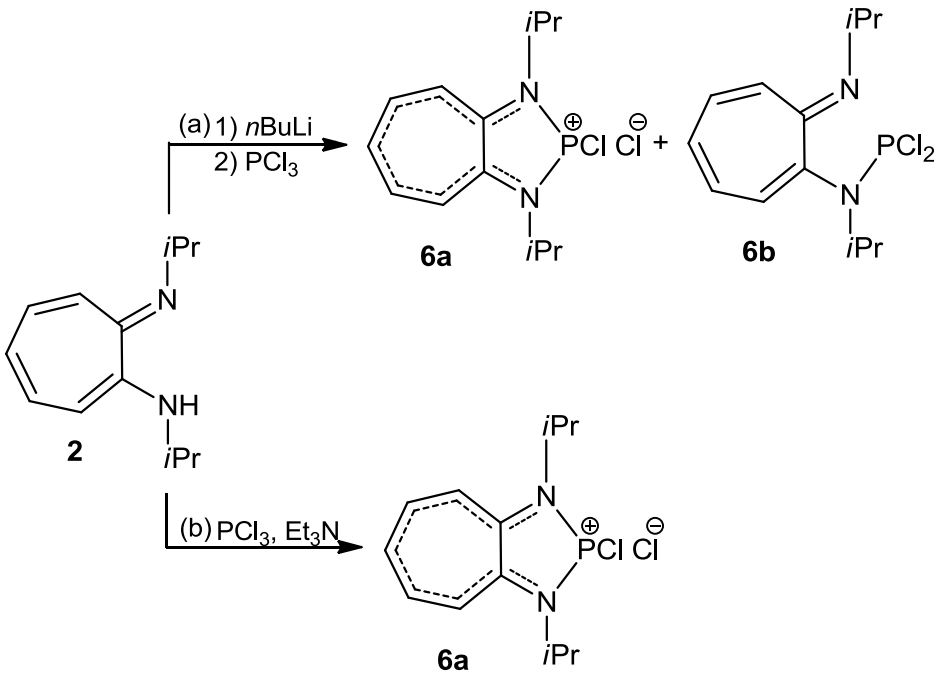

Ces réactions conduisent à la formation de dichloropnictogènes ou de chloropnictogéniums par rupture spontanée d'une liaison élément-chlore dans des pourcentages variables suivant la voie utilisée. Par exemple, la formation exclusive de chlorophosphénium a été obtenue en présence de triéthylamine. L'étude par RMN (^{31}P, ^{1}H et ^{13}C) montre un fort déplacement vers les champs faibles des protons du cycle à 7 chaînons par rapport aux signaux des ligands de départ en accord avec une délocalisation de la charge positive portée sur le système insaturé.

Ce caractère dissociatif de la liaison E-Cl dépend également de la nature du ligand et de l'élément du groupe 15. Il faut également noter que la stabilité des pnictogenium cations diminue dans le sens phosphore → antimoine. De plus, les stibéniums sont beaucoup moins solubles et donc plus difficiles à isoler. Ils évoluent très rapidement vers la formation de sels.

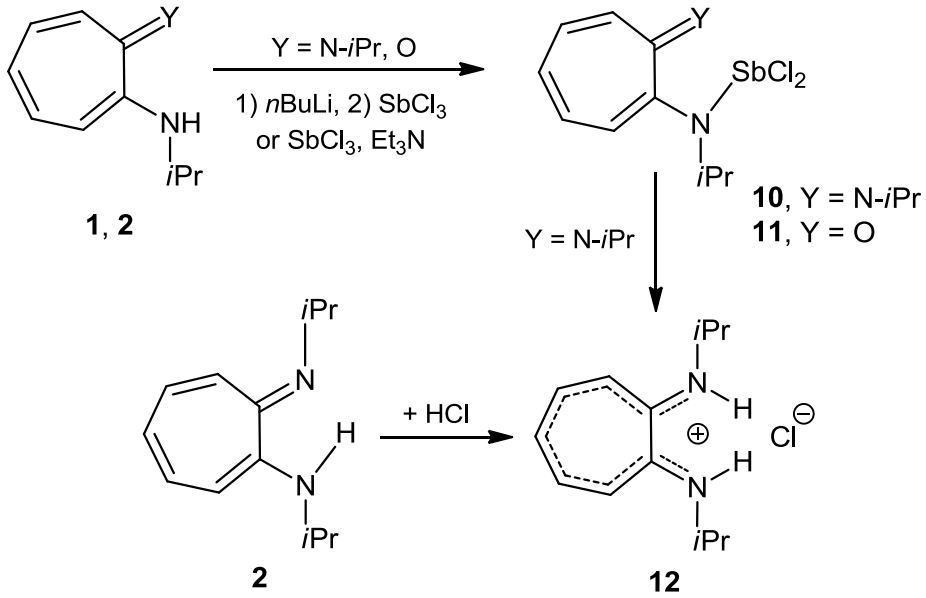

Dans le cas du phosphore, l'étude de leur structure par diffraction des rayons X a confirmé l'existence de formes totalement dissociées; aucune intéraction phosphore/chlore n'a été observée. Par contre, un dimère d'association a été mis en évidence dans le cas de l'arsenic et de l'aminotroponate comme substituant.

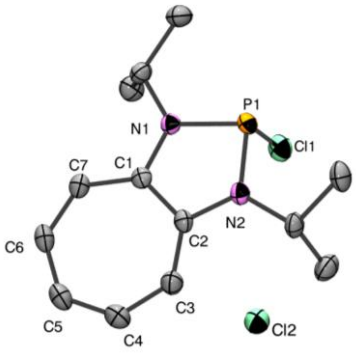

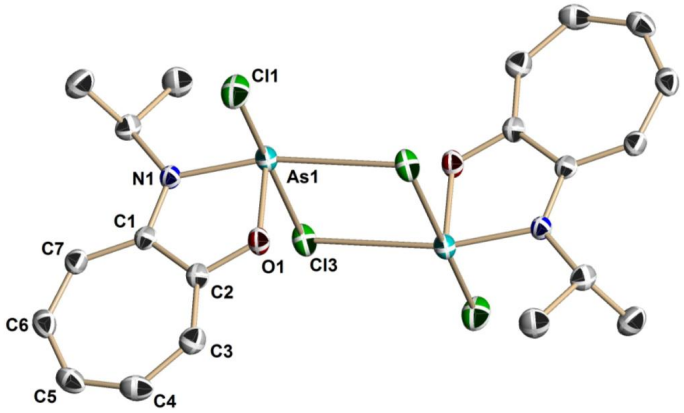

Des calculs DFT ont été réalisés à partir des données cristallographiques des chlorophosphéniums et chloroarséniums pour les deux ligands (N/N, aminotroponiminate et N/O, aminotroponate).

La localisation de la charge positive a été calculée à partir des valeurs NICS et de la fonction de Fukui. Ces calculs montrent que la délocalisation de la charge positive sur le cycle à 7 chaînons est la même pour tous les composés, par contre on note quelques différences sur l'hétérocycle à 5 chaînons. La délocalisation semble moins importante dans le cas de système N/O que dans le système N/N.

Nous avons également calculé les diagrammes moléculaires. Dans tous les cas, la HOMO est localisée sur le système bicyclique et les hétéroatomes (N ou O, Cl) et la LUMO un peu plus sur le cycle à 7 chaînons et moins sur l'hétérocycle. La paire libre du phosphore réside dans les orbitales HOMO-1 situées à 0.79 et 0.76 eV de la HOMO alors que pour l'arsenic elle se situe dans l'orbitale HOMO-4 plus éloignée de la HOMO correspondante (2.04 et 2.05 eV). Ces résultats semblent montrer que les phosphéniums soient plus aptes à se comporter comme des ligands vis-à-vis des métaux de transition que leurs analogues arséniés.

Introduction

Pnictogenium cations $[R_2E_{15}]^+$ (E_{15} = N, P, As, Sb, Bi) have attracted steady interest since the discovery of the first stable phosphenium some 40 years ago[1] both for fundamental purposes and for applications in the design of novel catalysts[2-3].

Phosphenium cations ($[R_2P:]^+$) are the isolobal and isovalent analogues of singlet carbenes[4]. Carbenes are compounds with a neutral divalent carbon atom and only six electrons in its valence shell[5],[6] having the general formula R_2C:. In terms of the electronic theory of bonding, which says that bonds between atoms are formed by a sharing of electrons, a carbene is a compound in which only two of the four valence, or bonding electrons of a carbon atom are actually engaged in bonding with other atoms. Phosphenium cations as carbenes have a formally sp^2-hybridized central element and a lone pair of electrons in a σ-type orbital, as well as an unhybridized, empty ***n***p π-type orbital (Chart 1). Because of this electronic structure, such species are expected to be both amphiphilic and amphoteric[4].

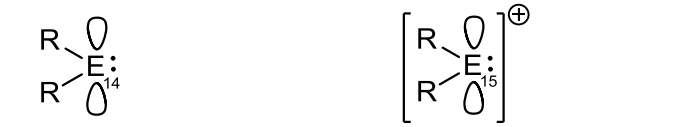

E_{14} = C - carbene
Si - silylene
Ge - germylene
Sn - stannylene
Pb - plumbylene

E_{15} = N - nitrenium
P - phosphenium
As - arsenium
Sb - stibenium
Bi - bismuthenium

Chart 1

In another view, phosphenium ions can be also considered to constitute one member of an isoelectronic series that extends from silicenium[7] to chloronium[8] ions (Chart 2).

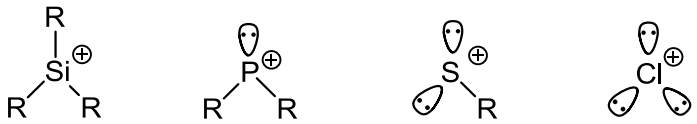

Chart 2

The birth certificate was signed in 1964 when the first stable phosphenium cations (**I**, **II**) were synthesized by Dimroth and Hoffmann[1] (Chart 3).

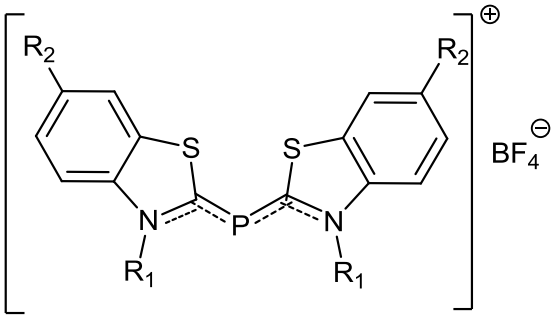

R_1 = Me, Et; R_2 = H, OH

I

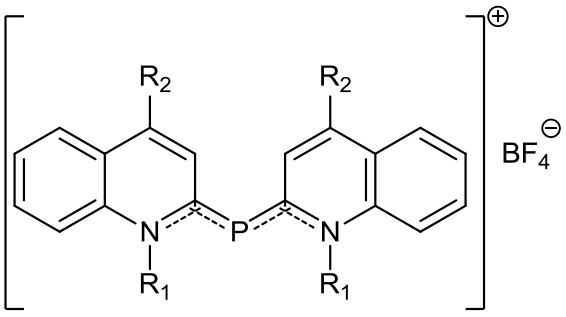

R_1 = Et; R_2 = H, Me

II

Chart 3

In 1972 the first stable cyclic phosphenium cations were reported independently by Fleming et al.[9] **III** and by Maryanoff and Hutchins[10] **IV**. From 1972 and onwards, the chemistry of these species has grown strongly; the first three X-Ray structural determinations (**V - VII**) date from 1978 (Cowley et al.[11], Schmidpeter et al.[12]) and 1979 (Pohl et al.[12-13]) for the following species (Chart 4).

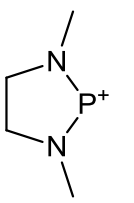

III

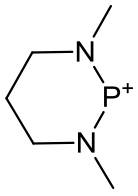

IV

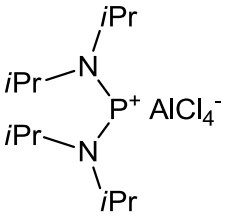

V

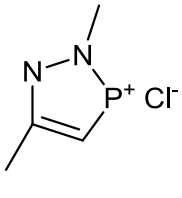

VI

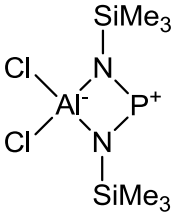

VII

Chart 4

In 1985, Cowley and Kemp[14] emphasized the increasing interest in the study of this species isoelectronic with carbene. The presence of a vacant orbital and a lone pair confers to these amphoteric derivatives a great diversity in reactivity in organic chemistry and in coordination chemistry.

Their stability depends on charge delocalization by using heteroatom bonding or/and by incorporation of the pnictogen atom into a conjugated π-system. Generally, the used substituents present electron rich centers that allow π-donation upon the cationic phosphorus

center [**V**[11], $Me_2N(Cl)P^+$][15-16]. A large variety of cyclic structures has been reported[14, 17-19] represented by **IX** – **XIV**[3] (Chart 5), among them the cyclic five membered one seems to dominate.

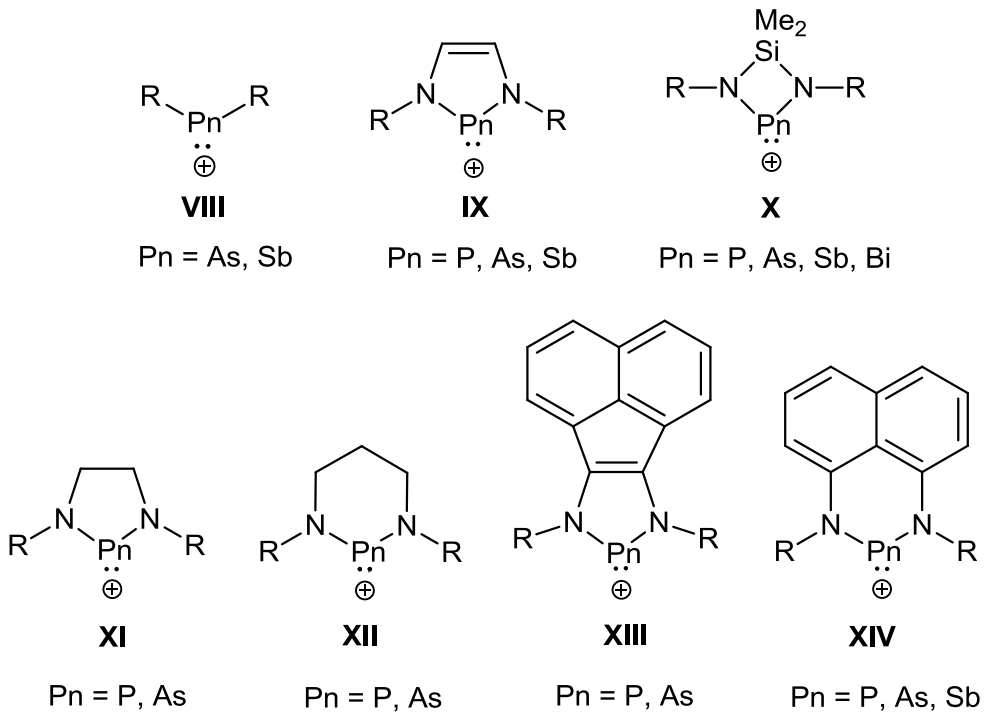

Chart 5

More recently, some tricoordinated species having aminoiminoligands with a covalent E_{15}–N bond and a coordinative $E_{15}\rightarrow N$ bond have been reported. Examples of such ligands include β-diketiminates[20] and amidinates[21]. However, the use of a β-diketiminato ligand suffers from a lack of generality since the preparation of a N,N'-chelated phosphenium cation supported by a β-diketiminato ligand hinges on the use of: i) an electronegative substituent (e.g. C_6F_5) at the nitrogen atoms and/or ii) of an alkyl substituent at the γ-carbon of the β-diketiminate to circumvent phosphorus substitution at this site (Equation 1). Moreover, computational studies suggest that a β-diketiminato ligand was unsuitable for stabilization of pnictogenium cations[22].

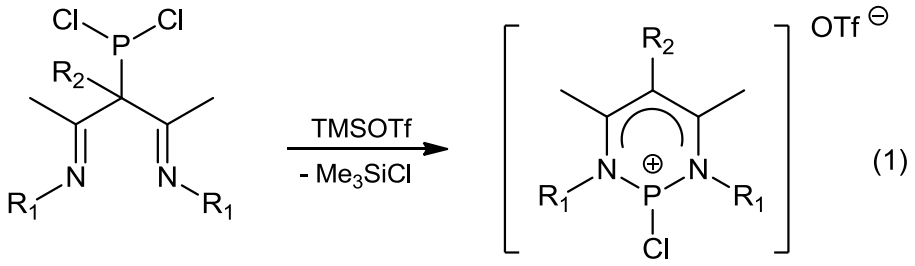

(1)

$R_1 = C_6F_5$; $R_2 = H$
$R_1 = Dipp$; $R_2 = Me$

In spite of the fact that the major part of work has been dedicated to phosphenium ions, cations with other group - 15 elements were also prepared. Today, stable cations centered at dicoordinate arsenic and antimony are known as well, even if examples of low valent antimony complexes are not as common as their phosphorus counterparts.

Examples of genuine cations **VIII**[23-24] became known[25] only over the last decades. Their stability relies commonly on mesomeric interaction with π-donor substituents[14],[19, 23-24] and practically all stable cations known contain one or two amino (NR'_2) or thiolato (SR') groups. As previously described in the case of phosphenium, this mesomeric stabilization can be enhanced by incorporating the dicoordinate species into an insaturated ring (**IX**[18, 26-28], Chart 5).

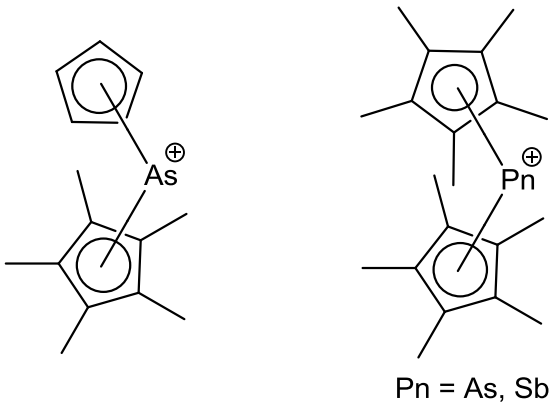

XV **XVI**

Chart 6

Low coordinate cationic arsenic centres have also been observed in the particular Cp*AsCp and Cp^*_2Pn, **XV** and **XVI**[29], which involve a bent sandwich π-complex coordination (Chart 6). Isolation of the first structurally characterized example was only made possible by incorporating the dicoordinate As unit into a diaminonaphthenic framework (**XIII**, Chart 5)[3].

Just a few compounds with amino-imino ligands were reported and in all cases only the formation of antimony and bismuth dichloro species was observed (**XVII**, **XVIII**, Chart 7)[30-31].

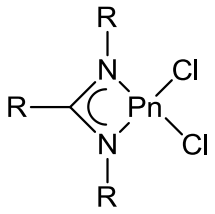

Pn = Sb, Bi

XVII

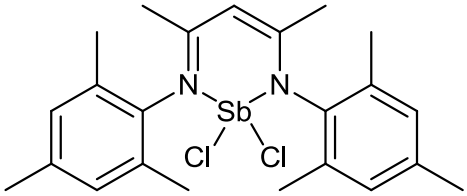

XVIII

Chart 7

All attempts to chloride ion abstraction failed leading to the ligand salt.

As a part of our ongoing studies of strategies to stabilize low-coordinate phosphorus atom,[32] [33] we identified the monoanionic ligands: tropolonate (from the neutral 2-hydroxy-2,4,6-cycloheptatrien-1-one), aminotroponate (from the neutral 2-(isopropylamino)cyclohepta-2,4,6-trien-1-one) and aminotroponiminate (from the neutral N-isopropyl-7-(isopropylimino)cyclohepta-l,3,5-trien-1-amine) where the hydroxy and carbonyl groups are successively replaced par amino or/and imino groups (Chart 8) as highly promising candidates for stabilizing phosphenium ions. These ligands are particularly useful as they can be prepared in high yields, crystallize easily and have the ability to stabilize low oxidation state compounds.

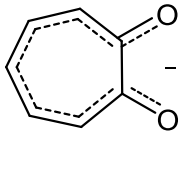

Tropolonate

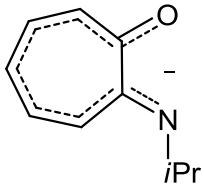

Aminotroponate

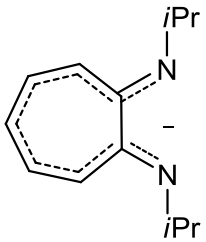

Aminotroponiminate

Chart 8

Tropolone is formally an α-diketone, non-benzenoid aromatic compound in the form of a seven-membered ring. The tropolonato anion is a bidentate ligand, which forms a five-membered chelate ring upon complexation to a metal ion. The functional groups of tropolone (carbonyl and hydroxyl) make it possible to coordinate a number of different d-block and f-block metal ions (in oxidation states from +I to +VI). Having all these properties, tropolone and its derivatives have been studied in various fields such as medicine, material science and agriculture[34-37].

Aminotroponiminates ([ATI]$^-$) are a well known class of ligands which have found extensive use in coordination chemistry leading to a large number of transition-metal and main-group complexes[38-39]. On one hand, this ligand displays heteroatom bonding and a highly conjugated 10 π-electron system that should allow charge delocalization when incorporating the pnictogenium atom in the π-electron backbone. On the other hand, and in marked contrast to the β-diketiminate scaffold, [ATI]$^-$ is expected to form stable five-membered chelate rings and its anticipated fused ring structure should disfavor side reactions analogous to those observed in the β-diketiminate system. Some of us have also demonstrated the potentialities of this fragment compared to that of amidinate or β-diketiminate in the context of the chemistry of cationic three-coordinate Group 13 elements[40-42]. By contrast, aminotroponates ([AT]$^-$), which may formally be considered as a combination of amido and carbonyl donors, have been much less investigated. Only a few aminotroponate complexes of main-group[43] and transition-metals[44-48] are known. However, in both cases the coordination chemistry of these ligands by electron-rich elements from Groups 15 to 17 remains totally unexplored.

1.1 Synthesis of complexes of P, As and Sb

Besides the tropolone which was purchased from Aldrich and used as received, we prepared the ligand precursors, the aminotropone and aminotroponimine.

1.1.1 Synthesis of ligand precursors

The 2-(isopropylamino)tropone [(*i*Pr)AT]H, **1**, was synthesized by a direct nucleophilic displacement of the tosyl group from the 2-(tosyloxy)tropone using an excess of isopropylamine and was isolated in 77 % yield (Equation 2).

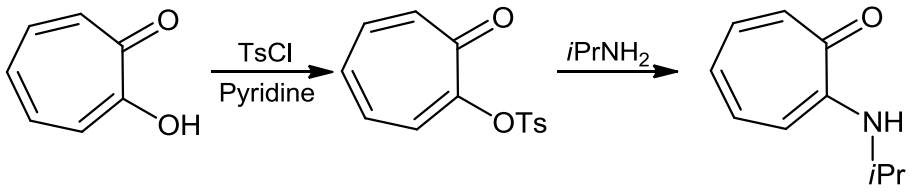

(2)

1

Starting from 2-(isopropylamino)tropone, an ethylation reaction with $Et_3O{\cdot}BF_4$ followed by the treatment with excess of isopropylamine gave [(*i*Pr)$_2$ATI]H **2** as a bright yellow solid (Equation 3). Yellow crystals of [(*i*Pr)$_2$ATI]H were obtained in 95 % yield from hexanes at -25 °C. This ligand is very soluble in almost all organic solvents, including saturated hydrocarbons such as n-pentane or hexanes.

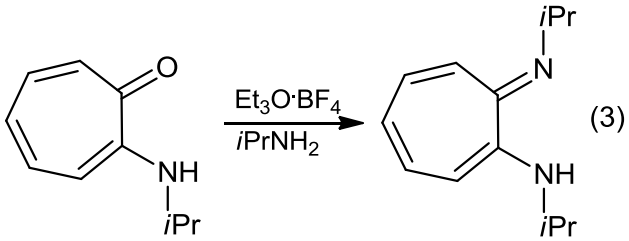

(3)

1 **2**

All these compounds were characterized by ^{1}H and ^{13}C NMR spectroscopies, the results being in accordance with the literature data[49].

1.1.2 Synthesis of tropolone complexes of P and As

The chemical reactions starting from tropolone proved to be much more complex regardless of the path followed: dehydrochloride coupling reaction or action of lithiated derivatives. Indeed, the absence of bulky groups such as amino (N-*i*Pr) can promote the grafting of several tropolone entities on phosphorus.

It has already been shown in the literature[50-51] that the action of tropolone (Tp) on PCl_5 leads to the formation of chloro trisubstituted salt that is then stabilized by treatment with NaI (Equation 4).

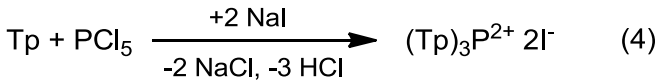

(4)

When using the phosphorus oxychloride, only the chlorination of OH group was observed without formation of the substituted product[52] (Equation 5).

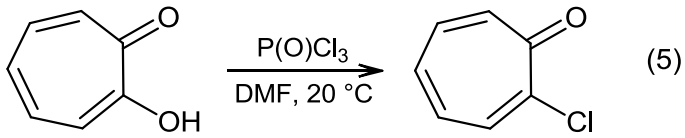

(5)

Up to date, no reaction using PCl_3 was reported in the literature. We first performed dehydrochloride coupling reaction with triethylamine as a base.

Phosphorus-31 NMR is one of the more routine NMR techniques because ^{31}P has an isotopic abundance of 100 % and a relatively high magnetogyric ratio. The ^{31}P nucleus also has a spin of ½, making spectra relatively easy to obtain and interpret. The ^{31}Phosphorus NMR experiment is much less sensitive than proton (^{1}H) but more sensitive than ^{13}Carbon. ^{31}Phosphorus is a medium sensitivity nucleus that yields sharp lines and has a wide chemical shift range[53].

The ^{31}P NMR spectrum of the reaction mixture indicates the formation of two products, one at 99 ppm and another one at -109 ppm in percentage that varies depending on the stoichiometry. When both reagents are used in stoichiometric quantity, we get a 50/50 ratio.

While an excess of PCl_3 leads to the sole formation of the first product, the reaction of two equivalents of tropolone only gives the second compound. In this last case the proton-decoupled ^{31}P NMR spectrum shows the presence of a hydrogen atom bonded to phosphorus with a very large coupling constant of 964 Hz characteristic of pentacoordinated phosphorus derivative **3** (Equation 6).

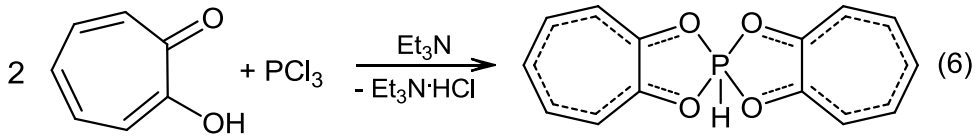

(6)

3

These compounds are practically insoluble in toluene but are very soluble in chlorinated solvents or THF. In these conditions, it was not possible to eliminate the triethylamine hydrochloride. A slow crystallization at low temperature always gives a mixture of products and salts. It was not possible to correctly identify the first product at 99 ppm.

A different result was obtained using the metalation reaction of tropolone followed by addition of PCl_3. The transient lithiated compound obtained by adding one equivalent of *n*BuLi to a diethyl ether solution of tropolone at 0 °C was reacted with PCl_3 at -78 °C

(Equation 7). The ^{31}P NMR analysis of the milky white filtrate indicated the presence of another product **4**, probably in the non-dissociated form, which displayed a resonance at 178.31 ppm in greater proportion. It was not possible to isolate pure **4** from the reaction mixture.

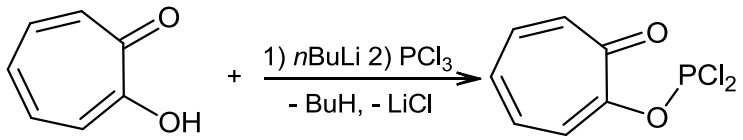

(7)

4

In the case of $AsCl_3$, the reaction also seems difficult. Using a base-induced dehydrohalogenation coupling reaction, a white solid with a low solubility in organic solvents was obtained. The ^{1}H NMR spectrum shows the formation of a new derivative having deshielded signals belonging to an aromatic system; the presence of this aromatic system, contrary to **4**, could be attributed to the arsenic derivate of tropolone **5** in the form of pair of ions (Equation 8). The mass spectroscopy data confirm this hypothesis with the presence of the [M-Cl] peak at 231 amu.

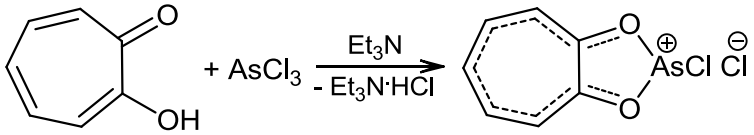

(8)

5

But this compound was very unstable in solution and rapidly gave the starting tropolone.

1.1.3 Synthesis of aminotroponiminate and aminotroponate complexes of P, As and Sb

We then extended these reactions to aminotroponiminate and aminotroponate ligands[54] (Scheme 1).

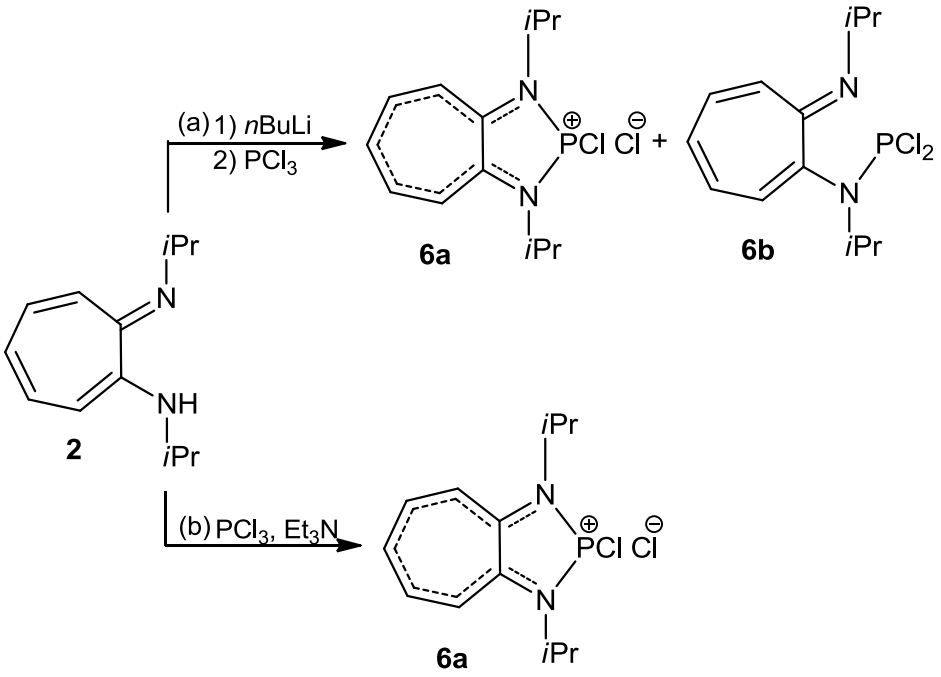

Scheme 1

Firstly, the addition of one equivalent of *n*BuLi to a diethyl ether solution of *N*-isopropyl-2-(isopropylamino)troponimine (*i*Pr$_2$ATI)H **2** at 0 °C afforded the transient lithiated compound which in turn reacted with PCl_3 (Scheme 1 (a)). The ^{31}P NMR analysis of the reaction mixture indicated two products which displayed resonances at 134.47 ppm and 160.95 ppm. Secondly, in sharp contrast, the reaction of PCl_3 with a mixture of triethylamine and (*i*Pr$_2$ATI)H in toluene at room temperature for 3 h yielded selectively the compound which exhibited a signal at 134.47 ppm (Scheme 1 (b)).

Single crystals suitable for X-ray crystallographic analysis were grown from a dichloromethane solution at -30 °C. The molecular representation (Figure 5) shows unambiguously the formation of the N,N'-chelated chlorophosphenium cation **6a**. If we consider the compound **6a** as a phosphenium, the chemical shift observed is among the most shielded. Indeed, in the case of phospheniums, the range of values is fairly wide ranging from 77 - 500 ppm[55] and depends heavily on the nature of the ligand and its ability to spread the positive charge. For example, in the case of aminophospheniums Me_2NP^+Y (Y = *t*Bu) the positive charge is mainly localized on the phosphorus, with a chemical shift of 513.2 ppm[56]. When Y = C≡N, a shielded signal is observed at 77 ppm[55] which can be attributed to a delocalization of the charge on the nitrile group.

The values generally observed for N-hererocyclic phosphenium cations are in the range of 200 to 260 ppm[12]. In our case, the ^{31}P chemical shift of 134.47 ppm is lower,

presumably because of the delocalization of the positive charge on the ligand backbone.

Concerning the second product **6b**, the ^{31}P NMR resonance (δ 160.95) is in the typical region for aminodichlorophosphines[57]. The simultaneous formation of both dissociated and non-dissociated forms has been already reported but not clearly evidenced with N,N',N'-trimethylethylenediamine[58-60] as substituent (Equation 9).

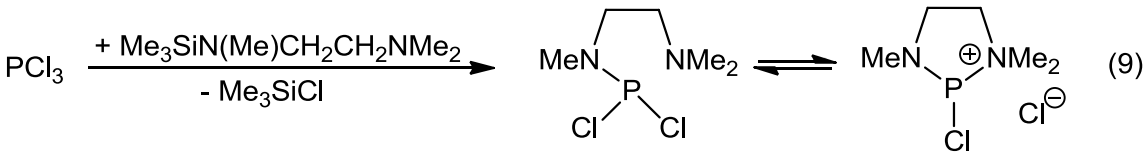

(9)

An equilibrium between covalent and ionic compounds has been suggested with displacement to covalent species upon heating[59]. In our case, the cationic form **6a** seems to be more stable than **6b** probably due to the presence of a conjugated backbone.

Next, we tested the coordinating properties of 2-(isopropylamino)tropone ((*i*PrAT)H **1** towards the phosphorous atom. Regardless of the procedure used (Equation 10), a mixture of two compounds **7a** and **7b** (^{31}P NMR: δ 155.70 ppm and 171.01 ppm respectively) was always obtained with ratios varying from 1:1 to 2:1.

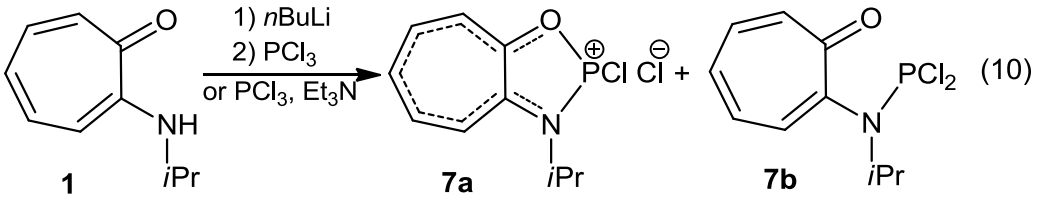

(10)

Yellow crystals were isolated by slow crystallization from dichloromethane in the case of the dehydrohalide coupling reaction, and structurally identified as the cationic form **7a**. However, it was more unstable than the N,N'-chelated analogue **6a**, particularly in solution with formation of ligand **1**. Moreover, compared to **6a**, the ^{31}P chemical shift (δ 155.70 ppm) is slightly shifted to low field, probably due to less effective charge dispersion, although a similar downfield shift of the ring protons was observed in the ^{1}H NMR spectrum. Compound **7b** has a signal at 171.01 ppm in the expected region for such a dichlorophosphine[57].

With $AsCl_3$, the resulting products strongly depend on the nature of the ligand. While, with the aminotroponiminate ligand, only the dissociated form **8** was obtained independently of the experimental conditions used, with the aminotroponate ligand the dichloroarsine **9** was formed exclusively (Scheme 2) as shown by X-ray structure analysis (Figure 7).

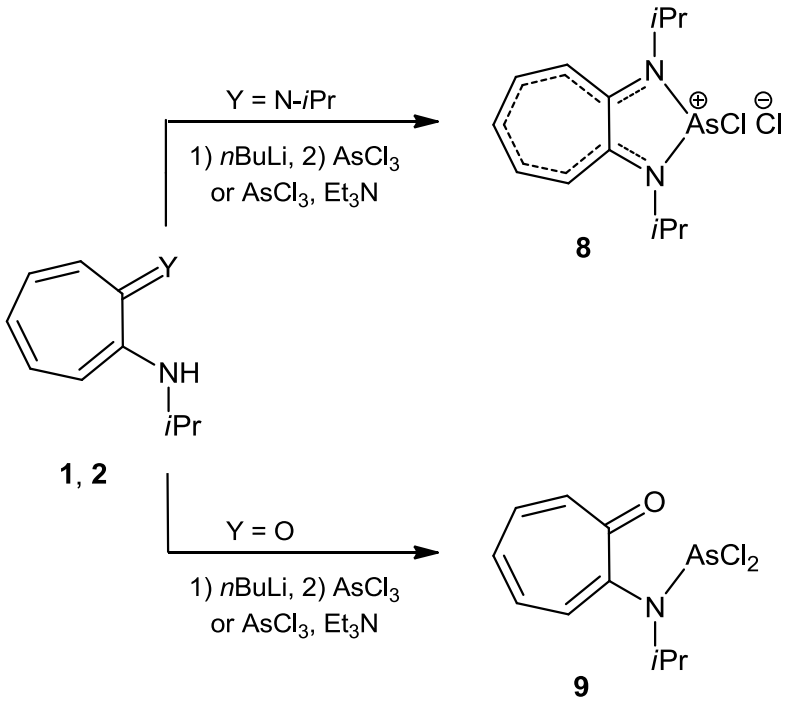

Scheme 2

All products supported by aminotroponate and aminotropoiminate were isolated as yellow air-sensitive solids in 48-60 yields. It should be note that, in all cases, higher yields have been obtained using the dehydrohalide coupling route and that the N,O-chelated products (**7** and **9**) were generally more unstable than the N,N'-chelated analogues (**6** and **8**), particularly in solution with formation of aminotropone. They were characterized by ^{1}H and ^{13}C NMR spectroscopy and in some cases by single-crystal X-ray diffraction studies.

In the case of $SbCl_3$, regardless of the path (nucleophilic substitution reaction using the monolithiated ligand or a base induced dehydrohalide coupling reaction) the ^{1}H NMR spectrum shows the formation of the same product having deshielded signals belonging to the aromatic system. This suggests the major presence of ionic species but without structural confirmation it was difficult to specify the correct molecular structure. These compounds **10** and **11** not only are practically insoluble in toluene but also have the same solubility in chlorinated solvents than the ammonium salt $Et_3N{\cdot}HCl$. So, they could not be separated from the salt and we cannot obtain suitable crystals for X-ray analysis.

Moreover, compound **10** quickly decomposes in solution giving the aminotroponiminate chlorhydrate salt **12** (Scheme 3), which can be obtained easily by adding HCl to an Et_2O solution of **2**. Recently, this phenomenon was observed in the case of $MesnacnacSbCl_2$ which decomposes towards the ligand salt, $[MesnacnacH_2]^+$, a protonated species at both nitrogen atoms[30].

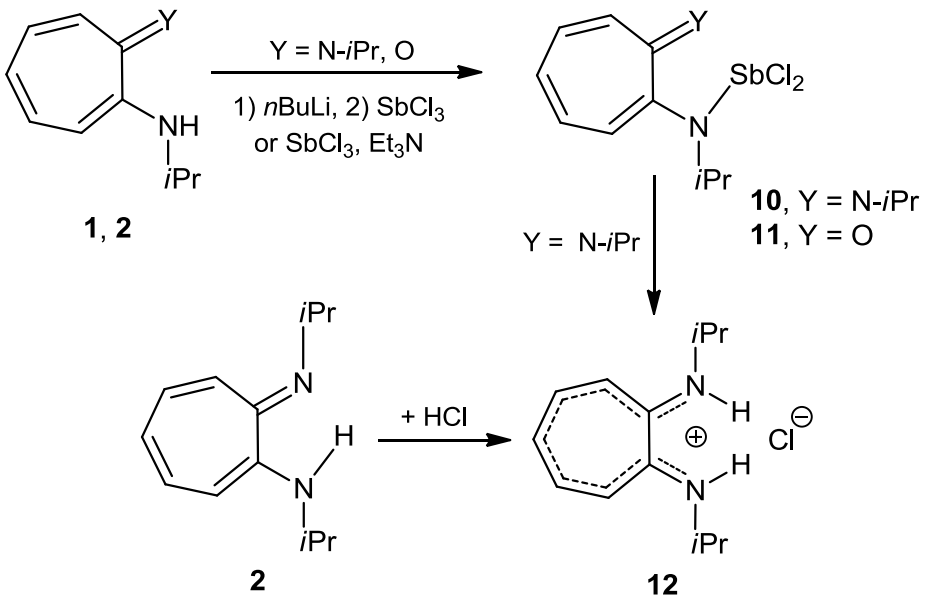

Scheme 3

Attempts to prepare the desired bismuthenium cations supported by these ligands were unsuccessful.

1.2 Spectroscopic characterization of aminotroponiminate and aminotroponate complexes of P, As and Sb

The ideal method to characterize and determine the structure of these compounds is NMR spectroscopy due to the fact that all of them are diamagnetic and there are several nuclei which can be thoroughly analyzed by this means. These include the classical ^{1}H, ^{13}C and ^{31}P NMR all of which have a nuclear spin number + ½. Since ^{13}C NMR detects only the ^{13}C isotope of carbon, whose natural abundance is only 1.1 %, because the main carbon isotope, ^{12}C, is not detectable by NMR since it has zero spin, the sensitivity of Carbon-13

NMR in extremely low; thus, highly concentrated samples and long measurement time are required[53].

Mass spectrometry was employed for elucidating the chemical structures of the new sensitized compounds. The MS principle consists of ionizing chemical compounds to generate charged molecules or molecule fragments and measurement of their mass-to-charge ratios[61].

Elemental analysis and X-ray diffraction studies were also carried out for some of these compounds.

1.2.1 NMR Properties

Atom labeling used in the NMR assignments of **1**, **2**, **6a, 6b**, **7a**, **7b**, **8**, **9**, **10**, **11** and **12** is given below (e.g. **6a**):

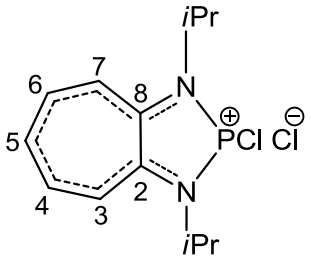

Figure 1: Numbering of atoms in compound **6a**

1.2.1.1 ^{1}H NMR

Depending on the local chemical environment, different protons in a molecule resonate at slightly different frequencies. Methyl and methine groups present characteristic signals as well as the aromatic protons in position 3-7 which range from 6.00 to 8.65 ppm.

The chemical shift values of pnictogen compounds and ligands are listed in Tables 1 and 2. The methyl groups of the isopropyl substituents appear as one doublet except for the dichlorophosphine **6b** which displays two close doublets ($\Delta\delta$: 0.03 ppm). This is perhaps due to the asymmetry caused by the two chloride atoms on the phosphorous center. The more interesting feature is the high deshielding of the ring protons in the cationic species compared to those of the starting ligands. This can be explained by the delocalization of the positive charge on the ligand backbone. A similar effect (increased conjugation of π-electrons in the newly formed metallacycles), but less pronounced, has been already observed in the case of the isovalent germanium(II) aminotroponiminate complex (*i*Pr$_2$ATI)GeCl[62]. This deshielding decreases when going from the phosphorus to the arsenic compounds specially when

comparing **7a** and **9**. This could be attributed to the presence of an increased cation-anion interaction which weakens the positive charge on the atom as highlighted in structural studies (see Figures 6 and 7). In the case of antimony derivates **10** and **11** the weak deshielding of the protons seems in agreement with non dissociated forms.

For example we give the ^{1}H and ^{1}H $\{^{31}P\}$ NMR spectra of the phosphenium cation **6a** (Figure 2).

As expected, ^{1}H NMR shows the presence of equivalent CH_3 groups in **12** which are deshielded in relation to starting ligand. A septuplet signal for isopropyl CH of aminotropoiminate salt appears at 3.97 ppm being sensibly downfield shifted compared to that of **2** (3.76 ppm). The same effect can be noted for the aromatic protons of the 7-membered ring.

Because nuclei themselves are little magnets they influence each other, changing the energy and hence frequency of nearby nuclei as they resonate, a phenomenon known as spin-spin coupling. The coupling constant is independent of magnetic field strength because it is caused by the magnetic field of another nucleus, not by the spectrometer magnet. In the case of **6a** , **7a** and **7b** several coupling constants between P and H can be observed.

It is to note the long-range spin–spin coupling constants between P and H observed for **6a** ($^{6}J_{HP}$ = 3.4 Hz, H_5) and **7b** ($^{5}J_{HP}$ = 1.0 Hz, H_4). Long-range couplings over more than three bonds can often be observed in cyclic and aromatic compounds (Chart 9)[63].

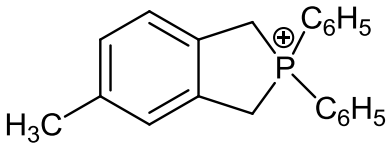

XIX

^{6}J = 0.9 Hz

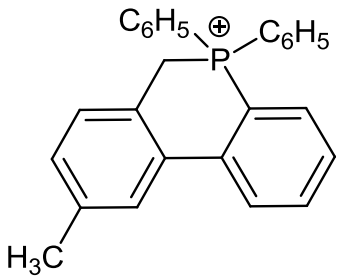

XX

^{7}J = 0.4 Hz

Chart 9

Table 1: Proton NMR chemical shifts for **2**, **10**, **6a**, **6b**, **8**, **12** (in ppm, J in Hz, in $CDCl_3$)

	CH_3	CH	H_5	$H_{4,6}$	$H_{3,7}$
2	1.19 (d, $^3J_{HH}$ = 6.2)	3.76 (sept, $^3J_{HH}$ = 6.2)	6.02 (t, $^3J_{HH}$ = 9.2)	6.65 (t, $^3J_{HH}$ = 10.3)	6.22 (d, $^3J_{HH}$ = 11.1)
6a	1.61 (d.d, $^3J_{HH}$ = 6.6, $^4J_{HP}$= 1.7)	4.77 (sept.d, $^3J_{HH}$ = 6.6, $^3J_{HP}$ = 10.9)	7.88 (t.d, $^3J_{HH}$ = 9.6, $^6J_{HP}$ = 3.4)	8.43 (t, $^3J_{HH}$ = 9.7)	8.55 (d.d, $^3J_{HH}$ = 11.0, $^4J_{HP}$ = 2.5)
6b	1.51 (d, $^3J_{HH}$ = 6.3), 1.54 (d, $^3J_{HH}$ = 6.3)	3.98 (sept, $^3J_{HH}$ = 6.8), 4.02 (sept, $^3J_{HH}$ = 6.8)	6.80-6.87 (m, C_7H_5), 7.35-7.44 (m, C_7H_5),7.89 (t, $^3J_{HH}$ = 9.0 Hz, C_7H_5), 8.30-8.41 (m, C_7H_5)		
8	1.74 (d, $^3J_{HH}$ = 6.6)	4.40 (sept, $^3J_{HH}$ = 6.6)	7.24 (t, $^3J_{HH}$ = 9.6)	7.69 (ps.t, $^3J_{HH}$ = 9.6)	7.30 (d, $^3J_{HH}$ = 11.4)
10	1.70 (d, $^3J_{HH}$ = 6.4)	4.43 (sept, $^3J_{HH}$ = 6.3)	6.99 (t, $^3J_{HH}$ = 9.4), 7.52 (ps.t), 7.08 (d, $^3J_{HH}$ = 11.5)		
12	1.51 (d, $^3J_{HH}$ = 6.4)	3.97 (sept, $^3J_{HH}$ = 6.4)	6.83-6.89 (m, C_7H_5), 7.43 (t, $^3J_{HH}$ = 9.6 Hz, C_7H_5)		

Table 2: Proton NMR chemical shifts for **1**, **7a**, **7b**, **9**, **11** (in ppm, J in Hz, in $CDCl_3$)

	CH_3	CH	H_5	$H_{4,6}$	$H_{3,7}$
1	1.27 (d, $^3J_{HH}$ = 6.4)	3.78 (sept, $^3J_{HH}$ = 6.4)	6.59 (t, $^3J_{HH}$ = 9.2)	7.06-7.22 (m, $H_{4,6,7}$)	6.50 (d, $^3J_{HH}$ = 10.5, H_3)
7a	1.71 (d.d, $^3J_{HH}$ = 6.6, $^4J_{PH}$ = 2.2)	4.69 (sept, $^3J_{HH}$ = 6.9)	8.13-8.15 (m)	8.28-8.35 (m)	8.65 (br.d, $^3J_{HH}$ = 5.5)
7b	1.36 (d, $^3J_{HH}$ = 6.4)	3.98-4.08 (m)	7.30 (t, $^3J_{HH}$ = 12.0)	7.62 (t.d, $^3J_{HH}$ = 10.3, $^5J_{HP}$ = 1.0, H_4), 7.80 (d.d, $^3J_{HH}$ = 9.3, $^3J_{HP}$ = 10.0, H_6)	7.31 (d, $^3J_{HH}$ = 9.4, H_3), 8.48 (d, $^3J_{HH}$ = 10.6, H_7)
9	1.74 (d, $^3J_{HH}$ = 6.4)	4.36 (sept, $^3J_{HH}$ = 6.7)	7.89 (ps.t)	7.40-7.50 (m)	7.70 (ps.d)
11	1.55 (d, $^3J_{HH}$ = 6.4)	4.25 (sept, $^3J_{HH}$ = 6.4)	6.88 (t, $^3J_{HH}$ = 9.4)	7.41 (ps.t)	7.01-7.10 (m)

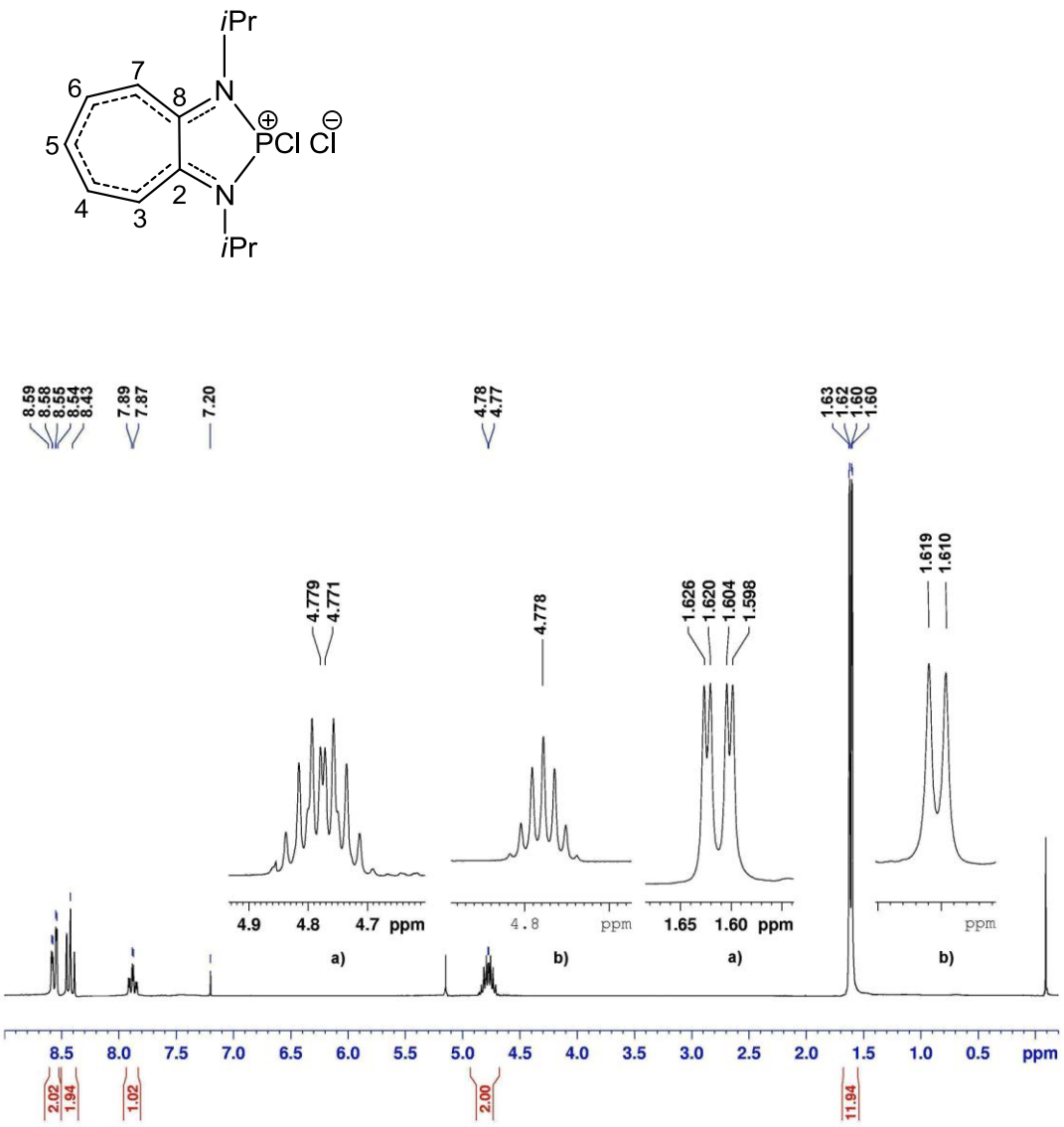

Figure 2: ^{1}H NMR spectrum for compound **6a**. a) signals of CH_3 and CH non decoupled of P; b) signals of CH_3 and CH decoupled of P

1.2.1.2 ^{13}C NMR

The Carbon-13 NMR spectrum can be divided into two groups. First, the signals between 21.18 and 51.20 ppm belong to an alkyl group. Secondly, those which ranged from 108.65 to 176.52 ppm belong to the aromatic carbon atoms.

For **6b** we also observe two signals for CH_3, CH and $C_{2,8}$ due to the asymmetry of the molecule (Table 3).

As previously observed in the ^{1}H NMR spectra, the resonances for the ring carbons are significantly shifted downfield compared to those of the ligands. Among the series, the parameters of the aromatic carbons change little (Table 4).

The correct assignment of all these signals requires a bidimensional NMR experiment. The HMBC (Heteronuclear Multiple Bond Correlation) is a 2D experiment that allows correlating carbons (or other X nuclei) and protons separated by multiple bonds (usually 2 or 3) and gives information about weak proton-carbon J-couplings. A weak proton-carbon J-coupling indicates that the proton is two, three, or four bonds away from the carbon. This experiment gives information about which protons are near to (but not directly bonded to) different carbons. This experiment (in conjunction with the HMQC) can give an enormous amount of information about molecular structure, since the long range proton-carbon correlations can include quaternary carbons, in addition to protonated carbons[64].

Quaternary carbons ($C_{2,8}$) have weaker and narrower signals than those of carbons attached to protons and present the highest chemical shifts. For phosphenium cations, the coupling constant P-C is decreasing from 12.7 to 5.0 Hz ($C_{2,8}$ to C_5) in the case of **6a** and from 15.5 to 2.0 Hz (C_2 to C_5) for compound **7a**.

If we compare the neutral ligand **2** and the salt **12**, no very different signals can be seen in Carbon-13 NMR for the two compounds due to the similarity of these two molecules.

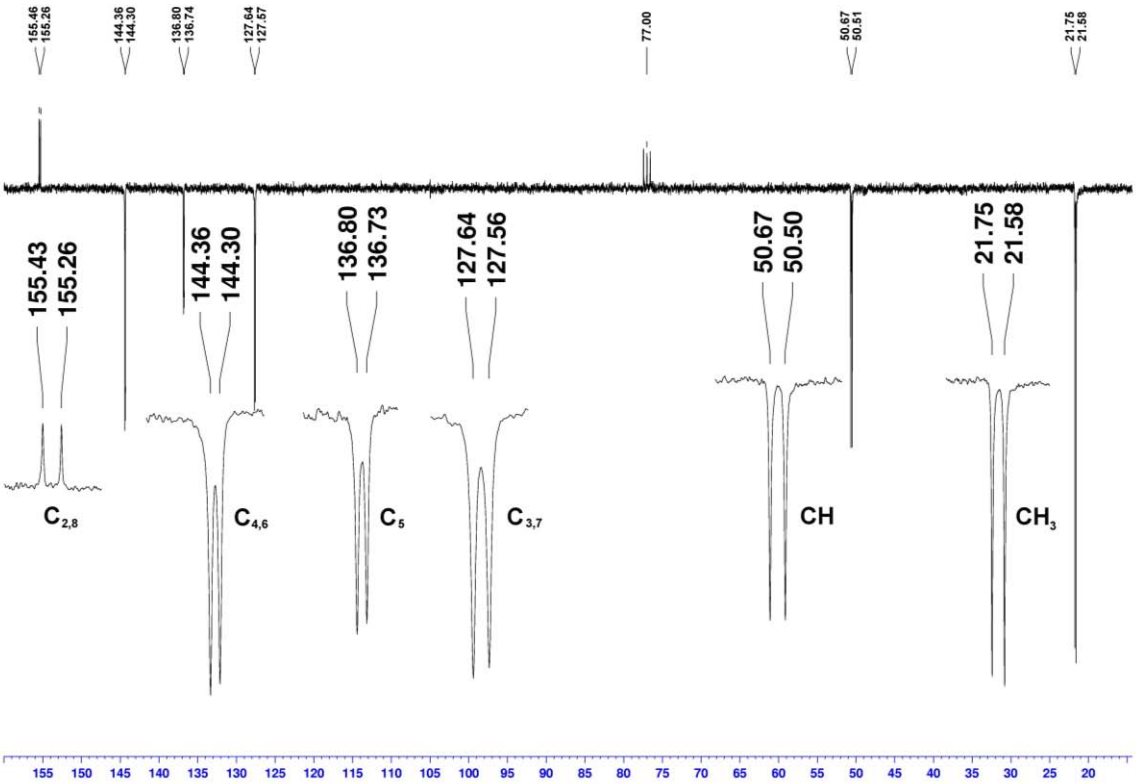

Figure 3: ^{13}C NMR spectrum for compound **6a** (for atom numbering see Figure 1 section 1.2.1)

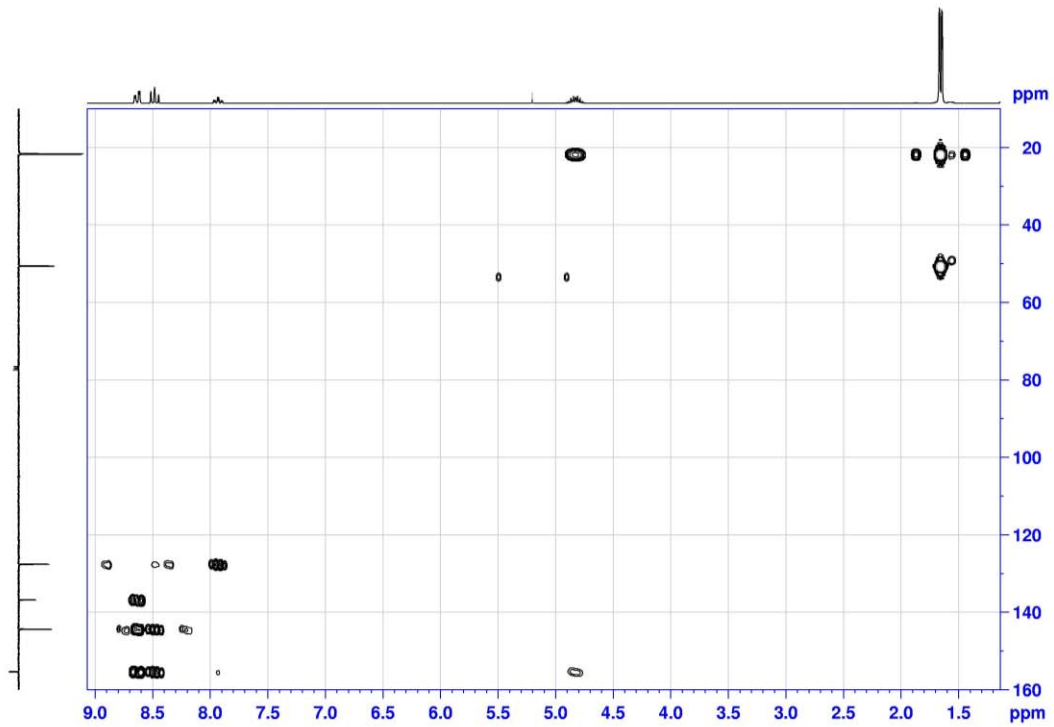

Figure 4: Correlation spectra $^{1}H/^{13}C$ (HMBC) for compound **6a**

Table 3: Carbon-13 NMR chemical shifts for **2**, **10**, **6b**, **6a**, **8**, **12** (in ppm, J in Hz, in $CDCl_3$)

	CH_3	CH	C_5	$C_{3,7}$	$C_{4,6}$	$C_{2,8}$
2	22.87	45.72	109.73	116.98	132.45	151.41
6a	21.89 (d, $^3J_{CP}$ = 12.6)	50.91 (d, $^2J_{CP}$ = 12.6)	136.99 (d, $^5J_{CP}$ = 5.0)	127.83 (d, $^3J_{CP}$ = 5.7)	144.56 (d, $^4J_{CP}$ = 5.7)	155.57 (d, $^2J_{CP}$ = 12.7)
6b	21.20 and 21.35	48.02 and 49.03	125.09	115.80	140.50	150.64 and 151.47
8	21.62	51.00	130.00	121.99	139.97	158.78
10	23.36	50.69	127.46	121.05	138.39	162.17
12	21.38	48.02	125.31	115.98	139.35	150.63

Table 4: Carbon-13 NMR chemical shifts for **1**, **7b**, **7a**, **9**, **11** (in ppm, J in Hz, in $CDCl_3$)

	CH_3	CH	C_7	C_3	C_5	C_4	C_6	C_2	C_8
1	21.92	43.71	108.65	121.66	128.17	137.01	136.11	154.58	176.52
7a	21.18 (d, $^3J_{CP}$ = 11.3)	51.12 (d, $^2J_{CP}$ = 8.3)	128.62 (d, $^3J_{CP}$ = 3.1)	130.34 (d, $^3J_{CP}$ = 2.9)	138.79 (d, $^5J_{CP}$ = 2.0)	147.57 (d, $^4J_{CP}$ = 2.1)	143.55 (d, $^4J_{CP}$ = 2.6)	156.39 (d, $^2J_{CP}$ = 4.6)	166.41 (d, $^2J_{CP}$ = 15.5)
7b	21.79	45.81	120.46, 125.95, 130.85			140.90, 142.56		155.33	163.25
9	21.54	51.20	124.33	128.25	133.40	140.69 and 142.56		150.00 and 158.13	
11	22.49	50.32	122.49 and 123.05		127.41	136.97 and 138.35		161.37 and 168.83	

1.2.2 Mass spectrometry study

The existence of the molecular peak depends on the dissociated or non dissociated character of the molecule. In the case of **6b** and **10** (non dissociated species) we observed in the mass spectrum the presence of the [M^+] peak at 304 and 396 amu respectively and [M-Cl] peak at 269 and 361 amu while for the dissociated species **8**, and partial dissociated species **9** and **11** the presence of the [M^+ - Cl] peak at 313 amu, 272 amu and 320 amu, respectively was only observed. In the particular case of **6a** a protonated fragment, [M-Cl+H], at 270 amu can be seen.

1.2.3 X-ray analyses

X-ray structure determinations were carried out for **6a**, **7a**, **8** and **9**. Their molecular structures (including selected bond lengths and bond angles) are shown in Figures 5-7.

All compounds show the same general features in the solid state: they consist in separated ion-pairs with chloride as anion. The nearest distances between the anion $Cl^{-\cdots}H$ [cation (methyl of isopropyl group)] are 2.54 Å (**6a**) and 2.64 Å (**7a**), and the shortest distances between the chloride anion and the phosphorus atoms are 5.36 Å and 3.05 Å for **6a** and **7a**, respectively. The compounds **6a** and **7a** show the same general features in the solid state consisting of separated ion-pairs with chloride as anions. Crystals of **8** are of poor quality and provide only limited data. Nevertheless, the distinctly ionic structure shows no evidence of interactions between cation and chloride anion.

The cationic parts are formed by PCl and AsCl units, which are stabilized by the chelating ligand systems. The three-coordinated phosphorus atoms adopt pyramidal geometries [the sum of the angles are 291.0° (**6a**) and 287.5° (**7a**)], with the bonded chloride atoms in approximately orthogonal positions towards the heterobicyclic planes. In the case of **6a**, the P-N distances, 1.697(1) and 1.708(1) Å, are in good agreement with the values observed by Cowley et al. in cyclic phosphenium cations: 1.694(4) and 1.689(4) Å for 1,2-bis(arylamino)acenaphthene[17], and 1.701(2) and 1.731(2) Å with β-diketiminate ligands[20].

In the asymmetric compound **7a**, the P-O bond [1.646(2) Å] is between a typical P-O single bond (1.71 Å) and a P=O double bond (1.40 Å),[65] which confirms the very strong covalent bond character of this formally donor bond. Consequently, the CO bond (1.365 Å) is about 10 pm longer than in the neutral corresponding tropone (1.245 Å),[66] and other comparable tropones, like 2-amino-5-methoxycarbonyltropone (1.255 Å),[67] 2-(4-fluoroanilino)tropone (1.251 Å, mean value)[68] or 2-(2,6-di-isopropylanilino)tropone (1.252

Å)[46]. The P-N distance is slightly longer [1.732(2) Å] compared to those of **6a**. These strong interactions between the formally P^+ and As^+ centers and the chelating systems are also reflected in the C-C bond lengths in the carbon backbones. Such small differences between the C-C bond distances combined with the nearly perfect planarity are strong evidence for a high degree of electron delocalization in the systems, which means delocalization of the positive charge.

Interestingly, compound **9**, which is closely related to **7a**, adopts a very different structure. The asymmetric unit contains two molecules of **9** which are very similar with little difference in the bond distances (Figure 7). One chloride atom seems to be linked to the arsenic in a covalent fashion with a As(1)-Cl(1) bond distance of 2.3206(6) Å. This value is slightly shorter than those observed in alkylated chloroarsines ($MeNCH_2CH_2NMe$)AsCl [2.390(5) Å] and {$MeN(CH_2)_3NMe$}AsCl [2.357(2) Å][24] but comparable with that observed in chloroarsine containing delocalized backbone as diamidonaphthalene ligand [2.2820(8) Å][3]. The second chloride atom is located 2.722 Å from the arsenic atom which is beyond the range of covalent bonds but within the sum of van der Waals radii (As, 2.0; Cl, 1.8)[69]. In the solid state, the neutral dichloroarsine presents a dimeric arrangement involving a four-membered As_2Cl_2 contact. The As-Cl distances (2.722 Å and 2.874 Å) of the As_2Cl_2 parallelogram are significantly elongated compared with that of the exocyclic As-Cl bond (2.3202 Å) which is in the range of covalent bonds[3, 18]. Similar halogen-bridged arrangements have been reported for chloroarsenic compounds such as chorobenzothiazarsole[70] or chloroarsines[71-72]. The N-heterobicyclic unit is planar and perpendicular to the As_2Cl_2 system. As previously observed for phosphenium **7a**, the As-O bond length [1.8194(16) Å is close to that of a single bond (1.78 Å)[73-74] and the As-N distance 1.9250(16) Å] is elongated compared to those of Arduengo type arsenium [1.812(9)][18] which confirmed a strong interaction between the arsenic atom and the chelating system. If we take into account the lengthening of the cyclic As-Cl distances and the near-perfect planarity of the heterobicyclic, compound **9** should be considered as a compound with some degree of ionic character between the arsenic and chloride atoms. The ^1H NMR data are in good agreement with the solid-state structure and the observation of down-field shifted ring protons.

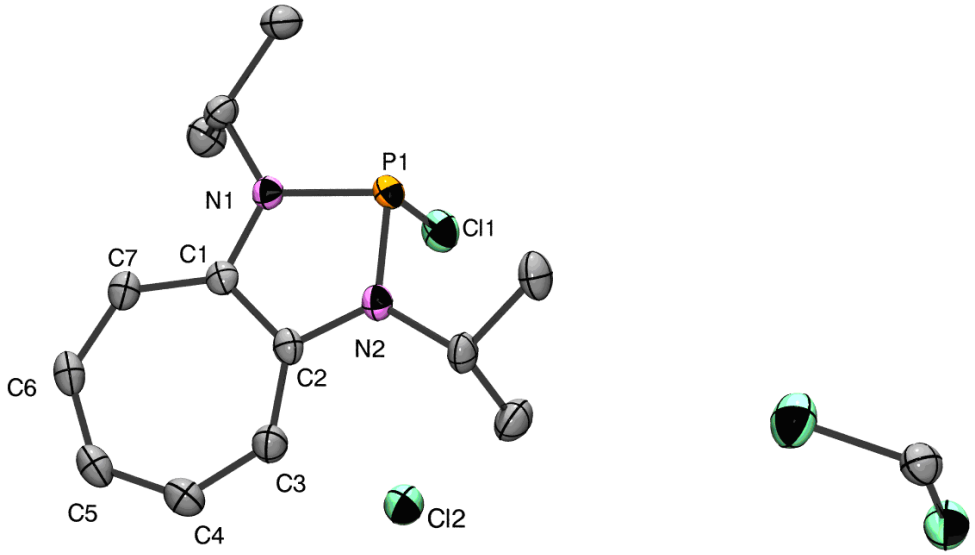

Figure 5: Molecular structure of compound **6a** (50 % probability level for the thermal ellipsoids). All H atoms have been omitted for clarity. Selected bond distances [Å] and angles [°] are: P(1)-N(1) 1.7075(13), P(1)-N(2) 1.6969(13), P(1)-Cl(1) 2.1543(6), C(1)-C(2) 1.441(2), C(2)-C(3) 1.392(2), C(3)-C(4) 1.390(2), C(4)-C(5) 1.390(2), C(5)-C(6) 1.387(2), C(6)-C(7) 1.385(2); N(2)-P(1)-N(1) 88.88(6), N(1)-P(1)-Cl(1) 101.70(5), N(2)-P(1)-Cl(1) 100.41(5), C(2)-N(1)-P(1) 114.94(10), C(8)-N(2)-P(1) 114.84(10).

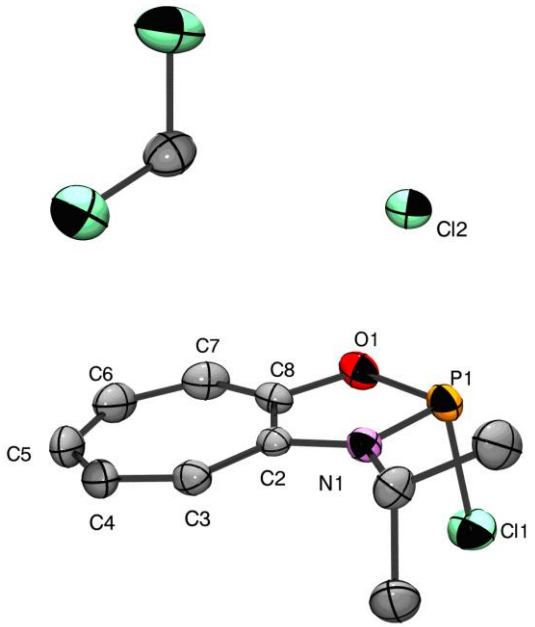

Figure 6: Molecular structure of compound **7a** (50 % probability level for the thermal ellipsoids). All H atoms have been omitted for clarity. Selected bond distances [Å] and angles [°] are: P(1)-O(1) 1.646(2), P(1)-N(1) 1.732(2), P(1)-Cl(1) 2.1262(12), C(1)-C(2) 1.423(4),

C(2)-C(3) 1.406(4), C(2)-C(8) 1.423(4), C(7)-C(8) 1.364(4), C(6)-C(7) 1.394(4), C(5)-C(6) 1.364(4), C(4)-C(5) 1.397(5); O(1)-P(1)-N(1) 89.95(11), O(1)-P(1)-Cl(1) 97.88(9), N(1)-P(1)-Cl(1) 97.63(9), C(2)-N(1)-P(1) 112.82(18), C(2)-O(1)-P(1) 114.83(18).

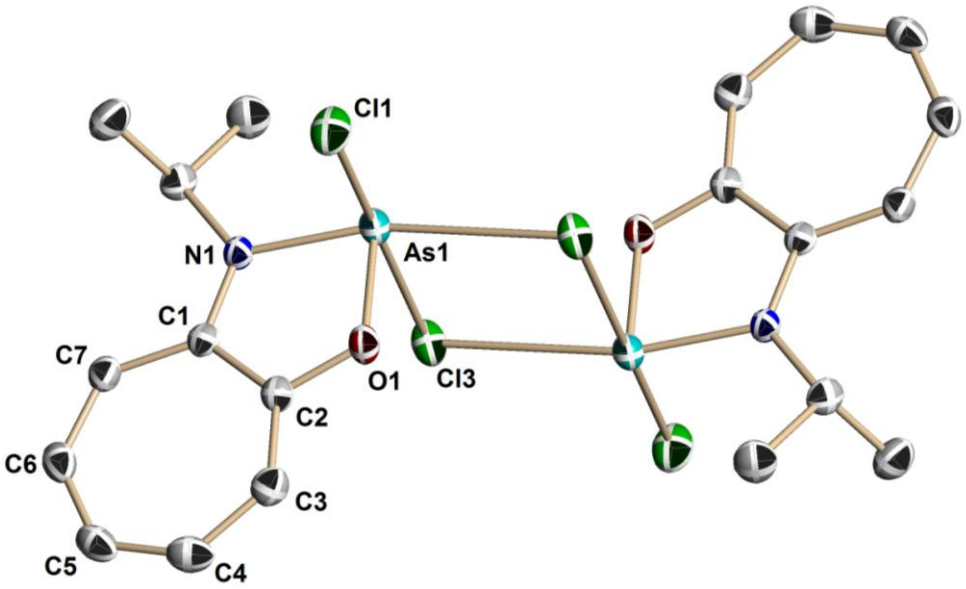

Figure 7: Molecular structure of compound **9** (50 % probability level for the thermal ellipsoids). All H atoms have been omitted for clarity. Selected bond distances [Å] and [°] are: As(1)-O(1) 1.8194(16), As(1)-N(1) 1.9250(17), As(1)-Cl(1) 2.3202(6), N(1)-C(1) 1.333(3), O(1)-C(2) 1.348(3), C(1)-C(7) 1.420(3), C(1)-C(2) 1.446(3), C(2)-C(3) 1.365(3), C(3)-C(4) 1.404(3), C(4)-C(5) 1.371(3), C(5)-C(6) 1.393(3), C(6)-C(7) 1.373(3); O(1)-As(1)-N(1) 83.56(7), O(1)-As(1)-Cl(1) 93.76(5), N(1)-As(1)-Cl(1) 93.24(6), C(1)-N(1)-As(1) 114.19(14), C(2)-O(1)-As(1) 115.97(13).

1.3 Computational studies

In order to gain more insight about the electronic state of these cations, Density Functional Theory (DFT) calculations were done on pnictogenium cations (P and As) **6a**, **7a**, **8** and **9** using the Amsterdam Density Functional package, ADF 2005[75]. The input parameters for the geometry optimization were generated from the X-ray crystallographic data of **6a**, **7a**, **8** and **9**. As shown in Figure 8, for **6a** and **7a**, the HOMO are localized into the bicyclic systems and the heteroatoms (N, O, Cl), whereas the LUMO are more localized on the seven-membered cycle and less on the heterocycle. The phosphorous lone-pair resides in HOMO-1 orbitals that are at 0.79 and 0.76 eV below their corresponding HOMO while in **8** and **9** the arsenic lone-pair resides in HOMO-4 orbitals that are at 2.04 and 2.05 eV below their corresponding HOMO (Figure 9).

The NICS (Nucleus-Independent Chemical Shifts) values[76-77] calculated at the centre of the rings (NICS(0)) and 1.0 Å above and below the ring (NICS(1)) for the four systems (**6a**, **7a**, **8** and **9**) are given in Table 6. NICS(0) are influenced by the sigma bonds so the NICS(1) values are considered as better indicators of π-electron delocalization. These data show that the electron delocalization in the seven-membered ring is similar in all compounds; however, the five-membered ring exhibits some differences, displaying somewhat lower NICS(1) values for **7a** and **9** than for **6a** and **8** respectively. Thus, the π-electrons in the five-membered ring are less delocalized, in accordance with the bond lengths in this ring and the chemical shifts in the ^{31}P NMR. The out-of-plane component of the NICS(1) value, $NICS(1)_{ZZ}$, might be considered as another indicator of the electron delocalization[78].

The localization of the positive charge was also calculated from the Fukui's function,[79-81] $f^{+}_{(r)}$ (Figure 10). In both cases, it is delocalized into the seven-membered cycle which is consistent with the ^{1}H NMR observations.

These computational studies and the X-ray structural data indicate an extensive delocalization of the positive charge over the seven-membered ring cycle suggesting that these species could be formally better described as chlorophosphines bearing a cationic substituent.

Table 6: B3LYP/6-31G(d,p) calculated NICS and NICSzz values for **6a**, **7a**, **8**, and **9**

Distance from the center (Å)	**6a**				**7a**			
	C_7 ring		**CNENC ring**		**C_7 ring**		**CNENC ring**	
	NICS	$NICS_{zz}$	NICS	$NICS_{zz}$	NICS	$NICS_{zz}$	NICS	$NICS_{zz}$
1	-7.49	-17.07	-4.04	-11.17	-7.64	-17.90	-3.28	-11.25
0	-5.40	-6.21	-6.81	-26.21	-5.49	-6.37	-6.36	-26.17
-1*	-7.56	-16.84	-6.47	-10.75	-7.75	-17.12	-5.07	-8.47
Distance from the center (Å)	**8**				**9**			
	C_7 ring		**CNENC ring**		**C_7 ring**		**CNENC ring**	
	NICS	$NICS_{zz}$	NICS	$NICS_{zz}$	NICS	$NICS_{zz}$	NICS	$NICS_{zz}$
1	-7.48	-3.43	-4.16	-5.12	-7.67	-3.47	-3.51	-6.38
0	-5.58	-5.75	-6.24	-13.63	-5.71	-5.36	-5.59	-12-11
-1*	-7.83	-3.58	-5.81	-1.72	-7.85	-3.51	-4.57	-1.77

*face opposite to the E-Cl bond

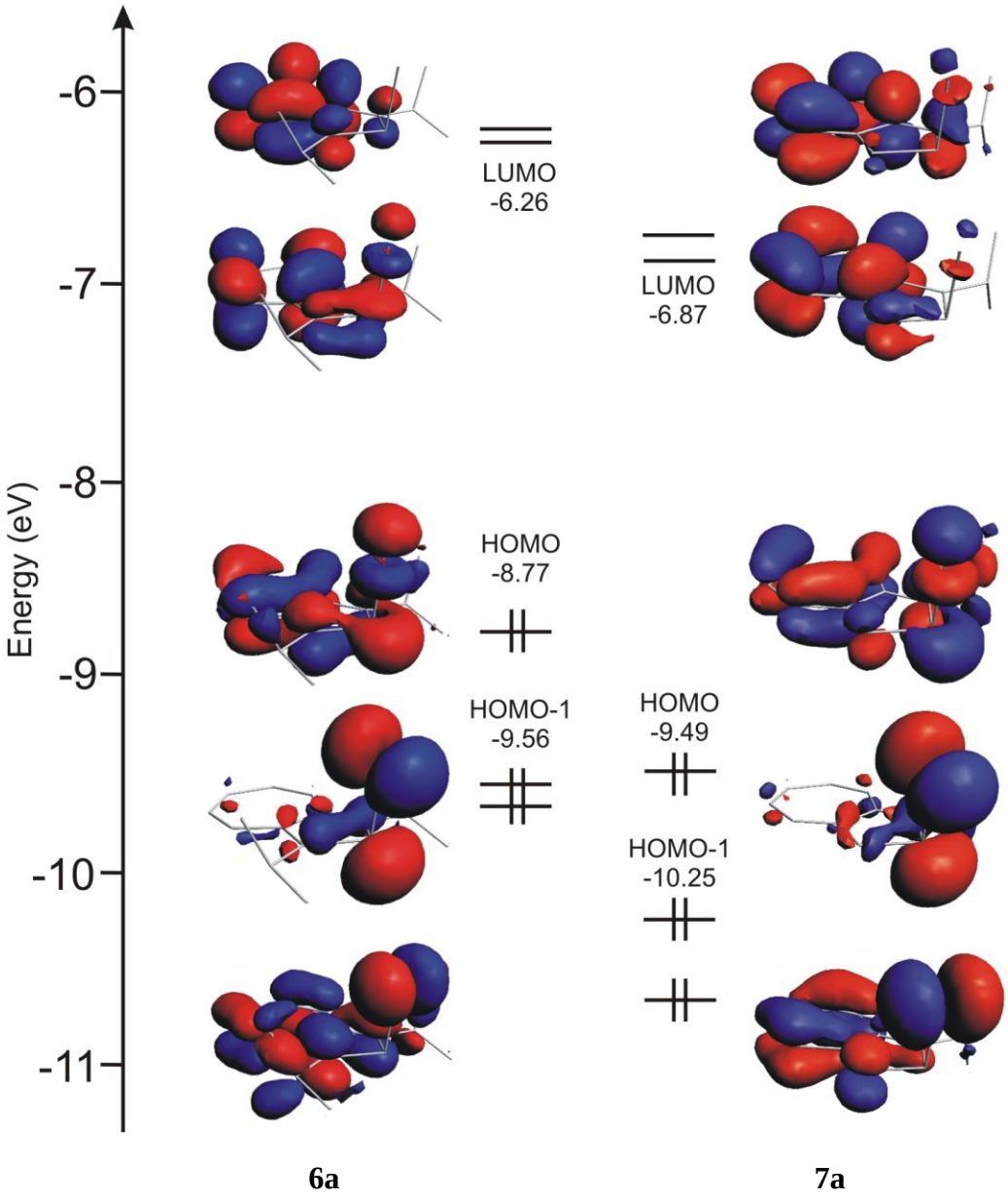

Figure 8: Molecular orbital diagrams and orbital contour plots of **6a** and **7a**.

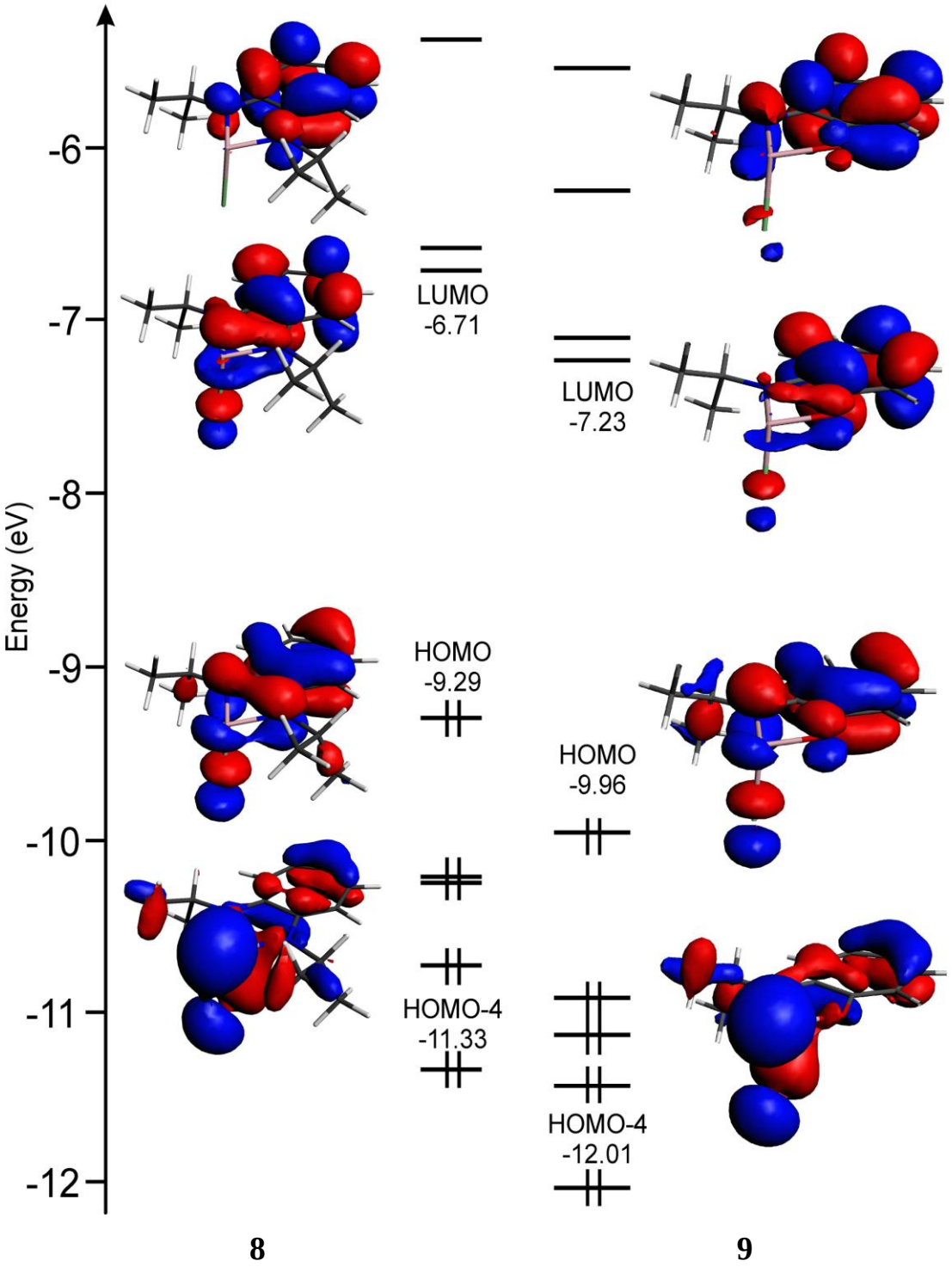

Figure 9: Molecular orbital diagrams and orbital contour plots of **8** and **9**.

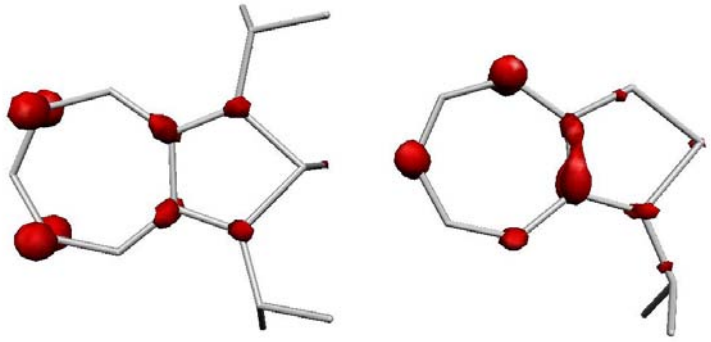

6a **7a**

Figure 10: Representation of Fukui's function, [$f^{+}_{(r)} = \rho_{N+1}(r) - \rho_{N}(r)$] of **6a** and **7a**.

Conclusions and perspectives

An easy and direct route to the first phosphenium and arsenium cations supported by N,N' or N,O-chelation derived from a tropolone scaffold was achieved. The presence of a π-unsaturated backbone in the aminotroponiminate and aminotroponate ligands not only prevents the competitive γ-carbon substitution previously observed for diketiminate ligand but also allows a complete positive charge delocalization on the seven-membered cycles. This result was confirmed by the X-ray structural data and DFT calculations.

Experimental section

Synthesis of 2-(tosyloxy)tropone

To a cold solution of tropolone 5.00 g (40.90 mmol) in dry pyridine (20 ml) was added tosyl chloride (9.36 g, 49.10 mmol) at 5 °C. The mixture was stirred at 20 °C for 12 h and then cold distillated water (200 ml) was added. The precipitate was filtered off and washed with cold distillated water. The precipitate was dried under reduced pressure to obtain tosyloxytropone as a white powder (11.08 g, 98 %, mp 158 °C).

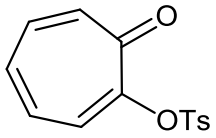

^{1}H NMR (300 MHz, $CDCl_3$): δ (ppm)

2.38 (s, 3H, CH_3),
6.92-7.18 (m, 4H, $H_{4,5,6,7}$),
7.29 (d, $^3J_{HH}$ = 8.6 Hz, 2H, H_o(Ts)),
7.40 (d.d, $^3J_{HH}$ = 9.1 Hz, $^4J_{HH}$ = 1.0 Hz, 1H, H_3),
7.86 (d, $^3J_{HH}$ = 8.4 Hz, 2H, H_m(Ts)).

Synthesis of 2-(isopropylamino)tropone 1

Finely powdered 2-(tosyloxy)tropone (11.0 g, 39.9 mmol) was slowly added at 0 °C to isopropylamine (44.0 ml, 514.6 mmol) over a period of 20 min. After the addition, the resulting yellow solution was stirred for 2 h at 0 °C. During this period, the solid slowly dissolved in the isopropylamine solution. The mixture was allowed to warm to room temperature and stirred for 12 h. The excess of isopropylamine was removed by vacuum. The resulting yellow residue was dried under vacuum, extracted into diethyl ether (3 × 100 ml), and filtered. The filtrate was concentrated under reduced pressure to obtain 2-(isopropy1amino)-tropone as a yellow solid (4.99 g, 77 %). It can be recrystallized from hexanes at -20 °C; mp 45 °C.

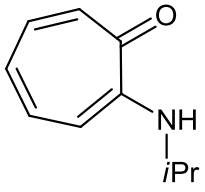

^{1}H NMR (300 MHz, $CDCl_3$): δ (ppm)

1.27 (d, $^{3}J_{HH}$ = 6.4 Hz, 6H, CH-CH_3),
3.78 (sept, $^{3}J_{HH}$ = 6.4 Hz, lH, CH-CH_3),
6.50 (d, $^{3}J_{HH}$ = 10.5 Hz, 1H, H_3),
6.59 (t, $^{3}J_{HH}$ = 9.2 Hz, 1H, H_5),
7.06-7.22 (m, 3H, $H_{4,6,7}$).

^{13}C {^{1}H} NMR (75 MHz, $CDCl_3$): δ (ppm)

21.92 (CH-$C$$H_3$),
43.71 (CH-CH_3),
108.65 (C_7),
121.66 (C_3),
128.17 (C_5),
136.11 (C_6),
137.01 (C_4),
154.58 (C_2),
176.52 (C_8).

N-Isopropyl-2-(isopropylamino)troponimine 2

$Et_3O{\cdot}BF_4$ (3.83 g, 20.2 mmol) in 20 ml of methylene chloride was slowly added to a methylene chloride (20 ml) solution of 2-(isopropylamino)tropone (3.00 g, 18.4 mmol). After stirring for 3 h, 20 ml (235.3 mmol) of isopropylamine was slowly added to the resulting reddish yellow solution. Immediately, the colour of the solution became yellow. The reaction mixture was stirred for a further 2 h, and the volatiles were removed under vacuum. The residue was extracted into hexane (300 ml), filtered and concentrated under vacuum to obtain **2** as a yellow solid (3.56 g, 95 %, mp 53-56 °C).

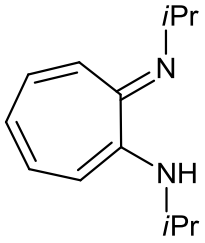

^{1}H NMR (300 MHz, $CDCl_3$): δ (ppm)

1.19 (d, $^{3}J_{HH}$ = 6.2 Hz, 12H, CH-CH_3),
3.76 (sept, $^{3}J_{HH}$ = 6.2 Hz, 2H, CH-CH_3),
6.02 (t, $^{3}J_{HH}$ = 9.2 Hz, 1H, H_5),
6.22 (d, $^{3}J_{HH}$ = 11.1 Hz, 2H, $H_{3,7}$),
6.65 (t, $^{3}J_{HH}$ = 10.3 Hz, 2H, $H_{4,6}$).

^{13}C {^{1}H} NMR (75 MHz, $CDCl_3$): δ (ppm)

22.87 (CH-$C$$H_3$),
45.72 (CH-CH_3),
109.73 (C_5),
116.98 ($C_{3,7}$),

132.45 ($C_{4,6}$),
151.41 ($C_{2,8}$).

Reaction of tropolone with PCl_3 in the presence of Et_3N

A solution of PCl_3 (0.23 g, 1.65 mmol) in toluene (1 ml) was added dropwise to a solution of tropolone (0.40 g, 3.28 mmol) and Et_3N (0.33 g, 3.30 mmol) in toluene (10 ml). The mixture became immediately brown. After 6 h of stirring, the volatiles were removed to yield a white brown powder. ^{1}H and ^{31}P NMR spectra showed the formation of only one product identified as **3**. It was no possible to separate the product from the $Et_3N{\cdot}HCl$.

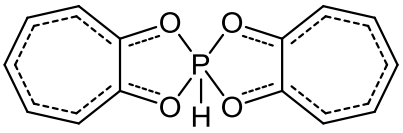

$^{31}P\{^{1}H\}$ NMR (121 MHz, $CDCl_3$): δ (ppm) −109.55 (J_{HP} = 964 Hz).

Reaction of lithiated tropolone with equimolecular quantity of PCl_3

Tropolone (0.21 g, 1.72 mmol) and *n*BuLi (1.15 ml of 1.6 M solution, 1.90 mmol) were mixed together in pre-cold diethyl ether (10 ml) and the resulting mixture was stirred at 0 °C for 0.5 h. To this mixture, PCl_3 (0.24 g, 1.72 mmol) was slowly added at -78 °C and stirred for 40 min. The white-yellow mixture was filtrated and the filtrate was dried to yield a light brown powder identified as **4**. It was not possible to isolate the pure product.

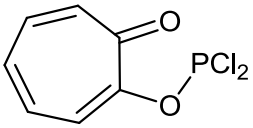

$^{31}P\{^{1}H\}$ NMR (121 MHz, $CDCl_3$): δ (ppm) 178.31.
^{1}H NMR (300 MHz, $CDCl_3$): δ (ppm)
7.55-7.66 (m, 2H, C_7H_5),
7.77-7.85 (m, 1H, C_7H_5),
7.87-7.90 (m, 1H, C_7H_5),
8.28 (d, $^{3}J_{HH}$ = 11.7 Hz, 1H, C_7H_5).

^{1}H NMR (300 MHz, $CDCl_3$): δ (ppm) 8.15-8.70 (m, 5H, C_7H_5).

Synthesis of tropolone arsenic derivate 5

To a mixture of tropolone (0.40 g, 3.27 mmol) and Et_3N (0.35 g, 3.46 mmol) in toluene (10 ml) was added $AsCl_3$ (0.59 g, 3.27 mmol) in toluene (5 ml). The mixture was stirred for 5 h at 35 °C. After filtration, volatiles were removed under vacuo and the residue was washed with CH_2Cl_2 and dried under vacuum (0.70 g, 80 %, mp 144 °C (dec.)).

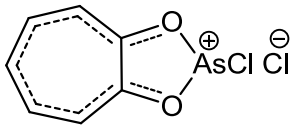

^{1}H NMR (300 MHz, $CDCl_3$): δ (ppm)
7.54-7.65 (m, 1H, H_5),
7.77-7.91 (m, 4H, $H_{4,6}$).

^{13}C {^{1}H} NMR (75 MHz, $CDCl_3$): δ (ppm)
129.96 ($C_{3,7}$),
133.82 (C_5),
140.78 ($C_{4,6}$),
177.63 ($C_{2,8}$).

EI-MS: m/z 231 [M^+ - Cl, 100 %], 196 [M^+ - 2 Cl, 14 %].

Preparation of 6a

To a mixture of (*i*Pr_2ATI)H **2** (0.52 g, 2.5 mmol) and Et_3N (0.26 g, 2.5 mmol) in toluene (15 ml) was added PCl_3 (0.35 g, 2.5 mmol) in toluene (5 ml). The mixture was stirred for 3 h. After filtration, volatiles were removed under vacuo and the residue was dissolved in CH_2Cl_2. The saturated solution was placed in a freezer at – 30 °C for 7 days to yield yellow crystals of **6a** (0.40 g, 52 %, mp 122-125 °C (dec.)).

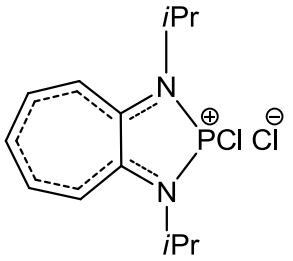

^{31}P NMR {^{1}H} (121 MHz, $CDCl_3$): δ (ppm) 134.47.

^{1}H NMR (300 MHz, $CDCl_3$): δ (ppm)
1.61 (d.d, $^3J_{HH}$ = 6.6 Hz, $^4J_{HP}$= 1.7 Hz, 12H, CH-CH_3),
4.77 (sept.d, $^3J_{HH}$ = 6.6 Hz, $^3J_{HP}$ = 10.9 Hz, 2H, C*H*-CH_3),
7.88 (t.d, $^3J_{HH}$ = 9.6 Hz, $^6J_{HP}$ = 3.4 Hz, 1H, H_5),

8.43 (t, $^{3}J_{HH}$ = 9.7 Hz, 2H, $H_{4,6}$),
8.55 (d.d, $^{3}J_{HH}$ = 11.0 Hz, $^{4}J_{HP}$ = 2.5 Hz, 2H, $H_{3,7}$).

^{13}C {^{1}H} NMR (75 MHz, $CDCl_3$): δ (ppm)
21.89 (d, $^{3}J_{CP}$ = 12.6 Hz, CH-*C*H_3),
50.91 (d, $^{2}J_{CP}$ = 12.6 Hz, *C*H-CH_3),
127.83 (d, $^{3}J_{CP}$ = 5.7 Hz, $C_{3,7}$),
136.99 (d, $^{5}J_{CP}$ = 5.0 Hz, C_5),
144.56 (d, $^{4}J_{CP}$ = 5.7 Hz, $C_{4,6}$),
155.57 (d, $^{2}J_{CP}$ = 12.7 Hz, $C_{2,8}$).

EI-MS: m/z 270 [M^+ - Cl + H, 16 %], 235 [M^+ - 2 Cl + H, 42 %].
Anal. $C_{14}H_{21}Cl_4N_2P$ (390.11): calc. C 43.10, H 5.43, N 7.18;
found C 43.29, H 6.08, N 7.45.

Reaction of (*i*Pr$_2$ATI)Li with PCl_3: 6b

A 1.6 M solution of *n*BuLi in hexanes (2.0 mmol) was slowly added to a cooled (0 °C) solution of **2** (0.34 g, 1.6 mmol) in diethyl ether (30 ml). The suspension was warmed to room temperature and stirred for 30 min, and it was slowly added to a cooled (-75 °C) solution of PCl_3 (0.22 g, 1.6 mmol) in diethyl ether (20 ml). The mixture was allowed to reach room temperature and stirred for 3h. After filtration, the remaining solid was washed with diethyl ether and dried under vacuum, leading to a yellow powder. The ^{1}H spectrum of the crude product indicated the presence of **6a** (20 %) and **6b** (80 %). **6b**:

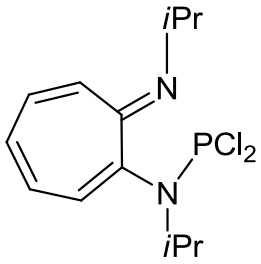

^{31}P NMR {^{1}H} (121 MHz, $CDCl_3$): δ (ppm) 160.95.
^{1}H NMR (300 MHz, $CDCl_3$): δ (ppm)
1.51 (d, $^{3}J_{HH}$ = 6.3 Hz, 6H, CH-CH_3),
1.54 (d, $^{3}J_{HH}$ = 6.3 Hz, 6H, CH-CH_3),
3.98 (sept, $^{3}J_{HH}$ = 6.8 Hz, 1H, C*H*-CH_3),
4.02 (sept, $^{3}J_{HH}$ = 6.8 Hz, 1H, C*H*-CH_3),
6.80-6.87 (m, 2H, C_7H_5),
7.35-7.44 (m, 1H, C_7H_5),
7.89 (t, $^{3}J_{HH}$ = 9.0 Hz, 1H, C_7H_5),
8.30-8.41 (m, 1H, C_7H_5).

^{13}C {^{1}H} NMR (75 MHz, $CDCl_3$): δ (ppm)
21.20 and 21.35 (CH-*C*H_3),
48.02 and 49.03 (*C*H-CH_3),
115.80 ($C_{3,7}$),
125.09 (C_5),

140.50 ($C_{4,6}$),
150.64 and 151.47 ($C_{2,8}$).

EI-MS: m/z 304 [M^+, 16 %], 289 [M^+ - CH_3, 21 %], 269 [M^+ - Cl, 7 %].

Synthesis of 7a

Using the same procedure described for **6a**, **1** (0.40 g, 2.5 mmol), Et_3N (0.26 g, 2.5 mmol) and PCl_3 (0.34 g, 2.5 mmol) in toluene (15 ml) gave a mixture of **7a** (45 %) and **7b** (55 %) (% determined from the ^{1}H NMR spectrum). A slow crystallization from dichloromethane at – 30 °C gave **7a** as yellow crystals (0.31 g, 48 %).

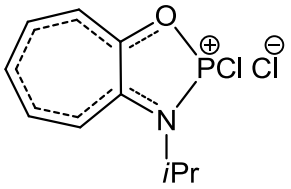

^{31}P {^{1}H} NMR (121 MHz, $CDCl_3$): δ (ppm) 155.70.

^{1}H NMR (300 MHz, $CDCl_3$): δ (ppm)

1.71 (d.d, $^3J_{HH}$ = 6.6 Hz, $^4J_{PH}$ = 2.2 Hz, 6H, CH-CH_3),
4.69 (sept, $^3J_{HH}$ = 6.9 Hz, 1H, CH-CH_3),
8.13-8.15 (m, 1H, H_5),
8.28-8.35 (m, 2H, $H_{4,6}$),
8.65 (br.l, $^3J_{HH}$ = 5.5 Hz, 2H, $H_{3,7}$).

^{13}C {^{1}H} NMR (75 MHz, $CDCl_3$): δ (ppm)

21.18 (d, $^3J_{CP}$ = 11.3 Hz, CH-$C$$H_3$),
51.12 (d, $^2J_{CP}$ = 8.3 Hz, CH-CH_3),
128.62 (d, $^3J_{CP}$ = 3.1 Hz, C_7),
130.34 (d, $^3J_{CP}$ = 2.9 Hz, C_3),
138.79 (d, $^5J_{CP}$ = 2.0 Hz, C_5),
143.55 (d, $^4J_{CP}$ = 2.6 Hz, C_6),
147.57 (d, $^4J_{CP}$ = 2.1 Hz, C_4),
156.39 (d, $^2J_{CP}$ = 4.6 Hz, C_2),
166.41 (d, $^2J_{CP}$ = 15.5 Hz, C_8).

7a is very sensitive to hydrolysis and oxidation. Reproducible analyses could not be obtained.

Reaction of (*i*PrAT)Li with PCl_3

Using the same procedure described for **6b**, 2.0 mmol of *n*BuLi (1.6 M) in hexanes, **1** (0.30 g, 1.8 mmol), and PCl_3 (0.28 g, 2.0 mmol) in diethyl ether (15 ml) gave a mixture of **7a** (65 %) and **7b** (35 %) identified by ^{1}H NMR analyses. **7b**:

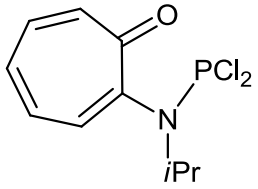

^{31}P {^{1}H} NMR (121 MHz, $CDCl_3$): δ (ppm) 171.01.
^{1}H NMR (300 MHz, $CDCl_3$): δ (ppm)
1.36 (d, $^3J_{HH}$ = 6.4 Hz, 6H, CH-CH_3),
3.98-4.08 (m, 1H, C*H*-CH_3),
7.30 (t, $^3J_{HH}$ = 12.0 Hz, 1H, H_5),
7.31 (d, $^3J_{HH}$ = 9.4 Hz, 1H, H_3),
7.62 (t.d, $^3J_{HH}$ = 10.3 Hz, $^5J_{HP}$ = 1.0 Hz, 1H, H_4),
7.80 (d.d, $^3J_{HH}$ = 9.3 Hz, $^3J_{HP}$ = 10.0 Hz, 1H, H_6),
8.48 (d, $^3J_{HH}$ = 10.6 Hz, 1H, H_7).
^{13}C {^{1}H} NMR (75 MHz, $CDCl_3$): δ (ppm)
21.79 (CH-*C*H_3),
45.81 (*C*H-CH_3),
120.46, 125.95, 130.85 ($C_{3,5,7}$),
140.90, 142.56 ($C_{4,6}$),
155.33 (C_2),
163.25 (C_8).

Preparation of 8

To a mixture of (*i*Pr_2ATI)H **2** (0.40 g, 1.96 mmol) and Et_3N (0.20 g, 1.96 mmol) in toluene (15 ml) was added dropwise over a period of 5 min $AsCl_3$ (0.36 g, 1.96 mmol) in toluene (5 ml). The mixture was stirred for 3 h. After filtration, volatiles were removed under vacuo and the residue was dissolved in CH_2Cl_2. The saturated solution was placed in a freezer at – 30°C for 2 days to yield yellow crystals of **8** (0.34 g, 50 %, mp 138-142 °C).

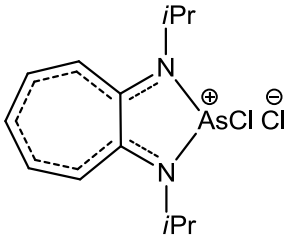

^{1}H NMR (300 MHz, $CDCl_3$): δ (ppm)
1.74 (d, $^3J_{HH}$ = 6.6 Hz, 12H, CH-CH_3),
4.40 (sept, $^3J_{HH}$ = 6.6 Hz, 2H, C*H*-CH_3),
7.24 (t, $^3J_{HH}$ = 9.6 Hz, 1H, H_5),

7.30 (d, $^{3}J_{HH}$ = 11.4 Hz, 2H, $H_{3,7}$),
7.69 (ps.t, $^{3}J_{HH}$ = 9.6 Hz, 2H, $H_{4,6}$).

^{13}C {^{1}H} NMR (75 MHz, $CDCl_3$): δ (ppm)

21.62 (CH-*C*H_3),
51.00 (*C*H-CH_3),
121.99 ($C_{3,7}$),
130.00 (C_5),
139.97 ($C_{4,6}$),
158.78 ($C_{2,8}$).

EI-MS: m/z 313 [M^+ - Cl, 100 %], 278 [M^+ - 2 Cl, 17 %], 235 [M^+ - (2 Cl, *i*Pr), 95 %].

Reaction of (*i*Pr_2ATI)Li with $AsCl_3$

A 1.6 M solution of *n*BuLi in hexanes (1.60 mmol) was slowly added at 0 °C to a solution of **2** (0.29 g, 1.42 mmol) in diethyl ether (10 ml). The resultant yellow colored mixture was removed from the cooling bath, allowed to reach room temperature and stirred for 0.5 h; then it was slowly added to a cooled (-75 °C) solution of $AsCl_3$ (0.26 g, 1.42 mmol) in diethyl ether (5 ml). The reaction mixture was allowed to reach ambient temperature and stirred for 3 h. After filtration, the remaining solid was washed with diethyl ether and dried under vacuo, leading to a yellow powder identified as **8** (0.28 g, 57 %).

Preparation of 9

Following the same experimental procedure as for the synthesis of **8**, **1** (0.40 g, 2.45 mmol), Et_3N (0.26 g, 2.50 mmol) and $AsCl_3$ (0.45 g, 2.50 mmol) in toluene (15 ml) gave **9**. Crystallization from dichloromethane at – 30 °C gave **9** as yellow crystals (0.42 g, 56 %, mp 106 °C (dec.)).

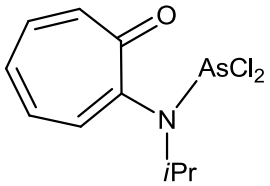

^{1}H NMR (300 MHz, $CDCl_3$): δ (ppm)

1.74 (d, $^{3}J_{HH}$ = 6.4 Hz, 6H, CH-CH_3),
4.36 (sept, $^{3}J_{HH}$ = 6.7 Hz, 1H, C*H*-CH_3),
7.40-7.50 (m, 2H, $H_{4,6}$),
7.70 (ps.d, 2H, $H_{3,7}$),
7.89 (ps.t, 1H, H_5).

^{13}C {^{1}H} NMR (75 MHz, $CDCl_3$): δ (ppm)

21.54 (CH-*C*H_3),
51.20 (*C*H-CH_3),
124.33 (C_7),

128.25 (C_3),
133.40 (C_5),
140.69 and 142.56 ($C_{4,6}$),
150.00 and 158.13 ($C_{2,8}$).

EI-MS: m/z 272 [M^+ - Cl, 100 %], 194 [M^+ - (2 Cl, *i*Pr), 70 %].

Reaction of (*i*PrAT)Li with $AsCl_3$

A 1.6 M solution of *n*BuLi in hexanes (0.85 mmol) was slowly added at 0 °C to a solution of 2-(isopropylamino) tropone (0.20 g, 1.23 mmol) in diethyl ether (15 ml). The yellow solution was warmed to room temperature and stirred for 30 min, and it was slowly added by cannula to a stirred diethyl ether (5 ml) solution of $AsCl_3$ (0.22 g, 1.23 mmol) at -75 °C. The reaction mixture was allowed to reach ambient temperature and stirred for a further 3 h. After filtration, the remaining solid was washed with diethyl ether (3 × 10 ml); volatiles were removed under reduced pressure to yield a yellow powder. The ^{1}H NMR showed the formation of **9** (50 %) and the presence of the starting ligand **1** (50 %).

Reaction of (*i*Pr_2ATI)Li with $SbCl_3$

A 1.6 M solution of *n*BuLi in hexanes (1.20 mmol) was slowly added to a cooled (0 °C) solution of **2** (0.22 g, 1.08 mmol) in diethyl ether (10 ml). The suspension was warmed to room temperature and stirred for 30 min, and it was slowly added to a cooled (-75 °C) solution of $SbCl_3$ (0.25 g, 1.08 mmol) in diethyl ether (5 ml). The mixture was allowed to reach room temperature and stirred for 3 h. After filtration, the remaining solid was washed with diethyl ether and dried under vacuo, leading to **10**, a yellow powder. The product decomposes in solution towards the starting ligand (0.37 g, 87 %, mp 196-200 °C).

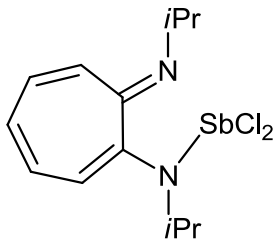

^{1}H NMR (300 MHz, $CDCl_3$): δ (ppm)

1.71 (d, $^3J_{HH}$ = 6.4 Hz, 12H, CH-CH_3),
4.43 (sept, $^3J_{HH}$ = 6.4 Hz, 2H, C*H*-CH_3),
6.99 (t, $^3J_{HH}$ = 9.4 Hz, 1H, C_7H_5),
7.08 (d, 2H, C_7H_5),
7.48-7.55 (m, 2H, C_7H_5).

^{13}C {^{1}H} NMR (75 MHz, $CDCl_3$): δ (ppm)

23.33 (CH-*C*H_3),
50.67 (*C*H-CH_3),
121.05 ($C_{3,7}$),
127.46 (C_5),
138.39 ($C_{4,6}$),
162.17 ($C_{2,8}$).

EI-MS: m/z 396 [M^+, 7 %], 361 [M^+ - Cl, 100 %], 239 [M^+ - Sb - Cl, 20 %].

Preparation of 10

To a solid mixture of (*i*Pr_2ATI)H **2** (0.22 g, 1.09 mmol) and $SbCl_3$ (0.25 g, 1.09 mmol) toluene (10 ml) was added. To this solution Et_3N (0.12 g, 1.20 mmol) was added dropwise over a period of 5 min. The mixture was stirred for 3 h. After filtration, volatiles were removed under vacuo to obtain **10** as a yellow powder. It was not possible to separate **10** from the ammonium salt Et_3N·HCl.

Synthesis of 11

Following the same experimental procedure as for the synthesis of **10**, **1** (0.20 g, 1.23 mmol), Et_3N (0.13 g, 1.23 mmol) and $SbCl_3$ (0.28 g, 1.23 mmol) in toluene (12 ml) gave **11**. Like **10**, **11** decomposes in solution towards the starting ligand.

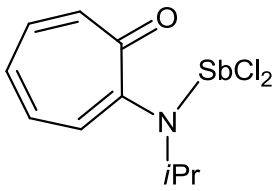

^{1}H NMR (300 MHz, $CDCl_3$): δ (ppm)
1.55 (d, $^3J_{HH}$ = 6.4 Hz, 6H, CH-C*H*$_3$),
4.25 (sept, $^3J_{HH}$ = 6.4 Hz, 1H, C*H*-CH_3),
6.88 (t, $^3J_{HH}$ = 9.4 Hz 1H, H_5),
7.01-7.10 (m, 2H, $H_{3,7}$),
7.41 (ps.t, 2H, $H_{4,6}$).

^{13}C {^{1}H} NMR (75 MHz, $CDCl_3$): δ (ppm)
22.49 (CH-*C*H_3),
50.32 (*C*H-CH_3),
122.49 and 123.05 ($C_{3,7}$),
127.41 (C_5),
136.97 and 138.35 ($C_{4,6}$),
161.37 and 168.83 ($C_{2,8}$).

EI-MS: m/z 320 [M^+ - Cl, 6 %].

Reaction of (*i*PrAT)Li with $SbCl_3$

Using the same procedure described for reaction of (*i*Pr_2ATI)Li with $SbCl_3$, (1.35 mmol) of *n*BuLi (1.6 M) in hexanes, **1** (0.20 g, 1.23 mmol), and $SbCl_3$ (0.28 g, 1.23 mmol) in diethyl ether (10 ml) gave a yellow powder. The ^{1}H NMR showed the formation of **11** (25 %) and the presence of the starting ligand **1** (75 %).

Synthesis of (*i*Pr_2ATI)H·HCl 12

A yellow precipitate was formed immediately after addition of HCl (0.04 g, 1.10 mmol) at room temperature to a solution of **2** (0.20 g, 0.98 mmol) in diethylether (5 ml). After 5 minutes of stirring, the volatiles were removed to yield a yellow precipitate, **12**, in nearly quantitative yield (mp 106 °C).

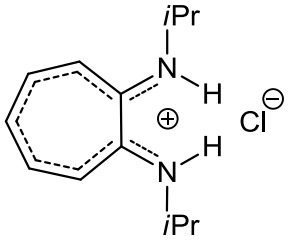

^{1}H NMR (300 MHz, $CDCl_3$): δ (ppm)
1.51 (d, $^3J_{HH}$ = 6.4 Hz, 12H, CH-CH_3),
3.97 (sept, $^3J_{HH}$ = 6.4 Hz, 1H, CH-CH_3),
6.83-6.89 (m, 3H, C_7H_5),
7.43 (t, $^3J_{HH}$ = 9.6 Hz, 2H, C_7H_5).

^{1}H NMR (500 MHz, $CDCl_3$): δ (ppm)
1.45 (d, $^3J_{HH}$ = 6.5 Hz, 12H, CH-CH_3),
3.95 (sept, $^3J_{HH}$ = 6.5 Hz, 1H, CH-CH_3),
6.99-7.06 (m, 3H, C_7H_5),
7.56 (ps.t, $^3J_{HH}$ = 9.6 Hz, 2H, C_7H_5).

^{13}C {^{1}H} NMR (75 MHz, $CDCl_3$): δ (ppm)
21.38 (CH-$C$$H_3$),
48.02 (CH-CH_3),
115.98 ($C_{3,7}$),
125.31 (C_5),
139.35 ($C_{4,6}$),
150.63 ($C_{2,8}$).

^{13}C {^{1}H} NMR (125.75 MHz, $CDCl_3$): δ (ppm)
21.16 (CH-$C$$H_3$),
47.89 (CH-CH_3),
117.47 ($C_{3,7}$),
127.10 (C_5),
140.20 ($C_{4,6}$),
150.70 ($C_{2,8}$).

EI-MS: m/z 161 [M^+ - HCl - *i*Pr, 100 %], 204 [M^+ - HCl, 95 %], 189 [M^+ - HCl - CH_3, 93 %].

X-ray structures

Structural data were collected at low temperature (193 K) using an oil-coated shock-cooled crystal on a Bruker-AXS CCD 1000 diffractometer with Mo-K_α radiation (λ = 0.71073 Å). Structures were solved by direct methods[82] and all non-hydrogen atoms were refined anisotropically using the least-squares method on F^2[83].

Structural data of **6a**, **7a** and **9** are given in Tables 7 and 8.

Table 7 Structural refinement data for **6a** and **7a**

	6a	**7a**
Empirical formula	$C_{14}H_{21}Cl_4N_2P$	$C_{11}H_{14}Cl_4NOP$
Formula weight	390.00	349.00
Temperature (K)	173(2)	193(2)
Crystal system	Triclinic	Monoclinic
Space group	$P\ \bar{1}$	$P2_1/c$
a (Å)	9.2570(6)	7.0170(7)
b (Å)	9.6340(7)	11.4932(12)
c (Å)	12.4169(9)	19.630(2)
α (°)	87.538(1)	90
β (°)	70.060(1)	92.484(2)
γ (°)	62.132(1)	90
Volume ($Å^3$)	911.17(11)	1581.7(3)
Z	2	4
Density (calculated)(Mg/m^3)	1.422	1.466
Absorption coefficient (mm^{-1})	0.732	0.837
Reflections collected	5306	9066
Independent reflections	3658 [R(int) = 0.0117]	3260 [R(int) = 0.0501]
Absorption correction	Semi-empirical	Semi-empirical
Max. and min. transmission	1.000000 and 0.570048	1.000000 and 0.783046
Final R indices [I>2sigma(I)]	R_1= 0.0289 wR_2 = 0.0749	R_1 = 0.0476 wR_2 = 0.0878
R indices (all data)	R_1= 0.0338 wR_2 = 0.0783	R_1 = 0.0891 wR_2 = 0.1009
Largest diff. peak and hole ($eÅ^{-3}$)	0.446 and -0.243	0.494 and -0.444

with $R_1 = \Sigma||F_o|-|F_c||/\Sigma|F_o|$ and $wR_2 = (\Sigma w (F_o^2-F_c^2)^2/\Sigma w(F_o^2)^2)^{0.5}$.

Table 8 Structural refinement data for **9**

	9
Empirical formula	$C_{10}H_{12}AsCl_2NO$
Formula weight	308.03
Temperature (K)	193(2)
Crystal system	Triclinic
Space group	$P\ \bar{1}$
a (Å)	9.6348(2)
b (Å)	11.0251(2)
c (Å)	13.3230(2)
α (°)	98.4130(10)
β (°)	100.5440(10)
γ (°)	113.0890(10)
Volume ($Å^3$)	1242.12(4)
Z	4
Density (calculated)(Mg/m^3)	1.647
Absorption coefficient (mm^{-1})	3.140
Reflections collected	19949
Independent reflections	6121 [R(int) = 0.0418]
Absorption correction	Semi-empirical from equivalents
Max. and min. transmission	0.6502 and 0.5724
Final R indices [I>2sigma(I)]	R1 = 0.0314 wR2 = 0.0641
R indices (all data)	R1 = 0.0469 wR2 = 0.0692
Largest diff. peak and hole ($eÅ^{-3}$)	0.474 and -0.502

with $R_1 = \Sigma||F_o|-|F_c||/\Sigma|F_o|$ and $wR_2 = (\Sigma w\ (F_o^2-F_c^2)^2/\Sigma w(F_o^2)^2)^{0.5}$.

Details on Computations

Density functional calculations were made with the Amsterdam Density Functional package, ADF 2005[84]. Structures were fully optimized via analytical energy gradient techniques employing the local density approximation (LDA)[85] and the generalized gradient approximation (GGA) method using Vosko-Wilk-Nusair local exchange correlations[86] with nonlocal exchange corrections by Becke[87] and nonlocal electronic correlations by Perdew[88]. We used uncontracted type IV basis sets using triple-ζ accuracy sets of Slater-type orbitals[89] (STO) with a single polarization function added for the main group elements (2p on H, 3d on C, N and O and 4d on P). Frozen core approximations[90] were applied to the inner orbitals of the constituent atoms: the C, N, O core up to 1s and P up to 2p.

References

[1] K. Dimroth, P. Hoffman, *Angew. Chem. Int. Ed. Engl.* **1964**, *3*, 384.

[2] N. J. Hardman, M. B. Abrams, M. A. Pribisko, T. M. Gilbert, R. L. Martin, G. J. Kubas, R. T. Baker, *Angew. Chem. Int. Ed. Engl.* **2004**, *43*, 1955.

[3] H. A. Spinney, I. Korobkov, G. A. DiLabio, G. P. A. Yap, D. S. Richeson, *Organometallics* **2007**, *26*, 4972.

[4] B. D. Ellis, P. J. Ragogna, C. L. B. Macdonald, *Inorg. Chem.* **2004**, *43*, 7857.

[5] A. J. Arduengo, *Acc. Chem. Res.* **1999**, *32*, 913.

[6] H. M. Tuononen, R. Roesler, J. L. Dutton, P. J. Ragogna, *Inorg. Chem.* **2007**, *46*, 10693.

[7] J. B. Lambert, W. J. Schulz, *J. Am. Chem. Soc.* **1983**, *105*, 1671.

[8] G. A. Olah, *Halonium Ions, Wiley: New York* **1975**.

[9] S. Fleming, M. K. Lupton, K. Jekot, *Inorg. Chem.* **1972**, *11*, 2534.

[10] B. E. Maryanoff, R. O. Hutchins, *J.Org. Chem.* **1972**, *37*, 3475.

[11] A. H. Cowley, M. C. Cushner, J. S. Szobota, *J. Am. Chem. Soc.* **1978**, *100*, 7784.

[12] P. Friedrich, G. Huttner, J. Luber, A. Schmidpeter, *Chem. Ber.* **1978**, *111*, 1558.

[13] S. Pohl, *Chem. Ber.* **1979**, *112*, 3159.

[14] A. H. Cowley, R. A. Kemp, *Chem. Rev.* **1985**, *85*, 367.

[15] M. G. Thomas, C. W. Schultz, R. W. Parry, *Inorg. Chem.* **1977**, *16*, 994.

[16] R. W. Kopp, A. C. Bond, R. W. Parry, *Inorg. Chem.* **1976**, *15*, 3042.

[17] G. Reeske, C. R. Hoberg, N. J. Hill, A. H. Cowley, *J. Am. Chem. Soc.* **2006**, *128*, 2800.

[18] C. J. Carmalt, V. Lomeli, B. G. McBurnett, A. H. Cowley, *Chem. Commun.* **1997**, 2095.

[19] D. Gudat, *Coord. Chem. Rev.* **1997**, *163*, 71.

[20] D. Vidovic, Z. Lu, G. Reeske, J. A. Moore, A. H. Cowley, *Chem. Commun.* **2006**, 3501.

[21] S. P. Green, C. Jones, G. Jin, A. Stasch, *Inorg. Chem.* **2007**, *46*, 8.

[22] B. D. Ellis, C. L. B. Macdonald, *Inorg. Chim. Acta* **2007**, *360*, 329.

[23] N. Burford, T. M. Parks, B. W. Royan, J. F. Richardson, P. S. White, *Can. J. Chem.* **1992**, *71*, 703.

[24] N. Burford, C. L. B. Macdonald, T. M. Parks, G. Wu, B. Borecka, W. Kiviatkowski, T. S. Cameron, *Can. J. Chem.* **1996**, *74*, 2209.

[25] D. Gudat, T. Gans-Eichler, M. Nieger, *Heteroatom Chem*, **2005**, *16*, 327.

[26] M. K. Denk, S. Gupta, A. J. Lough, *Eur. J. Inorg. Chem.* **1999**, 41.

[27] I. A. Litvinov, V. A. Naumov, T. V. Gryaznova, A. N. Pudovik, A. M. Kibadin, *Dolk. Akad. Nauk. SSSR* **1990**, *312*, 623.

[28] D. Gudat, H. Haghverdi, H. Hupfer, M. Nieger, *Chem. -Eur. J.* **2000**, *6*, 3414.

[29] P. Jutzi, T. Wippermann, C. Kruger, H. Kraus, *Angew. Chem. Int. Edit.* **1983**, *22*, 250.

[30] L. A. Lesikar, A. F. Richards, *J. Organomet. Chem.* **2006**, *691*, 4250.

[31] B. Lyhs, S. Schultz, U. Westphal, D. Blaser, R. Boese, M. Bolte, *Eur. J. Inorg. Chem.* **2009**, 2247.

[32] R. Menye-Biyogo, F. Delpech, A. Castel, V. Pimienta, H. Gornitzka, P. Rivière, *Organometallics* **2007**, *26*, 5091.

[33] R. Menye Biyogo, F. Delpech, A. Castel, P. Rivière, H. Gornitzka, *Angew. Chem. Int. Ed. Engl.* **2003**, *42*, 5610.

[34] J. Zhang, P. D. Badger, S. J. Geib, S. Petoud, *Inorg. Chem.* **2007**, *46*, 6473.

[35] K. Lyczko, W. Starosta, I. Persson, *Inorg. Chem.* **2007**, *46*, 4402.

[36] Y. Jianlin, Y. Yaxian, G. Renao, *Spect. Acta Part A* **2006**, *64*, 1072.

[37] A. T. Balaban, I. Haiduc, H. Hopfl, N. Farfan, R. Santillan, *Main Group Metal Chem.* **1996**, *19(6)*, 385.

[38] P. W. Roesky, *Chem. Soc. Rev.* **2000**, *29*, 335.

[39] H. V. R. Dias, Z. Wang, W. Jin, *Coord. Chem. Rev.* **1998**, *176*, 67.

[40] A. V. Korolev, F. Delpech, S. Dagorne, I. A. Guzei, R. F. Jordan, *Organometallics* **2001**, *20*, 3367.

[41] A. V. Korolev, E. Ihara, I. A. Guzei, V. G. Young, R. F. Jordan, *J. Am. Chem. Soc.* **2001**, *123*, 8291.

[42] F. Delpech, I. A. Guzei, R. F. Jordan, *Organometallics* **2002**, *21*, 1167.

[43] D. Pappalardo, M. Mazzeo, P. Montefusco, C. Tedesco, C. Pellecchia, *Eur. J. Inorg. Chem.* **2004**, 1292.

[44] N. Meyer, K. Löhnwitz, A. Zulys, P. W. Roesky, M. Dochnahl, S. Blechert, *Organometallics* **2006**, *25*, 3730.

[45] S. Dehnen, M. R. Bürgstein, P. W. Roesky, *J. Chem. Soc., Dalton Trans.* **1998**, 2425.

[46] F. A. Hicks, M. Brookhart, *Organometallics* **2001**, *20*, 3217.

[47] S. Datta, P. W. Roesky, S. Blechert, *Organometallics* **2007**, *26*, 4392.

[48] N. Meyer, R. Rüttinger, P. W. Roesky, *Eur. J. Inorg. Chem.* **2008**, 1830.

[49] H. V. R. Dias, W. Jin, R. E. Ratcliff, *Inorg. Chem.* **1995**, *34*, 6100.

[50] E. L Muetterties, C. M. Wright, *J. Am. Chem. Soc.* **1964**, *86*, 5132.

[51] J. Lacour, L. Vial, G. Bernardinelli, *Org. Lett.* **2002**, *14*, 2309.

[52] K. Kikuchi, M. Yagi, K. Takada, *Bull. Chem. Soc. Jap.* **1968**, *41*, 424.

[53] D. M. Grant, R. K. Harris, *Encyclopedia of Nuclear Magnetic Resonance, John Wiley & Sons* **1996**.

[54] L.-C. Pop, N. Katir, A. Castel, L. Silaghi-Dumitrescu, F. Delpech, I. Silaghi-Dumitrescu, H. Gornitzka, D. MacLeod-Carey, N. Saffon, *J. Organomet. Chem.* **2009**, *694*, 1562.

[55] M. Sanchez, M. R. Mazières, L. Lamandé, R. Wolf, *Multiple Bonds and Low Coordination Chemistry in Phosphorous Chemistry, (Eds: M. Regitz, O. Scherer), Georg Thieme Verlag, Stuttgart* **1990**, 129.

[56] A. H. Cowley, M. Lattman, J. C. Wilburn, *Inorg. Chem.* **1981**, *20*, 2916.

[57] R. B. King, N. D. Sadani, *Synth. React. Inorg. Met.-Org. Chem.* **1985**, 149.

[58] N. Burford, P. J. Ragogna, *J. Chem. Soc., Dalton Trans.* **2002**, 4307.

[59] W. Becker, D. Schomburg, P. G. Jones, R. Schmutzler, *Phosphorus Sulfur Silicon* **1990**, *49/50*, 109.

[60] T. Kaukorat, I. Neda, R. Schmutzler, *Coord. Chem. Rev.* **1994**, *137*, 53.

[61] O. D. Sparkman, *Mass spectrometry desk reference. Pittsburgh: Global View Pub.* **2000**.

[62] H. V. R. Dias, Z. Wang, *J. Am. Chem. Soc.* **1997**, *119*, 4650.

[63] K. Gholivand, S. Ghadimi, H. Naderimanesh, A. Forouzanfar, *Magn. Reson. Chem.* **2001**, *39*, 684.

[64] Atta-ur-Rahman, *One or two dimentional NMR spectroscopy, Elsevier Science Publisher* **1989**.

[65] L. Pauling, *Nature of the Chemical Bond, Cornell University Press, Ithaca, N. Y.,* **1960**.

[66] P. W. Roesky, M. R. Bürgstein, *Inorg. Chem.* **1999**, *38*, 5629.

[67] K. Kubo, T. Matsumoto, M. Hashimoto, A. Mori, *Acta Cryst.* **2006**, *E62*, o3584.

[68] G. Steyl, *Acta Cryst.* **2007**, *E63*, o4353.

[69] *CRC handbook of chemistry and physics. 67th ed. CRC Press, Boca Raton, Florida* **1986**, *D-188*.

[70] N. Burford, T. M. Parks, B. W. Royan, J. F. Richardson, P. S. White, *Can. J. Chem.* **1992**, *70*, 703.

[71] M. Veith, B. Bertsch, *Z. Anorg. Allg. Chem.* **1988**, *7*, 557.

[72] D. J. Willliams, M. G. Newton, K. J. Wynne, *Cryst. Struct. Commun.* **1977**, *6*, 167.

[73] A. L. Rheingold, A. J. DiMaio, *Organometallics* **1986**, *5*, 393.

[74] J. Kopf, K. Von Deuten, G. Klar, *Inorg. Chim. Acta* **1980**, *38*, 67.

[75] S. ADF2006.01, Theoretical Chemistry, Vrije Universiteit, Amsterdam, The Netherlands, http://www.scm.com/. Methods and results are presented in Supporting Information.

[76] P. v. R. Schleyer, C. Maerker, A. Dransfeld, H. Jiao, N. J. R. v. E. Hommes, *J. Am. Chem. Soc.* **1996**, *118*, 6317.

[77] P. v. R. Schleyer, H. Jiao, N. J. R. v. E. Hommes, V. G. Malkin, O. L. Malkina, *J. Am. Chem. Soc.* **1997**, *119*, 12669.

[78] C. Corminboeuf, T. Heine, G. Seifert, P. v. R. Schleyer, J. Weber, *Phys. Chem. Chem. Phys.* **2004**, *6*, 273.

[79] K. Fukui, *Science* **1982**, *218*, 747.

[80] R. G. Parr, W. Yang, *J. Am. Chem. Soc.* **1984**, *106*, 4049.

[81] W. Yang, R. G. Parr, R. Pucci, *J. Chem. Phys.* **1984**, *81*, 2862.

[82] G. M. Sheldrick, *Acta Cryst.* **1990**, *A46*, 467.

[83] G. M. Sheldrick, *SHELXL-97 Program for Crystal Structure Refinement; University of Göttingen* **1997**.

[84] G. te Velde, E. J. Baerends, *J. Comput. Phys.* **1992**, *99*, 84.

[85] W. Kohn, L. J. Sham, *Phys. Rev.* **1965**, *140*, A1133.

[86] S. H. Vosko, L. Wilk, M. Nusair, *Can. J. Phys.* **1980**, *58*, 1200.

[87] A. D. Becke, *Phys. Rev. A* **1988**, *38*, 3098.

[88] J. P. Perdew, *Phys. Rev. B* **1986**, *33*, 8822.

[89] J. G. Snijders, P. Vernooijs, E. J. Baerends, *At. Nucl. Data Tables* **1982**, *26*, 483.

[90] E. J. Baerends, D. E. Ellis, P. Ros, *Chem. Phys.* **1973**, *2*, 41.

CHAPTER II

Pnictogenium cations: reactivity

RESUME

Dans le chapitre précédent, nous avons décrit la synthèse des premiers pnictogenium cations stabilisés par des substituants aminotroponiminate et aminotroponate. Leur étude physicochimique et structurale a montré l'existence de structures très originales. Ces composés peuvent être considérés soit comme des pnictogenium cations stabilisés par N-chélation ou des composés du groupe 15 à ligand cationique.

Dans le but d'obtenir plus d'information sur leur structure, nous avons réalisé des réactions caractéristiques comme des réactions d'oxydation, de cycloaddition et de complexation avec des métaux de transition.

Les phosphéniums se sont révélés les plus réactifs. Leurs réactions d'oxydation avec le DMSO, le soufre et le sélénium conduisent très facilement aux composés hydroxylés correspondants stables et isolables dans le cas du soufre et du selenium.

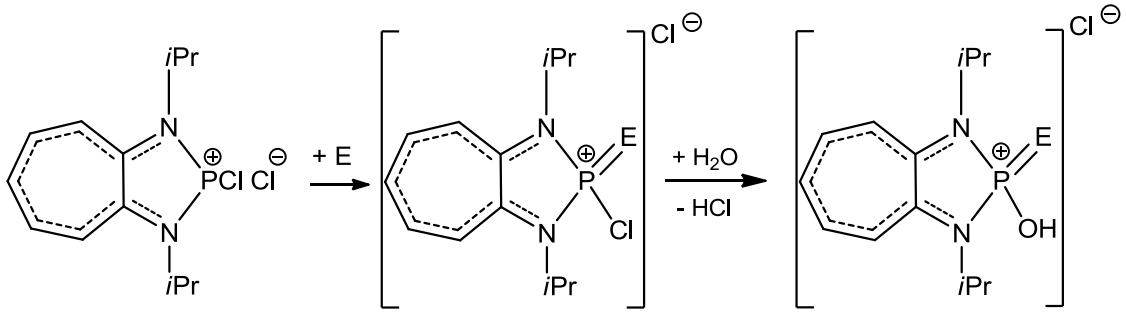

6a

21, E = S
22, E = Se

Leur étude physicochimique (RMN du ^{1}H, ^{13}C et ^{31}P, spectrométrie de masse) ainsi que structurale a permis de mettre en évidence l'existence de formes parfaitement dissociées et la présence de double liaison P=E.

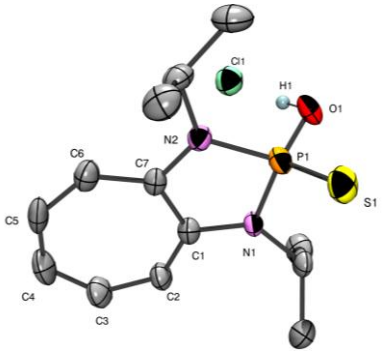

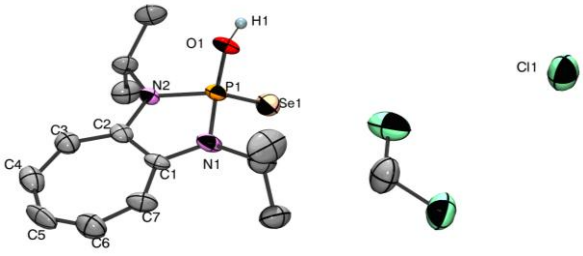

Une réaction inattendue d'élimination de HCl en présence de triéthylamine a conduit à des di-oxo et thiooxophosphoranes. Il faut noter que ce sont les premiers exemples d'aminométaphosphonate et de son équivalent soufré stabilisés par complexation intramoléculaire.

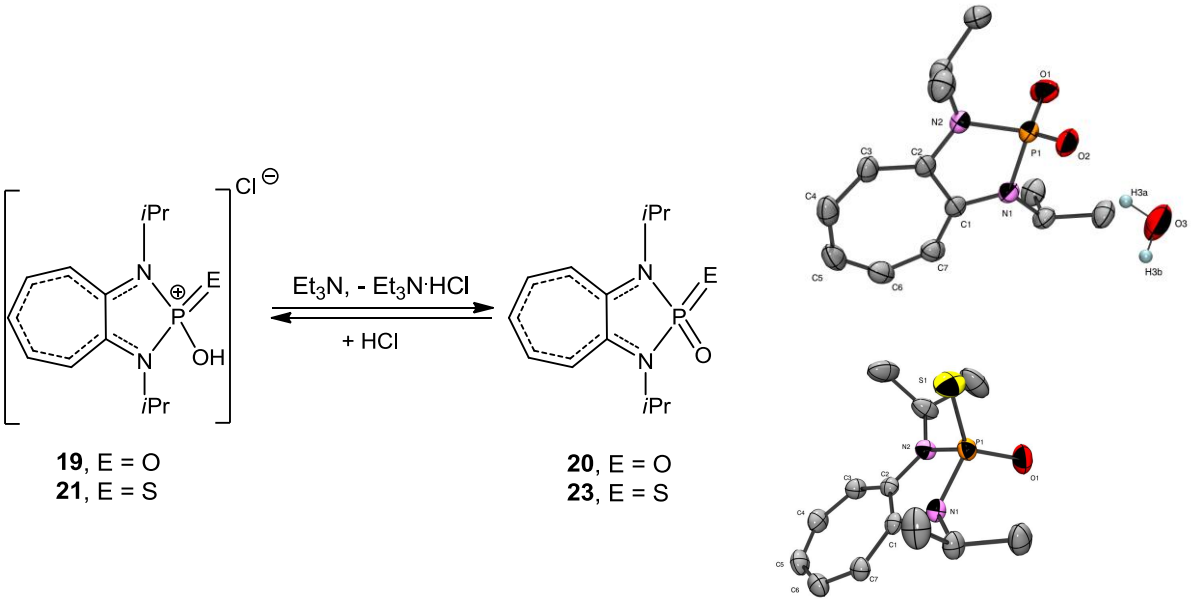

Les phosphéniums sont connus pour donner des réactions de cycloaddition avec des 1,3-diènes. La 3,5-di-*tert*-butyl-*o*-quinone réagit très facilement en donnant le cycloadduit correspondant. Comme cela a été observé précédemment, la liaison P-Cl est très sensible à l'hydrolyse conduisant rapidement à la formation d'hydroxyphosphorane en équilibre avec la forme ester. La structure de cette dernière a pu être confirmée par diffraction des rayons X.

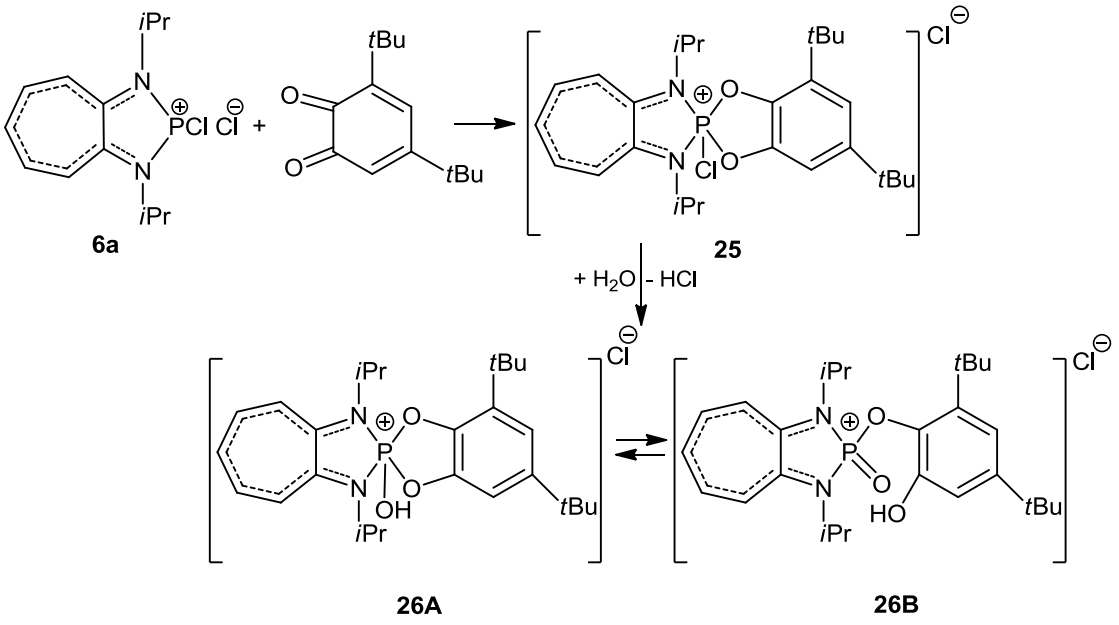

La dernière partie de ce chapitre porte sur l'aptitude de ces phosphéniums cations à former des complexes avec les métaux de transition. Les calculs DFT avaient montré que la paire libre de ce phosphénium cation résidait dans l'orbitale HOMO-1 et donc était accessible. Effectivement, le chlorophosphénium **6a** donne facilement une réaction d'échange de ligand dans le complexe $W(CO)_5THF$ conduisant à la formation transitoire du complexe **27** qui évolue rapidement vers la forme hydroxylée **28**.

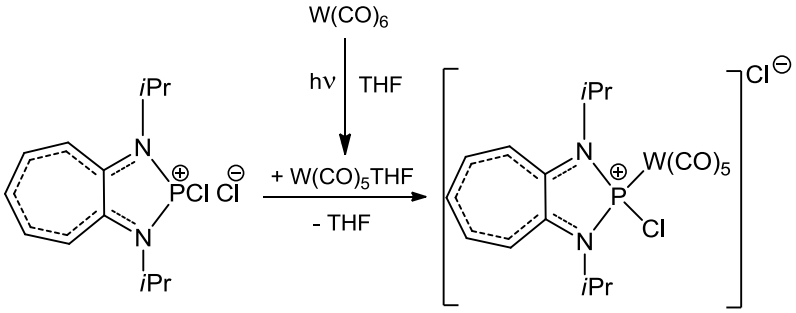

6a **27** **28**

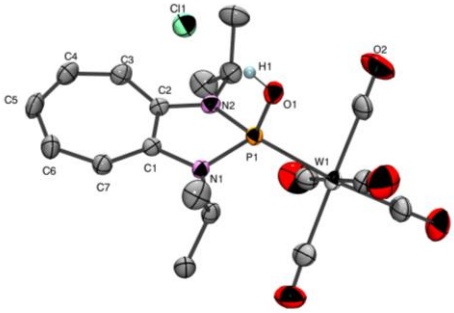

Ce complexe a été caractérisé en solution par la spectroscopie de RMN multinoyaux (^{1}H, ^{13}C, ^{31}P) et à l'état solide par diffraction de rayons X.

Introduction

In the first chapter, we have described the syntheses of new pnictogenium cations (P, As) supported by aminotroponate and aminotroponiminate ligands. The physicochemical and structural studies showed the existence of very special structures for these pnictogenium cations which can be regarded either as phosphenium or arsenium species stabilized by intramolecular complexation or as a phosphine or arsine with cationic ligand.

The main goal of this chapter is to perform some characteristic reactions such as halide ion exchange, oxidative addition, cycloaddition, and complexation with transition metals in an attempt to learn more about their structures.

2.1 Halide ion exchange

Firstly we investigated substitution reactions of chloride anion by trimethylsilyl triflate.

Treatment of phosphenium cation **6a** with stoichiometric amount of Me_3SiOTf in dichloromethane at room temperature resulted in Me_3SiCl elimination and formation of two new compounds **13** (35 %) and **14** (65 %) which display ^{31}P chemical signals at 136.16 and 111.05 ppm (Scheme 1).

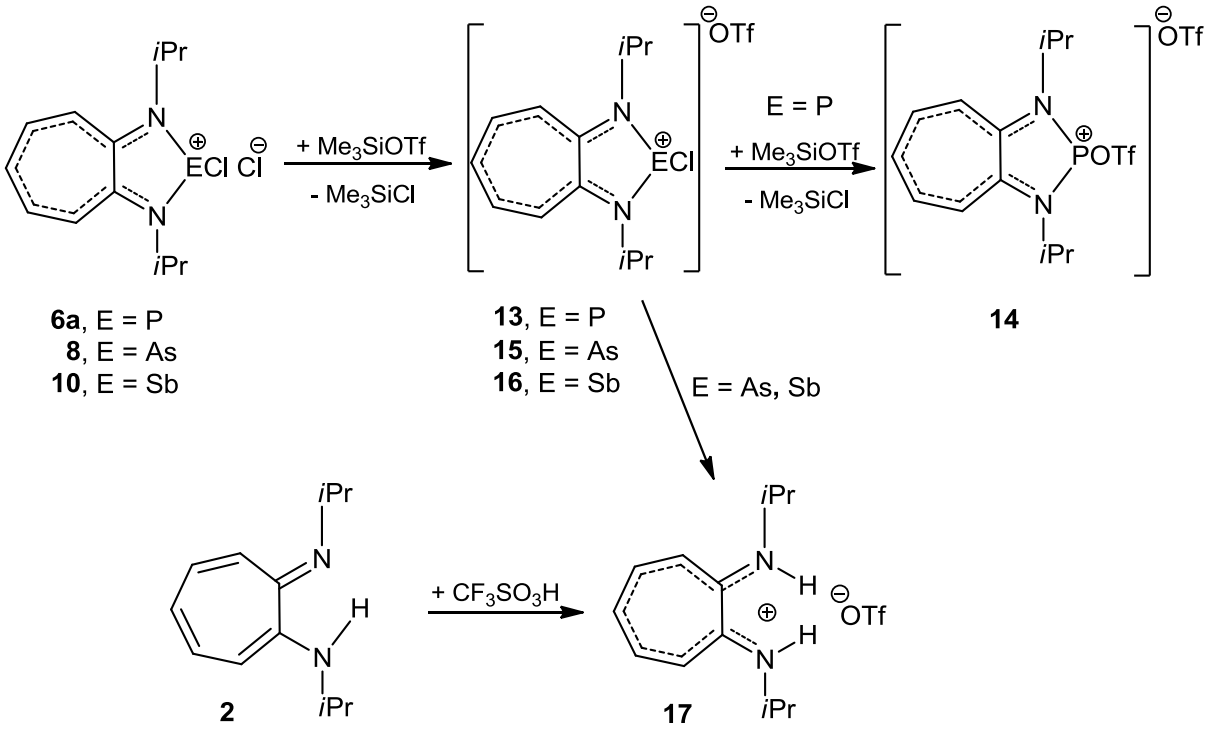

Scheme 1

Compound **6a** has two possible sites for such reactions: either the chloride anion or the chlorine atom of the P-Cl covalent bond. Because of the weak coordinating character of the triflate anion, we envisaged the substitution of the chloride anion in the first step leading to compound **13**. The ^{31}P chemical shift of 136.16 ppm which is almost similar to that of the chlorophosphenium cation **6a** seems in agreement with such a structure. Comparable phosphenium cations supported by a β-diketiminate ligands were previously reported[1]. Moreover, when adding two equivalents of Me_3SiOTf, we can see the major formation of disubstituted compound **14** which correspond to the signal at 111.05 ppm.

Starting from **8** or **10**, only one product **15** or **16** was obtained; **15** was structurally identified as a cationic species. However these compounds are unstable in solution, particularly the antimony compound **16**. They decompose leading to the triflate salt **17** which can be prepared by addition of a stoichiometric quantity of trifluoromethanesulfonic acid on aminotroponimine in Et_2O at room temperature (Scheme 1).

If compared with the parent pnictogenium compounds, the ^1H NMR data show almost similar deshielding of the ring protons confirming the formation of cationic species and delocalization of the positive charge on the ligand (Table 1). Within the group 15 series, a slightly deshielding effect can be seen for the aromatic protons of **13** (except for H_5) and **14** while for **15** and **16** the inverse phenomenon of shielding was found.

The same effect was observed for carbon signals. It is to note the presence of the characteristic quadruplet of CF_3 group with an average spin-spin coupling constant J_{CF} of 318 Hz.

As in the case of salt derivative **12**, **17** shows in ^1H and ^{13}C NMR deshielded signals compared to the neutral ligand.

^{19}Fluorine is a sensitive nucleus which yields sharp signals, has a spin of ½ and a relative abundance of 100 %, making measurements very fast (comparable with ^1H NMR).

All these derivatives display in ^{19}F NMR resonances between -78.44 ppm and -77.17 ppm which correspond to values expected for these triflate compounds[2]. We present the ^{19}F NMR spectrum for **15** in Figure 1.

In the mass spectra, the presence of the $[M^+ - Cl]$ peaks at 427 and 473 amu and the $[M^+ - OTf]$ peaks at 313 and 361 amu was observed for the triflate species **15** and **16** respectively (Figure 2). The molecular peak $[M^+]$ was also observed in the case of **16** at 510

amu suggesting some degree of associated form as observed for the similar chloride compound **10**.

Table 1: Proton NMR chemical shifts for **6a**, **13**, **14**, **15**, **16** and **17** (in ppm, J in Hz, in $CDCl_3$)

	CH_3	CH	H_5	$H_{4,6}$	$H_{3,7}$
6a	1.61 (d.d, $^3J_{HH}$ = 6.6, $^4J_{HP}$= 1.7)	4.77 (sept.d, $^3J_{HH}$ = 6.6, $^3J_{HP}$ = 10.9)	7.88 (t.d, $^3J_{HH}$ = 9.6, $^6J_{HP}$ = 3.4)	8.43 (t, $^3J_{HH}$ = 9.7)	8.55 (d.d, $^3J_{HH}$ = 11.0, $^4J_{HP}$ = 2.5)
13	1.62 (d, $^3J_{HH}$ = 6.5), 1.72 (d.d, $^3J_{HH}$ = 6.5, $^4J_{HP}$= 2.6)	4.64 (sept.d, $^3J_{HH}$ = 6.6, $^3J_{HP}$= 11.2)	7.92 (t.d, $^3J_{HH}$ = 9.6, $^6J_{HP}$ = 3.5)	8.31 (t, $^3J_{HH}$ = 10.2)	8.13 (d.d, $^3J_{HH}$ = 10.8, $^4J_{HP}$ = 2.7)
14	1.52 (d, $^3J_{HH}$ = 6.6)	4.48 (sept, $^3J_{HH}$ = 6.9)	7.59 (t.d, $^3J_{HH}$ = 9.7, $^6J_{HP}$ = 1.7)	8.04 (t, $^3J_{HH}$ = 10.1)	7.74 (d, $^3J_{HH}$ = 11.1)
8	1.74 (d, $^3J_{HH}$ = 6.6)	4.40 (sept, $^3J_{HH}$ = 6.6)	7.24 (t, $^3J_{HH}$ = 9.6)	7.69 (ps.t, $^3J_{HH}$ = 9.6)	7.30 (d, $^3J_{HH}$ = 11.4)
15	1.58 (d, $^3J_{HH}$ = 6.4), 1.81 (d, $^3J_{HH}$ = 6.4)	4.55 (sept, $^3J_{HH}$ = 6.5)	7.56 (t, $^3J_{HH}$ = 9.5)	7.95 (ps.t, $^3J_{HH}$ = 9.6)	7.63 (d, $^3J_{HH}$ = 11.1)
10	1.70 (d, $^3J_{HH}$ = 6.4)	4.43 (sept, $^3J_{HH}$ = 6.3)	6.99 (t, $^3J_{HH}$ = 9.4)	7.52 (ps.t)	7.08 (d, $^3J_{HH}$ = 11.5)
16	1.70 (d, $^3J_{HH}$ = 6.4)	4.52 (sept, $^3J_{HH}$ = 6.3)	7.23 (t, $^3J_{HH}$ = 9.5)	7.28 (d, $^3J_{HH}$ = 11.6)	7.71 (ps.t)
17	1.41 (d, $^3J_{HH}$ = 6.5)	3.94 (sept, $^3J_{HH}$ = 6.4)	6.97-7.04 (m, 3H), 7.55 (ps.t, 2H)		

Table 2: Carbon-13 NMR chemical shifts for **6a**, **13**, **14**, **15**, **16** and **17** (in ppm, J in Hz, in $CDCl_3$)

	CH_3	CH	CF_3	C_5	$C_{4,6}$	$C_{3,7}$	$C_{2,8}$
6a	21.89 (d, $^3J_{CP}$ = 12.6)	50.91 (d, $^2J_{CP}$ = 12.6)	-	136.99 (d, $^5J_{CP}$ = 5.0)	144.56 (d, $^4J_{CP}$ = 5.7)	127.83 (d, $^3J_{CP}$ = 5.7)	155.57 (d, $^2J_{CP}$ = 12.7)
13	21.70 (d, $^3J_{CP}$ = 8.9), 21.79 (d, $^3J_{CP}$ = 13.6)	51.55 (d, $^2J_{CP}$ = 3.3)	119.13 (q, J_{CF} = 318.4)	136.94 (d, $^5J_{CP}$ = 5.3)	143.95 (d, $^4J_{CP}$ = 4.9)	126.65 (d, $^3J_{CP}$ = 6.0)	155.69 (d, $^2J_{CP}$ = 12.8)
14	22.07 (d, $^3J_{CP}$ = 18.0)	49.37 (d, $^2J_{CP}$ = 14.3)	119.13 (q, J_{CF} = 318.4)	133.54 (d, $^5J_{CP}$ = 2.7)	142.82 (d, $^4J_{CP}$ = 2.7)	121.95 (d, $^3J_{CP}$ = 2.1)	155.74 (d, $^2J_{CP}$ = 10.1)
8	21.62	51.00	-	130.00	121.99	139.97	158.78
15	20.81	51.16	118.40 (q, J_{CF} = 317.4)	134.08	141.52	124.46	157.95
10	23.36	50.69	-	127.55	121.10	138.44	162.17
16	23.63	50.78	120.03 (q, J_{CF} = 319.0)	129.82	139.10	122.39	161.14
17	20.98	47.75	120.22 (q, J_{CF} = 319.6)	127.12	140.18	117.49	150.63

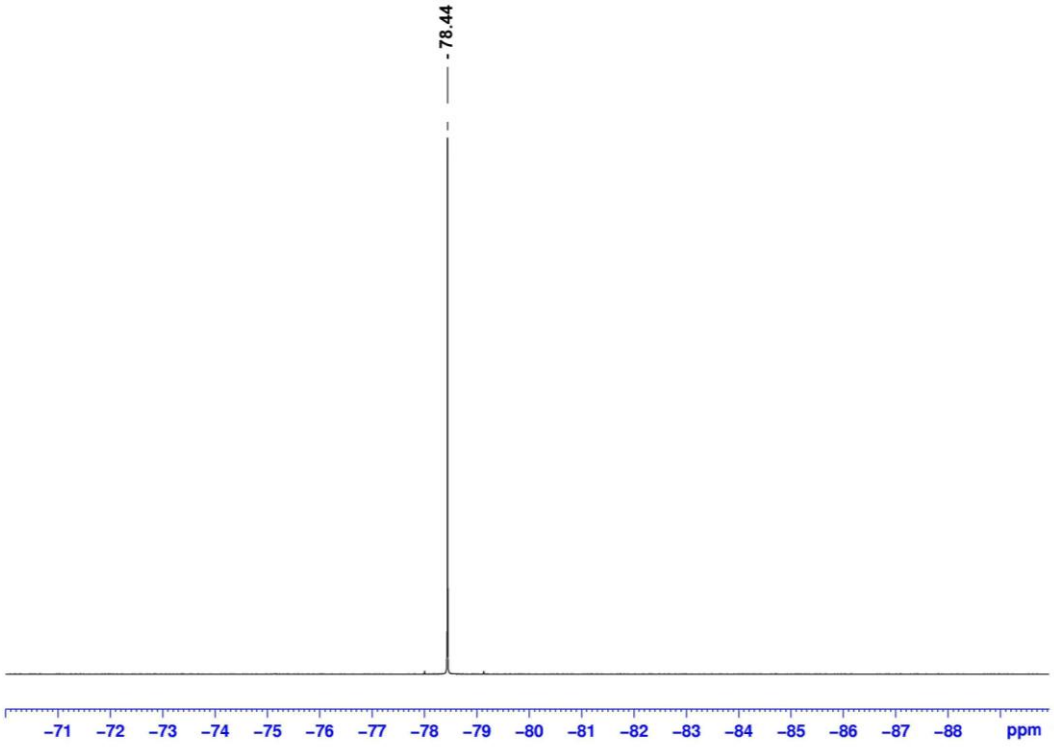

Figure 1: ^{19}F NMR spectrum of **15**

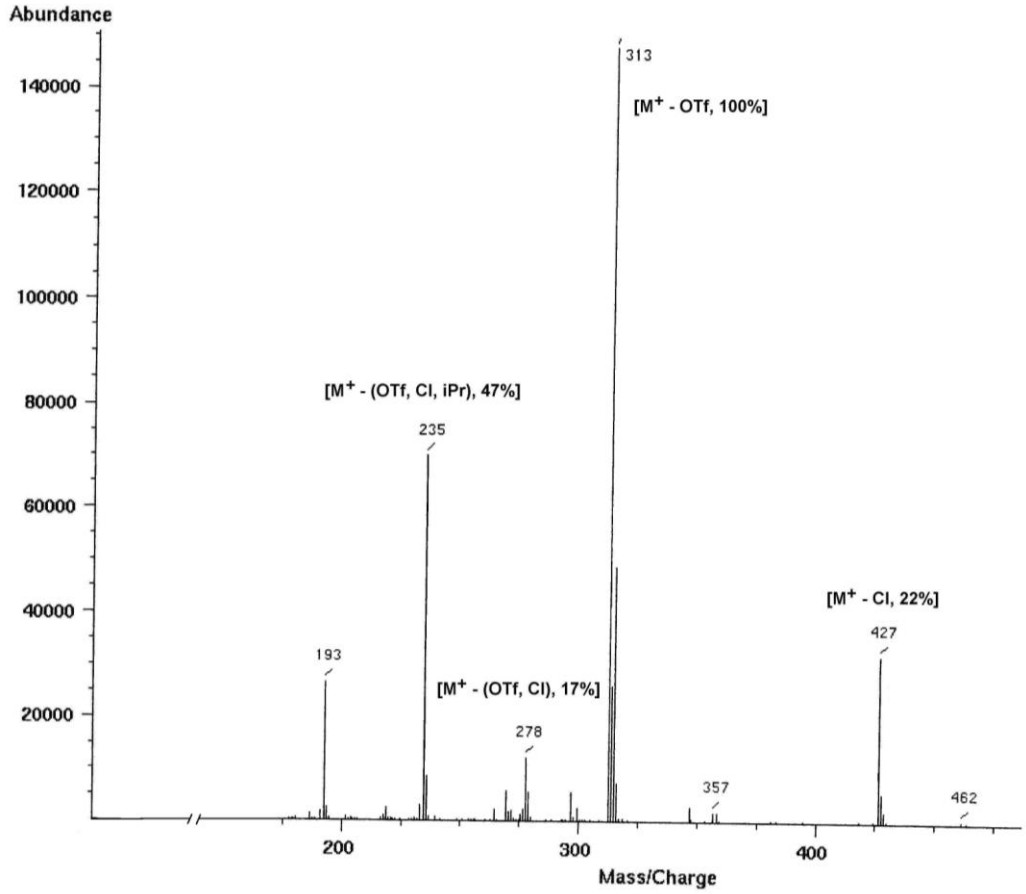

Figure 2: Mass spectrometry spectrum of **15**

Single crystals of **15** suitable for an X-ray crystallographic analysis were grown from dichloromethane solution at – 30 °C.

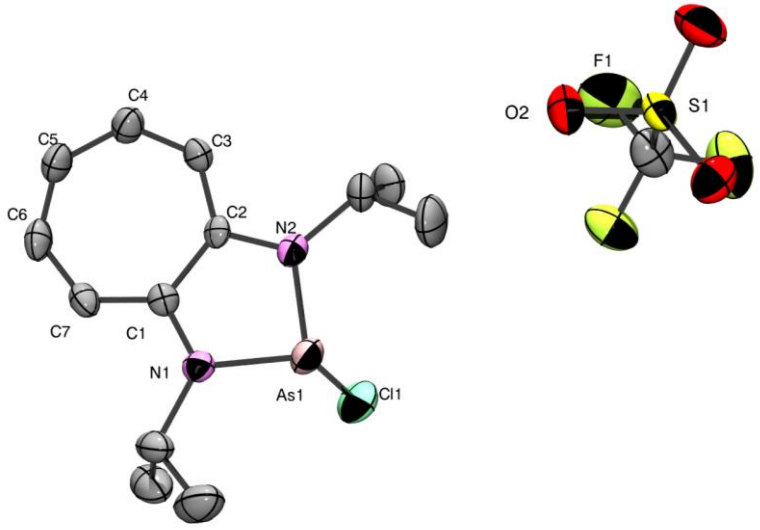

Figure 3: Molecular structure of **15** (50 % probability level for the thermal ellipsoids). All H atoms have been omitted for clarity. Selected bond distances [Å] and angles [°] are: As(1)-N(1) 1.837(4), As(1)-N(2) 1.840(4), As(1)-Cl(1) 2.2808(15), N(1)-C(1) 1.356(5), N(2)-C(2) 1.360(5), C(1)-C(7) 1.396(6), C(1)-C(2) 1.447(6), C(2)-C(3) 1.396(6), C(3)-C(4) 1.385(6), C(4)-C(5) 1.393(7), C(5)-C(6) 1.371(7), C(6)-C(7) 1.390(7); N(1)-As(1)-N(2) 84.77(16), N(1)-As(1)-Cl(1), 99.44(12), N(2)-As(1)-Cl(1) 98.63(12), C(1)-N(1)-As(1) 115.5(3), C(2)-N(2)-As(1) 114.9(3).

The molecular representation (Figure 3) shows the formation of well-separated N,N'-chelated arsenium cation and triflate anion, the nearest distance between the F^- atom of the anion and the hydrogen atom of the *i*Pr group of the cation being 2.729 Å. The shortest distance between the triflate anion and the arsenic atom is 6.910 Å. The three-coordinated arsenic atom adopts a pyramidal geometry (the sum of the angles are 282.8°), with the bonded chlorine atom in approximately orthogonal position in relation to the heterobicyclic plane. The As-N bond lengths (average 1.839 Å) in **15** are very similar to those reported in cyclic diaminoarsenium species[3-4]. The bond length of As-Cl (2.2808(15) Å) compares well with that obtained for chloroarsine containing a diaminonaphthalene ligand (2.2820(8) Å)[5] and is close to the sigma bond value for {tBu $N(CH_2)_2$tBu}AsCl (2.375 Å)[6]. The N-heterobicyclic unit is almost perfectly planar confirming the high degree of delocalization.

2.2 Oxidative reactions with dimethylsulfoxide, sulfur and selenium

We first tried a reaction with DMSO. The addition of a stoichiometric amount of DMSO at room temperature leads to the formation of oxidation product **18** after removal of dimethyl sulfide. As previously described in the literature for chlorophosphines[7] a side reaction of hydroxylation was observed in the presence of an excess of DMSO (Scheme 2). The hydroxyoxophosphonium cation **19**, obtained by this way, is very sensitive to hydrolysis and rapidly evolves towards the formation of aminometaphosphonate **20** whose structure was determined by X-ray diffraction.

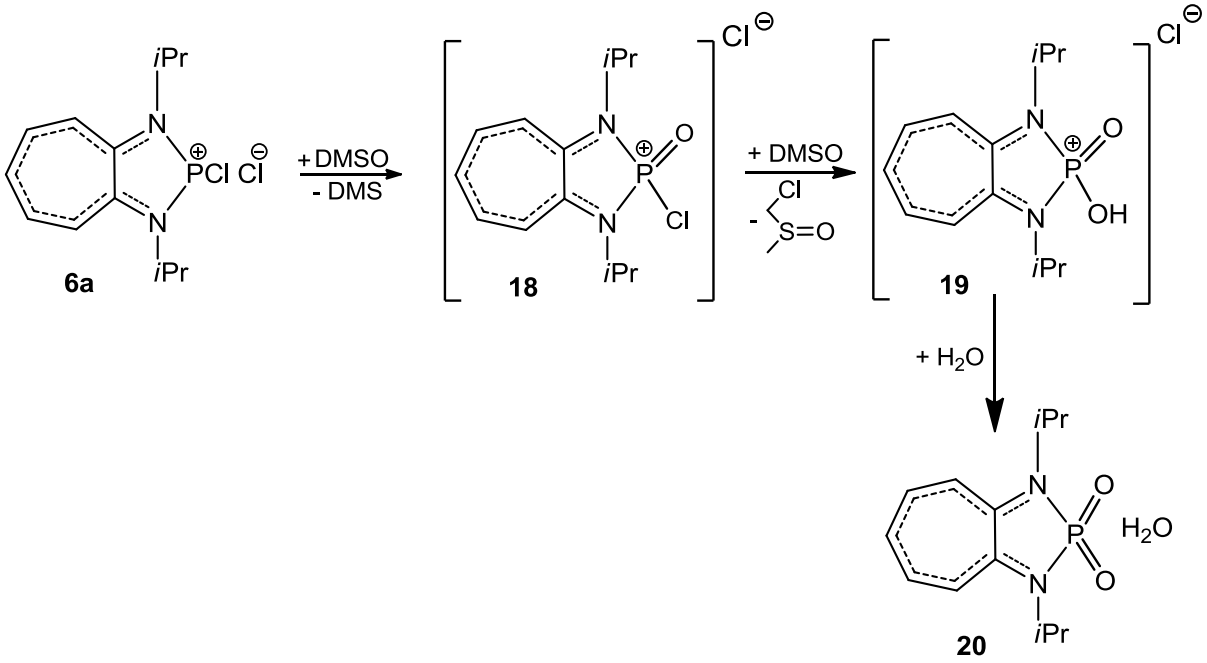

Scheme 2

In ^{31}P NMR spectra, chemical shifts are in the field of phosphine oxides and very slight differences of chemical shifts were observed: 13.40, 6.81 and 4.00 ppm for **18**, **19** and **20** respectively.

We also tried another route to prepare the phosphorus oxide **18** starting from phosphoryl chloride (Equation 1). No dehydrochloride coupling reaction was observed using triethylamine even under heating.

When using the metallation reaction with *n*BuLi, the ^{31}P NMR spectrum indicates the disappearance of the phosphoryl chloride and the formation of small amounts of oxide (4.33 ppm) probably the compound **20**. The ^{1}H NMR spectrum of the mixture showed the presence of the starting ligand **2** (76 %) and the corresponding salt **12** (24 %).

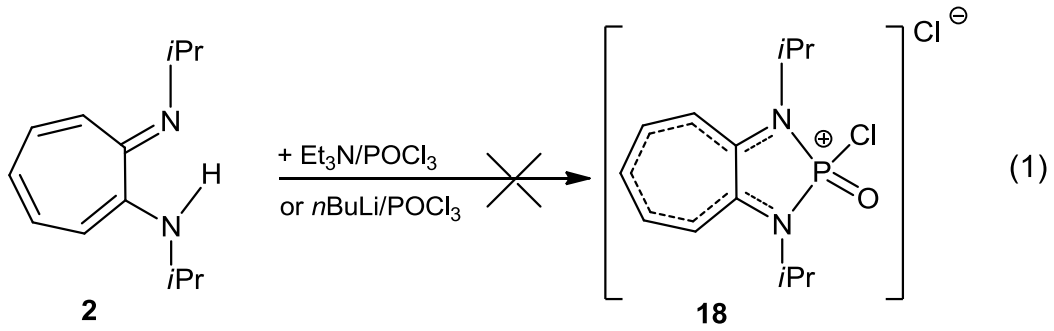

The oxidation reaction with sulfur seems more difficult and was only observed at dichloromethane reflux for 14 hours. The dichlorothiophosphoryl intermediate compound could not be characterized in this case and evolved very rapidly towards hydroxythiophosphonium cation **21** whose structure was determined by X-ray diffraction (Scheme 3).

The same reaction carried out with selenium in chloroform at reflux gives the hydroxyselenophosphonium **22**.

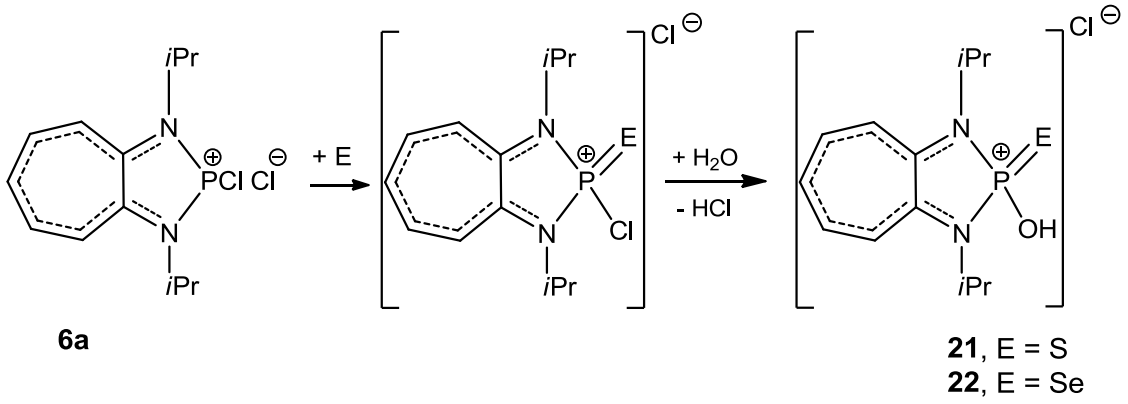

Scheme 3

Starting from hydroxyoxo- and hydroxythio-phosphonium **19** and **20**, the elimination of HCl was performed in the presence of a base such as Et_3N leading to the corresponding di-oxo- and thiooxophosphorane **20** and **23**. It should be noted that the reaction is reversible and that addition of HCl in diethyl ether gives again the hydroxy-derivatives (Equation 2). By contrast, the hydroxyselenophosphonium **22** does not react with Et_3N.

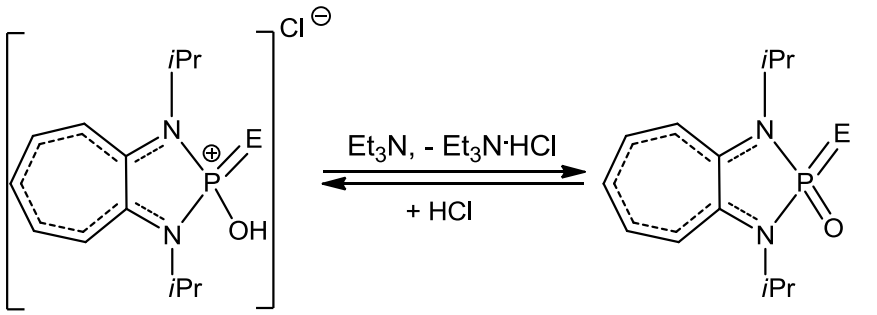

(2)

19, E = O
21, E = S

20, E = O
23, E = S

It must be underlined that compounds **20** and **23** are respectively the first examples of aminometaphosphonate and of its sulfur equivalent stabilized by intramolecular complexation. Several approaches have been tested to stabilize metaphosphonates (including their sulfur and selenium congeners) such as coordination to transition-metal centers. In this context, we have already reported the first ruthenium-stabilized monomeric metaphosphonate **XXI** (Chart 1)[8]. There are only few examples of phosphine-stabilized metaphosphonate and their sulfur and selenium analogs **XXII**, **XXIII** (Chart 1)[9-10]. The route we propose is easily to implement and the obtained products are not air sensitive.

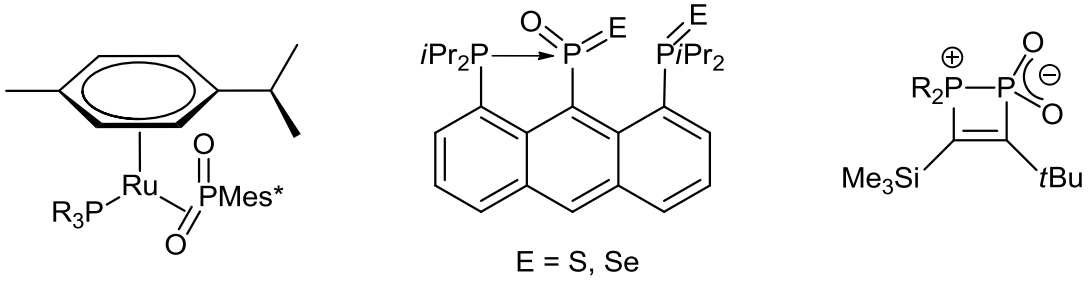

XXI **XXII** **XXIII**

Chart 1

All the compounds have been perfectly characterized spectroscopically. The ^{31}P NMR spectra of **21**, **22** and **23** display close signals at 59.04, 48.44 and 55.53 ppm, respectively. For the selenium derivative, we observe a singlet with satellites of selenium, due to the weak abundance of ^{77}Se (7.63 %)[11] with a coupling constant $^{2}J_{PSe}$ of 871 Hz (Figure 4a). This value corresponds to a coupling through a double bond (800-1200 Hz)[12]. In the ^{77}Se NMR spectrum (Figure 5), the signal at 46.00 ppm was too large to allow the measurement of the coupling constant with phosphorus atom. Moreover, the positive chemical shift suggests the predominant character of double bond without contribution of a dipolar mesomeric structure

(R_3P-Se ↔ R_3P^+ Se^-)[13]. Selenium also shows couplings to other nuclei, ^1H, ^{13}C. In the ^{13}C NMR spectrum, a coupling constant $^3J_{CSe}$ = 49.4 Hz can be seen (Figure 4b).

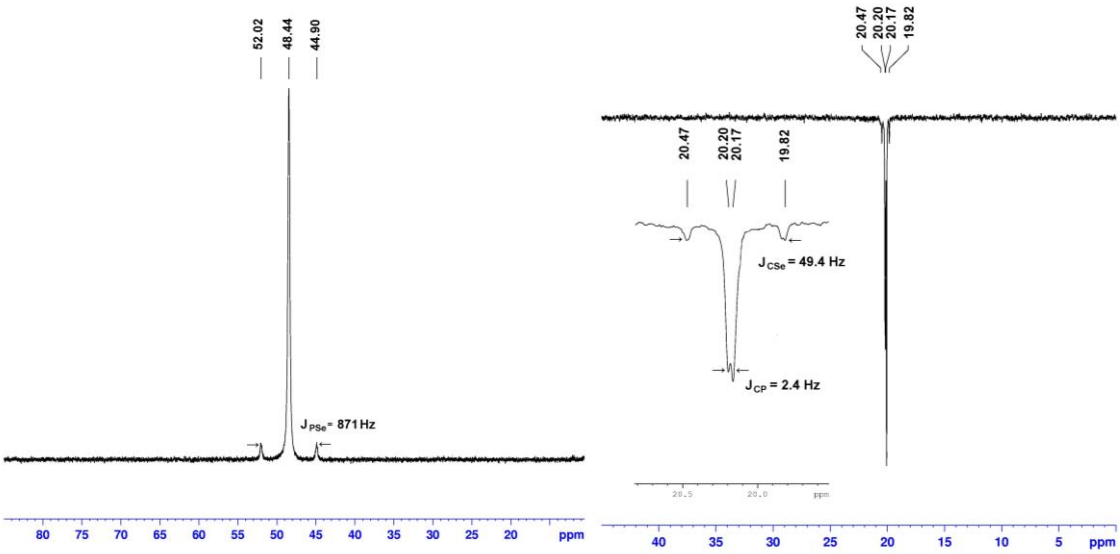

a) **b)**

Figure 4: ^{31}P (a) and ^{13}C NMR (b) spectra for compound **22**; in both cases the coupling constant with ^{77}Se can be observed

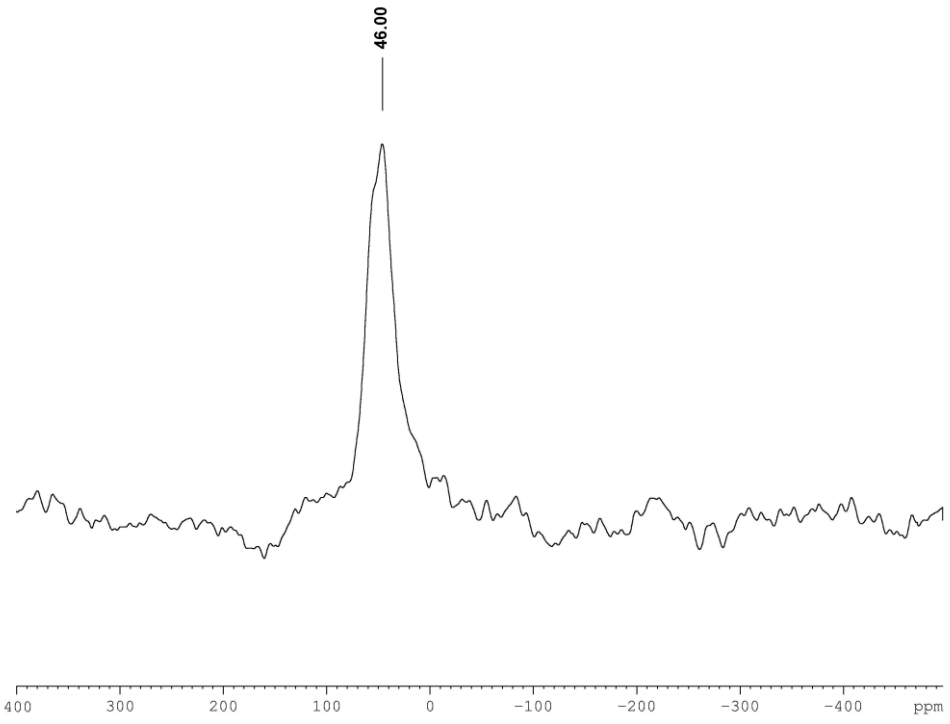

Figure 5: ^{77}Se NMR spectrum for compound **22**

Table 3: Proton NMR chemical shifts for **6a**, **18**, **19**, **20**, **22** and **23** (in ppm, J in Hz, in $CDCl_3$)

	CH_3	CH	H_5	$H_{4,6}$	$H_{3,7}$
6a	1.61 (d.d, $^3J_{HH}$ = 6.6, $^4J_{HP}$= 1.7)	4.77 (sept.d, $^3J_{HH}$ = 6.6, $^3J_{HP}$ = 10.9)	7.88 (t.d, $^3J_{HH}$ = 9.6, $^6J_{HP}$ = 3.4)	8.43 (t, $^3J_{HH}$ = 9.7)	8.55 (d.d, $^3J_{HH}$ = 11.0, $^4J_{HP}$ = 2.5)
18	1.52 (d, $^3J_{HH}$ = 6.7), 1.60 (d, $^3J_{HH}$ = 6.6)	4.80-5.10 (m)	8.00 (t, $^3J_{HH}$ = 9.6)	8.61 (t, $^3J_{HH}$ = 10.0)	8.84 (d, $^3J_{HH}$ = 10.9)
19	1.49 (d, $^3J_{HH}$ = 6.6)	4.35 (sept.d, $^3J_{HH}$ = 7.0, $^3J_{HP}$= 14.1)	7.46 (t, $^3J_{HH}$ = 9.5)	7.94 (t, $^3J_{HH}$ = 10.2)	7.60 (d, $^3J_{HH}$ = 10.9)
19*	1.42 (d, $^3J_{HH}$ = 6.6)	4.40 (sept.d, $^3J_{HH}$ = 6.7, $^3J_{HP}$ = 1.6)	7.39 (t.d, $^3J_{HH}$ = 9.4, $^6J_{HP}$ = 4.4)	7.86 (t.d, $^3J_{HH}$ = 9.5, $^4J_{HP}$ = 3.4)	7.39 (t.d, $^3J_{HH}$ = 9.4, $^6J_{HP}$ = 4.4)
21	1.68 (d, $^3J_{HH}$ = 6.9), 1.81 (d, $^3J_{HH}$ = 6.9)	4.58 (sept.d, $^3J_{HH}$ = 6.9, $^3J_{HP}$= 12.0)	7.31 (t, $^3J_{HH}$ = 9.6)	7.38 (d, $^3J_{HH}$ = 11.1)	7.75 (t, $^3J_{HH}$ = 10.0)
22	1.64 (d, $^3J_{HH}$ = 6.8), 1.77 (d, $^3J_{HH}$ = 6.8)	4.64 (sept, $^3J_{HH}$ = 6.3)	7.26 (t, $^3J_{HH}$ = 9.3)	7.36 (d, $^3J_{HH}$ = 10.4)	7.76 (t, $^3J_{HH}$ = 10.1)
20	1.60 (d, $^3J_{HH}$ = 6.6)	4.23 (sept.d, $^3J_{HH}$ = 6.6, $^3J_{HH}$ = 13.2)	7.04-7.14 (m, C_7H_5), 7.59 (t, $^3J_{HH}$ = 10.4, C_7H_5)		
23	1.66 (d, $^3J_{HH}$ = 6.9), 1.79 (d, $^3J_{HH}$ = 6.9)	4.52 (sept.d, $^3J_{HH}$ = 6.9, $^3J_{HP}$= 12.0)	7.07 (t, $^3J_{HH}$ = 10.0)	7.14 (d, $^3J_{HH}$ = 11.2)	7.56 (t, $^3J_{HH}$ = 10.8)

* recorded in DMSO-d6

Table 4: Carbon-13 NMR chemical shifts for **6a**, **18**, **19**, **20**, **22** and **23** (in ppm, J in Hz, in $CDCl_3$)

	CH_3	CH	C_5	$C_{4,6}$	$C_{3,7}$	$C_{2,8}$
6a	21.89 (d, $^3J_{CP}$ = 12.6)	50.91 (d, $^2J_{CP}$ = 12.6)	136.99 (d, $^5J_{CP}$ = 5.0)	144.56 (d, $^4J_{CP}$ = 5.7)	127.83 (d, $^3J_{CP}$ = 5.7)	155.57 (d, $^2J_{CP}$ = 12.7)
18	19.80 (d, $^3J_{CP}$ = 1.9), 21.24 (d, $^3J_{CP}$ = 1.3)	51.55 (d, $^2J_{CP}$ = 3.3)	139.14	146.82	128.19 (d, $^3J_{CP}$ = 9.8)	149.91 and 150.14
19	20.37	49.30 (d, $^2J_{CP}$ = 3.8)	132.55	142.83	120.93 (d, $^3J_{CP}$ = 8.6)	150.59 (d, $^2J_{CP}$ = 16.0)
21	20.61	47.21	131.63	142.30	120.63 (d, $^3J_{CP}$ = 9.1)	151.55 (d, $^3J_{CP}$ = 10.7)
22	20.20 ($^3J_{CP}$ = 2.4, $^4J_{CSe}$ = 49.4)	49.32	132.17	141.87 (d, $^4J_{CP}$ = 6.4)	120.76 (d, $^3J_{CP}$ = 6.6)	150.67 (d, $^2J_{CP}$ = 4.8) and150.80 (d, $^2J_{CP}$ = 5.0)
20	20.28	48.61 (d, $^2J_{CP}$ = 4.2)	127.90	140.47	116.76 (d, $^3J_{CP}$ = 7.4)	150.54 (d, $^2J_{CP}$ = 139)
23	20.20	48.86 (d, $^2J_{CP}$ = 5.9)	128.74	140.55	117.89 (d, $^3J_{CP}$ = 6.5)	150.83 (d, $^2J_{CP}$ = 10.7)

The ^{1}H and ^{13}C{^{1}H}NMR spectra of compounds **18** - **23** show the expected set of signals for the (*i*Pr$_2$ATI) ligand. The ^{1}H NMR spectra of all these compounds display three well-separated signals which correspond to H_5, $H_{4,6}$ and $H_{3,7}$, except **20** for which we cannot distinguish the signals for the aromatic system. The methyl groups of the isopropyl substituents of **18**, **21**, **22** and **23** appear as two sets of doublets in the ^{1}H NMR spectrum suggesting different environments for the methyl groups. This is perhaps due to the asymmetry caused by the Cl atom for **18**, OH group for **21** and **22** in the pnictogenium atom. Noticeable, methyl groups of **19** and **20**, which contain oxygen and hydroxyl groups, appear as only one doublet. The signals of the isopropyl C*H* proton of **19**, **21**, **22** and **23** are well

resolved into a septuplet and show only a slight upfield shift [δ = 4.23 (**20**), 4.35 (**19**), 4.58 (**21**), 4.64 (**22**), 4.52 (**23**) ppm] compared to that of the departing phosphenium cation **6a** (δ = 4.77 ppm)[14].

The aromatic protons follow the same upfield trend indicating a weaker degree of delocalization of the electrons in the system. It can be noticed that with decreasing of ^{31}P NMR chemical shift from 13.40 to 4.00 for compounds **18**, **19** and **20** and from 59.04 to 55.53 ppm for compounds **21** and **23**, the shielding increases for the aromatic protons, the same observation being valid for the aromatic carbons as well. That seems in agreement with more associated structures. In Tables 3 and 4 are listed the chemical shift for **6a**, **18**, **19**, **20**, **22** and **23**.

Noticeable, when the ^{1}H NMR spectrum for **19** is recorded in DMSO all the coupling constants between aromatic protons and phosphorus, even the long coupling constant between H_5 - P, can be observed ($^{6}J_{HP}$ = 4.4 Hz).

A slow crystallization at low temperature in dichloromethane allowed the isolation of crystals of compounds **21** and **22** (Figures 6 and 7).

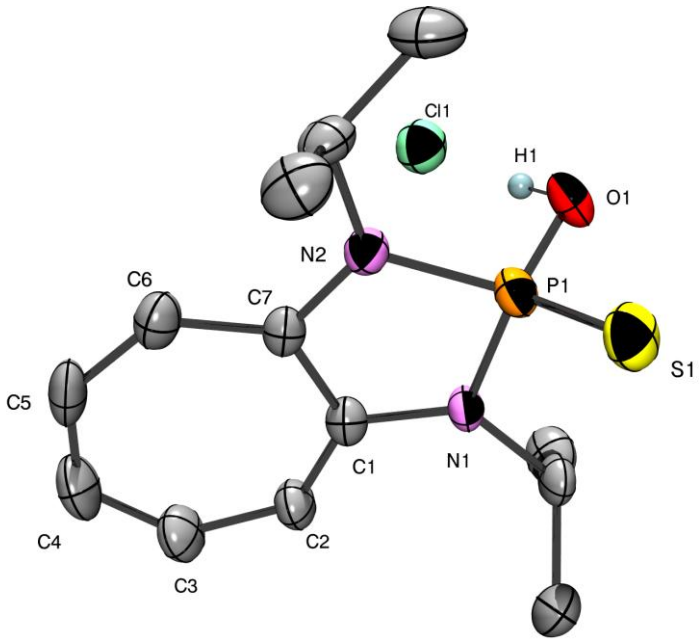

Figure 6: Molecular structure of **21** (50 % probability level for the thermal ellipsoids). All H (except H1) atoms have been omitted for clarity. Selected bond distances [Å] and angles [°] are: N(1)-P(1) 1.694(3), N(2)-P(1) 1.699(3), P(1)-O(1) 1.542(3), P(1)-S(1) 1.9147(16), O(1)-H(1) 0.8400, C(1)-N(1) 1.353(5), C(1)-C(2) 1.393(5), C(1)-C(7) 1.456(5), C(2)-C(3) 1.379(5), C(3)-C(4) 1.381(6), C(4)-C(5) 1.372(6), C(5)-C(6) 1.396(6), C(6)-C(7) 1.389(5);

O(1)-P(1)-N(1) 107.76(16), O(1)-P(1)-N(2) 109.85(17), N(1)-P(1)-N(2) 90.67(16), O(1)-P(1)-S(1) 112.68(12), N(1)-P(1)-S(1) 115.67(13), N(2)-P(1)-S(1) 118.02(13), P(1)-O(1)-H(1) 109.5.

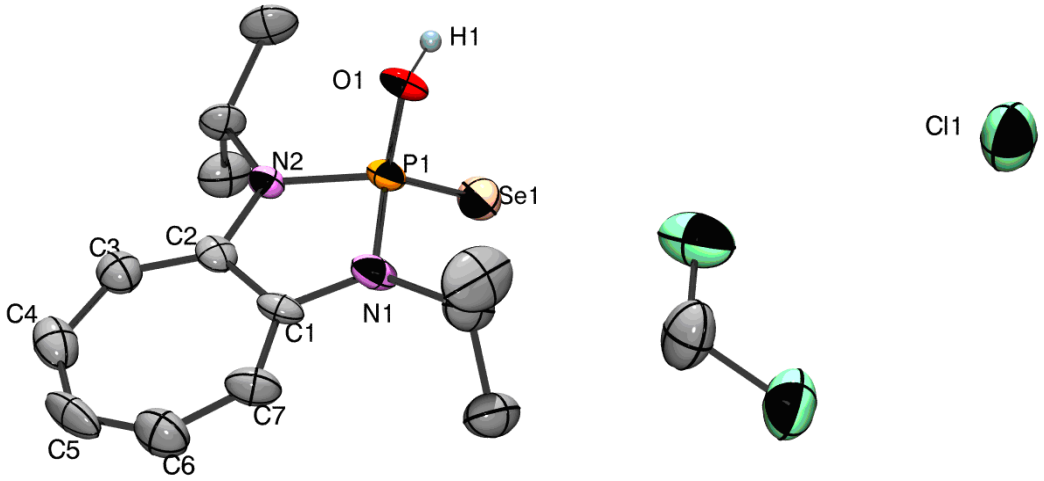

Figure 7: Molecular structure of **22** (50 % probability level for the thermal ellipsoids). All H (except H1) atoms have been omitted for clarity. Selected bond distances [Å] and angles [°] are: P(1)-O(1) 1.516(4), P(1)-N(1) 1.701(6), P(1)-N(2) 1.709(5), P(1)-Se(1) 2.0840(19), N(1)-C(1) 1.358(8), N(2)-C(2) 1.369(8), C(1)-C(7) 1.385(9), C(1)-C(2) 1.471(9), C(2)-C(3) 1.382(9), C(3)-C(4) 1.408(10), C(4)-C(5) 1.386(11), C(5)-C(6) 1.360(11), C(6)-C(7) 1.358(10); O(1)-P(1)-N(1) 106.5(3), O(1)-P(1)-N(2) 109.0(3), N(1)-P(1)-N(2) 90.1(3), O(1)-P(1)-Se(1) 117.07(19), N(1)-P(1)-Se(1) 114.8(2), N(2)-P(1)-Se(1) 115.96(19).

The study of their structures by X-ray diffraction shows that there is no interaction between the cationic phosphorus species and the chloride anion, the shorter P-Cl distances being 3.757 Å and 8.500 Å for **21** and **22**, respectively. The OH group of the cation is hydrogen-bonded to the chloride anion with a distance of 2.031 Å for the sulfur compound while there is no interaction for the selenium compound. This may explain the different behavior of these hydroxyphospheniums towards triethylamine, particularly the lack of reactivity of **22**. The heterobicyclic system is almost planar with P-N bond distances (1.694 and 1.699, 1.701 and 1.709 Å for **21** and **22**, respectively) comparable to those observed for **6a** [1.6969(13) and 1.7075(13) Å].

The phosphorus atom is four-coordinate with small N-P-N angles (90.67 and 90.1°) due to the N-chelation of the ligand. The P-OH bond lengths [1.542(3) and 1.516(4) Å for **21** and **22**, respectively] are in the range of P-OH distances (1.503-1.611 Å)[15-17]. The bond lengths of P=S [1.9147(16) Å] and P=Se [2.0840(19) Å] correspond to the double bond values (1.954 Å for $Ph_3P=S$[18] and 2.057 Å, which is the average for P=Se[9]).

For compounds **20** and **23** (Figures 8 and 9), the main structural features are the quasi planarity of the bicyclic system and the presence of tetracoordinate phosphorus atoms. Note, however, slightly longer P-N bond distances [1.7198(15) and 1.7269(17) Å for **20**, 1.7300(16) and 1.7379(15) Å for **23**] compared to those obtained in the starting phosphenium cation. The second important point is the environment of the phosphorus atom and the nature of the bonds with the elements of group 16, oxygen and sulfur. In both cases, the bond lengths of phosphorus-oxygen [1.4674(16), and 1.4773(15) Å for **20** and 1.4764(15) Å for **23**] are slightly shorter than the P=O bond in phosphine-stabilized sulfur analogues of metaphosphonates (Chart 1, compound **XXII**) [1.495(1) Å][9] and that in $Ph_3PO{\cdot}H_2O$ [1.482(3) Å][19]. In the same manner, the P=S bond length [1.9442(7) Å] is shortened compared to those in compound **XXII** [1.9575(8) Å] and in Ph_3PS [1.9545(9) Å][18]. In addition compound **20** has a water molecule in the lattice which is involved in a hydrogen bonding interaction with one oxygen of the PO_2 fragment (1.965 Å, distance within the sums of the respective van der Waals radii: H, 1.20; O, 1.52)[20-21]. Water acts as a bridge with two molecules in the same way as described for the silver complex of bis(pyrazol-1-yl) phosphinate[22].

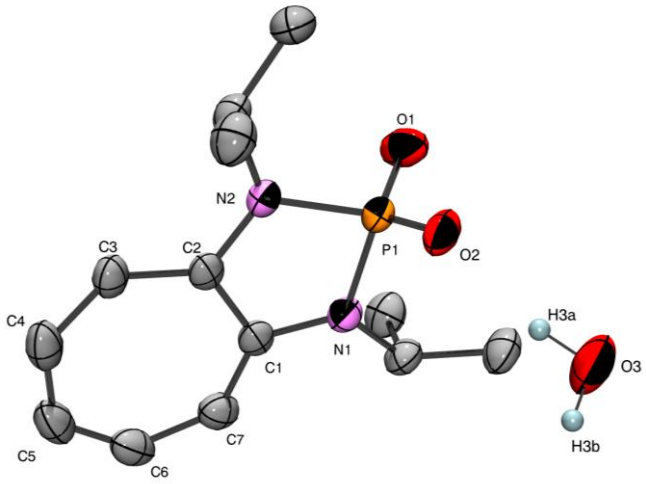

Figure 8: Molecular structure of **20** (50 % probability level for the thermal ellipsoids). All H (except H from H_2O) atoms have been omitted for clarity. Selected bond distances [Å] and angles [°] are: P(1)-O(1) 1.4674(16), P(1)-O(2) 1.4773(15), P(1)-N(1) 1.7269(17), P(1)-N(2) 1.7198(15), C(1)-C(2) 1.463(3), C(2)-C(3) 1.402(3), C(3)-C(4) 1.390(3), C(4)-C(5) 1.380(3), C(5)-C(6) 1.386(3), C(6)-C(7) 1.383(3), C(1)-C(7) 1.400(3); O(1)-P(1)-O(2), 119.81(10), O(1)-P(1)-N(2) 112.26(8), O(2)-P(1)-N(2) 109.40(8), O(1)-P(1)-N(1) 109.70(9), O(2)-P(1)-N(1) 112.15(8), N(2)-P(1)-N(1) 89.43(8), C(1)-N(1)-P(1) 114.29(13), C(2)-N(2)-P(1), 114.39(13).

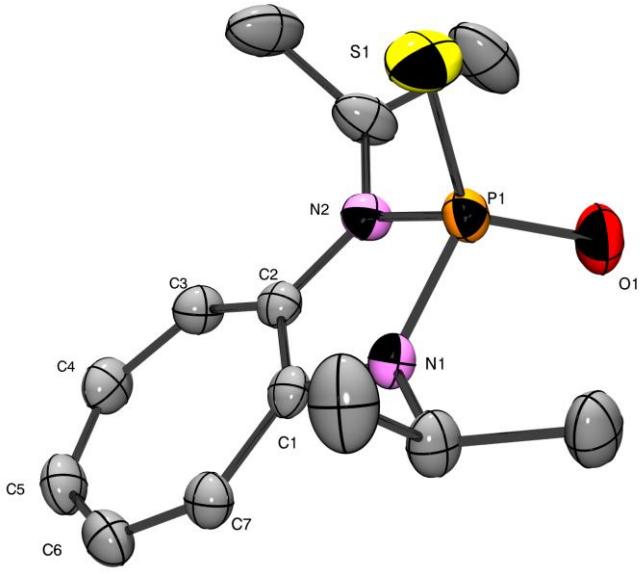

Figure 9: Molecular structure of **23** (50 % probability level for the thermal ellipsoids). All H atoms have been omitted for clarity. Selected bond distances [Å] and angles [°] are: P(1)-O(1) 1.4764(15), P(1)-N(2) 1.7300(16), P(1)-N(1) 1.7379(15), P(1)-S(1) 1.9442(7), C(1)-C(7)

1.404(2), C(1)-C(2) 1.454(2), C(2)-C(3) 1.404(2), C(3)-C(4) 1.386(3), C(4)-C(5) 1.379(3), C(5)-C(6) 1.386(3), C(6)-C(7) 1.391(3); O(1)-P(1)-N(2) 111.40(9), O(1)-P(1)-N(1) 110.79(8), N(2)-P(1)-N(1) 88.54(7), O(1)-P(1)-S(1) 120.34(7), N(2)-P(1)-S(1) 109.86(6), N(1)-P(1)-S(1) 111.40(6).

No reaction between tellurium and **6a** was observed under similar reaction conditions.

All these oxidative reactions with chlorophophenium cation supported by aminotroponate ligand **7a** appeared to be more difficult because of its lower stability in solution and thermally.

The oxidation of **7a** with DMSO occurs very rapidly giving a new product which displays a ^{31}P NMR signal at 4 ppm in the typical region of the phosphorus oxides. However, due to the fast decomposition, the new phosphorus oxide could not be characterized by X-ray crystallography; so the real structure remains unknown. The decomposition product **24** was identified as the ligand salt of **1** (Scheme 4).

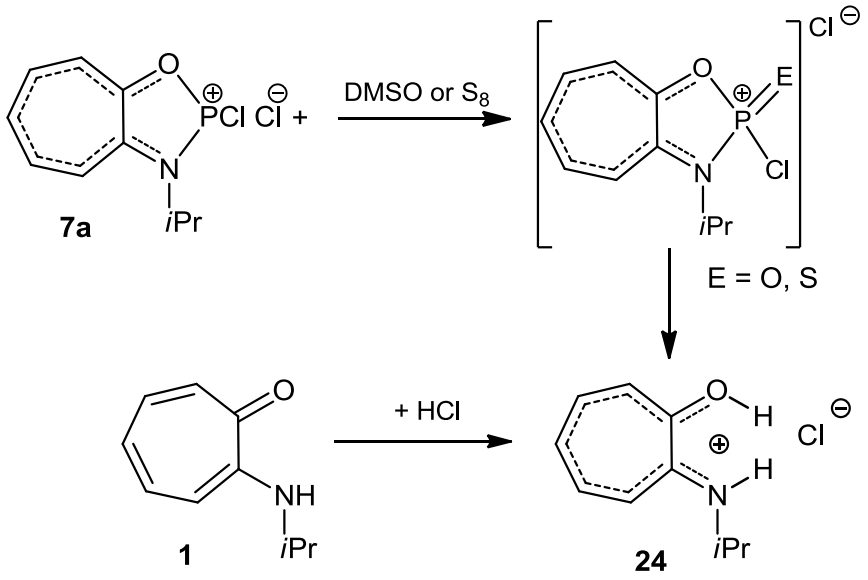

Scheme 4

The oxidative addition of elemental sulfur to **7a** goes slowly. After 8 h of reaction at 40 °C the ^{31}P RMN spectrum shows a total conversion of the starting product and a new signal at 60 ppm appears which could be the equivalent compound of **21**, but in the same time the ^{1}H RMN spectrum showed other products including the ligand salt **24**. This later was synthesized by adding aminotropone to stoichiometric quantity of hydrochloric acid in Et_2O and characterized by ^{1}H and ^{13}C NMR spectrometries.

By contrast, the arsenium analogues **8** and **9** proved to be unreactive towards these oxidizing reactants.

2.3 Cycloaddition reaction with *o*-quinone

One of the characteristic reactions of phospheniums is the cycloaddition reaction with dienes in which they behave as dienophiles[23]. In fact, for phospenium cation **6a**, no reaction was observed with dimethylbutadiene, whatever the experimental conditions used (in dichloromethane solution[24-25] or in a sealed tube at 100 °C[26]).

When we tried a reaction with glyoxal-bis-(2,4,6-trimethylphenyl)imine, the ^{31}PNMR spectrum revealed a new signal at 30.88 ppm but we were unsuccessful in identifying this product.

By contrast, an immediate reaction was observed with 3,5-di-*tert*-butyl-1,2-benzoquinone at room temperature.

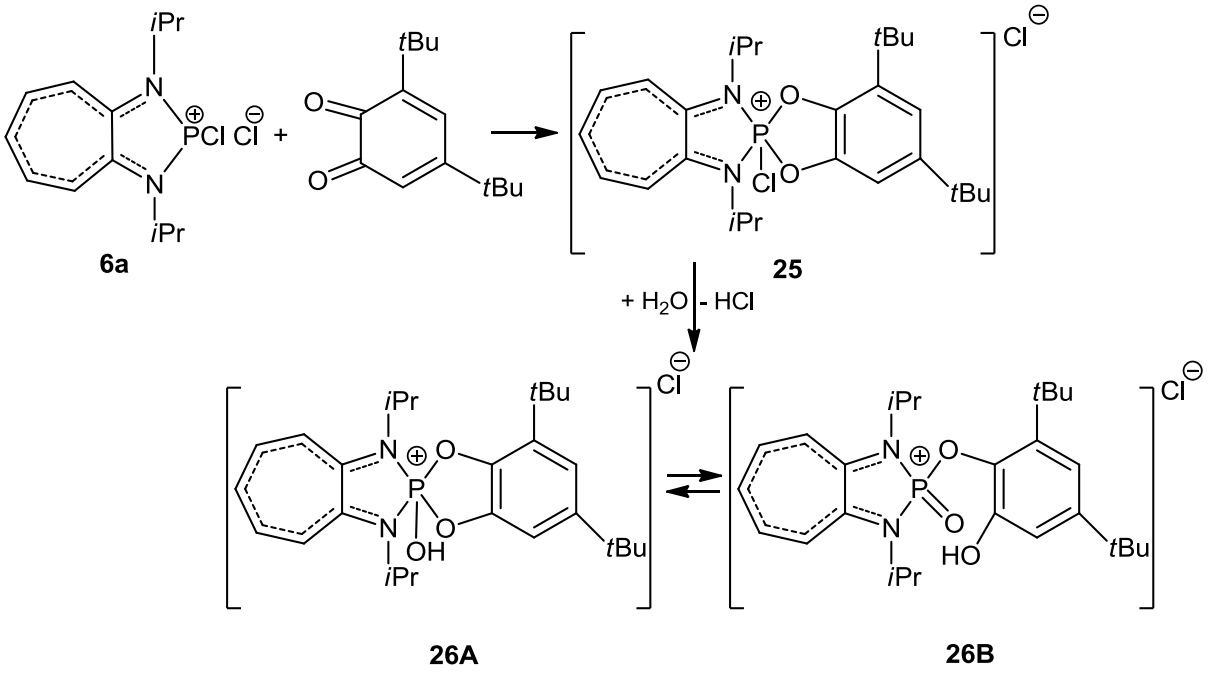

Scheme 5

When a solution of *o*-quinone in CH_2Cl_2 is slowly added to a solution of **6a** in the same solvent at room temperature, a slow discoloration of the quinone solution can be noticed. The reaction is monitored by ^{31}P NMR and shows the formation of a single product at 7.83 ppm which could then be easily isolated after evaporation of the solvent and identified as **25**

(Scheme 5). Compound **25** is extremly sensitive to hydrolysis in solution and rapidly gives the corresponding hydroxy compound **26A**. It has been shown in literature[27] that such hydroxyphosphoranes were in equilibrium with their phosphate ester form **26B** and that this balance would be shifted to the B form in the presence of an acid. In our case, hydrolysis of compound **25** would release HCl which could serve as a catalyst in shifting the equilibrium towards the form **26B**. A slow crystallization in CH_2Cl_2 at -30 °C gave suitable crystals for X-ray analysis which confirms the presence of the form **26B** in the solid state (Figure 10).

The ^{1}H NMR spectrum for the two phosphorus cycloadducts shows all the protons are more deshielded for **25** if compared with **26B**; the same conclusion can be drawn for the quinonic system which is in agreement with the chemical shifts in ^{31}P NMR (7.83 for **25** and - 3.33 ppm for **26B**). For carbon signals the same effect was seen.

In the mass spectrum, the presence of the fragment peak $[M^+ - 1]$ was found in the case of **26B** at 506 amu while for **25** only the $[M^+ - Cl + H]$ at 490 amu was observed.

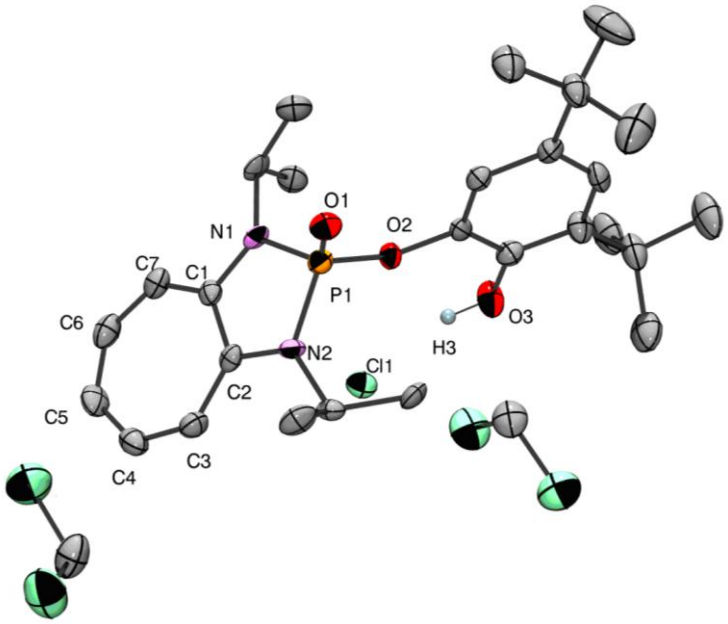

Figure 10: Molecular structure of **26B** (50 % probability level for the thermal ellipsoids). All H (except H3) atoms have been omitted for clarity. Selected bond distances [Å] and angles [°] are: P(1)-O(1) 1.456(3), P(1)-O(2) 1.568(3), P(1)-N(1) 1.667(4), P(1)-N(2) 1.669(4), N(1)-C(1) 1.384(5), N(1)-C(8) 1.498(5), C(1)-C(7) 1.380(6), C(1)-C(2) 1.440(6), C(2)-C(3) 1.407(6), C(3)-C(4) 1.375(6), C(4)-C(5) 1.382(6), C(5)-C(6) 1.381(6), C(6)-C(7) 1.384(6); O(1)-P(1)-O(2) 115.05(18), O(1)-P(1)-N(1) 120.62(18), O(2)-P(1)-N(1) 101.95(18), O(1)-

P(1)-N(2) 115.43(19), O(2)-P(1)-N(2) 108.67(18), N(1)-P(1)-N(2) 92.20(19), C(1)-N(1)-P(1) 113.2(3), C(2)-N(2)-P(1) 113.1(3).

The molecular structure of **26B** is shown in Figure 10. No interaction was detected between the phosphorus atom and the chloride anion (P^+....Cl^-, 3.920 Å) and the two heterocycles are almost in the same plane. The phosphorus atom is tetracoordinate. The P-O bond length (1.568 Å) is comparable to those observed for the hydroxy compounds **21** and **22** and corresponds to a covalent bond. The P=O bond length (1.456 Å) is very close to the value of the standard P=O double bond of compound **20**. The quinonic system lies in a plane perpendicular to the heterocyclic in order to limit the steric constraints.

The same reaction was much more complex in the case of phosphenium cation **7a**. The ^{31}P NMR spectrum of the reaction mixture showed the presence of two products which display resonances at 13.05 ppm (predominant) which could correspond to the product of monocycloaddition and at - 89.19 ppm corresponding to the product of dicycloaddition. The analysis by mass spectrometry reveals the presence of two molecular ion peaks at 449 and 633, respectively, corresponding to the mono- and di-cycloadducts.

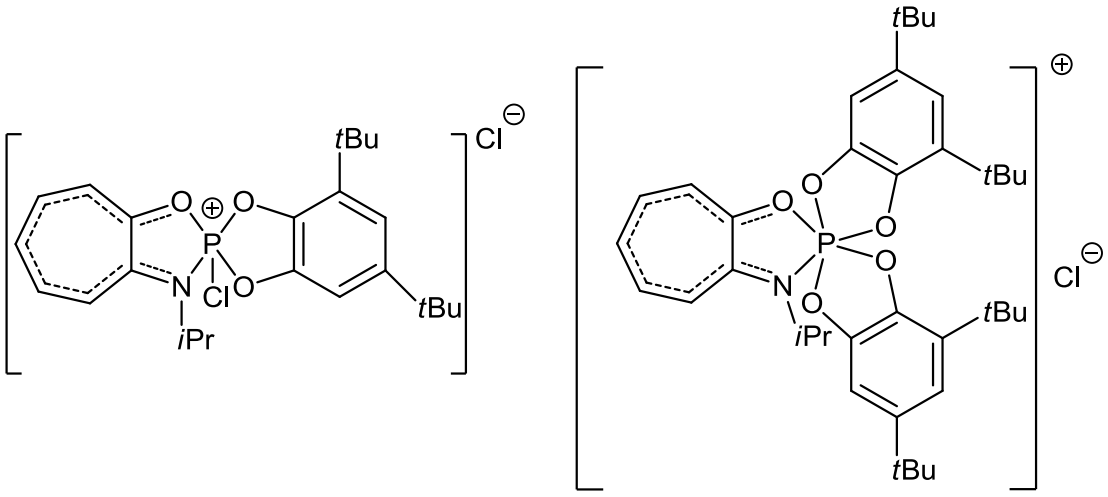

No reaction between 3,5-di-*tert*-butyl-1,2-benzoquinone and the arsenium compound **8** was observed under similar reaction conditions.

2.4 Complexation with transition metals

Thanks to a high-lying phosphorus lone-pair orbital (HOMO-1), the phosphenium cation **6a**, can behave as valuable ligand for metal-transition complexation. To evaluate its ability, we tried a test with a tungsten complex.

The $W(CO)_5THF$ complex was prepared by UV-photolysis of a THF solution of $W(CO)_6$ with a 300 W high-pressure Hg lamp for 2 h at room temperature. The photogeneration reaction of $M(CO)_5L$ from $M(CO)_6$ has been extensively studied. These 16-electron $M(CO)_5$ fragments react avidly with any available donor atom[28]. The reaction was performed using stoichiometric amount of cation **6a** and complex $W(CO)_5THF$ in THF at room temperature (Scheme 6) and led to a mixture of complex **27** and its hydroxyl analogue **28** which were perfectly characterized by NMR analyses. A slow crystallization in deuterated chloroform solution at room temperature gave brown crystals identified to complex **28** by X-ray analysis.

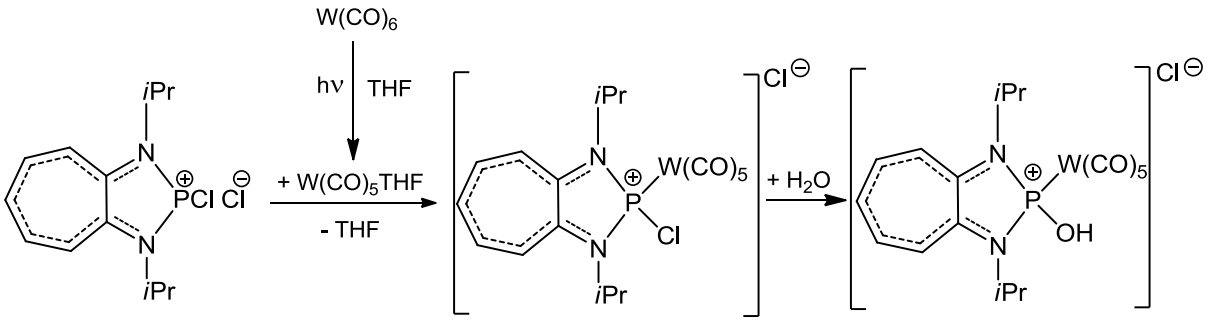

6a **27** **28**

Scheme 6

The ^{31}P NMR spectra show two resonances at 150.03 and 128.65 ppm accompanied by satellites of tungsten with coupling constants J_{WP} = 385 and 386 Hz for **27** (75 %) and **28** (25 %) respectively (Figure 11 and 12). These values are lower than those previously observed for the similar complex $[\{(C_5Me_5)(t\text{BuNH})P\}W(CO)_3(MeCN)_2\}]^+$ $AlCl_4^-$ (404 Hz)[29] and seem to indicate a small π character. Indeed, a very large constant (847 Hz) was reported in complexes with tungsten-phosphorus double bond such as $Cp(CO)_2W{=}P[OC(CH_3)_2\text{-}C(CH_3)_2O]$[30].

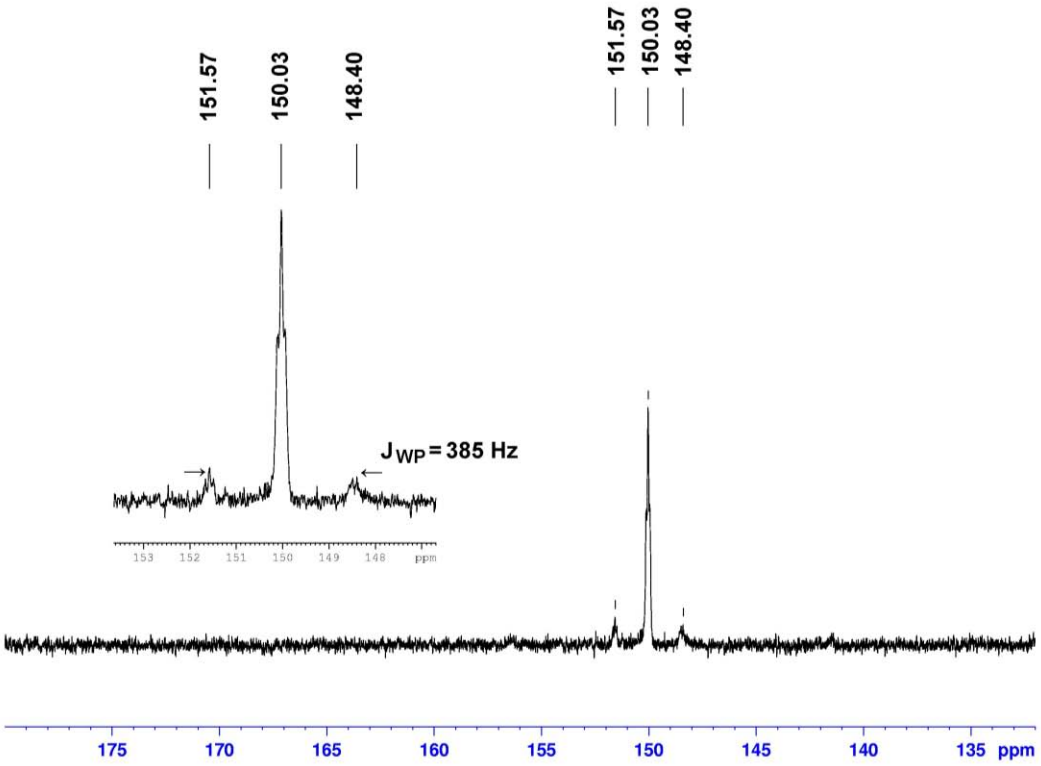

Figure 11: ^{31}P NMR spectrum for compound **27**

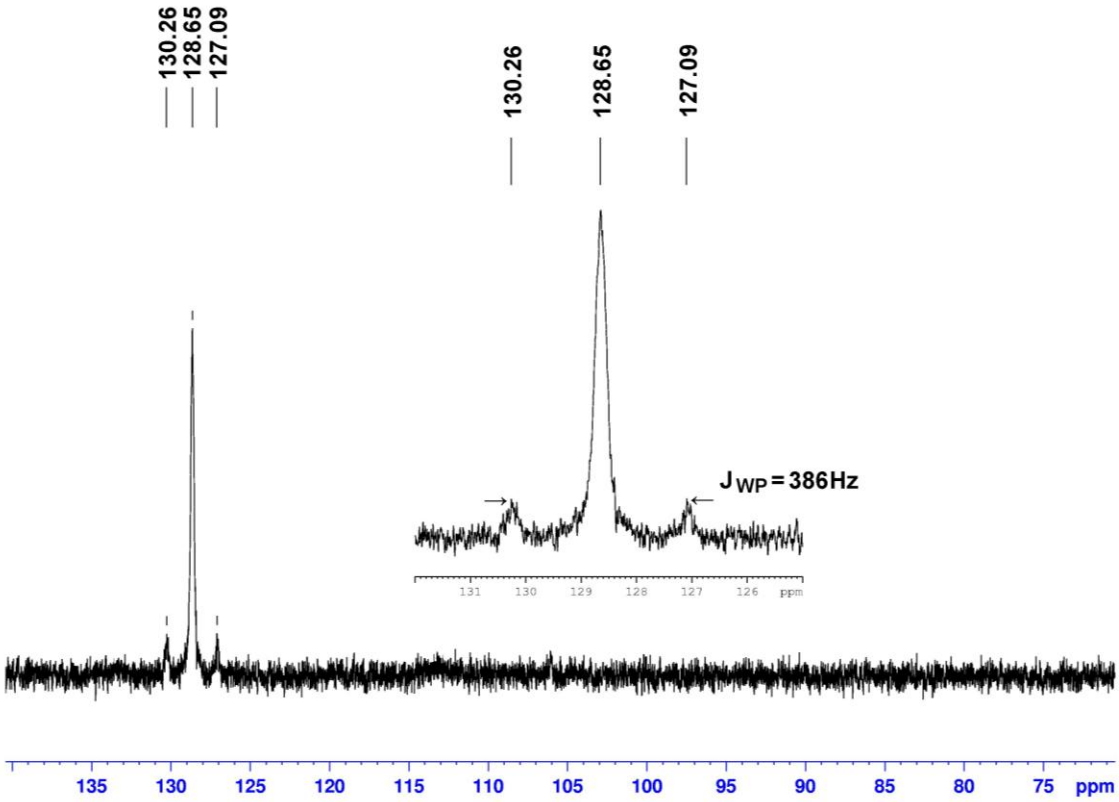

Figure 12: ^{31}P NMR spectrum for compound **28**

Due to the great resemblance of these two transition metal complexes, both ^{1}H and ^{13}C NMR spectra show nearly identical signal, but shielded for aromatic system compared with **6a**.

Each ^{13}C NMR spectra of **27** and **28** show two sharp resonances at low field of relative intensity 1:4, belonging to the axial and equatorial carbonyl groups which are split by C-P coupling constant (201.76, $^{2}J_{CP}$ = 8.5 Hz, 204.02, $^{2}J_{CP}$ = 6.2 Hz (Figure 13) and 195.20 $^{2}J_{CP}$ = 9.3 Hz, 196.18 $^{2}J_{CP}$ = 8.6 Hz for **27** and **28** respectively). The trans carbonyl resonance is slightly deshielded relatively to the cis carbonyl one as previously observed in the literature for complexes $Y_3PW(CO)_5$, (Y = Me, Bu, Ph, OPh)[31-34].

The IR spectrum exhibits the characteristic pattern for the $LW(CO)_5$[31] moiety with three CO stretching bands at 1833, 1904 and 2017 cm^{-1}.

All attempts to obtain suitable mass spectra by various methods (EI, CI) were unsuccessful. Moreover, complex **28** is very air-sensitive and rapidly decomposes in solution towards the ligand salt **12**.

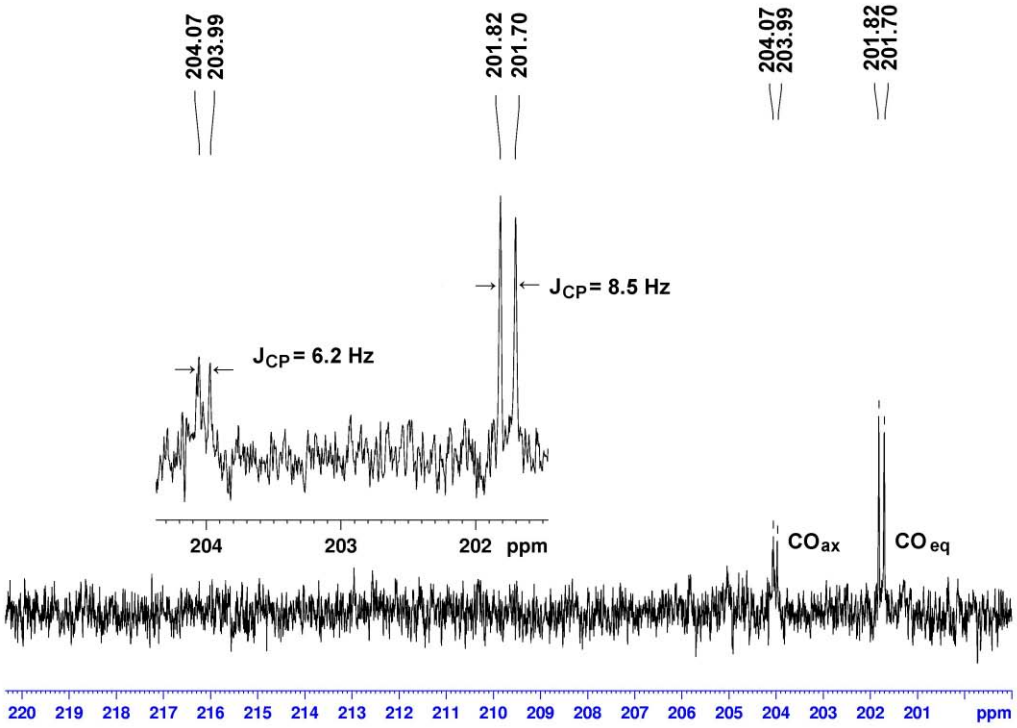

Figure 13: ^{31}C NMR spectrum for compound **27**; the resonances of relative intensity 1:4, for CO_{ax} and CO_{eq} and the C-P coupling constant, can be observed

The molecular representation (Figure 14) shows unambiguously the formation of the N,N'-chelated tungstenphosphenium cation **28**.

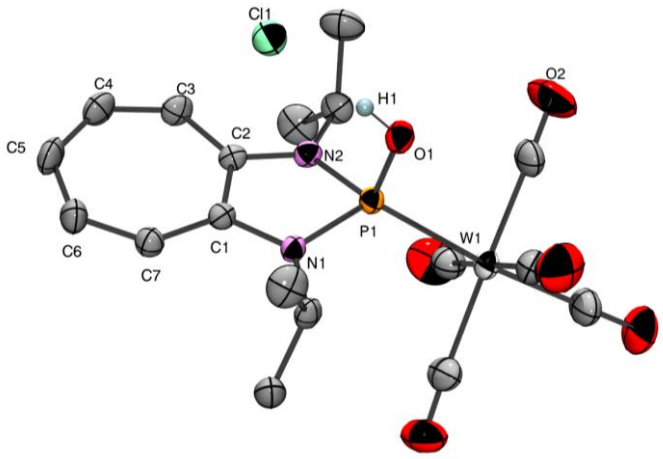

Figure 14: Molecular structure of **28** (50 % probability level for the thermal ellipsoids). All H (except H1) atoms have been omitted for clarity. Selected bond distances [Å] and angles [°] are: P(1)-O(1) 1.573(3), P(1)-N(1) 1.717(3), P(1)-N(2) 1.724(3), P(1)-W(1) 2.4584(9), N(1)-C(1) 1.372(4), N(2)-C(2) 1.368(5), W(1)-C(16) 2.025(5), W(1)-C(18) 2.049(5), O(2)-C(14) 1.136(6), O(4)-C(16) 1.129(6), C(1)-C(7) 1.396(5), C(1)-C(2) 1.444(5), C(2)-C(3) 1.394(5), C(3)-C(4) 1.376(6), C(4)-C(5) 1.381(6), C(5)-C(6) 1.384(6), C(6)-C(7) 1.380(5); O(1)-P(1)-N(1) 105.73(16), N(1)-P(1)-N(2) 88.44(15), C(1)-N(1)-P(1) 114.0(2), C(2)-N(2)-P(1) 113.9(2), O(1)-P(1)-W(1) 107.42(11), N(1)-P(1)-W(1) 123.99(11), N(2)-P(1)-W(1) 122.87(12), C(16)-W(1)-C(14) 89.05(19), C(16)-W(1)-P(1) 173.33(15).

The phosphorus atom is tetracoordinate with a nearly identical N-P-N angle, 88.44(15)°, compared with **6a**, 88.88(6)°. The long distance between the phosphorus atom and the chloride anion (P^+....Cl^-, 3.833 Å) suggests that there is no interaction between them. The OH group of the cation is hydrogen-bonded to the chloride anion with a distance of 2.047 Å, as observed for hydroxy-thiophosphonium **21**. If we compare the P-N distances from **6a**, 1.697(1) and 1.708(1) Å, to those of **28**, we observe that they are slightly longer [1.717(3) and 1.724(3) Å].

The N-heterobicyclic unit is nearly planar and almost perpendicular to the $W(CO)_5$ system. The P-O bond length, 1.573(3) Å, is in the range of P-OH distances (1.503-1.611 Å)[15-17]. The tungsten atom is octahedrally coordinated with an almost linear C_{ax}-W-P angle

of 173.33(15)°. The angles C_{ax}-W-C_{eq} are close to 90° with small deviations from the ideal octahedral. The carbons 14 and 18 from the carbonyl group which are in cis in relation to OH are slightly inclined towards the phosphorus ligand. The bond length of P-W (2.4584(9) Å) is between the bond value of $W(PCl_3)(CO)_5$ [2.378(2) Å][35] and $W(PMe_3)(CO)_5$ [2.516(2) Å][35] and nearly identical with the P-W bond value in the structure described by Mathey et al [2.4516(8) Å][36]. These bond distances are longer than the value expected for a W-P double bond (2.26 Å)[30]. The difference between the W-C_{ax} [2.025(5) Å] and W-C_{eq} [2.039(5) - 2.060(5) Å] for **28** is small. In the carbonyl groups the distances C-O are practically identical, the smallest one belonging to CO_{ax} [1.129(6) Å] which is smaller than CO_{ax} [1.17(2) Å] of $W(PCl_3)(CO)_5$[37].

The existence and the importance of metal-phosphorus π-interaction in addition to M-P σ-bonding in complexes of type $ML(CO)_5$ is still a subject of controversy because many factors are involved such as the electronic and steric properties of the substituent of the phosphorus ligand, the nature of the phosphorus acceptor orbital[31]. In our case, the bond lengths and the NMR spectroscopic data seem in agreement with a poor π-acceptor behavior of the phosphenium cation ligand.

We extended the reactions with the tungsten complex to the arsenium analogue **8**. The reaction with $W(CO)_5$THF, gives a yellow compound tentatively identified as **29** by ^{1}H NMR (Scheme 7).

The IR spectrum of the compound recorded using KBr pellet exhibits a pattern of three CO stretching vibrations at 1848, 1910 and 1984 cm^{-1} respectively, similar with those obtained for the equivalent phosphorus. All attempts to obtain crystals suitable for a X-ray structure determination failed. Thus, determination of the exact structure was not possible.

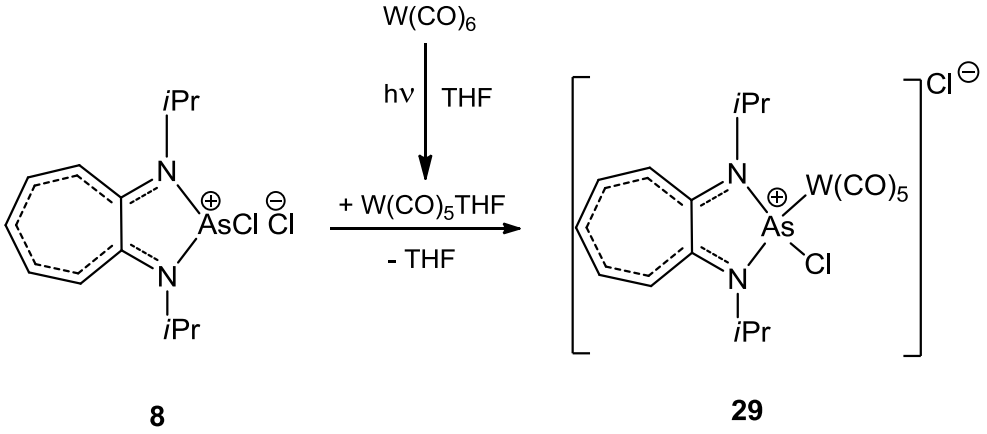

8 **29**

Scheme 7

We also tried direct substitution of a carbonyl group by the phosphenium cation **6a** in $W(CO)_3(MeCN)_3$. The reaction was performed in dichloromethane at ambient temperature (Equation 3). We observed in ^{31}P NMR spectrum the appearance of a new signal at 271.63 ppm (Figure 15) comparable to that observed in the case of a phosphenium with a cyclopentadienyl ligand[38].

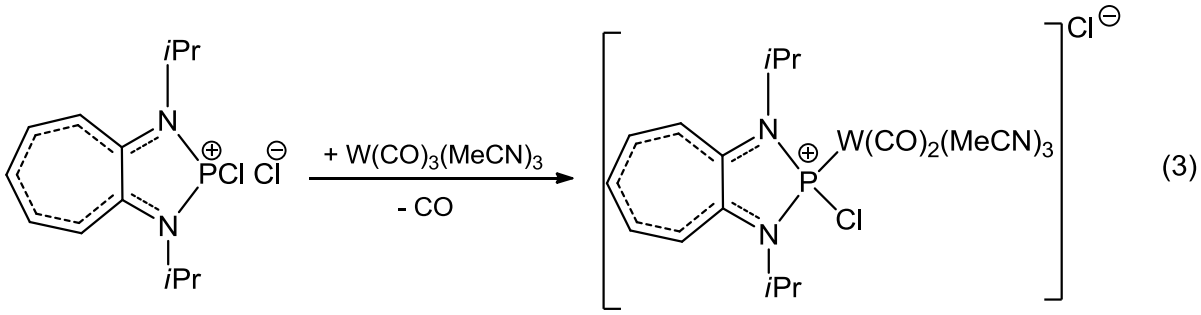

(3)

6a **30**

The infra-red analysis of complex **30** also shows the presence of two new characteristic bands ν (CO) at 1896 and 1985 cm^{-1}. Unfortunately, all the crystallization attempts to isolate the pure product failed. Moreover, it seems that this complex **30** decomposes slowly in solution with formation of insoluble products.

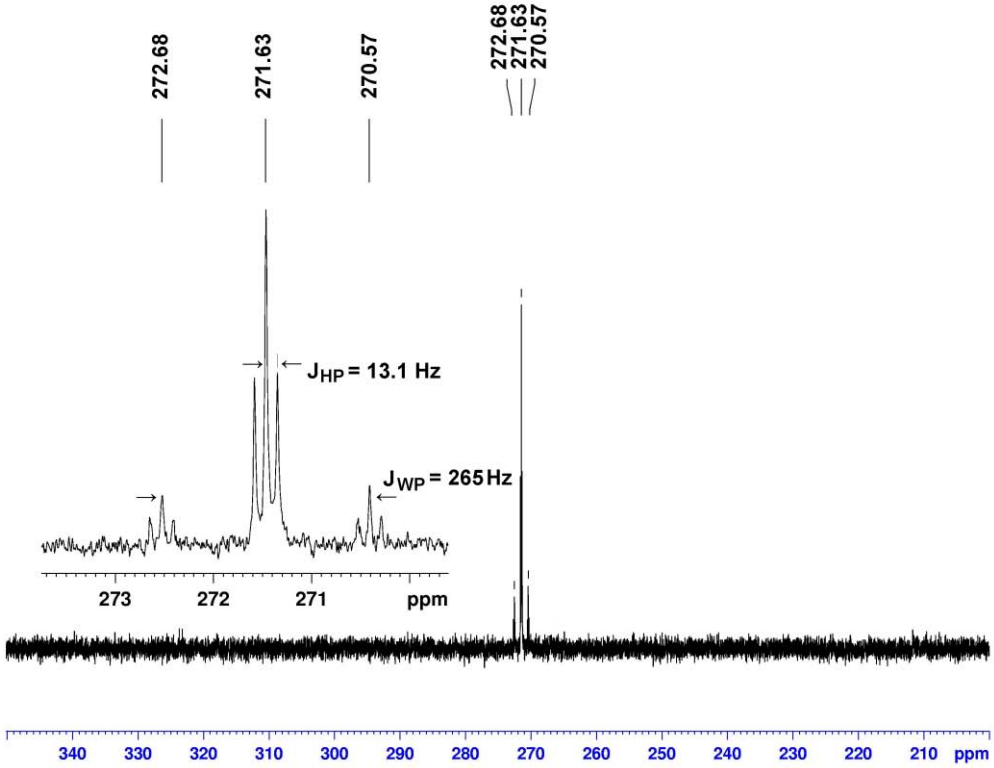

Figure 15: ^{31}P NMR spectrum for compound **30**; the coupling constant between ^{1}H and ^{183}W can be observed

We then conducted a test with tetrakis (triphenylphosphine) platinum (0) (Scheme 8). The reaction proved to be quite complex, although we observed the liberation of PPh_3 with a signal in the ^{31}P NMR spectrum at -6 ppm.

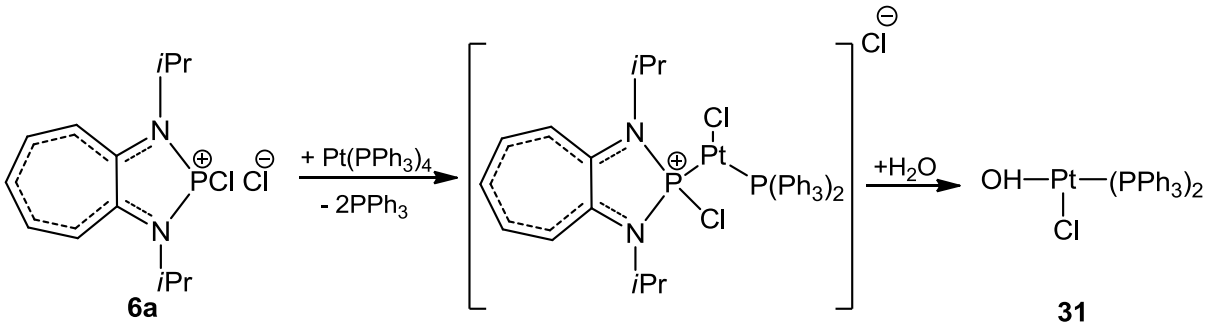

Scheme 8

The new postulated complex is very air-sensitive and we could only characterize hydroxychlorobis(triphenylphosphine) platinum (II) **31**[39].

Conclusions and perspectives

The study of pnictogenium cations reactivity has been further developed. A particularly rich chemistry surrounds these species, which undergo a variety of transformations including halide ion exchange, oxidative and cycloaddition reactions.

Several oxidative reactions were carried out using dimethylsulfoxide, sulfur or selenium. In all cases, the phosphenium cation has been, not only more reactive, but also gave stable and unexpected products. In particular, it allowed the syntheses and the structural characterization of the first examples of an aminometaphosphonate and of its sulfur equivalent stabilized by intramolecular complexation.

The cycloaddition reaction with *o*-quinone confirms their dienophilic nature with formation of a phosphate ester derivatives.

Another interesting feature is their ability to act as ligand in the sphere of coordination of transition-metal complexes. A novel cationic tungsten complex which is isolobal to transition metal carbene complexes could be synthesized and structurally characterized.

Experimental Section

Reaction of 6a with Me_3SiOTf

Trimethylsilyl trifluoromethanesulfonate (0.11 g, 0.54 mmol) was combined with a solution of **6a** (0.15 g, 0.49 mmol) in dichloromethane (5 ml) and the mixture stirred for 10 minutes at room temperature. Then the volatiles were removed under reduced pressure leading to a yellow solid. The ^{1}H NMR analysis shows the formation of **13** (75 %) and **14** (25 %).

Compound **13**

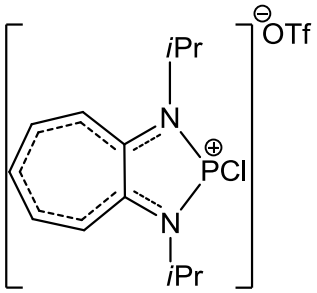

^{19}F NMR (282 MHz, $CDCl_3$): δ (ppm) –77.47.
^{31}P {^{1}H} NMR (121 MHz, $CDCl_3$): δ (ppm) 136.16.
^{1}H NMR (300 MHz, $CDCl_3$): δ (ppm)

1.62 (d, $^3J_{HH}$ = 6.5 Hz, 6H, CH-CH_3),
1.72 (d.d, $^3J_{HH}$ = 6.5 Hz, $^4J_{HP}$= 2.6 Hz, 6H, CH-CH_3),
4.64 (sept.d, $^3J_{HH}$ = 6.6 Hz, $^3J_{HP}$= 11.2 Hz, 2H, C*H*-CH_3),
7.92 (t.d, $^3J_{HH}$ = 9.6 Hz, $^6J_{HP}$ = 3.5 Hz, 1H, H_5),
8.13 (d.d, $^3J_{HH}$ = 10.8 Hz, $^4J_{HP}$ = 2.7 Hz, 2H, $H_{3,7}$),
8.31 (t, $^3J_{HH}$ = 10.2 Hz, 2H, $H_{4,6}$).

^{13}C {^{1}H} NMR (75 MHz, $CDCl_3$): δ (ppm)

21.70 (d, $^3J_{CP}$ = 8.9 Hz, CH-*C*H_3),
21.79 (d, $^3J_{CP}$ = 13.6 Hz, CH-*C*H_3),
50.63 (d, $^2J_{CP}$ = 12.8 Hz, *C*H-CH_3),
119.13 (q, J_{CF} = 318.4 Hz, CF_3),
126.65 (d, $^3J_{CP}$ = 6.0 Hz, $C_{3,7}$),
136.94 (d, $^5J_{CP}$ = 5.3 Hz, C_5),
143.95 (d, $^4J_{CP}$ = 4.9 Hz, $C_{4,6}$),
155.69 (d, $^2J_{CP}$ = 12.8 Hz, $C_{2,8}$).

EI-MS: m/z 384 [M^+ - Cl +1, 1 %].

Compound **14**

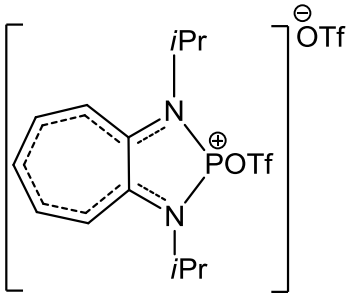

^{19}F NMR (282 MHz, $CDCl_3$): δ (ppm) –77.90.
^{31}P {^{1}H} NMR (121 MHz, $CDCl_3$): δ (ppm) 111.05.
^{1}H NMR (300 MHz, $CDCl_3$): δ (ppm)
1.52 (d, $^3J_{HH}$ = 6.6 Hz, 12H, CH-CH_3),
4.48 (sept, $^3J_{HH}$ = 6.9 Hz, 2H, CH-CH_3),
7.59 (t.d, $^3J_{HH}$ = 9.7 Hz, $^6J_{HP}$ = 1.7 Hz, 1H, H_5),
7.74 (d, $^3J_{HH}$ = 11.1 Hz, 2H, $H_{3,7}$),
8.04 (t, $^3J_{HH}$ = 10.1 Hz, 2H, $H_{4,6}$).
^{13}C {^{1}H} NMR (75 MHz, $CDCl_3$): δ (ppm)
22.07 (d, $^3J_{CP}$ = 18.0 Hz, CH-$C$$H_3$),
49.37 (d, $^2J_{CP}$ = 14.3 Hz, CH-CH_3),
119.13 (q, J_{CF} = 318.4 Hz, CF_3),
121.95 (d, $^3J_{CP}$ = 2.1 Hz, $C_{3,7}$),
133.54 (d, $^5J_{CP}$ = 2.7 Hz, C_5),
142.82 (d, $^4J_{CP}$ = 2.7 Hz, $C_{4,6}$),
155.74 (d, $^2J_{CP}$ = 10.1 Hz, $C_{2,8}$).

Reaction of 8 with Me_3SiOTf

To a solution of **8** (0.20 g, 0.57 mmol) in CH_2Cl_2 (5 ml), was added dropwise over a period of 5 min Me_3SiOTf (0.13 g, 0.59 mmol). The orange solution was filtered after 0.5 h of magnetic stirring (elimination of the triflate salt **17**). After drying, the precipitate was dissolved in CH_2Cl_2, followed by cooling for 24 h at -30 °C giving **15** as yellow crystals (0.15 g, 59 %, mp 160-163 °C).

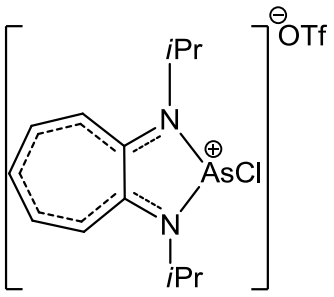

^{19}F {^{1}H} NMR (282 MHz, $CDCl_3$): δ (ppm) -78.44.

^{1}H NMR (300 MHz, $CDCl_3$): δ (ppm)
1.58 (d, $^{3}J_{HH}$ = 6.4 Hz, 6H, CH-CH_3),
1.81 (d, $^{3}J_{HH}$ = 6.4 Hz, 6H, CH-CH_3),
4.55 (sept, $^{3}J_{HH}$ = 6.5 Hz, 2H, CH-CH_3),
7.56 (t, $^{3}J_{HH}$ = 9.5 Hz, 1H, H_5),
7.63 (d, $^{3}J_{HH}$ = 11.1 Hz, 2H, $H_{3,7}$),
7.95 (ps.t, $^{3}J_{HH}$ = 9.6 Hz, 2H, $H_{4,6}$).

^{13}C {^{1}H} NMR (75 MHz, $CDCl_3$): δ (ppm)
20.81 (CH-$C$$H_3$),
51.16 (CH-CH_3),
118.40 (q, J_{CF} = 317.4 Hz, CF_3),
124.46 ($C_{3,7}$),
134.08 (C_5),
141.52 ($C_{4,6}$),
157.95 ($C_{2,8}$).

EI-MS: m/z 427 [M^+ - Cl, 22 %], 313 [M^+ - OSO_2CF_3, 100 %], 278 [M^+ - (OSO_2CF_3, Cl), 17 %], 235 [M^+ - (OSO_2CF_3, Cl, *i*Pr), 47 %].

Anal. $C_{14}H_{19}ClN_2AsO_3SF_3$ (462.74) calc. C 36.33, H 4.14, N 6.06;
found C 35.92, H 3.91, N 5.90.

Reaction of 10 with Me_3SiOTf

Trimethylsilyl trifluoromethanesulfonate (0.08 g, 0.38 mmol) was combined with a solution of **10** (0.15 g, 0.38 mmol) in dichloromethane and the mixture stirred for 10 minutes at room temperature, then the volatiles were removed under reduced pressure leading to **16** a yellow solid.

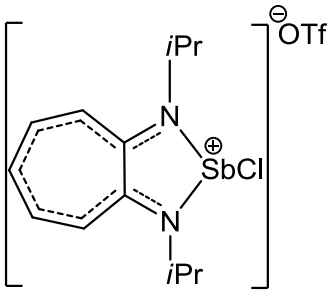

^{19}F NMR (282 MHz, $CDCl_3$): δ (ppm) –77.84.

^{1}H NMR (300 MHz, $CDCl_3$): δ (ppm)
1.67 (d, $^{3}J_{HH}$ = 6.3 Hz, 12H, CH-CH_3),
4.52 (sept, $^{3}J_{HH}$ = 6.3 Hz, 1H, CH-CH_3),
7.25 (t, $^{3}J_{HH}$ = 9.5 Hz, 1H, H_5),
7.32 (d, $^{3}J_{HH}$ = 11.5 Hz, 2H, $H_{3,7}$),
7.72 (ps.t, 2H, $H_{4,6}$).

^{1}H NMR (500 MHz, $CDCl_3$): δ (ppm)
1.70 (d, $^{3}J_{HH}$ = 6.4 Hz, 12H, CH-CH_3),
4.52 (sept, $^{3}J_{HH}$ = 6.3 Hz, 1H, CH-CH_3),
7.23 (t, $^{3}J_{HH}$ = 9.5 Hz, 1H, H_5),
7.28 (d, $^{3}J_{HH}$ = 11.6 Hz, 2H, $H_{3,7}$),
7.71 (ps.t, 2H, $H_{4,6}$).
^{13}C {^{1}H} NMR (125.75 MHz, $CDCl_3$): δ (ppm)
23.63 (CH-$C$$H_3$),
50.78 (CH-CH_3),
120.03 (q, J_{CF} = 319.0 Hz, CF_3),
122.39 ($C_{3,7}$),
129.82 (C_5),
139.10 ($C_{4,6}$),
161.14 ($C_{2,8}$).
EI-MS: m/z 510 [M^+, 3 %], 473 [M^+ - Cl, 8 %], 361 [M^+ - OTf, 6 %], 281 [M^+ - OTf - Cl - *i*Pr, 7 %].

Preparation of aminotroponiminate triflate salt (*i*Pr_2ATI)H·$HOSO_2CF_3$

Trifluoromethanesulfonic acid (0.07 g, 0.49 mmol) was added dropwise at room temperature to a solution of (*i*Pr_2ATI)H (0.10 g, 0.49 mmol) in diethylether (3 ml). Immediately, a yellow precipitate appeared. After 15 minutes of stirring, the volatiles where removed from the precipitate yielding **17** as a yellow solid (168 mg, 98 %, mp 120 °C).

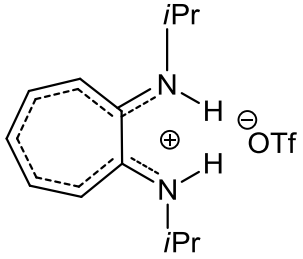

^{19}F NMR (282 MHz, $CDCl_3$): δ (ppm) –78.17.
^{1}H NMR (300 MHz, $CDCl_3$): δ (ppm)
1.41 (d, $^{3}J_{HH}$ = 6.5 Hz, 12H, CH-CH_3),
3.94 (sept, $^{3}J_{HH}$ = 6.4 Hz, 2H, CH-CH_3),
6.97-7.04 (m, 3H, C_7H_5),
7.55 (ps.t, 2H, C_7H_5).
^{13}C {^{1}H} NMR (75 MHz, $CDCl_3$): δ (ppm)
20.98 (CH-$C$$H_3$),
47.75 (CH-CH_3),
120.22 (q, J_{CF} = 319.6 Hz, CF_3),
117.49 ($C_{3,7}$),
127.12 (C_5),
140.18 ($C_{4,6}$),
150.63 ($C_{2,8}$).

Reaction of 6a with DMSO

To a solution of **6a** (0.20 g, 0.65 mmol) in CH_2Cl_2 (6 ml) was added dropwise dry dimethyl sulfoxide (51 mg, 0.65 mmol). The reaction mixture was stirred at room temperature for 0.5 h. The NMR analyses show the formation of **18**.

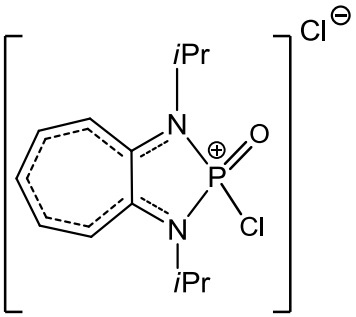

^{31}P {^{1}H} NMR (121 MHz, $CDCl_3$): δ (ppm) 13.40 (t, $^{3}J_{HP}$ = 18.2 Hz).
^{1}H NMR (300 MHz, $CDCl_3$): δ (ppm)
1.52 (d, $^{3}J_{HH}$ = 6.7 Hz, 6H, CH-CH_3),
1.60 (d, $^{3}J_{HH}$ = 6.6 Hz, 6H, CH-CH_3),
4.80-5.10 (m, 2H, CH-CH_3),
8.00 (t, $^{3}J_{HH}$ = 9.6 Hz, 1H, H_5),
8.61 (t, $^{3}J_{HH}$ = 10.0 Hz, 2H, $H_{4,6}$),
8.84 (d, $^{3}J_{HH}$ = 10.9 Hz, 2H, $H_{3,7}$).
^{13}C {^{1}H} NMR (75 MHz, $CDCl_3$): δ (ppm)
19.80 (d, $^{3}J_{CP}$ = 1.9 Hz, CH-$C$$H_3$),
21.24 (d, $^{3}J_{CP}$ = 1.3 Hz, CH-$C$$H_3$),
51.55 (d, $^{2}J_{CP}$ = 3.3 Hz, CH-CH_3),
128.19 (d, $^{3}J_{CP}$ = 9.8 Hz, $C_{3,7}$),
139.14 (C_5),
146.82 ($C_{4,6}$),
149.91 and 150.14 ($C_{2,8}$).

Reaction of 6a with excess of DMSO

To a solution of **6a** (0.20 g, 0.65 mmol) in CH_2Cl_2 (6 ml) was added dropwise dry dimethyl sulfoxide (102 mg, 1.30 mmol). The reaction mixture was stirred at room temperature for 0.5 h and then the solvent was removed under vacuum giving **19** as a yellow powder (1.91 g, 92 %, mp 115-117 °C (dec.)).

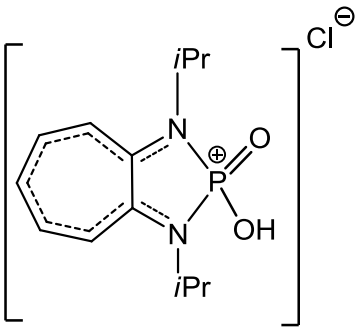

^{31}P {^{1}H} NMR (121 MHz, $CDCl_3$): δ (ppm) 6.81 (t, $^{3}J_{HP}$ = 14.4 Hz).
^{1}H NMR (300 MHz, $CDCl_3$): δ (ppm)
1.49 (d, $^{3}J_{HH}$ = 6.6 Hz, 12H, CH-CH_3),
4.35 (sept.d, $^{3}J_{HH}$ = 7.0 Hz, $^{3}J_{HP}$ = 14.1 Hz, 2H, C*H*-CH_3),
7.46 (t, $^{3}J_{HH}$ = 9.5 Hz, 1H, H_5),
7.60 (d, $^{3}J_{HH}$ = 10.9 Hz, 2H, $H_{3,7}$),
7.94 (t, $^{3}J_{HH}$ = 10.2 Hz, 2H, $H_{4,6}$).
^{13}C {^{1}H} NMR (75 MHz, $CDCl_3$): δ (ppm)
20.37 (CH-*C*H_3),
49.30 (d, $^{2}J_{CP}$ = 3.8 Hz, *C*H-CH_3),
120.93 ($C_{3,7}$),
132.55 (C_5),
142.83 ($C_{4,6}$),
150.48 and 150.69 ($C_{2,8}$).
^{31}P {^{1}H} NMR (121 MHz, DMSO): δ (ppm) 4.40.
^{1}H NMR (300 MHz, DMSO): δ (ppm)
1.42 (d, $^{3}J_{HH}$ = 6.6 Hz, 12H, CH-CH_3),
4.40 (sept.d, $^{3}J_{HH}$ = 6.7 Hz, $^{3}J_{HP}$ = 1.6 Hz, 2H, C*H*-CH_3),
7.39 (t.d, $^{3}J_{HH}$ = 9.4 Hz, $^{6}J_{HP}$ = 4.4 Hz, 1H, H_5),
7.61 (d.d, $^{3}J_{HH}$ = 10.5 Hz, $^{3}J_{HP}$ = 5.6 Hz, 2H, $H_{3,7}$),
7.86 (t.d, $^{3}J_{HH}$ = 9.5 Hz, $^{4}J_{HP}$ = 3.4 Hz, 2H, $H_{4,6}$).
^{13}C {^{1}H} NMR (75 MHz, DMSO): δ (ppm)
20.53 (CH-*C*H_3),
48.05 (d, $^{2}J_{CP}$ = 3.3 Hz, *C*H-CH_3),
119.58 ($C_{3,7}$),
130.73 (C_5),
142.23 ($C_{4,6}$),
149.88 and 150.07 ($C_{2,8}$).

A slow crystallisation at -30 °C gave yellowish crystals of **20**.

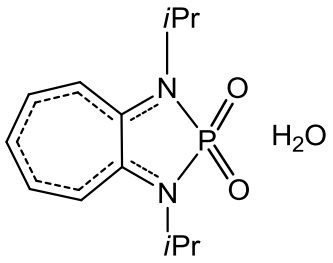

^{31}P {^{1}H} NMR (121 MHz, $CDCl_3$): δ (ppm) 4.00 (t, $^{3}J_{HP}$ = 13.0 Hz).
^{1}H NMR (300 MHz, $CDCl_3$): δ (ppm)
1.60 (d, $^{3}J_{HH}$ = 6.6 Hz, 12H, CH-CH_3),
4.23 (sept.d, $^{3}J_{HH}$ = 6.6 Hz, $^{3}J_{HP}$ = 13.2 Hz, 2H, C*H*-CH_3),
7.04-7.14 (m, 3H, C_7H_5),
7.59 (t, $^{3}J_{HH}$ = 10.4 Hz, 2H, C_7H_5).

^{13}C {^{1}H} NMR (75 MHz, $CDCl_3$): δ (ppm)
20.28 (CH-*C*H_3),
48.61 (d, $^{2}J_{CP}$ = 4.2 Hz, *C*H-CH_3),
116.76 (d, $^{3}J_{CP}$ = 7.4 Hz, $C_{3,7}$),
127.90 (C_5),
140.47 ($C_{4,6}$),
150.54 (d, $^{2}J_{CP}$ = 139 Hz, $C_{2,8}$).
EI-MS: m/z 284 [M^+, 3 %], 266 [M^+ - H_2O, 35 %], 224 [M^+ - H_2O - *i*Pr + H, 33 %], 251 [M^+ - H_2O - CH_3, 5 %].

Reaction of 19 with H_2O

To a solution of **19** (0.20 g, 0.65 mmol) in CH_2Cl_2 (6 ml) was added H_2O (23 mg, 1.30 mmol). The reaction mixture was stirred at room temperature for 10 minutes. The ^{31}P and ^{1}H NMR confirm the presence of **20**.

Reaction of 19 with Et_3N

Dry triethylamine (33 mg, 0.32 mmol) was added with a microsyringe to a solution of **19** (0.10 g, 0.32 mmol) in CH_2Cl_2 (5 ml). The reaction mixture was stirred at room temperature for 5 min, then the volatiles were removed. The ^{1}H and ^{31}P NMR spectra showed a total conversion of the initial product towards **20**, quantitative yields being obtained.

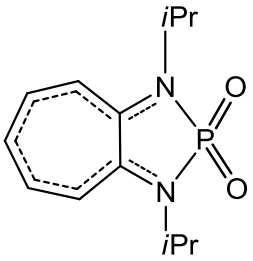

Reaction of (*i*Pr_2ATI)Li with $POCl_3$

A 1.6 M solution of *n*BuLi in hexanes (2.10 mmol) was slowly added at 0 °C to a solution of **2** (0.40 g, 1.98 mmol) in diethyl ether (15 ml). The resultant yellow colored mixture was removed from the cooling bath, allowed to reach room temperature and stirred for 0.5 h. It

was slowly added to a cooled (-75 °C) solution of phosphoryl chloride ($POCl_3$) (0.32 g, 2.10 mmol) in diethyl ether (5 ml). The reaction mixture was allowed to reach ambient temperature and stirred for 3 h. The reaction mixture was dried under vacuo, leading to a yellow powder. NMR spectrum showed that one major product, **2**, was formed in addition to a small amount of **12** and trace of a phosphorated product, probably **20**. The compounds could not be isolated from the mixture.

^{31}P {^{1}H} NMR (121 MHz, $CDCl_3$): δ (ppm) 41.95 (t, J = 22.0 Hz) and 4.33.

Reaction of 6a with elemental sulfur

A solution of **6a** (0.25 g, 0.82 mmol) in CH_2Cl_2 (5 ml) was added to a stirred suspension of sulfur (0.026 g, 0.10 mmol) in CH_2Cl_2 (5 ml). The reaction mixture was heated at 40 °C during 14 h. Storage of the reaction mixture at 4 °C afforded yellowish crystals of **21** (0.22 g, 81 %, mp 121 °C (dec.)).

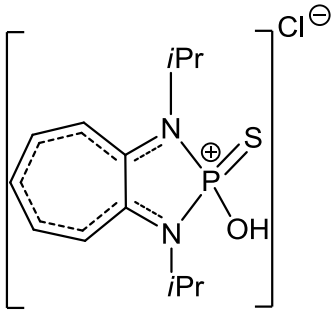

^{31}P {^{1}H} NMR (121 MHz, $CDCl_3$): δ (ppm) 59.04.
^{1}H NMR (300 MHz, $CDCl_3$): δ (ppm)
1.68 (d, $^{3}J_{HH}$ = 6.9 Hz, 6H, CH-CH_3),
1.81 (d, $^{3}J_{HH}$ = 6.9 Hz, 6H, CH-CH_3),
4.58 (sept.d, $^{3}J_{HH}$ = 6.9 Hz, $^{3}J_{HP}$= 12.0 Hz, 2H, CH-CH_3),
7.31 (t, $^{3}J_{HH}$ = 9.6 Hz, 1H, H_5),
7.38 (d, $^{3}J_{HH}$ = 11.1 Hz, 2H, $H_{4,6}$),
7.75 (t, $^{3}J_{HH}$ = 10.0 Hz, 2H, $H_{3,7}$).
^{13}C {^{1}H} NMR (75 MHz, $CDCl_3$): δ (ppm)
20.22 (CH-$C$$H_3$),
48.92 (d, $^{2}J_{CP}$ = 5.8 Hz, CH-CH_3),
117.76 (d, $^{3}J_{CP}$ = 7.5 Hz, $C_{3,7}$),
128.58 (C_5),
140.43 ($C_{4,6}$),
150.88 ($C_{2,8}$).

Reaction of 6a with elemental selenium

10 ml of dry chloroform was added to a mixture of 0.079 g (0.70 mmol) selenium and 0.209 g (0.70 mmol) of **6a**, the mixture was then stirred for 5 h at 60 °C. The resulting red-black

solution, with a strong smell of garlic, was filtered and the volatiles were removed from the filtrate under vacuo to obtain the product **22** as a yellow solid (0.21 g, 82 %, mp 130-132 °C (dec.)). The obtained product is dissolved in a minimum quantity of CH_2Cl_2. A slow crystallisation at -30 °C gave yellowish crystals of **22**.

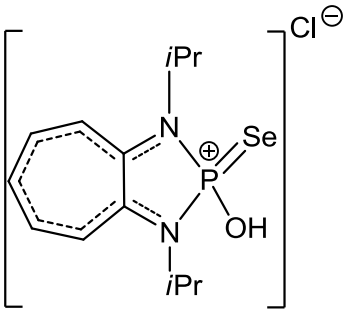

^{77}Se NMR (76 MHz, $CDCl_3$): δ (ppm) 46.00.
^{31}P NMR {^{1}H} (121 MHz, $CDCl_3$): δ (ppm) 48.44 (J_{PSe} = 871 Hz).
^{1}H NMR (300 MHz, $CDCl_3$): δ (ppm)
1.64 (d, $^3J_{HH}$ = 6.8 Hz, 6H, CH-CH_3),
1.77 (d, $^3J_{HH}$ = 6.8 Hz, 6H, CH-CH_3),
4.64 (sept, $^3J_{HH}$ = 6.3 Hz, 2H, CH-CH_3),
7.26 (t, $^3J_{HH}$ = 9.3 Hz, 1H, H_5),
7.36 (d, $^3J_{HH}$ = 10.4 Hz, 2H, $H_{3,7}$),
7.76 (t, $^3J_{HH}$ = 10.1 Hz, 2H, $H_{4,6}$).
^{13}C {^{1}H} NMR (75 MHz, $CDCl_3$): δ (ppm)
20.20 (d, $^3J_{CP}$ = 2.4 Hz, $^3J_{CSe}$ = 49.4 Hz, CH-$C$$H_3$),
49.32 (CH-CH_3),
120.76 (d, $^3J_{CP}$ = 6.6 Hz, $C_{3,7}$),
132.17 (C_5),
141.87 (d, $^4J_{CP}$ = 6.4 Hz, $C_{4,6}$),
150.67 (d, $^2J_{CP}$ = 4.8 Hz) and 150.80 (d, $^2J_{CP}$ = 5.0 Hz $C_{2,8}$).
EI-MS: **m/z** 330 [M^+ - 1, 53 %], 249 [M^+ - SeH - 1, 25 %], 207 [M^+ - SeH - *i*Pr, 83 %], 165 [M^+ - SeH - 2*i*Pr, 100 %], 149 [M^+ - SeH - 2*i*Pr - O, 100 %].

Reaction of 21 with Et_3N

A solution of **21** (0.25 g, 0.82 mmol) in CH_2Cl_2 (5 ml) was treated with Et_3N (0.83 g, 0.82 mmol). The reaction mixture was stirred for 10 minutes. Cooling of the reaction mixture at 4 °C afforded yellowish crystals of **23** (mp 142-145 °C).

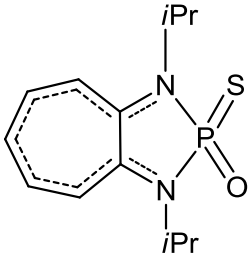

^{31}P {^{1}H} NMR (121 MHz, $CDCl_3$): δ (ppm) 55.53.
^{1}H NMR (300 MHz, $CDCl_3$): δ (ppm)
1.66 (d, $^{3}J_{HH}$ = 6.9 Hz, 6H, CH-CH_3),
1.79 (d, $^{3}J_{HH}$ = 6.9 Hz, 6H, CH-CH_3),
4.52 (sept.d, $^{3}J_{HH}$ = 6.9 Hz, $^{3}J_{HP}$= 12.0 Hz, 2H, C*H*-CH_3),
7.07 (t, $^{3}J_{HH}$ = 10.0 Hz, 1H, H_5),
7.14 (d, $^{3}J_{HH}$ = 11.2 Hz, 2H, $H_{4,6}$),
7.56 (t, $^{3}J_{HH}$ = 10.8 Hz, 2H, $H_{3,7}$).
^{13}C {^{1}H} NMR (75 MHz, $CDCl_3$): δ (ppm)
20.20 (CH-*C*H_3),
48.86 (d, $^{2}J_{CP}$ = 5.9 Hz, *C*H-CH_3),
117.89 (d, $^{3}J_{CP}$ = 6.5 Hz, $C_{3,7}$),
128.74 (C_5),
140.55 ($C_{4,6}$),
150.83 (d, $^{2}J_{CP}$ = 10.7 Hz, $C_{2,8}$).
EI-MS: m/z 282 [M^+ - 57 %], 239 [M^+ - *i*Pr, 17 %], 207 [M^+ - S - *i*Pr, 41 %].

Reaction of 23 with HCl

A solution of **23** (0.25 g, 0.82 mmol) in CH_2Cl_2 (5 ml) was treated with HCl (37 %). The reaction mixture was stirred for 10 minutes. ^{31}P and ^{1}H NMR analyses showed the formation of **21**.

Reaction of 7a with DMSO

A 0.014g (0.18 mmol) amount of DMSO was slowly injected to a deuterated chloroform (0.6 ml) solution of 0.047g (0.18 mmol) of **7a**. The solution was stirred for 10 minutes at room temperature. The NMR analyses show the formation of a new compound, probably the equivalent of **20**.

^{31}P NMR (121 MHz, $CDCl_3$): δ (ppm) 4.00 (d, $^{3}J_{PH}$ = 14.6 Hz).
^{31}P {^{1}H} NMR (121 MHz, $CDCl_3$): δ (ppm) 4.00.
^{1}H NMR (300 MHz, $CDCl_3$): δ (ppm)
1.56 (d, $^{3}J_{HH}$ = 6.7 Hz, 6H, CH-CH_3),
4.28 (sept.d, $^{3}J_{HH}$ = 7.1 Hz, $^{3}J_{HP}$ = 14.1 Hz, 2H, C*H*-CH_3),
7.53 (ps.t, 1H, H_5),
7.66 (d, $^{3}J_{HH}$ = 10.5 Hz, 2H, $H_{4,6}$),

7.80 (t, $^{3}J_{HH}$ = 10.1 Hz, 1H, C_7H_5),
8.06 (ps.t, 1H, C_7H_5).

^{13}C {^{1}H} NMR (75 MHz, $CDCl_3$): δ (ppm)

20.29 (CH-*C*H_3),
49.26 (d, $^{2}J_{CP}$ = 3.5 Hz, *C*H-CH_3),
122.29 (C_7),
125.57 (C_3),
133.93 (C_5),
141.43 (C_6),
144.86 (C_4),
155.63 (C_2),
159.27 (C_8).

EI-MS: m/z 182 [M^+ - *i*Pr - H, 1 %].

Synthesis of (*i*PrAT)H·HCl 24

To a solution of **1** (0.150 g, 0.92 mmol) in CH_2Cl_2 (5 ml) HCl (0.037 g, 1.00 mmol) was syringed dropwise. The cloudy orange mixture was stirred for 20 minutes at room temperature. The solvent was removed in vacuo, and the NMR spectrum showed a total conversion of the starting product (mp 76-78 °C).

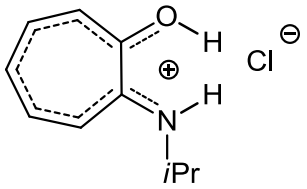

^{1}H NMR (300 MHz, $CDCl_3$): δ (ppm)

1.37 (br.s, 3H, CH-C*H*$_3$),
3.95-4.20 (m, lH, C*H*-CH_3),
7.20-7.95 (m, 5H, C_7H_5).

^{13}C {^{1}H} NMR (75 MHz, $CDCl_3$): δ (ppm)

22.02 (CH-*C*H_3),
46.21 (*C*H-CH_3),
122.00 (C_7),
125.55 (C_3),
131.57 (C_5),
140.87 (C_6),
143.55 (C_4),
155.25 (C_2),
162.17 (C_8).

Reaction of 7a with sulfur

A solution of **7a** (0.22 g, 0.83 mmol) in CH_2Cl_2 (5 ml) was added to a stirred suspension of

sulfur (0.027 g, 0.10 mmol) in CH_2Cl_2 (5 ml). The reaction mixture was heated at 40 °C for 8 h and monitored by ^{31}P NMR spectroscopy until all **7a** was consumed. The isolation of the product was impossible due to the partial decomposition of starting product. The ^{31}P NMR spectrum shows the presence of a new signal at 60 ppm. The ^{1}H NMR spectrum shows the presence of more than one product; consequently the analysis was difficult.

$^{31}P\{^{1}H\}$ NMR (121 MHz, $CDCl_3$): δ (ppm) 60.00.

Reaction of 6a with 3,5-di-*tert*-butyl-1,2–benzoquinone

A solution of 3,5-di-*tert*-butyl-1,2-benzoquinone (0.13 g, 0.6 mmol) in CH_2Cl_2 (2 ml) was added to **6a** (0.20 g, 0.7 mmol) in CH_2Cl_2 (4 ml). The mixture was stirred for 1 h at room temperature and then heated at 40 °C for 1 h. The mixture was kept at -30 ˚C for 12 h and then the resulting yellow powder was filtered and dried under vacuo to give compound **25** (0.24 g, 77 %, mp 176 °C).

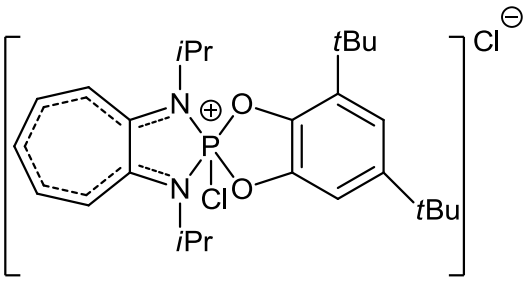

$^{31}P\{^{1}H\}$ NMR (121 MHz, $CDCl_3$): δ (ppm) 7.83.

^{1}H NMR (300 MHz, $CDCl_3$): δ (ppm)

1.22 (s, 9H, C(CH_3)$_3$),
1.31 (s, 9H, C(CH_3)$_3$),
1.51 (d, $^{3}J_{HH}$ = 6.5 Hz, 6H, CH-CH_3),
1.54 (d, $^{3}J_{HH}$ = 6.7 Hz, 6H, CH-CH_3),
4.63 (sept, $^{3}J_{HH}$ = 6.7 Hz, 2H, CH-CH_3),
7.04 (d, $^{4}J_{HH}$ = 2.2 Hz, 1H, C_6H_2),
7.47 (d, $^{4}J_{HH}$ = 2.2 Hz, 1H, C_6H_2),
7.78 (t, $^{3}J_{HH}$ = 9.4 Hz, 1H, C_7H_5),
8.16-8.30 (m, 4H, C_7H_5).

$^{13}C\{^{1}H\}$ NMR (75 MHz, $CDCl_3$): δ (ppm)

19.82 (d, $^{3}J_{CP}$ = 1.5 Hz, CH-CH$_3$),
21.21 (CH-CH$_3$),
29.50 and 31.55 (C-CH$_3$),
34.49 and 35.41 (C-CH$_3$),
50.19 (d, $^{2}J_{CP}$ = 3.3 Hz, CH-CH$_3$),
113.63 and 120.17 (C_6H_2, CH),
124.89 (d, $^{3}J_{CP}$ = 10.6 Hz, $C_{3,7}$),
135.62 (C_5),
137.95 and 141.05 (C_6H_2, quat),
139.61 (d, $^{2}J_{CP}$ = 8.0 Hz) and 143.64 (d, $^{2}J_{CP}$ = 8.7 Hz) C_6H_2, quat),

144.31 ($C_{4,6}$),
151.24 (d, $^{2}J_{CP}$ = 18.0 Hz, $C_{2,8}$).

CI:NH_3 m/z: 490 [M^+ - Cl + H, 14 %].

Analyse: $C_{27}H_{39}Cl_2N_2O_2P$ (524.21) calcd: C 61.71, H 7.48, N 5.33;
found: C 60.54, H 7.90, N 5.88.

A very slow recrystallization at -30˚C from CH_2Cl_2 gave the product **26B** (mp 140-142 °C).

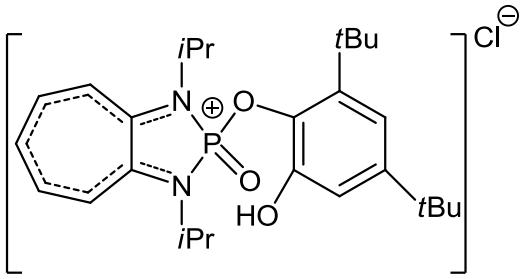

^{31}P {^{1}H} NMR (121 MHz, $CDCl_3$): δ (ppm) = -3.33.

^{1}H NMR (300 MHz, $CDCl_3$): δ (ppm)

1.13 (s, 9H, C(CH_3)$_3$),
1.28 (s, 9H, C(CH_3)$_3$),
1.48 (d, $^{3}J_{HH}$ = 6.4 Hz, 12H, CH-CH_3),
3.89-4.00 (m, 2H, C*H*-CH_3),
6.81-7.05 (m, 5H, C_6H_2 and C_7H_5),
7.37-7.44 (m, 2H, C_7H_5).

^{13}C {^{1}H} NMR (75 MHz, $CDCl_3$): δ (ppm)

20.35 (CH-*C*H_3),
28.55 and 30.51 (C-*C*H_3),
33.25 and 34.11 (*C*-CH_3),
46.82 (*C*H-CH_3),
115.19 and 124.27 (C_6H_2, *C*H),
125.04 (C_5),
127.20 and 128.00 ($C_{3,7}$),
135.70 and 140.28 (C_6H_2 quat),
136.81 and 142.77 (C_6H_2 quat),
138.74 ($C_{4,6}$),
149.58 ($C_{2,8}$).

EI-MS: **m/z** 506 [M^+- 1, 1 %].

Reaction of 7a with 3,5-di-*tert*-butyl-1,2–benzoquinone

Using the same experimental procedure than for the synthesis of **25**, the reaction of **7a** (0.20 g, 0.8 mmol) with 3,5-di-*tert*-butyl-1,2–benzoquinone (0.15 g, 0.7 mmol) gave the two cycloadducts identified by ^{31}P NMR spectroscopy and mass spectrometry.

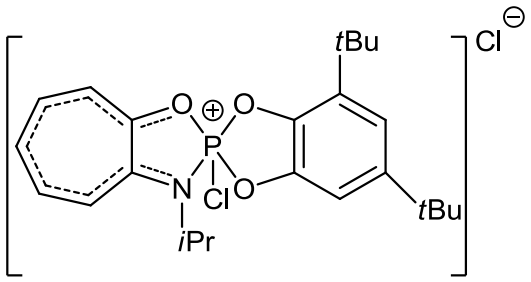

Monocycloadduct
^{31}P {^{1}H} NMR (121 MHz, $CDCl_3$): δ (ppm) 12.55.
CI:NH_3 m/z: 449 [M^+ - Cl, 1 %].

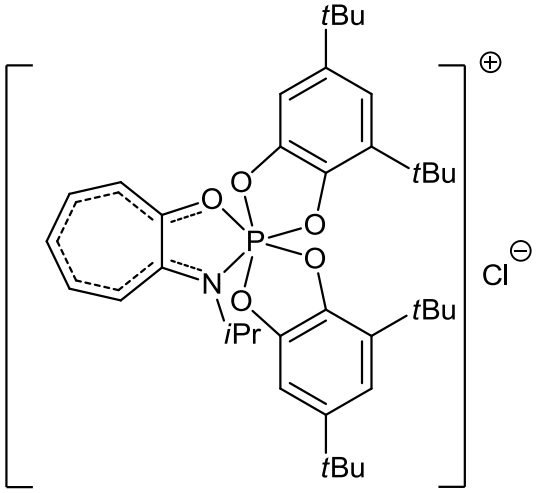

Dicycloadduct
^{31}P {^{1}H} NMR (121 MHz, $CDCl_3$): δ (ppm) - 89.19.
CI:NH_3 m/z: 633 [M^+ - Cl, 1 %].

Reaction of 6a with $W(CO)_5$THF

A solution of $W(CO)_5$THF (0.44 g, 1.10 mmol), freshly prepared by irradiation of $W(CO)_6$, in THF (20 ml), was added to a stirred suspension of **6a** (0.31 g, 1.00 mmol)) in THF (6 ml). The solution immediately turned red then, in 5 minutes the colour changed to deep red. The reaction mixture was stirred for 6 h at room temperature. The solvent was removed from the solution leaving a yellow powder which was identified as compound **27**.

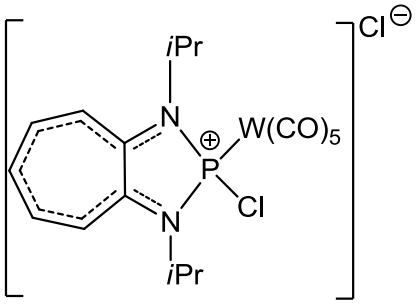

^{31}P {^{1}H} NMR (121 MHz, $CDCl_3$): δ (ppm) 150.03 (t, J_{WP} = 385 Hz, $^{3}J_{PH}$ = 10.7 Hz).
^{1}H NMR (300 MHz, $CDCl_3$): δ (ppm)
1.62 (d, $^{3}J_{HH}$ = 7.1 Hz, 6H, CH-CH_3),
1.74 (d, $^{3}J_{HH}$ = 7.1 Hz, 6H, CH-CH_3),
5.00 (sept.d, $^{3}J_{HH}$ = 7.0 Hz, $^{3}J_{HP}$ = 10.9 Hz, 2H, C*H*-CH_3),
7.49 (t, $^{3}J_{HH}$ = 9.0 Hz, 1H, H_5),
7.71 (d, $^{3}J_{HH}$ = 11.0 Hz, 2H, $H_{3,7}$),
7.89 (t, $^{3}J_{HH}$ = 10.2 Hz, 2H, $H_{4,6}$).
^{13}C {^{1}H} NMR (75 MHz, $CDCl_3$): δ (ppm)
20.20 (d, $^{3}J_{CP}$ = 3.6 Hz, CH-*C*H_3),
48.96 (d, $^{2}J_{CP}$ = 14.5 Hz, *C*H-CH_3),
122.12 (d, $^{3}J_{CP}$ = 5.7 Hz, $C_{3,7}$),
132.39 (C_5),
141.70 ($C_{4,6}$),
153.63 ($C_{2,8}$),
201.76 (d, $^{2}J_{CP}$ = 8.5 Hz, 4C, COeq),
204.02 (d, $^{2}J_{CP}$ = 6.2 Hz, 1C, COax).

A very slow crystallisation at room temperature gave crystals of **28**.

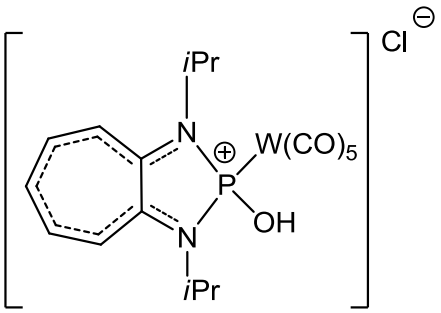

^{31}P {^{1}H} NMR (121 MHz, $CDCl_3$): δ (ppm) 128.65 (J_{WP} = 386 Hz).
^{1}H NMR (300 MHz, $CDCl_3$): δ (ppm)
1.74 (d, $^{3}J_{HH}$ = 7.0 Hz, 6H, CH-CH_3),
1.84 (d, $^{3}J_{HH}$ = 7.1 Hz, 6H, CH-CH_3),
4.72-4.90 (m, 2H, C*H*-CH_3),
7.50-7.60 (m, 1H),
7.68-7.95 (m, 4H).

^{13}C {^{1}H} NMR (75 MHz, $CDCl_3$): δ (ppm)
20.63 (d, $^{3}J_{CP}$ = 3.7 Hz, CH-*C*H_3),
49.05 (d, $^{2}J_{CP}$ = 13.2 Hz, *C*H-CH_3),
122.43 (d, $^{3}J_{CP}$ = 4.7 Hz, $C_{3,7}$),
133.22 (C_5),
143.37 ($C_{4,6}$),
154.06 ($C_{2,8}$),
195.20 (d, $^{2}J_{CP}$ = 9.3 Hz, 4C, COeq),
196.18 (d, $^{2}J_{CP}$ = 8.6 Hz, 1C, COax).
IR: $\nu_{(CO)}$ = 1833, 1904 and 2017 cm^{-1}.

Reaction of 8 with $W(CO)_5THF$

A solution of $W(CO)_5THF$ (0.44 g, 1.10 mmol), freshly prepared by irradiation of $W(CO)_6$, in THF (20 ml), was added to a stirred suspension of **8** (0.35 g, 1.00 mmol)) in THF (6 ml). The solution immediately turned red. The reaction mixture was stirred 9 h at room temperature. The solvent was removed from the solution leaving a yellow powder of **29**.

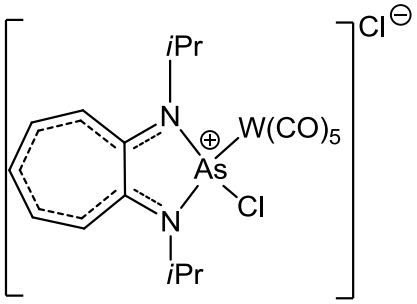

^{1}H NMR (300 MHz, $CDCl_3$): δ (ppm)

1.72 (d, $^3J_{HH}$ = 6.6 Hz, 12H, CH-CH_3),
4.58 (sept, $^3J_{HH}$ = 6.6 Hz, 2H, CH-CH_3),
7.55 (t, $^3J_{HH}$ = 9.6 Hz, 1H, H_5),
7.62 (d, $^3J_{HH}$ = 11.4 Hz, 2H, $H_{3,7}$),
7.95 (ps.t, 2H, $H_{4,6}$).

IR: $\nu_{(CO)}$ = 1848, 1910 and 1984 cm^{-1}.

Reaction of 6a with $W(CO)_3(CH_3CN)_3$

A solution of **6a** (0.32 g, 1.0 mmol) in CH_2Cl_2 (5 ml) was added to $W(CO)_3(CH_3CN)_3$ (0.38 g, 1.0 mmol) in CH_2Cl_2 (5 ml). After 12 h of stirring at ambient temperature the mixture was filtrated and the precipitate dried at reduced pressure. The compound **30** was obtained as a deep red powder.

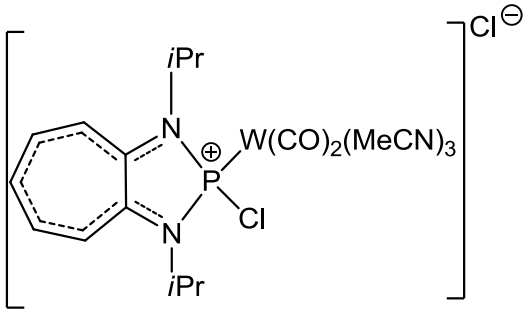

^{31}P {^{1}H} NMR (121 MHz, CH_2Cl_2): δ (ppm) 271.63 (t, J_{WP} = 265 Hz, $^3J_{PH}$ = 13.1 Hz).
IR: $\nu_{(CN)}$ = 2360, $\nu_{(CO)}$ = 1896 and 1985 cm^{-1}.

Reaction of 6a with $Pt(PPh_3)_4$

Solid **6a** (0.20 g, 0.65 mmol) was slowly added over one hour to a cold (0 °C) solution of tetrakis(triphenylphosphine)platinum(0) (0.80 g, 0.65 mmol) in CH_2Cl_2 (12 ml). The ^{31}P NMR analysis showed that within one hour all the starting product was consumed. A slow crystallization at -30˚C led to $PtOH(PPh_3)_2Cl$, **31**.

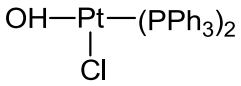

^{31}P {^{1}H} NMR (121 MHz, $CDCl_3$): δ (ppm) 28.24 (t, J_{PtP} = 3016 Hz).

X-ray Structural Determination

Structural data were collected at low temperature (193 K) using an oil-coated shock-cooled crystal on a Bruker-AXS CCD 1000 diffractometer with Mo-K_α radiation (λ = 0.71073 Å). Structures were solved by direct methods[40] and all non-hydrogen atoms were refined anisotropically using the least-squares method on F^2 (SHELXL-97)[41].

Structural data of **15**, **20**, **21**, **22**, **23**, **26B** and **28** are given in Tables 5, 6, 7 and 8.

Table 5: Structural refinement data for **15** and **20**

	15	**20**
Empirical formula	$C_{14}H_{19}AsClF_3N_2O_3S$	$C_{13}H_{21}N_2O_3P$
Formula weight	462.74	284.29
Temperature (K)	193(2)	193(2)
Crystal system	Monoclinic	Monoclinic
Space group	$P2_1/c$	*P2(1)/n*
a (Å)	11.5208(6)	7.3044(2)
b (Å)	8.7814(4)	13.5747(4)
c (Å)	19.0636(9)	14.8003(4)
α (°)	90.000	90.000
β (°)	95.614(3)	100.422(2)
γ (°)	90.000	90.000
Volume ($Å^3$)	1919.39(16)	1443.31(7)
Z	4	4
Density (calculated)(Mg/m^3)	1.601	1.308
Absorption coefficient (mm^{-1})	2.062	0.197
Reflections collected	5938	24094
Independent reflections	5955 [R(int) = 0.0000]	3557 [R(int) = 0.0632]
Absorption correction	Semi-empirical from equivalents	Semi-empirical from equivalents
Max. and min. transmission	0.8524 and 0.7338	1.000000 and 0.850578
Final R indices [I>2sigma(I)]	R1 = 0.0531, wR2 = 0.1384	R1 = 0.0456, wR2 = 0.0978
R indices (all data)	R1 = 0.0862, wR2 = 0.1488	R1 = 0.0831, wR2 = 0.1142
Largest diff. peak and hole ($eÅ^{-3}$)	0.604 and -0.560	0.365 and -0.308

with $R_1 = \Sigma||F_o|-|F_c||/\Sigma|F_o|$ and $wR_2 = (\Sigma w\,(F_o^2-F_c^2)^2/\Sigma w(F_o^2)^2)^{0.5}$.

Table 6: Structural refinement data for **21** and **22**

	21	**22**
Empirical formula	$C_{13}H_{20}ClN_2OPS$	$C_{14}H_{22}Cl_3N_2OPSe$
Formula weight	318.79	450.62
Temperature (K)	193(2)	193(2)
Crystal system	Orthorhombic	Triclinic
Space group	Pbca	P-1
a (Å)	16.6221(18)	9.5659(4)
b (Å)	10.5520(12)	10.6414(4)
c (Å)	18.0621(18)	10.7778(5)
α (°)	90	86.070(3)
β (°)	90	66.749(3)
γ (°)	90	75.424(3)
Volume ($Å^3$)	3168.0(6)	974.99(7)
Z	8	2
Density (calculated)(Mg/m^3)	1.337	1.535
Absorption coeff. (mm^{-1})	0.468	2.421
Reflections collected	29865	10214
Independent reflections	2904 [R(int) = 0.1985]	3065 [R(int) = 0.0864]
Absorption correction	Semi-empirical from equivalents	Semi-empirical from equivalents
Max. and min. transmission		0.9532 and 0.8299
Final R indices [I>2sigma(I)]	R1 = 0.0603, wR2 = 0.0890	R1 = 0.0590, wR2 = 0.1307
R indices (all data)	R1 = 0.1329, wR2 = 0.1112	R1 = 0.1166, wR2 = 0.1572
Largest diff. peak and hole ($eÅ^{-3}$)	0.279 and -0.315	1.042 and -0.581

with $R_1 = \Sigma||F_o|-|F_c||/\Sigma|F_o|$ and $wR_2 = (\Sigma w\,(F_o^2-F_c^2)^2/\Sigma w(F_o^2)^2)^{0.5}$.

Table 7: Structural refinement data for **23** and **26B**

	23	**26B**
Empirical formula	$C_{13}H_{19}N_2OPS$	$C_{29}H_{44}Cl_5N_2O_3P$
Formula weight	282.33	676.88
Temperature (K)	193(2)	173(2)
Crystal system	Monoclinic	Triclinic
Space group	P2(1)/n	P-1
a (Å)	9.3805(3)	10.0784(15)
b (Å)	12.0851(3)	10.7719(17)
c (Å)	12.9740(3)	17.733(3)
α (°)	90	73.226(3)
β (°)	106.231(2)	78.009(3)
γ (°)	90	70.202(3)
Volume ($Å^3$)	1412.17(7)	1721.3(5)
Z	4	2
Density (calculated)(Mg/m^3)	1.328	1.306
Absorption coefficient (mm^{-1})	0.333	0.499
Reflections collected	17555	10459
Independent reflections	3483 [R(int) = 0.0466]	4832 [R(int) = 0.1278]
Absorption correction	Semi-empirical from equivalents	Semi-empirical from equivalents
Max. and min. transmission	1.000000 and 0.824613	
Final R indices [I>2sigma(I)]	R1 = 0.0438, wR2 = 0.1075	R1 = 0.0461, wR2 = 0.0669
R indices (all data)	R1 = 0.0648, wR2 = 0.1181	R1 = 0.1444, wR2 = 0.0904
Largest diff. peak and hole ($eÅ^{-3}$)	40.345 and -0.256	0.233 and -0.210

with $R_1 = \Sigma||F_o|-|F_c||/\Sigma|F_o|$ and $wR_2 = (\Sigma w\,(F_o^2-F_c^2)^2/\Sigma w(F_o^2)^2)^{0.5}$.

Table 8: Structural refinement data for **28**

	28
Empirical formula	$C_{18}H_{20}ClN_2O_6PW$
Formula weight	610.63
Temperature (K)	193(2) K
Crystal system	Orthorhombic
Space group	Pbca
a (Å)	9.5289(2)
b (Å)	13.1917(2)
c (Å)	35.3309(6)
α (°)	90
β (°)	90
γ (°)	90
Volume ($Å^3$)	4441.18(14)
Z	8
Density (calculated)(Mg/m^3)	1.826
Absorption coefficient (mm^{-1})	5.429
Reflections collected	75313
Independent reflections	5470 [R(int) = 0.0557]
Absorption correction	Semi-empirical from equivalents
Max. and min. transmission	0.7730 and 0.1721
Final R indices [I>2sigma(I)]	R1 = 0.0325, wR2 = 0.0618
R indices (all data)	R1 = 0.0422, wR2 = 0.0648
Largest diff. peak and hole ($eÅ^{-3}$)	0.969 and -1.617

with $R_1 = \Sigma||F_o|-|F_c||/\Sigma|F_o|$ and $wR_2 = (\Sigma w (F_o^2-F_c^2)^2/\Sigma w(F_o^2)^2)^{0.5}$.

References

[1] D. Vidovic, Z. Lu, G. Reeske, J. A. Moore, A. H. Cowley, *Chem. Commun.* **2006**, 3501.

[2] C. H. Dungan, J. R. V. Wazer, *Compilation of reported F(19) NMR chemical shifts, 1951 to mid-1967*, **1970** *Wiley-Interscience, New York.*

[3] T. Gans-Eichler, D. Gudat, M. Nieger, *Heteroat. Chem.* **2005**, *16*, 327.

[4] G. Reeske, C. R. Hoberg, N. J. Hill, A. H. Cowley, *J. Am. Chem. Soc.* **2006**, *128*, 2800.

[5] H. A. Spinney, I. Korobkov, G. A. DiLabio, G. P. A. Yap, D. S. Richeson, *Organometallics* **2007**, *26*, 4972.

[6] C. J. Carmalt, V. Lomeli, B. G. McBurnett, A. H. Cowley, *Chem. Commun.* **1997**, 2095.

[7] E. H. Amonoo-Neize, S. K. Ray, R. A. Shaw, B. C. Smith, *J. Chem. Soc.* **1965**, 6250.

[8] R. Menye Biyogo, F. Delpech, A. Castel, H. Gornitzka, P. Rivière, *Angew. Chem. Int. Ed. Engl.* **2003**, *42*, 5610.

[9] P. Kilian, A. M. Z. Slawin, *Dalton Trans.* **2007**, 3289.

[10] M. Sanchez, R. Reau, H. Gornitzka, F. Dahan, M. Regitz, G. Bertrand, *J. Am. Chem. Soc.* **1997**, *119*, 9720.

[11] M. Lardon, *J. Am. Chem. Soc.* **1970**, *92*, 5063.

[12] B. A. Trofimov, A. V. Artem'ev, S. F. Malysheva, N. K. Gusarova, *J. Organomet. Chem.* **2009**, *694*, 4116.

[13] J. Hernandez-Dias, A. F. Parra, R. Contreras, *Heteroatom Chem,* **2004**, *15*, 307.

[14] L. C. Pop, N. Katir, A. Castel, L. Silaghi-Dumitrescu, F. Delpech, I. Silaghi-Dumitrescu, H. Gornitzka, D. MacLeod-Carey, N. Saffon, *J. Organomet. Chem.* **2009**, *694*, 1562.

[15] M. J. Pilkington, A. M. Z. Slawin, D. J. Williams, J. D. Woolins, *Main Group. Chem.* **1995**, *1*, 145.

[16] Z. Lu, M. Findlater, A. H. Cowley, *Chem. Commun.* **2008**, 184.

[17] W. W. Wieczorek, J. W. Karolak, M. Mikolajczyk, M. Witczak, W. S. Sheldrick, *Acta Crystallogr., Sect. B Struct. Crystallogr. Cryst. Chem.* **1978**, *34*, 3414.

[18] B. Ziemer, A. Rabis, H. U. Steinberger, *Acta Cryst., Sect. C* **2000**, *C56*, e58.

[19] P. W. Baures, *Acta Cryst., Sect. C* **1991**, *C47*, 2715.

[20] N. Burford, T. M. Parks, B. W. Royan, J. F. Richardson, P. S. White, *Can. J. Chem.* **1992**, *71*, 703.

[21] R. Steudel, *Chemistry of non-metal elements. de Guyter, New York* **1977**.

[22] E. Psilakis, J. C. Jeffery, J. A. McCleverty, M. D. Ward, *J. Chem. Soc., Dalton Trans.* **1997**, 1645.

[23] M. Sanchez, M. R. Mazières, L. Lamandé, R. Wolf, *Multiple Bonds and Low Coordination Chemistry in Phosphorous Chemistry, (Eds: M. Regitz, O. Scherer), Georg Thieme Verlag, Stuttgart* **1990**, 129.

[24] C. A. Caputo, J. T. Price, M. C. Jennings, R. McDonald, N. D. Jones, *Dalton Trans.* **2008**, 3461.

[25] C. K. SooHoo, S. G. Baxter, *J. Am. Chem. Soc.* **1983**, *105*, 7443.

[26] A. Bond, M. Green, S. C. Pearson, *J. Chem. Soc. B* **1968**, 929.

[27] F. Ramirez, M. Nowakowski, J. F. Marecek, *J. Am. Chem. Soc.* **1977**, *99*, 4515.

[28] F. A. Cotton, G. Wilkinson, *Advanced inorganic chemistry, Wiley Interscience, New York* **1988**.

[29] D. Gudat, M. Nieger, E. Niecke, *J. Chem. Soc., Dalton Trans.* **1989**, 693.

[30] E. Gross, K. Jörg, K. Fiederling, A. Göttlein, W. Malish, R. Boese, *Angew. Chem. Int. Ed. Engl.* **1984**, *23*, 738.

[31] M. S. Davies, R. K. Pierens, M. J. Aroney, *J. Organometal. Chem.* **1993**, *458*, 141.

[32] G. M. Bodner, *Inorg. Chem.* **1975**, *14*, 2694.

[33] W. Buchner, W. A. Schenk, *Inorg. Chem.* **1984**, *23*, 132.

[34] G. G. Mather, A. Pidcock, *J. Am. Chem. Soc. A.* **1970**, 1226.

[35] M. S. Davies, M. J. Aroney, I. E. Buys, T. W. Hambley, J. L. Calvert, *Inorg. Chem.* **1995**, *34*, 330.

[36] M. P. Duffy, F. Mathey, *J. Am. Chem. Soc.* **2009**, *131*, 7534.

[37] S. D. Murray, M. J. Aroney, I. E. Buys, T. W. Hambley, *Inorg. Chem.* **1995**, *34*, 330.

[38] D. Gudat, M. Nieger, E. Niecke, *J. Chem. Soc. Dalton. Trans.* **1989**, 693.

[39] J. C. Bailar, H. Itatani, *Inorg. Chem.* **1965**, *4*, 1618.

[40] G. M. Sheldrick, *Acta Cryst.* **1990**, *A46*, 467.

[41] G. M. Sheldrick, *SHELXL-97 Program for Crystal Structure Refinement; University of Göttingen* **1997**.

CHAPTER III

Bridged bis(pnictogenium cations) and bis-germylenes: syntheses, spectroscopic studies and reactivity

RESUME

Dans ce dernier chapitre, nous avons développé l'étude de nouveaux systèmes chélatants: les di-aminotroponimines et di-aminotropones pontées:

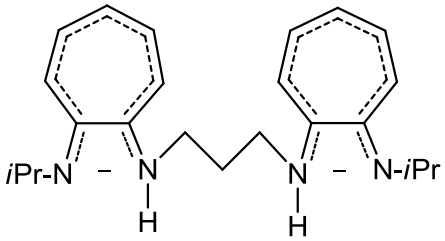

I

Ce nouveau ligand offre deux possibilités de coordination:

- tétrachélation d'un seul métal central
- complexation de deux métaux dans une structure pontée.

Le mode coordination dépend essentiellement de la taille des métaux ou des éléments utilisés. Nous avons testé plusieurs ligands avec des longueurs de chaîne carbonée différente. En série du groupe 15 (P, As et Sb) nous avons toujours obtenu les bis(pnictogenium)cations pontés quelle que soit la voie de synthèse utilisée.

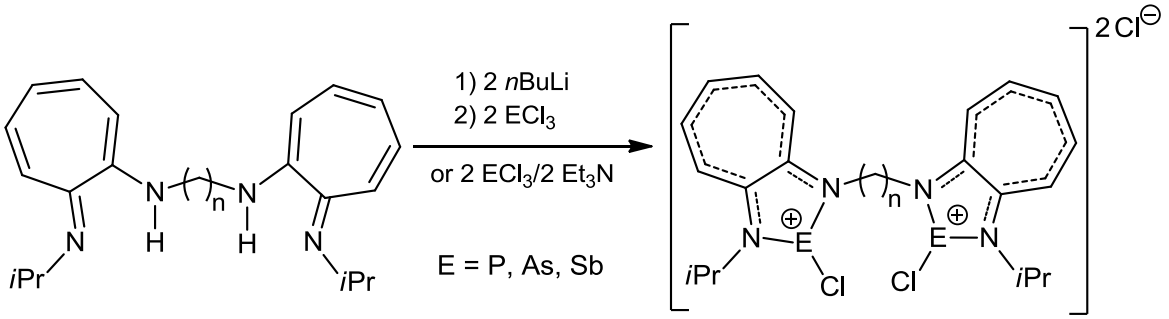

32, n = 2
33, n = 3

37, E = P, n = 2
38, E = As, n = 2
39, E = Sb, n = 2
40, E = P, n = 3
41, E = As, n = 3
42, E = Sb, n = 3

Ces composés sont assez peu solubles dans les solvants usuels et il a été impossible de les séparer du chlorhydrate de triéthylamine ou du chloure de lithium. Cependant ils ont été

parfaitement caractérisés par voie physicochimique (RMN du ^{1}H, ^{13}C et ^{31}P, spectrométrie de masse).

Nous avons ensuite réalisée une extension de ces réactions au germanium et pu ainsi accéder à de nouveaux germylènes.

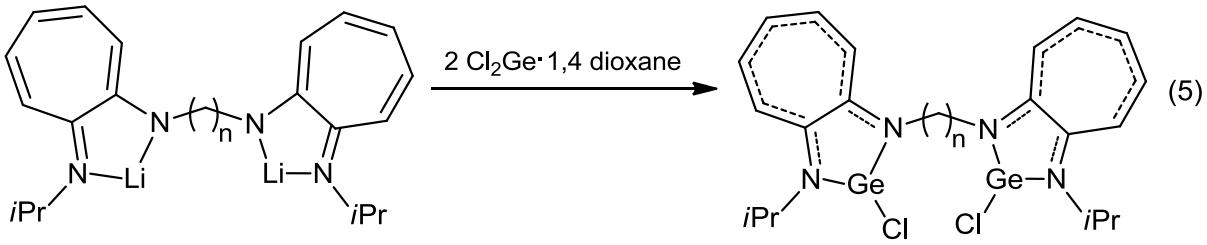

(5)

35, n = 2
36, n = 3

47, n = 2
48, n = 3

Dans ce cas également, nous avons obtenu les formes pontées qui ont pu être isolées et caractérisés. Leur étude par RMN du ^{1}H et du ^{13}C indique une augmentation de la conjugaison des électrons π sur les deux cycles comparativement aux ligands de départ comme cela avait été déjà observé dans le monogermylène correspondant. Des calculs DFT ont montré que la forme pseudo-Trans était légèrement plus stable que la forme pseudo-Cis.

Une étude de leur réactivité a été menée en comparaison avec celle des monogermylènes.

Ces espèces bien que tri-coordinnées conservent leur caractère divalent comme le montrent leurs réactions de cycloaddition avec une *o*-quinone.

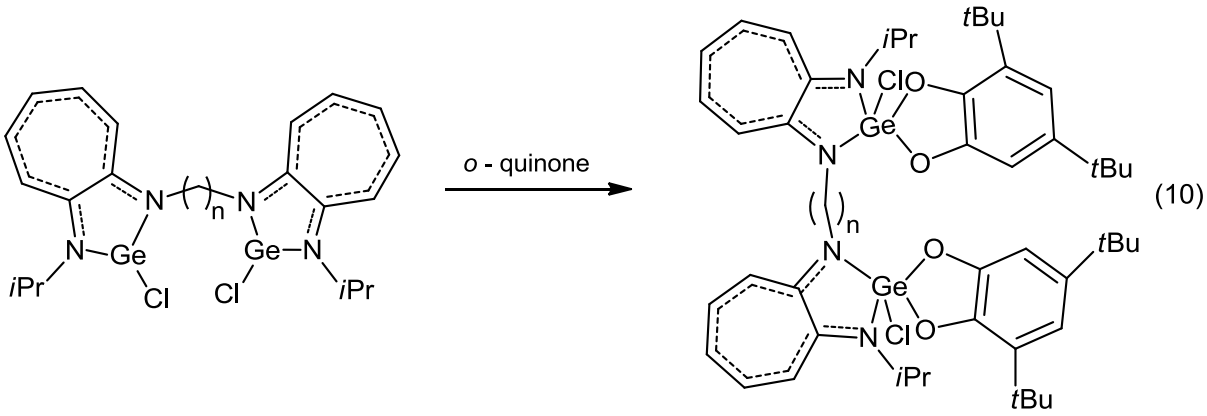

(10)

47, n = 2
48, n = 3

56, n = 2
57, n = 3

Par contre, ces bis-germylènes se sont montrés peu réactifs vis-à-vis d'agents oxydants comme le soufre ou le sélénium alors que les monogermylènes donnent facilement les germa-thiones ou sélénones correspondantes.

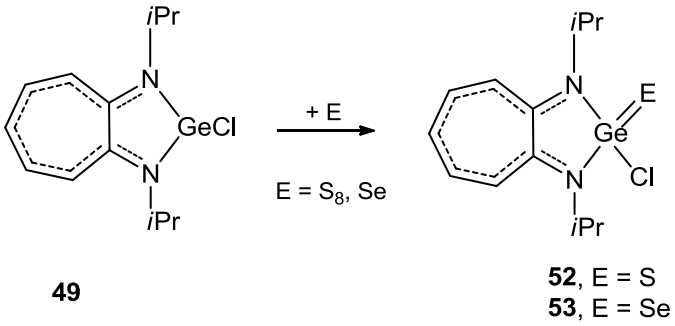

49

52, E = S
53, E = Se

(8)

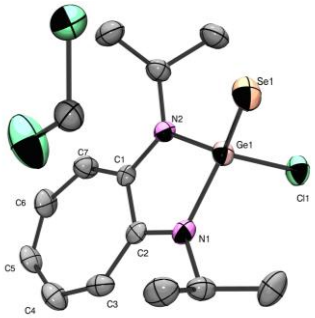

Ces bis-germylènes se sont révélés être de bons ligands vis-à-vis des métaux de transition.

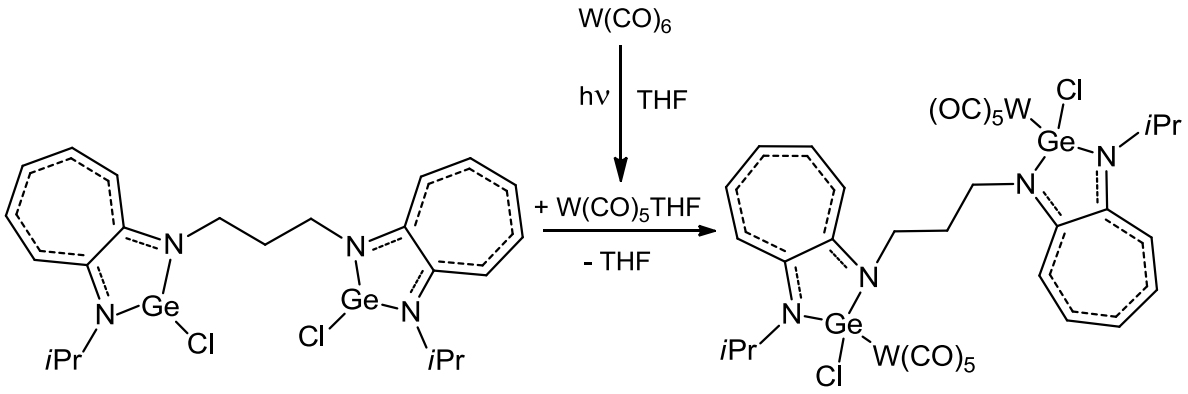

48

58

Un bis-germylène complexé par le tungstène a pu être isolé et sa structure déterminée par diffraction des rayons X. Il présente une conformation de type trans avec les deux unités germaniés de part et d'autre de la chaîne carbonée.

Introduction

Aminotroponiminates are a well known class of ligands which have found extensive use in coordination chemistry as formal substitutes for cyclopentadienyl groups[1-7]. In the first chapter, we have also demonstrated the high potential of this ligand in the stabilization of pnictogenium cations. Recently Roesky[8] has synthesized bridged aminotroponiminates (**I**, Chart 1) and tested them as "alternatives" for *ansa*-metallocenes in the lanthanide series[9-12].

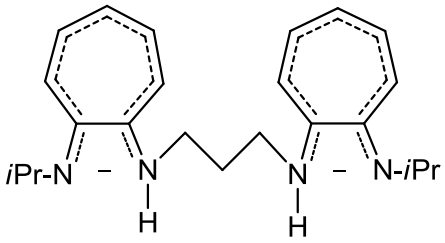

I

Chart 1

This new bridged bis(amino-imino) ligand exhibits two different coordination modes:

- tetradentate chelation of one metal center,
- complexation of two metals in the bridged structure.

It was demonstrated that the coordination mode depended mainly on the size of the ion radius of the metal atoms or chemical element used. For example, indium and gallium gave the chelated form[13], while the metal-bridging coordination was observed in the case of the smaller aluminium ion radius (**II**, **III**, Chart 2)[14].

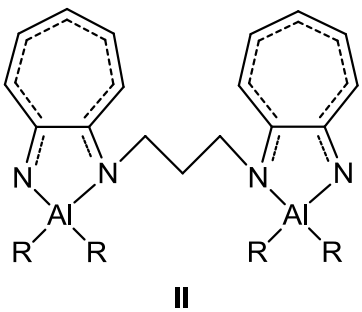

II

R = Me, Et, *i*Bu

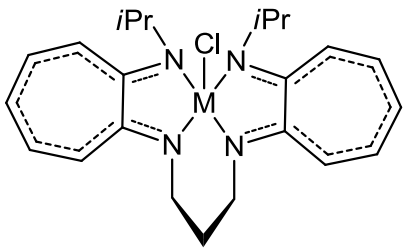

III

M = Ga, In

Chart 2

Up to date, the coordination chemistry of this bridged di-aminotroponiminate ligand remains totally unexplored for group 14 and 15 elements.

In this chapter, we describe the synthesis, characterization of novel bisphosphenium, arsenium and stibenium cations incorporating this ligand and the bridged di-aminotroponate group where the imino function was replaced by a carbonyl group. An extension to bis-germylenes will be also developed.

3.1 Bridged bis(pnictogenium cations) (P, As, Sb)

3.1.1 Synthesis of ligand precursors

In order to study the influence of the bridge length on the stability of new compounds we decided to prepare ligands with different bridge sizes. The direct synthesis of the bridged chelating ligands, a system in which two aminotroponimine moieties are linked together (1,2-di(2-(N-isopropylamino)troponimine)ethane (**32**) or 1,3-di(2-(N-isopropylamino)troponimine) propane (H_2[(*i*Pr)TP)] (**33**)) was performed starting from 2-(N-isopropylamino)-tropone **1** (Equation 1)[6]. Treatment of **1** with $Et_3O{\cdot}BF_4$, Et_3N, and 1,2-diaminoethane or 1,3-diaminopropane leads to the desired product **32** or **33** as yellow solids in 46.5 % and 78.6 % yields, respectively.

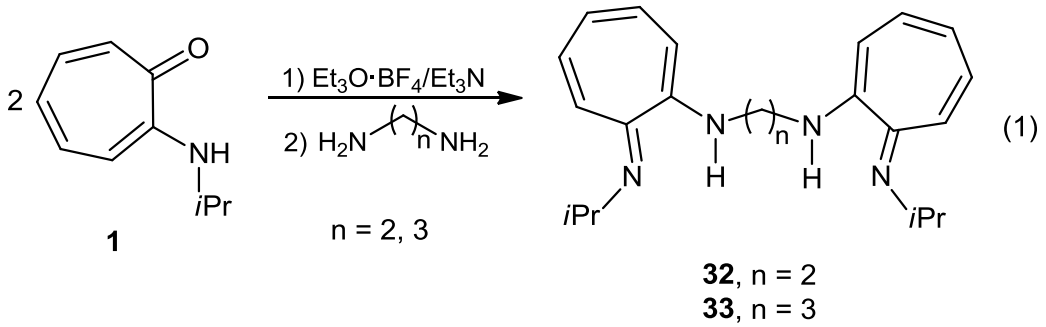

Both ligands were characterized by ^{1}H and ^{13}C NMR spectroscopy. The ^{1}H NMR spectra show a singlet at 3.65 ppm for the methylene groups of compound **32** and two well-defined signals for the propane bridge, a quintet at 2.14 ppm for the central CH_2 and a triplet for the CH_2N at 3.43 ppm respectively for compound **33** indicating the presence of a symmetric species in solution. For the seven-membered cycle and the isopropyl protons, no

noticeable difference can be seen between the bridged ligands and the aminotroponimine **2**; the same observation can be made for the corresponding carbon signals in ^{13}C NMR.

The bis-aminotropone **34** was synthesized using the tropolone tosylate as starting reagent (Equation 2). The latter was then treated with 1,3-diaminopropane and Et_3N giving **34** as yellow crystals after purification by chromatography on silica gel (eluent: chloroform / ether 5 / 1) with a yield of 50 %[15].

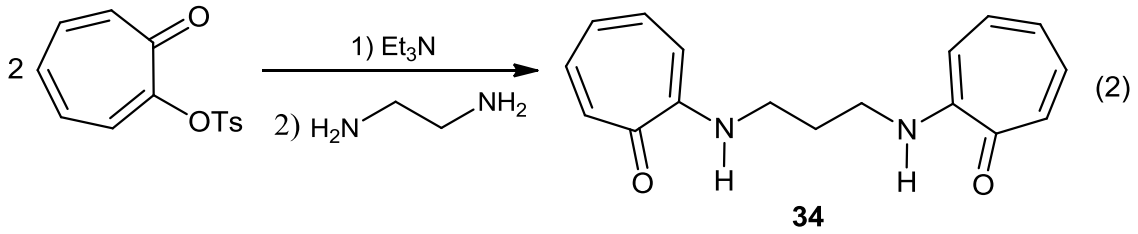

34 (2)

In the ^1H NMR spectrum, the propane bridge protons appear as two well-defined sets of multiplets, a quintet at 2.11 ppm for the central CH_2 and a triplet at 3.40 ppm for the CH_2N groups indicating the presence of a symmetric species in solution as previously observed for **32** and **33**. In the ^{13}C NMR spectrum, it can be mentioned the signal at 176.64 ppm characteristic of a carbonyl group.

These ligands **32** - **34** are very soluble in almost all organic solvents, including saturated hydrocarbons such as n-pentane or hexanes.

3.1.2 Synthesis of the dilithiated ligands salt

Deprotonation of 1,2-di(2-(N-isopropylamino)troponimine)ethane **32** and 1,3-di(2-(N-isopropylamino)troponimine)propane **33**, with *n*BuLi in hexanes affords the dilithium salts **35** and **36** as orange, air-sensitive crystalline solids which were characterized by ^7Li, ^1H and ^{13}C NMR spectroscopy (Equation 3).

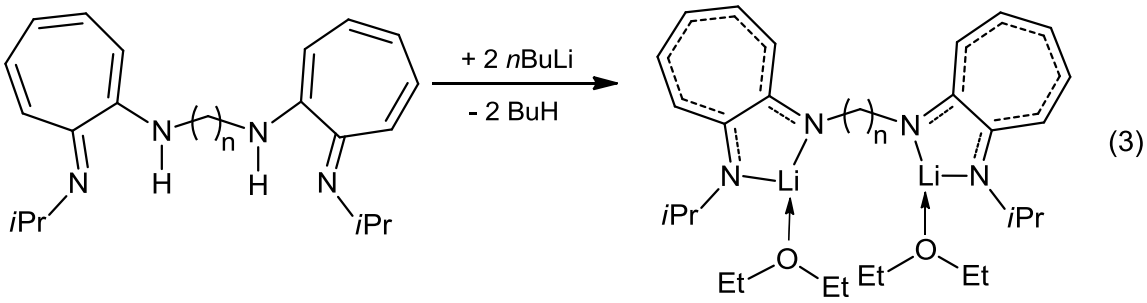

32, n = 2
33, n = 3

35, n = 2
36, n = 3

(3)

The ^{1}H NMR spectra of both lithiated salts, **35** and **36**, show shielded signals for the C*H* groups of the 7-membered ring compared to the starting ligands. Moreover, the ^{13}C NMR signals of the C_2 and C_8 carbons bonded to nitrogen atoms appear at about 10 ppm downfield compared to the corresponding carbons in the free ligands. Similar trends have been observed both for $K_2[(i\text{Pr})\text{TP}]$[16] and for $[(i\text{Pr})_2\text{ATI}]\text{Li}(\text{THF})_2$[5]. This can be explained by a weak delocalization of the positive charge on the 7-membered ring (Tables 1 and 2).

The two sets of multiplets at 1.07 and 3.33 for **35** and at 1.16 and 3.43 ppm for **36** can be assigned to the diethyl ether hydrogens. It is difficult to compare these with the chemical shift values of 1.12 and 3.38 ppm of free diethyl ether in THF[17]. It seems that an exchange of diethyl ether by THF probably occurs in solution.

^{7}Li nucleus has an isotopic abundance of 92.41 %, a spin of ½, is highly sensitive and yields broad signals in NMR due to its high quadrupolar moment. The chemical shift range is usually rather small from -16 to 11 ppm[18-19].

For **35** and **36** the observed lithium resonances are broad with signals at 1.64 and 1.66 ppm (Figure 1) not far from the value obtained for $[(Me_3Si)_2NLi]$ (1.10 ppm)[18].

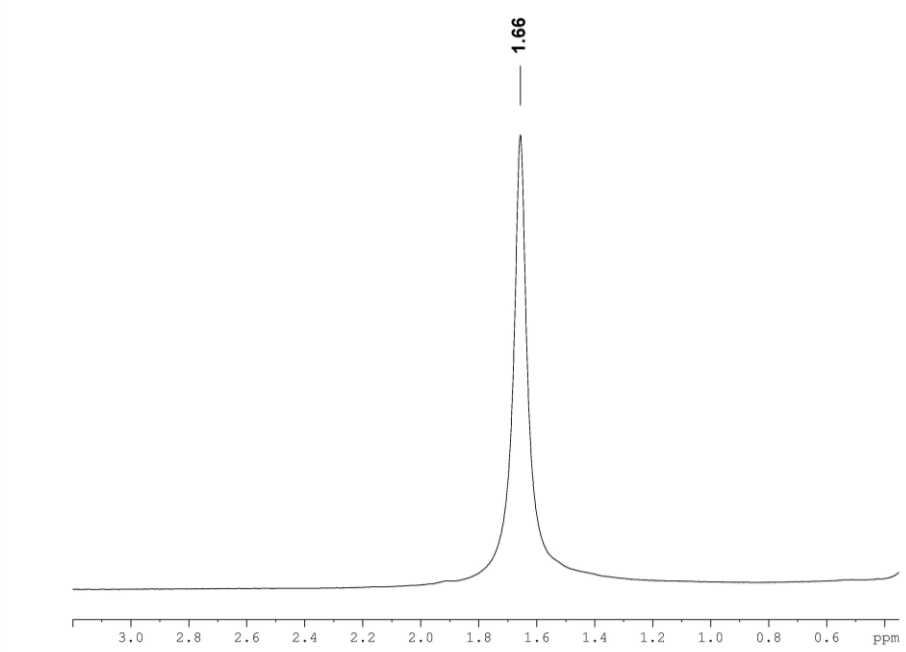

Figure 1: ^{7}Li NMR spectrum for **36** in THF, a broad signal can be seen

Table 1: Proton NMR chemical shifts for **35** and **36** (in ppm, J in Hz, in THF d_8)

	35	**36**
$(CH_3CH_2)_2O$	1.07 (t, $^3J_{HH}$ = 6.9)	1.16 (t, $^3J_{HH}$ = 7.0)
CH-CH_3	1.07 (d, $^3J_{HH}$ = 6.2)	1.18 (d, $^3J_{HH}$ = 6.2)
CH_2	-	2.04 (quint, $^3J_{HH}$ = 7.5)
$(CH_3CH_2)_2O$	3.33 (q, $^3J_{HH}$ = 7.0)	3.43 (q, $^3J_{HH}$ = 7.0)
NCH_2	3.47 (s)	3.50 (t, $^3J_{HH}$ = 7.0)
CH-CH_3	3.71 (sept, $^3J_{HH}$ = 6.2)	3.80 (sept, $^3J_{HH}$ = 6.2)
C_7H_5	5.45 (t, $^3J_{HH}$ = 8.9)	5.56 (t, $^3J_{HH}$ = 8.8)
C_7H_5	5.89 (d, $^3J_{HH}$ = 11.4)	5.95 (d, $^3J_{HH}$ = 11.2)
C_7H_5	5.97 (d, $^3J_{HH}$ = 11.4)	6.03 (d, $^3J_{HH}$ = 11.3)
C_7H_5	6.42 (ps.t)	6.50 (ps.t)

Table 2: Carbon-13 NMR chemical shifts for **35** and **36** (in ppm, in THF d_8)

	35	**36**
$(CH_3CH_2)_2O$	12.60	16.01
(CH-CH_3)	21.11	23.32
CH_2	-	32.69
N-CH_2	45.67	49.49
CH-CH_3	51.31	47.70
$(CH_3CH_2)_2O$	63.23	63.22
$C_{3,7}$	104.31 and 103.89	105.96 and 106.19
C_5	105.23	107.22
$C_{4,6}$	129.62 and 129.22	131.25 and 131.60
$C_{2,8}$	160.77 and 162.00	162.90 and 164.11

The solid-state structure of **36** was established by single crystal X-ray diffraction. In the solid state, each lithium atom is surrounded by two nitrogen atoms of an aminotroponiminate unit forming a five-membered LiN_2C_2 ring and by one diethyl ether molecule (Figure 2). The N–Li bond lengths: 1.997(3) and 2.031(4) Å, 1.998(3) and 2.002(3) Å are slightly longer than those of chiral aminolithiium compound [{(LiTHF)}{(*SS*)(*i*Pr$_2$ATI)$_2$diph}] (diph = 1,2-(*S*,*S*)-diamino-1,2-diphenylethane): 1.976(6), 1.951(6) Å and 1.932(6), 1.992(6) Å (**IV**, Chart 3)[20]. Moreover, the flexibility of the propane bridge allows folding of the molecule and further interaction of a lithium with the nitrogen atom of the neighbouring aminotroponiminate unit. These N–Li bond lengths (2.221(4) and 2.295(4) Å) are significantly smaller than those observed for chiral aminolithien (2.510(6) and 2.456(6) Å)[20] indicating stronger interactions.

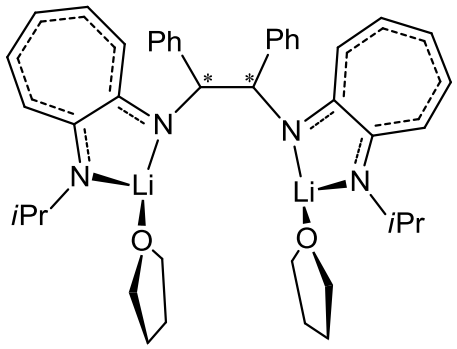

IV

Chart 3

The N-C distances in the LiN_2C_2 cycle [1.324(2), 1.322(2), 1.320(2), 1.322(2) Å] are between that of a carbon-nitrogen single bond [1.342(3) Å] and that of an imine bond [1.314(3) Å] of the starting ligand[6]. The five- and seven-membered rings are not in the same plane but the two aminotroponiminato units are almost parallel.

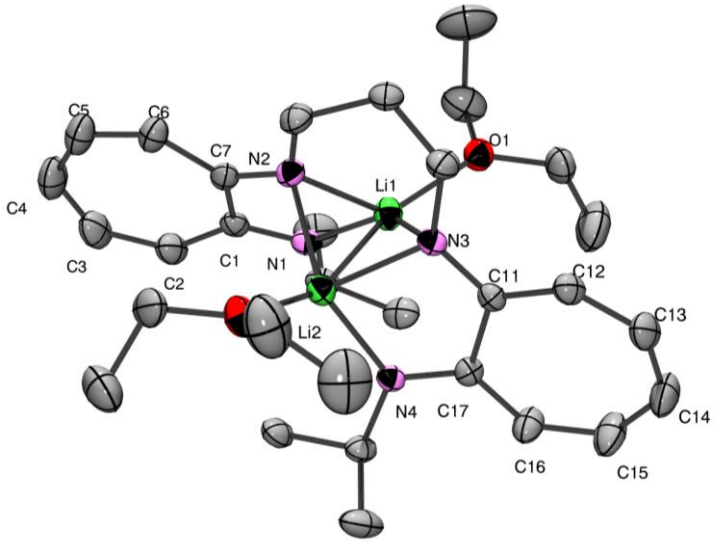

Figure 2: Molecular structure of compound **36** (30 % probability level for the thermal ellipsoids). All H atoms have been omitted for clarity. Selected bond distances [Å] and angles [°] are: Li(1)-N(2) 1.997(3), Li(1)-N(1) 2.031(4), Li(1)-N(3) 2.295(4), Li(2)-N(3) 1.998(3), Li(2)-N(4) 2.002(3), Li(2)-N(2) 2.221(4), C(1)-C(2) 1.433(3), C(1)-C(7) 1.511(3), C(2)-C(3) 1.384(3), C(3)-C(4) 1.380(4), C(4)-C(5) 1.371(4), C(5)-C(6) 1.379(3), C(6)-C(7) 1.423(3), C(11)-C(12) 1.425(2), C(11)-C(17) 1.508(2), C(12)-C(13) 1.385(3), C(13)-C(14) 1.370(3), C(14)-C(15) 1.387(3), C(15)-C(16) 1.378(3), C(16)-C(17) 1.427(3); N(2)-Li(1)-N(1) 79.41(13), N(2)-Li(1)-N(3) 83.52(13), N(1)-Li(1)-N(3) 141.90(18), N(3)-Li(2)-N(4) 80.29(13), N(3)-Li(2)-N(2) 85.42(13), N(4)-Li(2)-N(2) 129.69(17).

The salts of these new ligands are then used for the preparation of the phosphorus, arsenic and antimony compounds.

3.1.3 Synthesis of the bis-cations of P, As and Sb

The reactions of bridged diaminotroponimines $H_2\{(i\text{PrATI})_2(CH_2)_n\}$ with ECl_3/Et_3N in toluene or nBuLi/ECl_3 in Et_2O led to bridged di-pnictogenium products of composition $[\{(i\text{PrATI})_2(CH_2)_n\}(ECl_2)_2]$ [n = 2, E = P (**37**), As (**38**), Sb (**39**)] and n = 3, P (**40**), As (**41**), Sb (**42**)] (Scheme 1).

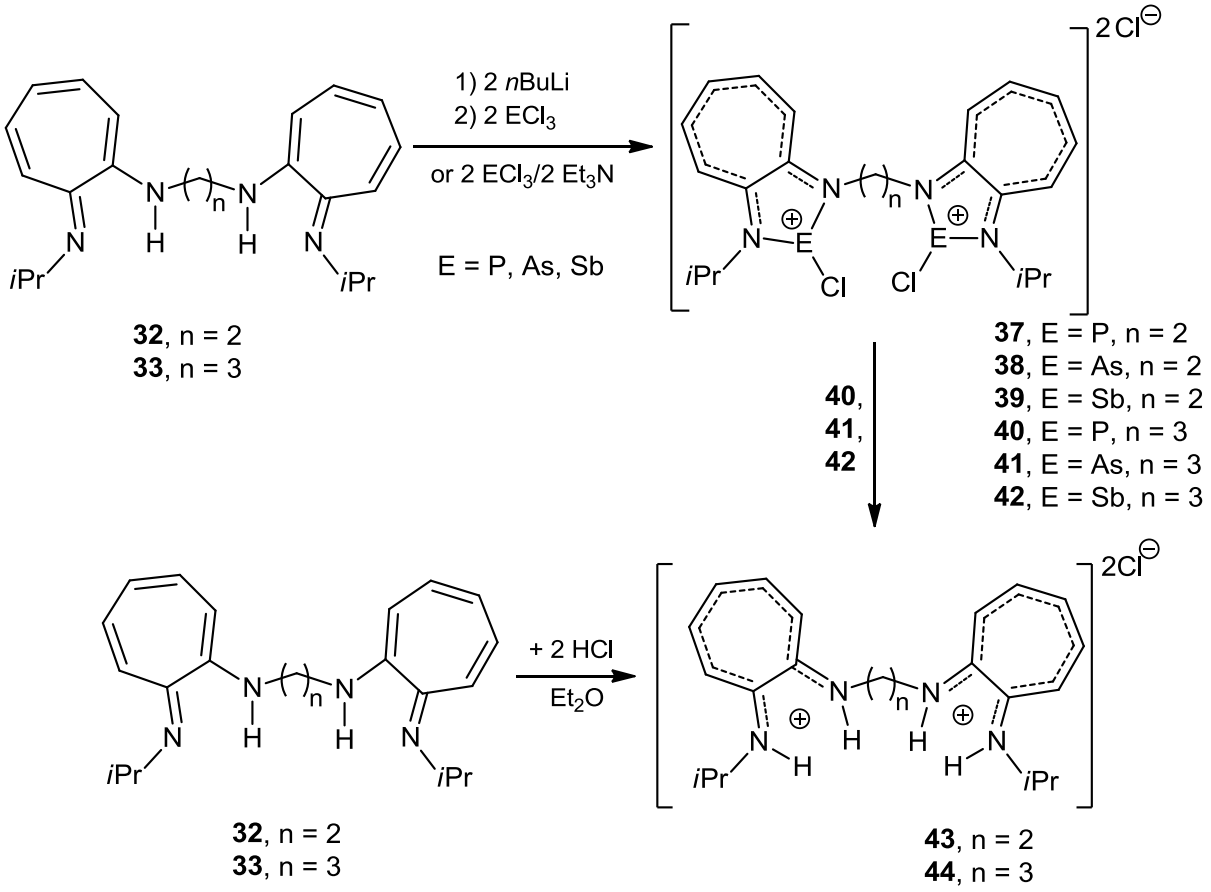

Scheme 1

Compounds **37** – **42** were obtained as yellow crystalline solids very slightly soluble in organic solvents with an appreciable sensitivity towards air and moisture. They cannot be separated from the salts (Et_3N·HCl or LiCl) and isolated in a pure state. Moreover, as in the case of antimony aminotroponiminato derivative **10**, a slow decomposition in solution was observed both for **40**, **41** and **42** leading to the corresponding salt **44**.

In order to determine the unknown products which are present in the reaction mixture of **37**, **38** and **39** we also synthesized the corresponding ligand salt **43**, but, surprisingly, the signals that correspond for the salt ligand does not match with the signals found for the impurities.

However, all the compounds could be perfectly characterized by standard spectroscopic techniques. The ^{1}H and ^{13}C NMR spectra point to a symmetrical coordination of the two aminotropiniminato anions in solution highlighted by the equivalence of the methylene groups of the bridging chain. The signals of the isopropyl C*H* proton are well resolved into a septuplet for **38**, **41** and **42** but appear as a complex multiplet for **37**, **39** and

40. They have shifted downfield [δ = 4.47 - 4.60 (**37**), 4.43 (**38**), 3.96 - 4.07 (**39**), 4.40 - 4.60 (**40**), 4.42 (**41**), 4.42 (**42**) ppm] compared to that of the free ligands **32** (δ = 3.76 ppm) and **33** (δ = 3.77 ppm) (Tables 3 and 4). Analogously, the resonances of the ring protons have significantly shifted downfield in agreement with increased conjugation of π-electrons on the cycles.

When the ^{1}H NMR and ^{13}C NMR spectra for **40** were recorded at high magnetic field (500 MHz for ^{1}H and 125.75 MHz for ^{13}C), a long range coupling constant between H_5-P and C_5-P can be observed ($^{6}J_{HP}$ = 2.9 Hz, $^{5}J_{CP}$ = 4.6 Hz). The P-decoupled Carbon-NMR spectra show, as expected, single signals for all the carbon atoms.

The ^{31}P NMR spectra show close resonances at 133.80 ppm (134.62 ppm when recorded in CD_2Cl_2) for **37** and 137.22 ppm for **40**. These values are similar to those previously observed for **6a**.

Table 3: Proton NMR chemical shifts for **32**, **43**, **37**, **38**, **39**, **33**, **44**, **40**, **41** and **42** (in ppm, J in Hz, in $CDCl_3$)

	CH_3	CH_2	N CH_2	CH	C_7H_5
32	1.19 (d, $^3J_{HH}$ = 6.3)	-	3.65 (s)	3.76 (sept, $^3J_{HH}$ = 6.2)	6.07 (t, $^3J_{HH}$ = 9.3), 6.17 (d, $^3J_{HH}$ = 10.7), 6.41 (d, $^3J_{HH}$ = 11.2), 6.69 (ps.t)
43	1.50 (d, $^3J_{HH}$ = 6.4)	-	4.12 (s)	3.98 (sept, $^3J_{HH}$ = 6.2)	6.92-7.07 (m, 4H), 7.48 (ps.t, 2H), 7.62-7.75 (m, 4H)
37	1.72 (d, $^3J_{HH}$ = 6.4)	-	4.95-4.99 (m)	4.47-4.60 (m)	7.75 (t, $^3J_{HH}$ = 9.7), 7.90 (d, $^3J_{HH}$ = 11.3), 8.12 (ps.t, 2H), 8.30 (ps.t), 9.23 (d, $^3J_{HH}$ = 10.6)
38	1.75 (d, $^3J_{HH}$ = 6.5)	-	4.21-4.33 (m)	4.43 (sept, $^3J_{HH}$ = 6.5)	7.52 (t, $^3J_{HH}$ = 10.3), 7.62 (d, $^3J_{HH}$ = 10.5), 7.77 (t, $^3J_{HH}$ = 10.3), 8.00 (t, $^3J_{HH}$ = 10.4), 8.34 (d, $^3J_{HH}$ = 10.9)
39	1.49 (d, $^3J_{HH}$ = 6.4)	-	4.08-4.15 (m)	3.96-4.07 (m)	7.47-7.59 (m, 4H), 7.86 (ps.t, 2H), 8.35 (ps.d, 2H), 8.95-9.01 (m, 2H)
33	1.21 (d, $^3J_{HH}$ = 6.3)	2.14 (quint, $^3J_{HH}$ = 6.9)	3.43 (t, $^3J_{HH}$ = 6.9)	3.77 (sept, $^3J_{HH}$ = 6.3)	6.05 (t, $^3J_{HH}$ = 9.3) 6.18 (d, $^3J_{HH}$ = 10.7), 6.32 (d, $^3J_{HH}$ = 11.3), 6.63-6.72 (m)
44	1.49 (d, $^3J_{HH}$ = 6.3)	2.58 (ps.q)	3.77 (ps.t, $^3J_{HH}$ = 6.9)	3.96 (sept, $^3J_{HH}$ = 6.3)	6.85-7.00 (m), 7.29 (d, $^3J_{HH}$ = 11.1), 7.45 (t, $^3J_{HH}$ = 10.3), 7.59 (t, $^3J_{HH}$ = 10.2)
40	1.71 (d.d, $^3J_{HH}$ = 6.6 Hz, $^4J_{HP}$ = 1.5)	2.75 (quint, $^3J_{HH}$ = 7.0)	4.68 (t.d, $^3J_{HH}$ = 7.6, $^3J_{HP}$ = 12.3)	4.40-4.60 (m)	7.87 (d, $^3J_{HH}$ = 11.0), 8.08 (d, $^3J_{HH}$ = 10.0), 8.33 (t, $^3J_{HH}$ = 9.9), 9.60 (d.d,$^3J_{HH}$ = 10.9, J_{HP} = 2.1)
41	1.75 (d, $^3J_{HH}$ = 6.4)	2.86 (quint, $^3J_{HH}$ = 7.1)	4.29 (t, $^3J_{HH}$ = 7.2)	4.42 (sept, $^3J_{HH}$ = 6.5)	7.25-7.35 (m), 7.70-7.90 (m)
42	1.76 (d, $^3J_{HH}$ = 6.4)	2.87 (quint, $^3J_{HH}$ = 7.1)	4.29 (t, $^3J_{HH}$ = 7.2)	4.42 (sept, $^3J_{HH}$ = 6.5)	7.27-7.34 (m), 7.67-7.89 (m)

Table 4: Carbon-13 NMR chemical shifts for **32**, **43**, **37**, **38**, **33**, **44**, **40**, **41** and **42** (in ppm, in $CDCl_3$)

	CH_3	CH_2	NCH_2	CH	$C_{3,7}$	C_5	$C_{4,6}$	$C_{2,8}$
32	22.72	-	48.18	45.06	107.84 and 112.58	117.42	133.14 and 132.63	151.22 and 154.00
43	21.36	-	42.04	47.48	117.16 and 118.59	127.09	139.77 and 140.68	150.77 and 151.36
38*	21.40	-	43.46	49.83	121.67 and 123.05	136.80	140.67 and 141.06	156.66 and 158.38
37	21.43 (d, $^3J_{CP}$ = 12.2)	-	43.22 (d, $^2J_{CP}$ = 25.9)	50.74 (d, $^2J_{CP}$ = 12.6)	125.60 and 128.20	135.98	143.09 and 144.64	155.32 and156.34
33	22.84	31.14	45.47	45.18	108.07 and 112.21	117.44	132.63 and 133.12	151.27 and 153.56
44	20.87	34.70	42.18	47.07	116.91 and 117.87	126.56	139.62 and 139.89	150.34 and 150.90
40	21.68 (d, $^3J_{CP}$ = 12.4)	27.33	43.33 (d, $^2J_{CP}$ = 18.9)	50.58 (d, $^2J_{CP}$ = 12.6)	125.43 (d, $^3J_{CP}$ = 5.2) and 128.89 (d, $^3J_{CP}$ = 5.1)	135.99	142.93 and 144.90 (d, $^4J_{CP}$ = 4.2)	154.99 (d, $^2J_{CP}$ = 12.8) and 157.21 (d, $^2J_{CP}$ = 12.6)
41	21.98	27.15	44.80	50.91	122.41 and 123.68	131.59	140.42 and 141.48	157.35 and 159.71
42	21.62	25.11	42.02	47.73	117.18 and 118.96	127.31	139.88 and 141.06	150.92 and 151.67

* recorded in DMSO d8

Starting from bis-aminotropone **34**, only the dehydrochlorination coupling reaction was carried out giving the bridged compounds **45** and **46** as yellow solids (Equation 4).

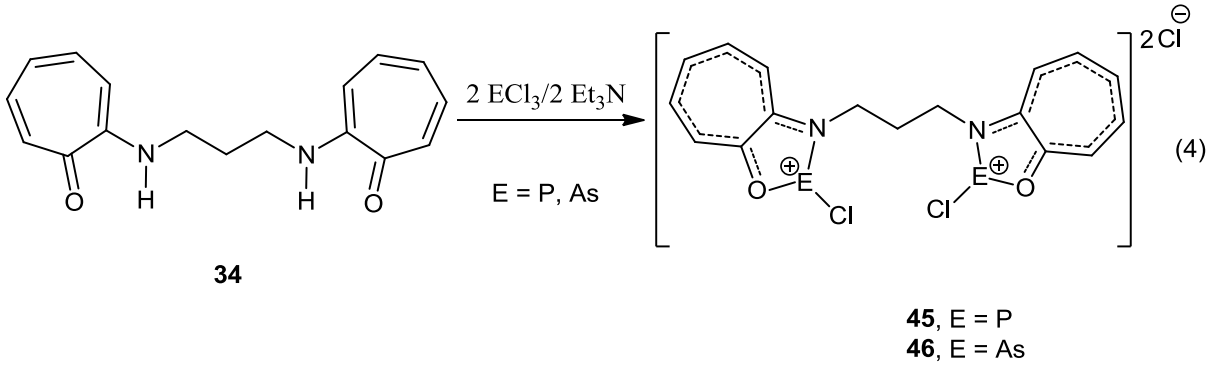

34

45, E = P
46, E = As

In the ^{1}H NMR spectra, the aromatic protons could not be distinguished; in both cases a large multiplet is present for all 10 hydrogen atoms, which are more deshielded for **45** than for **46** compared with the neutral ligand **34**. The low solubility of **45** in halogeno deuterated solvents prevented us to record the ^{13}C NMR spectra.

The use of these ligands was then extended to the stabilization of low coordinated group 14 species.

3.2 Bis-germylenes

Germylenes are heavier analogues of carbenes[21-25], where the germanium atom exists in a formal divalent oxidation state[26-28]. The germylenes are expected to be of great importance in fundamental and applied chemistry as a result of their differences and similarities to carbenes.

The dichlorogermylene complex Cl_2Ge·1,4-dioxane[29-30] is known to be stable and isolable compared to the very transient CCl_2.

In contrast to the carbon atom, the heavier germanium atom has a low ability to form hybrid orbitals. The germanium atom therefore prefers the $4s^2 4p^2$ valence electron configurations in its divalent species[31-32]. Since two electrons remain as a lone pair in the 4s orbital, the ground state of H_2Ge: is a singlet, unlike the case of H_2C:, where the ground state is a triplet. Substituted germylenes generally have a singlet ground state with a vacant p-orbital and a lone pair of valence orbitals. This extremely high reactivity must be due to their vacant p-orbitals, since 6 valence electrons are less than the 8 electrons of the “octet rule”.

Their lone pair is expected to be inert due to its high s-character. In order to stabilize germylenes enough to be isolated, either some thermodynamic and/or kinetic stabilization of the reactive vacant p-orbital is required. A range of "isolable" germylenes has been synthesized through the thermodynamic stabilization of coordinating Cp* ligands, the inclusion of heteroatoms such as N, O, and P, and/or the introduction of kinetic stabilization using bulky substituents[33].

Knowledge about bis-germylenes is limited to some cyclic (the first synthesis and characterization of such a compound, the trimeric species (GeNAr), where Ar = 2,6-*i*-$Pr_2C_6H_3$, was described in 1990)[34] or acyclic (stabilized using a bulky ligand such as -$N(SiMe_3)_2$)[35] derivatives.

In this context, our group reported the preparation of *p*-phenylene and *p*-biphenylene-bridged germanocenes where the germanium(II) atoms are linked to the cyclopentadienyl ring (**V**, Chart 4)[36].

More recently, the preparation and coordination chemistry of bis-germylenes containing two benzannulated NHGe (N-heterocyclic germylene) units that can coordinate to transition metals in a chelating fashion (**VI**, Chart 4) were described by Zabula et al.[37-39]. These studies only involved N-heterocyclic germylenes featuring two normal covalent bonds.

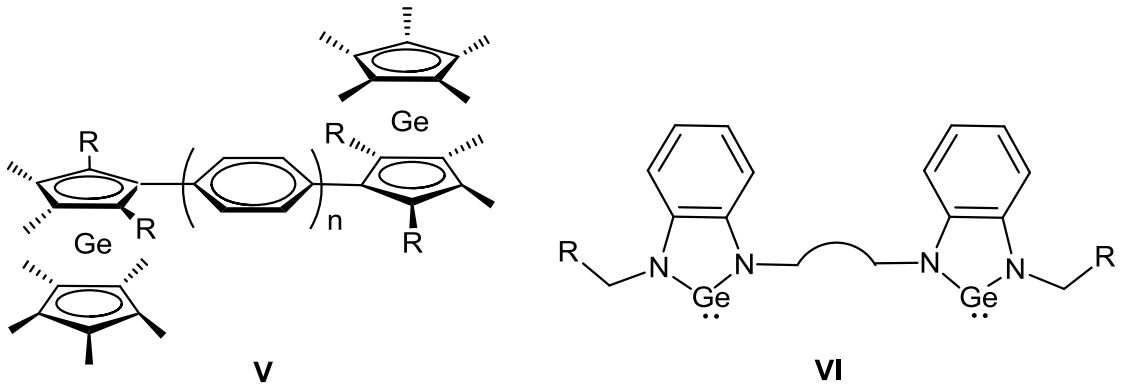

V **VI**

R = H, n = 1
R = CH_3, n = 1
R = CH_3, n = 2

= $C(CH_3)_2$, R = *t*Bu
= CH_2CH_2, R = Me, *t*Bu
= $CH_2CH_2CH_2$, R = Me, *t*Bu
= C_6H_4-1,2, R = *t*Bu
= C_6H_4-1,3, R = *t*Bu

Chart 4

3.2.1 Synthesis of monogermylenes and bis-germylenes

Bis-germylenes **47** and **48** were prepared by reaction of the di-lithiated derivatives **35** and **36** with $Cl_2Ge{\cdot}1,4$-dioxane in diethylether at -78°C (Equation 5). The orange-yellow products were isolated in good yields (42 % and 56 % respectively) and fully characterized.

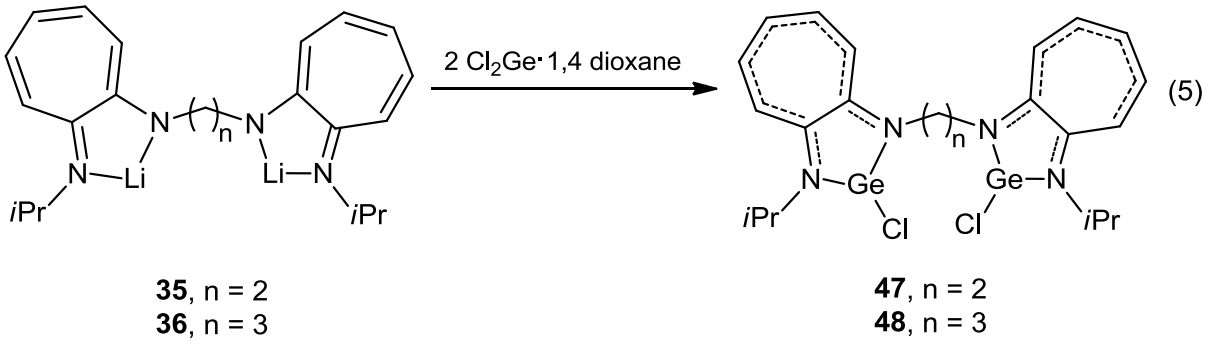

(5)

35, n = 2
36, n = 3

47, n = 2
48, n = 3

The ^{1}H NMR spectra show overlapped signals for methylene and methine groups at 4.10-4.30 ppm for the compound **47** and two well-defined signals for the propane bridge, a quintet at 2.53 ppm for the central CH_2 and a triplet for the CH_2N at 3.89 ppm for compound **48**. The signals of the isopropyl CH_3 protons of **47** and **48** show a downfield shift [δ = 1.55 (**47**), 1.60 (**48**) ppm] compared to that of the neutral ligand **32** (δ = 1.19 ppm) and **33** (δ = 1.21 ppm). The same trend can be seen for the the isopropyl C*H* protons of **47** and **48** which show a downfield shift [δ = 4.30 (**47**), 4.29 (**48**) ppm] compared to those of the free ligand **32** (δ = 3.76 ppm) and **33** (δ = 3.76 ppm). The seven-membered ring protons could not be well assigned for **47** and **48**, but in both cases the signals are deshielded compared with the starting ligands **32** and **33** as previously observed for the group 15 analogs (compounds **37** - **42**). For the aromatic and the isopropyl protons, no noticeable difference can be seen between **47** and **48**; the same observation can be made for the carbon signals in ^{13}C NMR.

Besides the NMR investigations, both **47** and **48** were characterized by EI or CI mass spectrometry. For both compounds, molecular ion peaks and their characteristic patterns were observed: [M^+] at 564 and 578 amu respectively. The loss of chlorine atom is then the main fragmentation, [M^+ - Cl] at 529 and 543 amu, respectively. These bis-germylens are air and moisture-sensitive and correct elemental analyses cannot be obtained. However for compound **48** we were able to determine the high resolution mass spectrometric weight (578.0307 amu). The measured mass agrees to 4.49 ppm with the calculated exact mass.

Concerning the aminotroponate units, their chelating properties remain totally unexplored in the germanium series not only for bis-germylenes but for monogermylene as well. In a first step, we prepared the chlorogermylene **50** by treatment of $Cl_2Ge{\cdot}1,4$-dioxane with the lithium salt of the aminotropone **1** using the experimental procedures described for the germylene containing aminotroponiminate ligand **49** (1:1 molar ratio in diethyl ether at low temperature)[40] (Equation 6). These yellow products were isolated in good yields (82-84 %).

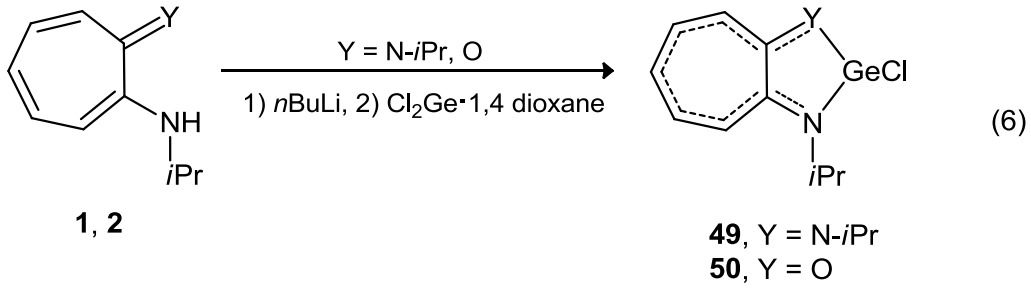

1, **2**

49, Y = N-*i*Pr
50, Y = O

(6)

Depending on the deuterated solvent used, the analysis of ^{1}H NMR spectrum of **50** shows a single doublet for the methyl of isopropyl groups like in the case of **49** when CD_3Cl is employed or two different large signals when C_6D_6 is utilized. One signal for the C*H* group can be also observed for both compounds **49** and **50**. While for compounds **49** the aromatic protons of the 7-membered ring appear as three well separated multiplets, for **50**, due to the lack of symmetry, four well distinct multiplets can be seen. It is to note a downfield shift of these protons relative to the starting ligands **1** and **2** for compounds **49** and **50** which would be consistent with an increased conjugation in the π electrons for the two cycles, the 7-membered ring and the 5-membered ring newly formed by the intramolecular complexation Y→Ge[41]. In the ^{13}C NMR spectra, the identification of the carbon atoms of the seven-membered chelated ring were made according to the literature[6, 42]. The deshielding of these carbons is observed for **49** and **50** confirming the phenomenon of conjugation. It is also worth noting the presence of a signal at 175.26 ppm for **50** corresponding to a carbonyl group. Thus, it seems that both chelated and non-chelated forms coexist in solution.

Then, in a similar fashion, the reaction of the lithium salt of **34** with the dichlorogermylene yielded the bis-germylene **51** as a yellow solid. This later was less stable in solution than both germanium(II) derivatives **48** and **50** but it could be kept for several months at low temperature in the solid state (Equation 7).

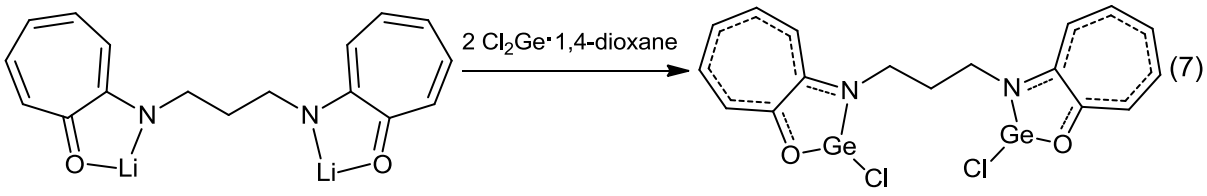

(7)

51

Compared with the starting ligand **34**, all the signals for **51** are deshielded in ^{1}H and ^{13}C NMR spectra. In both cases, for the neutral ligand and the bis-germylene, the signals for CH_2 are present in the form of quintets at 2.11 and 2.56 ppm, respectively, and for NCH_2 triplets are observed at 3.40 and 3.88 ppm in ^{1}H NMR spectra.

In the mass spectrum the peak [M^+ - HCl] at 461 amu with the correct isotopic distribution for a germanium compound can be seen.

3.2.2 Computational studies

In order to get further insight about the molecular structure and the electronic state of the bis-germylene **48**, DFT(B3LYP) calculations were performed using the program Gaussian[43] with 6-31G(d,p) basis set. The structures, total and relative energies are depicted in Figures 3 and 4. The relevant interatomic distances and torsion angle are given in Tables 5 and 6. The nature of the stationary points after optimization was checked by calculations of the harmonic vibration frequencies. No imaginary frequencies have been found which confirm that the molecules are minima on the surface energy potential. Two minima were found on the surface energy potential one with the two germanium atoms directed toward the same direction, named pseudo-*Cis* and another one with the germanium atoms in opposite position, named pseudo-*Trans.*

The conformation named pseudo-*Trans*, with a dihedral angle between the two aminotroponiminates systems of 78°, is the privileged one. Indeed, the conformation named pseudo-*Cis* lies 3.9 kcal/mol in energy above the pseudo-*Trans* probably because of both the steric hindrance (highest nuclear repulsion energy) and the length of the carbon bridge. Zabula *et al.*[37] reported an *anti* arrangement for bis-germylenes (**VI**, n = 2, Chart 4) and a *cis* orientation for n = 3.

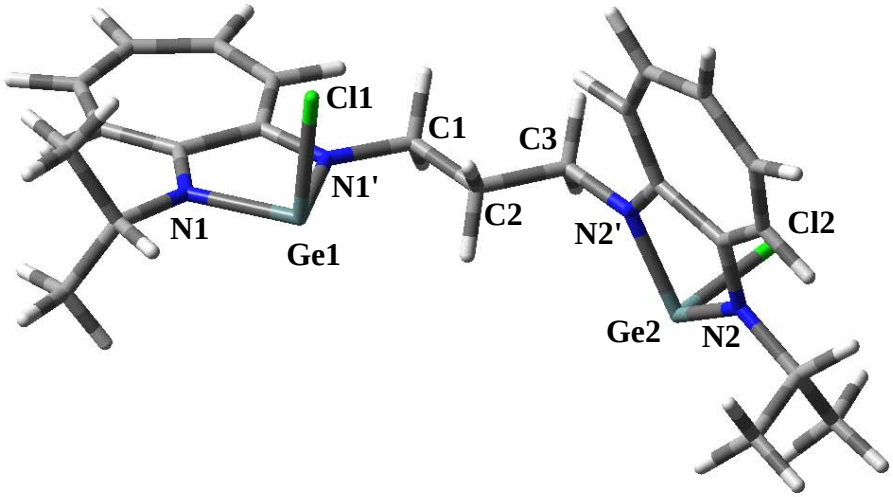

Figure 3: Compound **48**, pseudo-*Trans* conformer

Total energy (ZPE): -6183.597721 a.u. Relative energy 0 kcal/mol

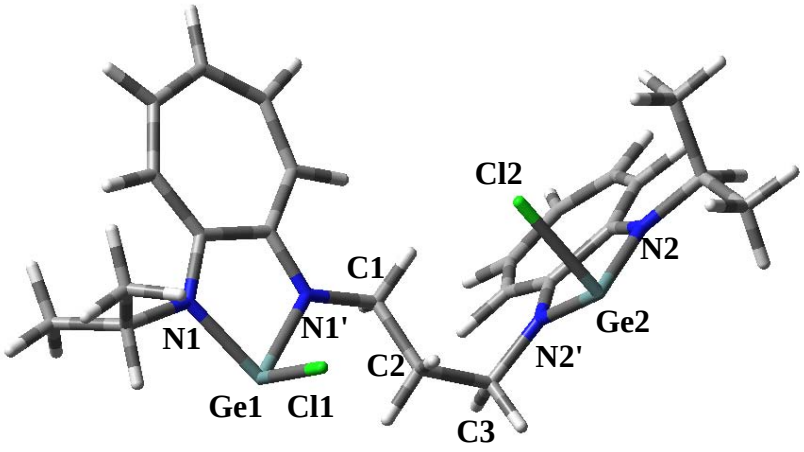

Figure 4: Compound **48**, pseudo-*Cis* conformer

Total energy(ZPE): -6183.591576 a.u. Relative energy 3.85 kcal/mol

If the tricoordinate pseudo-*Trans* conformer, which has the lowest energy (implicitly being the most stable) is compared with the twocoordinate bis-germylene (**V**, n = 2, Chart 3), a good accuracies of the calculated distances can be noticed. However the bond angles are wider, probably due to the change of coordination number of the germanium center. The Ge-Cl bond lengths (average 2.363 Å) found for this conformer are nearly identical with that found in **49**[40] [{(*i*Pr)$_2$ATI}GeCl] (2.368 Å). These values are shlighly longer than the average Ge-Cl distances reported in Ge(II) and Ge(IV) compounds (Ge-Cl: 2.11-2.20 Å)[44-49].

The chlorine atoms are nearly perpendicular on the five membered rings as previously observed for corresponding monogermylene[40].

Table 5: The bond distances and bond angle for pseudo-*Trans* conformer compared with Zabula's bis-germylene

Bond distances (Å)	Pseudo-*Trans*	Zabula's compound	Bond angles (°)	Pseudo-*Trans*	Zabula's compound
Ge1-N1	1.956	1.866	N1-Ge1-Cl1	95.96	-
Ge1-N1'	1.969	1.866	N1'-Ge1-Cl1	95.36	-
Ge2-N2	1.974	-	N2-Ge2-Cl2	97.72	-
Ge2-N2'	1.956	-	N2'-Ge2-Cl2	93.67	-
Ge1-Cl1	2.368	-	N1-Ge1-N1'	80.03	85.06
Ge2 -Cl2	2.357	-	N2-Ge2-N2'	79.66	-
N1'-C1	1.460	1.459	Ge1-N1'-Cl	122.18	-
N2'-C3	1.456	-	Ge2-N2'-C3	117.92	127.86
C1-C2	1.529	1.519	C1-C2-C3	111.28	-
C2-C3	1.536	-			

Table 6: The bond distances and bond angle for pseudo-*Cis* conformer

Bond	Distances (Å)	Bond angles	(°)
Ge1-N1	1.954	N1-Ge1-Cl1	95.669
Ge1-N1'	1.970	N1'-Ge1-Cl1	98.526
Ge2-N2	1.974	N2-Ge2-Cl2	94.228
Ge2-N2'	1.979	N2'-Ge2-Cl2	97.603
Ge1-Cl1	2.346	N1-Ge1-N1'	80.105
Ge2-Cl2	2.358	N2-Ge2-N2'	79.538
N1'-C1	1.464	Ge1-N1'-Cl	122.365
N2'-C3	1.464	Ge2-N2'-C3	117.434
C1-C2	1.529	C1-C2-C3	114.121
C2-C3	1.539		

In both conformers, the four first occupied MO correspond mainly to the lone pair orbital localized on the germanium atom (NBO calculation shows a strong s character (~85%) with ~15% of p character) in anti-bonding interaction with the corresponding chlorine lone pairs and for the two first ones with the aminotroponiminate π system. It is to note that taking into account the geometrical structure (two aminotroponiminate systems quasi perpendicular) the two aminotroponiminate moieties molecular orbitals do not interact between them.

From the energetically point of view, we can note a slightly more destabilized (nucleophile) germanium centre, considering the *Cis* form (-5.17 eV) *versus* the *Trans* one (-5.33 eV), that allows these two isomers to coordinate easily with a metallic centre.

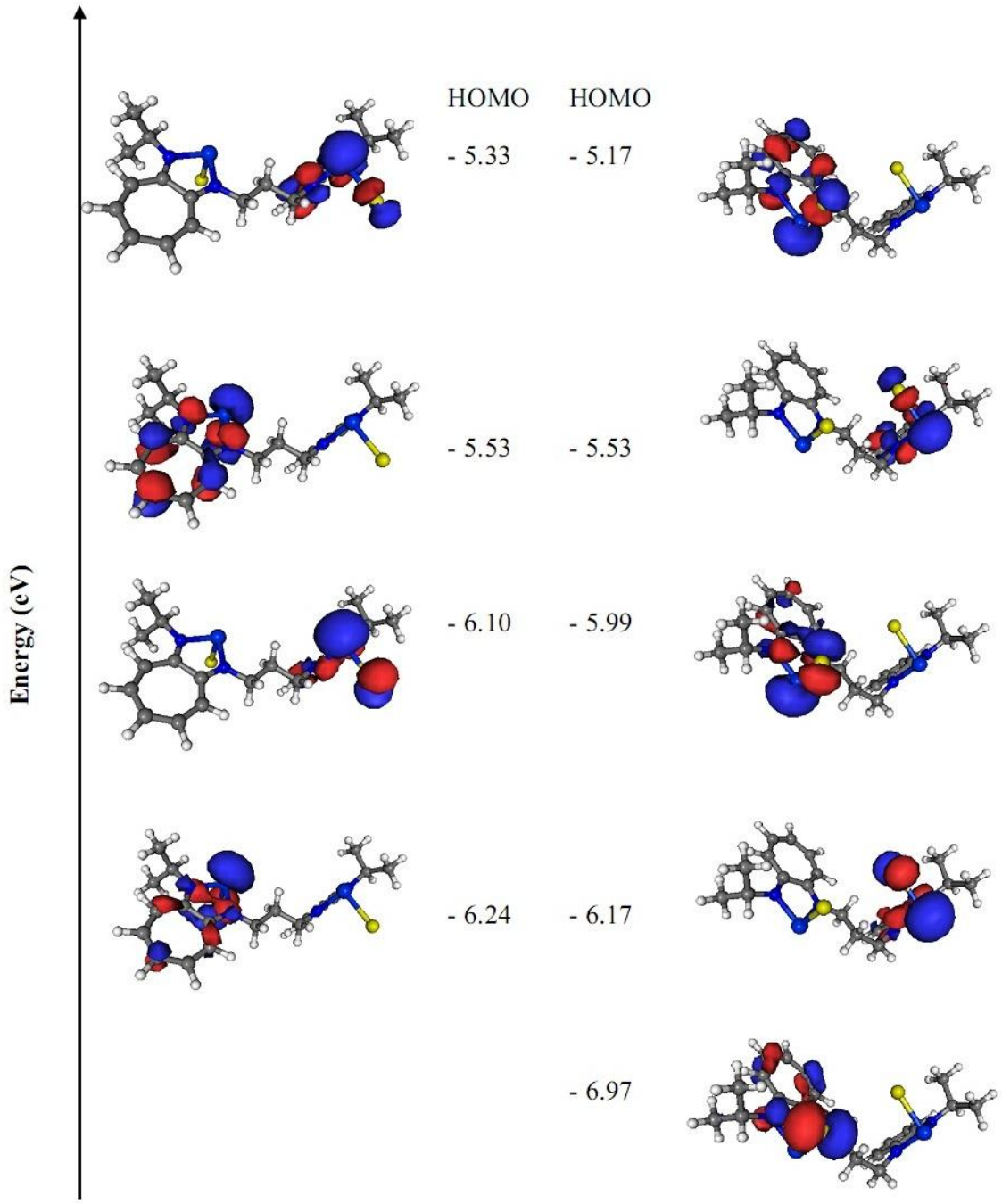

48 pseudo-*Trans* **48** pseudo-*Cis*

Figure 5: Molecular orbital diagrams and orbital contour plots of **48** pseudo-*Trans* and **48** pseudo-*Cis*

3.2.3 Chemical reactivity of germylenes

3.2.3.1 Oxidative reactions with sulfur and selenium

In recent years, the chemistry of double bonded species between group 14 and 16 heavier elements M=E (M = Si, Ge, Sn; E = S, Se, Te) analogues of ketone, has attracted steady interest[50]. Examples such as Si=E (E = S)[51-52], Ge=E (E = S, Se, Te)[53-59] and Sn=E (E = S, Se, Te)[60-65] have been synthesized and structurally characterized. In contrast, compounds involving double bonded elements bearing chlorines have been much less investigated. Only, few examples with β-diketiminates as ligands were reported[66]. The oxidation reaction of germylenes by chalcogens seems to constitute an efficient route to such species.

Firstly, we tried these reactions with monogermylenes **49** and **50**.

Treatment of chlorogermylene **49** with elemental sulfur and selenium in chloroform at 60 °C for 2 h and 4.5 h afforded the germanethioacid chloride **52** and germaneselenoacid chloride **53** as yellow solids (Equation 8). All these chalcogen derivatives were obtained in good yield. In contrast, with the phosphorus analogs **21** and **22**, these germathione and germaselenone were not very air and moisture sensitive and hydrolysis of the Ge-Cl bond was never observed.

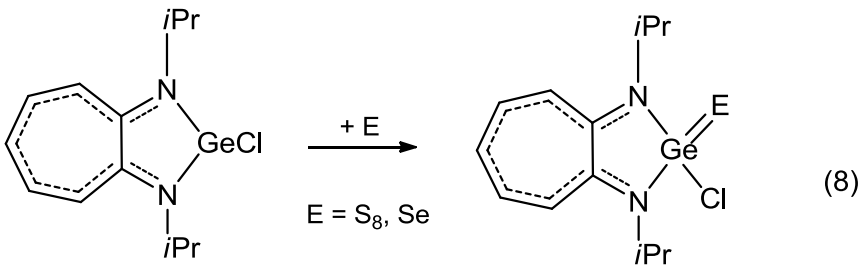

49

52, E = S
53, E = Se

(8)

The ^{1}H and ^{13}C NMR spectra of **52** and **53** show similar patterns and display the expected sets of signals. While for **49**[40] the ^{1}H NMR shows the presence of magnetically equivalent methyl groups, for **52** and **53** we can see two resonance signals for the isopropyl CH_3 groups due to the different environment on the germanium atom (Figures 6 and 7). The signals for isopropyl C*H* of **52** (4.30 ppm) and **53** (4.37 ppm) appear as septuplet and are slightly downfield shifted in comparaison with that of **49** (4.18 ppm)[40]. The same trend can be observed for the aromatic protons (Table 7).

^{77}Se NMR may act as a good probe for determining the nature of germanium-selenium interaction. The ^{77}Se chemical shift for Ge-Se single bond in $(H_3Ge)_2Se$ is -612 ppm[67]. Depending on the substituents, germaneselenones show signals from -288 ppm for [{HC(CMeNAr)$_2$}Ge(Se)Cl][68] to 941 ppm for [(Tbt)(Tip)Ge(Se)] (Tbt = 2,4,6-tris[bis(trimethylsilyl)methyl]phenyl, Tip = 2,4,6-triisopropylphenyl)[69]. In the ^{77}Se NMR spectrum of compound **53** the resonance was observed at -44.91 ppm. This value which is between that for a single bond, [Ge{(NSiMe$_3$)$_2$}$_2$(μ-Se)]$_2$ (δ = –476.0 ppm)[70] and that for a double bond, [(Tbt)(Tip)Ge=Se] (δ = 940 ppm)[71], seems to indicate that the bonding in solution can be described as intermediates between Ge$^+$-Se$^-$ and Ge=Se resonance structure[66].

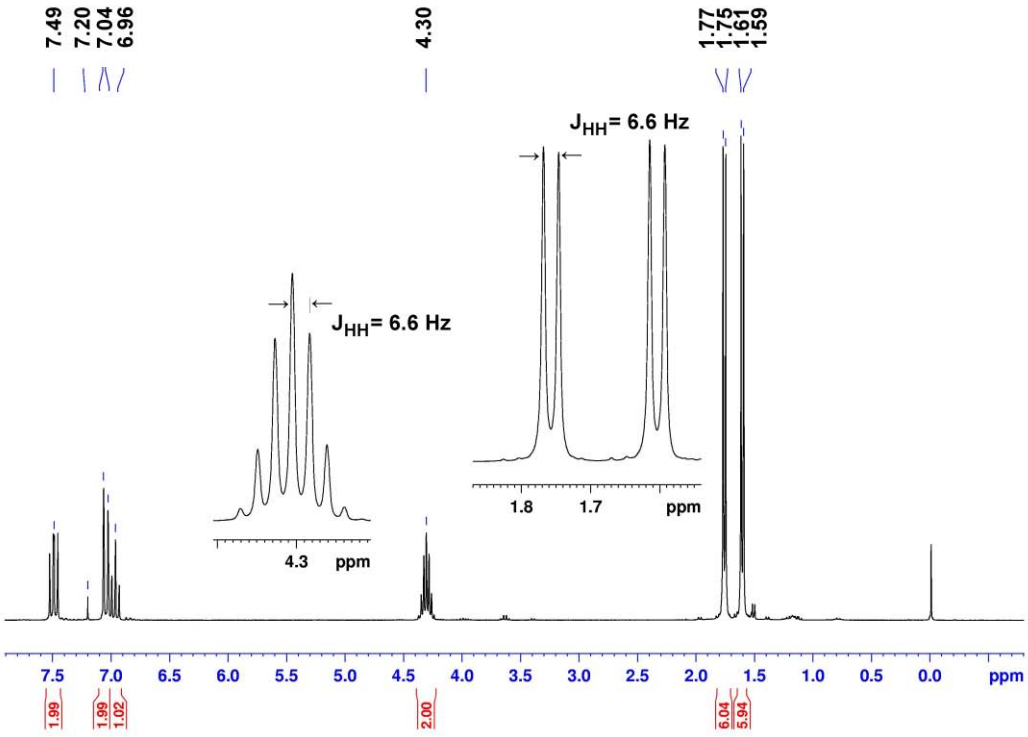

Figure 6: ^{1}H NMR spectrum for compound **52**, two different signals for CH_3 can be observed

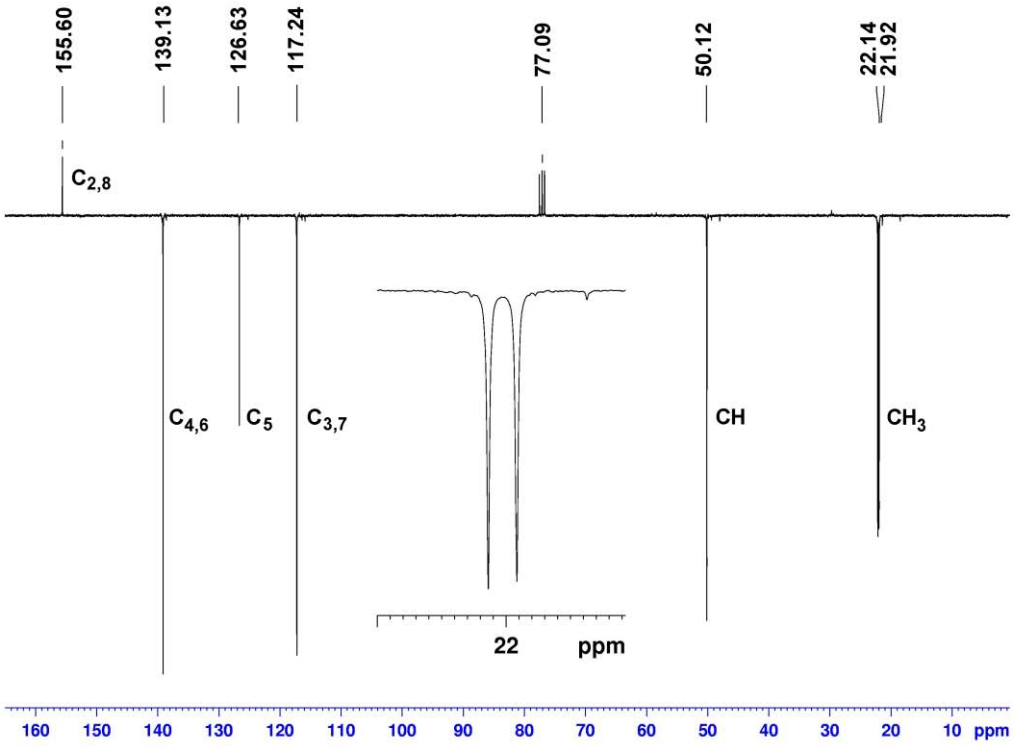

Figure 7: ^{13}C NMR spectrum for compound **52**, two different signals for CH_3 can be observed

Table 7: Proton NMR chemical shifts for **49**, **52** and **53** (in ppm, J in Hz, in $CDCl_3$)

	CH_3	CH	H_5	$H_{4,6}$	$H_{3,7}$
49	1.55 (d, $^3J_{HH}$ = 6.3)	4.18 (sept, $^3J_{HH}$ = 6.3 Hz)	6.66 (t, $^3J_{HH}$ = 9.3)	7.23 (t, $^3J_{HH}$ = 10.4)	6.84 (d, $^3J_{HH}$ = 11.2)
52	1.60 (d, $^3J_{HH}$ = 6.6), 1.75 (d, $^3J_{HH}$ = 6.6)	4.30 (sept, $^3J_{HH}$ = 6.6)	6.96 (t, $^3J_{HH}$ = 9.4)	7.04 (d, $^3J_{HH}$ = 11.4)	7.48 (t, $^3J_{HH}$ = 10.5)
53	1.61 (d, $^3J_{HH}$ = 6.6), 1.79 (d, $^3J_{HH}$ = 6.6)	4.37 (sept, $^3J_{HH}$ = 6.6)	6.94 (t, $^3J_{HH}$ = 9.4)	7.03 (d, $^3J_{HH}$ = 11.6)	7.49 (ps.t)

Table 8: Carbon-13 NMR chemical shifts for **49**, **52** and **53** (in ppm, in $CDCl_3$)

	CH_3	CH	C_5	$C_{4,6}$	$C_{3,7}$	$C_{2,8}$
49	23.80	49.30	123.00	136.80	115.70	160.50
52	21.92 and 22.14	50.12	126.63	139.13	117.24	150.60
53	20.37	50.26	126.80	138.92	117.35	155.70

In the mass spectrometry spectra, the molecular peaks [M^+] at 390 and 344 amu and [M^+ - Cl] at 309 and 311 amu are present for both germanechalcogenoacid. For **53** the peak [M^+ - Se] at 309 amu was observed while for **52** it was the peak [M^+ - SH] at 311 amu. For **52** and **53** the characteristic isotopic distribution for germanium can be seen in Figures 8a and 8c.

Isotope distributions can also be calculated using different programs. In Figures 8b and 8d we present the calculated molecular peaks for **52** and **53**.

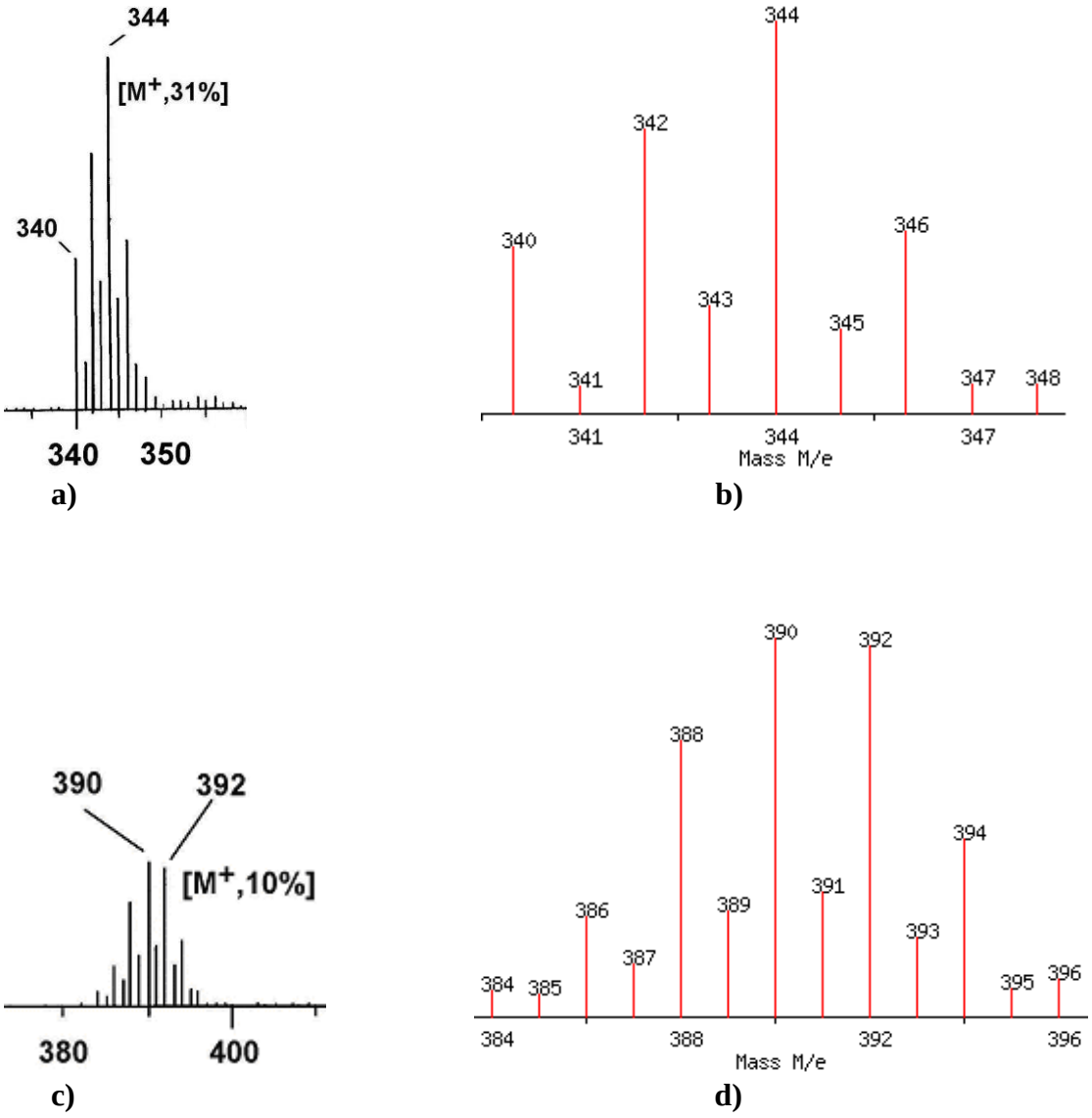

Figure 8: Molecular peaks for compounds **52** (a – experimental, b – calculated[72-73]) and **53** (c – experimental, d – calculated)

Single crystal of **53** has been subjected to X-ray diffraction analysis and the corresponding molecular structure is shown in Figure 9.

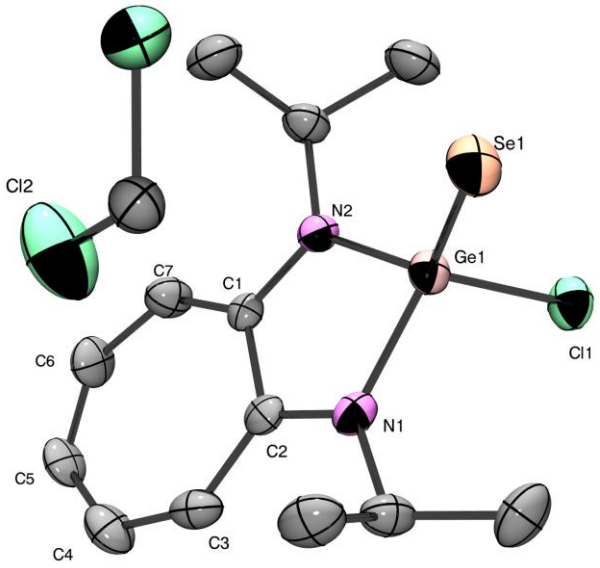

Figure 9: Molecular structure of compound **53** (50 % probability level for the thermal ellipsoids). All H atoms have been omitted for clarity. Selected bond distances [Å] and angles [°] are: Ge(1)-N(1) 1.874(5), Ge(1)-N(2) 1.876(4), Ge(1)-Se(1) 2.2109(9), Ge(1)-Cl(1) 2.2119(16), N(2)-C(1) 1.357(7), C(2)-N(1) 1.354(7), C(2)-C(3) 1.416(8), C(2)-C(1) 1.481(7), C(6)-C(5) 1.381(9), C(6)-C(7) 1.391(8), C(1)-C(7) 1.394(8), C(4)-C(5) 1.380(9), C(4)-C(3) 1.385(9); N(1)-Ge(1)-N(2) 85.7(2), N(1)-Ge(1)-Se(1) 121.40(15), N(2)-Ge(1)-Se(1) 123.19(14), N(1)-Ge(1)-Cl(1) 104.03(15), N(2)-Ge(1)-Cl(1) 103.09(15), Se(1)-Ge(1)-Cl(1) 114.57(5).

These data confirm that compound **53** is monomer in the solid state. Due to the higher oxidation state of the germanium (tetracoordinated instead of tricoordinated) the Ge–N distances [1.874(5) and 1.876(4) Å] and Ge–Cl distance [2.2119(16) Å] in **53** are shorter than the corresponding bond lengths of the parent germanium (II) species **49** [1.956(4) and 2.368(2) Å, respectively]. The germanium–selenium distances in compound **53** [Ge–Se 2.2109(9) Å] is more consistent with a double than a covalent bond, since the distance Ge=Se is between 2.180(2)[69] and 2.247(7) Å[58, 74] and the calculated germanium–selenium single bond distance is around 2.39 Å[75-76]. The N-Ge-N and N-Ge-Cl bond angles for **53** are several degrees larger compared to those of compound **49**.

No reaction between tellurium and **49** was observed under similar reaction conditions. Under heating, **49** decompose towards the neutral ligand **1**.

Reaction between **50** and sulfur is somewhat more complicated; after 4 h of stirring at room temperature a mixture of unidentified products was obtained.

Surprisingly, no reaction was found between **50** and selenium; after some time and under heating the mixture gives only the ligand **1**.

Starting from the bisgermylene **48**, the oxidation reaction with sulfur seems also more complex. After 3 h of stirring at 60 °C in toluene, the ^{1}H NMR shows the formation of more than one product; one of them could be the corresponding bis-germanedithioacid dichloride.

3.2.3.2 Cycloaddition reaction with *o*-quinone

One of the characteristic reactions for germylenes is the oxidative cycloaddition reaction with an *ortho* quinone.

The addition of 3,5-di-*tert*-butyl-*ortho*-quinone in THF solution at room temperature on germylenes **49** and **50** causes a slow discoloration of the quinone solution. The colour change is complete after 0.5 h for **49** and **50** at room temperature. The corresponding cycloadducts **54** and **55** could then be easily isolated after evaporation of the solvent and characterized (Equation 9).

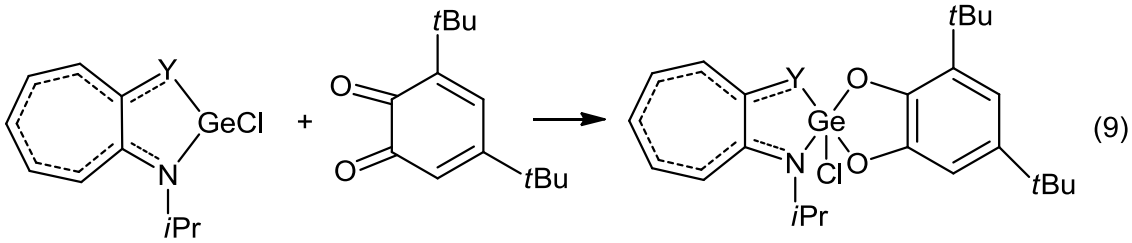

(9)

49, Y = N-*i*Pr
50, Y = O

54, Y = N-*i*Pr
55, Y = O

Similarly, treatment of bis-germylenes **47** and **48** with *o*-benzoquinone at room temperature in THF led to the cyclic products **56** and **57**. The discoloration process of the quinone solution is ended in 1.5 h. After evaporation of the THF, the corresponding cycloadducts were isolated as yellow powders (Equation 10).

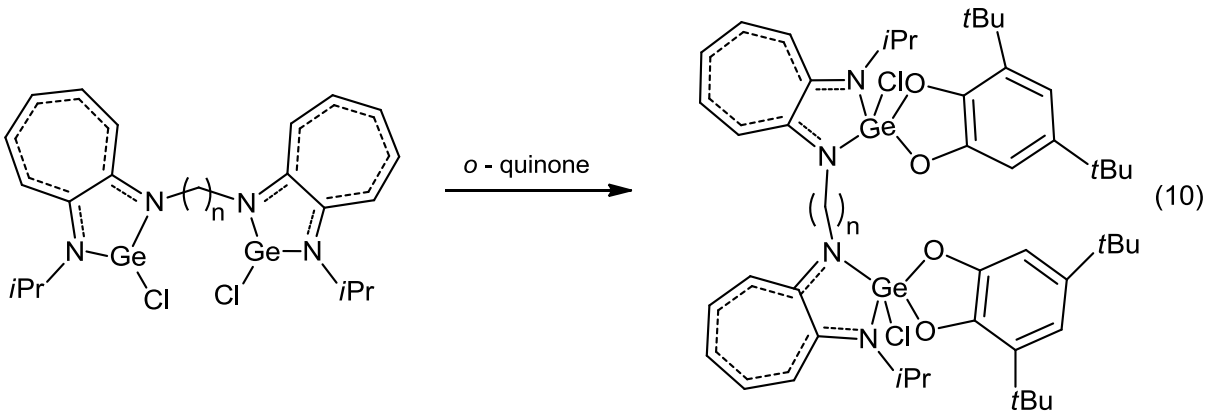

(10)

47, n = 2
48, n = 3

56, n = 2
57, n = 3

Cycloladducts **54** - **57** were fully characterized by multinuclear NMR spectroscopy and mass spectrometry. In the ^{1}H NMR spectra, the resonances of the methyl groups of the iso-propyl substituents are non equivalent due to their different environments.

EI-MS for **54** and **55** gave the corresponding molecular peaks [M^+] at 532 and 491 amu respectively and the fragments [M^+ - CH_3] at 517 and 476 amu, respectively. In contrast, CI-MS for **56** and **57** only indicates the presence of the fragments [M^+ - 2 HCl - H] at 950 amu and [M^+ - HCl] at 983 amu, respectively, both of them having the characteristic isotopic distribution of bis-germylenes.

Satisfactory analytical data were difficult to obtain owing to the sensibility of the compound toward moisture and air.

All attempts (different solvents and temperature of crystallization) to obtain suitable crystals for X-ray analysis were unsuccessful.

3.2.3.3 Complexation with transition metals

The lone pair on germanium could also allow the coordination on a transition metal[77].

During the past few years, the chemistry of stable homoleptic (where the transition metal has only one type of ligand)[78] and heteroleptic (where the transition metal has more than one type of ligand)[78] divalent compounds of germanium[79] and of their transition metal complexes[80-81] has been the focus of considerable attention.

Like cationic transition metal phosphenium complexes, the analogous $M_{14}(II)$-transition metal complexes are of potential interest for many applications (e.g., as catalysts for cationic or ring-opening polymerizations) because of the possibility that the increased electrophilicity that results from the positive charge may enhance substrate coordination and activation[75].

The reaction of the divalent species **48** with the pentacarbonyltungsten·THF intermediate in tetrahydrofuran gave the expected germylene tungsten complex in very good yield (80 %). The compound was fully characterized. X-ray quality crystal was grown from CH_2Cl_2 at room temperature (Scheme 2).

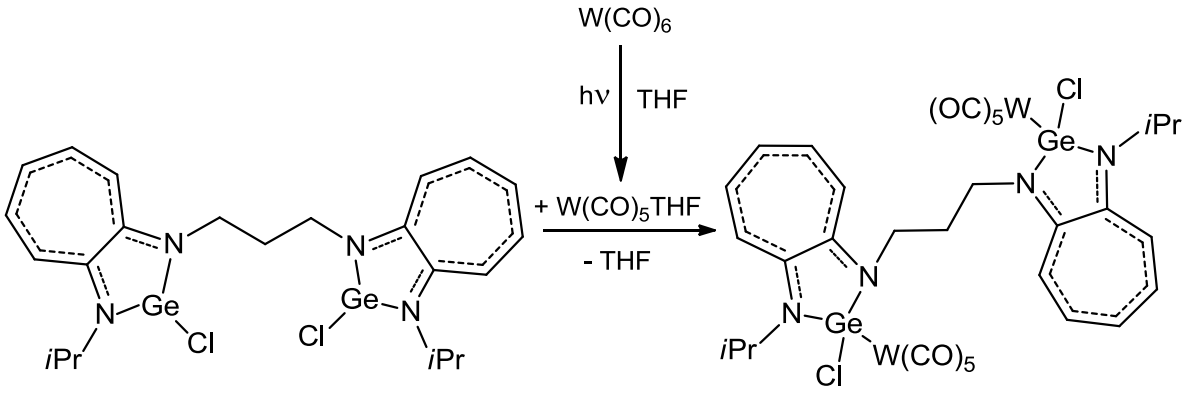

48 **58**

Scheme 2

While for **48** the ^{1}H NMR shows the presence of magnetically equivalent methyl groups, in **58** we can see four resonance signals for the isopropyl C*H*$_3$ groups due to the different environment on the germanium atom. The signal for isopropyl C*H* of **58** (4.35 ppm) appears as a septuplet and is sensibly downfield shifted in relation to that of the **48** (4.29 ppm). The same trend can be observed for the aromatic protons.

In ^{13}C NMR the presence of two signals for the *C*H$_2$ group is observed which denotes the lack of symmetry in solution for this compound.

All the carbon signals (except C_2 and C_8) of the seven-membered rings of **58** are deshielded compared with the parent germylene **48**. This deshielding is consistent with an increased positive charge on the ligand backbone.

The resonances for the CO groups are found in the expected zone (C_{ax} being deshielded compared with the C_{eq}) and with the relative intensity 1:4.

The infra-red analysis of this germanium – tungsten complex, shows the presence of three new characteristic bands ν (CO) at 1936, 1979 and 2070 cm^{-1}.

Microanalytical data for complex **58** could not be obtained owing to its sensibility toward moisture and air. The molecular structure of **58** was determined by X-ray diffraction.

This new complex with tungsten crystallizes as monomer with no interaction in the solid state; the structure of **58** is depicted in Figure 10.

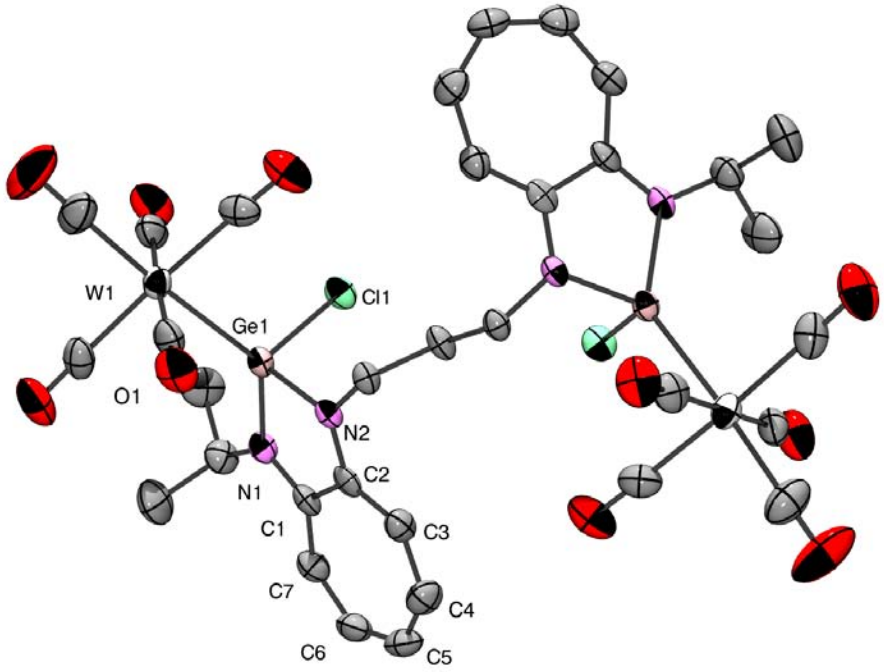

Figure 10: Molecular structure of compound **58** (50 % probability level for the thermal ellipsoids). All H atoms have been omitted for clarity. Selected bond distances [Å] and angles [°] are: W(1)-C(15) 2.010(8), W(1)-C(14) 2.040(8), W(1)-C(16) 2.050(8), W(1)-Ge(1) 2.5582(7), Ge(1)-N(2) 1.895(5), Ge(1)-N(1) 1.908(5), Ge(1)-Cl(1) 2.2843(16), N(1)-C(1) 1.349(8), C(1)-C(7) 1.419(9), C(1)-C(2) 1.482(8), C(2)-C(3) 1.387(9), C(3)-C(4) 1.398(9), C(4)-C(5) 1.367(10), C(5)-C(6) 1.389(10), C(6)-C(7) 1.390(9); N(2)-Ge(1)-N(1) 83.4(2), N(1)-Ge(1)-Cl(1) 100.73(16), N(2)-Ge(1)-W(1) 121.37(15), Cl(1)-Ge(1)-W(1) 111.00(5).

The germylene units adopt an *anti* arrangement toward each other and the alkyl bridge exhibits an all *trans* conformation.

The molecule has a distorted tetrahedral geometry around the germanium, with the sum of the angles at the metal center deviating from the sp^3 tetrahedral value, the sum of the N(1)–Ge–N(2) [83.4(2)°], N(1)–Ge–Cl [100.73(16)°], Cl–Ge–W [111.00(5)°], and N(2)–Ge–W [121.37(15)°], bond angles being 416.52°. The N(1)–Ge–N(2) bond angles observed in the four-coordinate complexes are slightly wider than those found in **49** [(*i*Pr)$_2$ATI]GeCl

[80.3(2)°], probably due to the change of coordination number of the germanium centers (tricoordinate for **49** and tetracoordinate for **58**) and a little more narrow than those observed in the similar bridged bis-germylene structures found in the literature [84.95, 85.06(8) for the bridged bis(benzimidazoline-2-germylene)[37]]. The Ge–N [1.895(5) and 1.908(5) Å] and Ge–Cl [2.2843(16) Å] bond lengths in complex **58** are shorter than those in divalent species **49**, respectively [Ge–N 1.956(4) Å and Ge–Cl 2.368(2) Å]. These differences may be attributable to the diminished electronic densities around the germanium in **58** compared to **49**. In complex **58**, the geometry around the tungsten is nearly octahedral. The Ge–W bond length [2.5582(7) Å] is nearly identical to those observed for (η^2-Cp*)(Cl)-GeW(CO)$_5$ [2.571(1) Å][82], and L(Cl)GeW(CO)$_5$ [L = PhNC(Me)CHC(Me)NPh] [2.567(5) Å][81] and for various halogermanium (IV) complexes (η^5-C$_5$R$_5$)M(CO)$_3$GeCl$_3$ (R = H, Me; M = Mo, W)[83-85]. They are among the shortest reported for compounds of R$_2$GeW(CO)$_5$ type[86-90]; they are even shorter than the Ge–W bond length of 2.593(1) Å determined for Ar$_1$Ar$_2$Ge–W(CO)$_5$ [Ar$_1$ = 2,4,6-tris[bis(trimethylsilyl)methyl]phenyl, Ar$_2$ = 2,4,6-triisopropylphenyl] in which the germanium atom is three-coordinated[86]. The range for an interatomic Ge–W single bond is 2.59–2.67 Å[87-88, 91]. It is noteworthy that in the complex **57** the W–Cax [2.010(8) Å] is slightly shorter than the W–Ceq bonds (average) [2.046 Å] and is the largest among the W–Cax bonds yet observed in germylene tungsten complexes[86-90, 92].

As shown in the literature[37], the linkage of two N-heterocyclic germylene units with a flexible alkyl chain makes the bis-germylenes **48** flexible enough to coordinate to a metal center in a chelating fashion; consequently we conducted a test with M(CO)$_4$COD (M = Mo, W). Complexes **59** and **60** were obtained together with a mixture of unidentified products from **48** in THF (Equation 11).

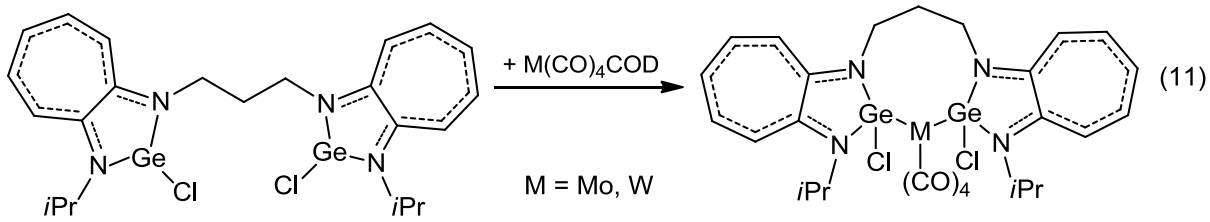

48

59, M = Mo
60, M = W

(11)

Between the two compounds **59** and **60** we cannot see a noticeable difference in ^{1}H NMR. If compared with **48**, four signals for C*H*$_3$, in the range from 1.62 to 1.90 pm for **59** and from 1.55 to 1.81 ppm for **59**, appear in the expected aliphatic zone which highlights four

different environments for each methyl group. In the case of **59** in ^{13}C NMR four signals are also present for CH_3. For **60** the two N-CH_2 groups are not equivalent and two multiplet signals can be observed. The ^{13}C NMR spectrum of **59** shows four deshielded signals belonging to carbonyl groups. The infra-red analysis of these new complexes, shows the presence of three new characteristic bands $\nu_{(CO)}$ 1893, 1919 and 2018 cm^{-1} for **59** and two large bands $\nu_{(CO)}$ = 1879 and 2045 cm^{-1} for **60**.

When we tried the same reaction with $W(CO)_4COD$ starting from **49** after 4 h of stirring at 60 °C no reaction was observed.

Conclusions and perspectives

In this last chapter, we have prepared the first bridged bis-pnictogenium (P, As and Sb) cations supported by aminotroponiminate (N,N') and aminotroponate (N,O) ligands using direct two-step synthetic pathways: a nucleophilic substitution reaction by an aminolithiated derivative or a base-induced dehydrohalogenation coupling reaction. The ^{31}P, ^{1}H and ^{13}C NMR analyses confirmed the formation of cationic species with high delocalization of the positive charge on the π-conjugated backbone.

An extension to the corresponding bis-germylenes was also described. Theoretical calculations using DFT(B3LYP) have been carried out showing that the conformation, named pseudo-*Trans* with the germanium atoms in opposite position, was slightly more stable than the pseudo-*Cis* conformation with the two germanium atoms directed toward the same direction.

Some tests of reactivity such as oxidative reaction with chalcogens (sulfur and selenium) and cycloaddition reaction with *o*-quinone were also performed in comparison with the corresponding monogermylenes. In both cases, these species retain their divalent character.

The σ-donor character of these bis-germylenes was highlighted by their easy complexation with transition metal complexes. For the first time, a stable trans-disubstituted germanium(II)-tungsten carbonyl complex was prepared and structurally characterized.

Experimental Section

Synthesis of ligand 32

A 2.50 g (13.15 mmol) amount of $Et_3O{\cdot}BF_4$ in 10 ml of methylene chloride was slowly added to a methylene chloride solution (10 ml) of 2.00 g (12.26 mmol) of 2-(N-isopropylamino)tropone under argon atmosphere. The solution was stirred for 3 h at room temperature, then 1.24 g (12.26 mmol) of NEt_3 was slowly added to the reddish solution. The mixture was stirred for another 5 min, and then 0.34 g (6.16 mmol) of freshly distilled 1,2-diaminoethane in 6 ml of NEt_3 was added. The mixture was stirred for 14 h, and the volatiles were eliminated under vacuo. The residue was extracted into pentane (350 ml), filtered through Celite, and concentrated under reduced pressure (1.00 g, 46.50 %, mp 104 °C).

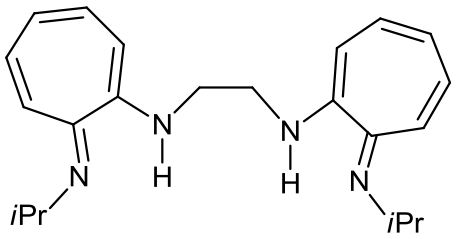

^{1}H NMR (300 MHz, $CDCl_3$): δ (ppm)
1.19 (d, $^3J_{HH}$ = 6.3 Hz, 12H, CH-CH_3),
3.65 (s, 4H, N-CH_2),
3.76 (sept, $^3J_{HH}$ = 6.2 Hz, 2H, CH-CH_3),
6.07 (t, $^3J_{HH}$ = 9.3 Hz, 2H, C_7H_5),
6.17 (d, $^3J_{HH}$ = 10.7 Hz, 2H, C_7H_5),
6.41 (d, $^3J_{HH}$ = 11.2 Hz, 2H, C_7H_5),
6.69 (ps.t, 4H, C_7H_5),
7.60-7.80 (m, 2H, NH).

^{1}H NMR (300 MHz, C_6D_6): δ (ppm)
1.06 (d, $^3J_{HH}$ = 6.3 Hz, 12H, CH-CH_3),
3.52 (s, 4H, N-CH_2),
3.55 (sept, $^3J_{HH}$ = 6.3 Hz, 2H, CH-CH_3),
6.10 (t, $^3J_{HH}$ = 9.2 Hz, 2H, C_7H_5),
6.14 (d, $^3J_{HH}$ = 10.6 Hz, 2H, C_7H_5),
6.27 (d, $^3J_{HH}$ = 10.9 Hz, 2H, C_7H_5),
6.54-6.69 (m, 4H, C_7H_5),
7.80-8.30 (m, 2H, NH).

^{1}H NMR (300 MHz, THF d8): δ (ppm)
1.17 (d, $^3J_{HH}$ = 6.3 Hz, 12H, CH-CH_3),
3.60 (s, 4H, N-CH_2),
3.79 (sept, $^3J_{HH}$ = 6.2 Hz, 2H, CH-CH_3),
6.02 (t, $^3J_{HH}$ = 9.2 Hz, 2H, C_7H_5),
6.23 (d, $^3J_{HH}$ = 10.8 Hz, 2H, C_7H_5),

6.39 (d, $^3J_{HH}$ = 11.2 Hz, 2H, C_7H_5),
6.66 (ps.t, 4H, C_7H_5),
7.58-8.17 (m, 2H, N*H*).

^{13}C {^{1}H} NMR (75 MHz, $CDCl_3$): δ (ppm)

22.72 (CH-*C*H_3),
45.06 (*C*H-CH_2),
48.18 (N-*C*H_2),
107.84 and 112.58 ($C_{3,7}$),
117.42 (C_5),
133.14 and 132.63 ($C_{4,6}$),
151.22 and 154.00 ($C_{2,8}$).

^{13}C {^{1}H} NMR (75 MHz, THF d8): δ (ppm)

21.87 (CH-*C*H_3),
44.63 (*C*H-CH_2),
47.14 (N-*C*H_2),
107.85 and 111.04 ($C_{3,7}$),
116.71 (C_5),
132.14 and 132.49 ($C_{4,6}$),
150.83 and 153.20 ($C_{2,8}$).

Synthesis of ligand 33

A 6.46 g (34.00 mmol) amount of $Et_3O{\cdot}BF_4$ in 35 ml of methylene chloride was slowly added to a methylene chloride solution (20 ml) of 5.00 g (30.67 mmol) of 2-(*N*-isopropylamino)tropone under inert atmosphere. After the solution was stirred for 3 h at room temperature, 3.10 g (30.67 mmol) of NEt_3 was slowly added to the reddish solution. The mixture was stirred for another 5 min, and then 1.13 g (15.34 mmol) of 1,3-diaminopropane in 15 ml of NEt_3 was added to the mixture. The mixture was stirred 14 h, and the volatiles were removed in vacuo. The residue was extracted into pentane (350 ml), filtered through Celite, and concentrated under vacuo (4.41 g, 78.60 %, mp 85 °C).

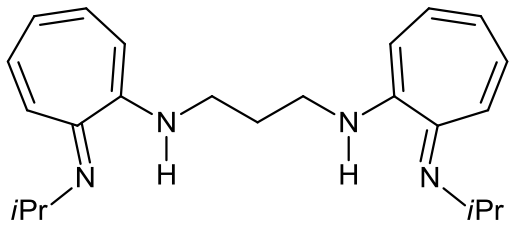

^{1}H NMR (300 MHz, $CDCl_3$): δ (ppm)

1.21 (d, $^3J_{HH}$ = 6.3 Hz, 12H, CH-C*H*$_3$),
2.14 (quint, $^3J_{HH}$ = 6.9 Hz, 2H, C*H*$_2$),
3.43 (t, $^3J_{HH}$ = 6.9 Hz, 4H, N-C*H*$_2$),
3.77 (sept, $^3J_{HH}$ = 6.3 Hz, 2H, C*H*-CH_3),
6.05 (t, $^3J_{HH}$ = 9.3 Hz, 2H, C_7H_5),
6.18 (d, $^3J_{HH}$ = 10.7 Hz, 2H, C_7H_5),

6.32 (d, $^{3}J_{HH}$ = 11.3 Hz, 2H, C_7H_5),
6.63-6.72 (m, 4H, C_7H_5),
8.05 (s, 2H, N*H*).

^{1}H NMR (300 MHz, THF d8): δ (ppm)
1.16 (d, ^{3}J = 6.3 Hz, 12H, CH-C*H*$_3$),
2.06 (quint, $^{3}J_{HH}$ = 6.9 Hz, 2H, C*H*$_2$),
3.39 (t, $^{3}J_{HH}$ = 6.9 Hz, 4H, N-C*H*$_2$),
3.77 (sept, $^{3}J_{HH}$ = 6.3 Hz, 2H, C*H*-CH$_3$),
5.99 (t, $^{3}J_{HH}$ = 9.2 Hz, 2H, C_7H_5),
6.20 (d, $^{3}J_{HH}$ = 10.7 Hz, 2H, C_7H_5),
6.28 (d, $^{3}J_{HH}$ = 11.3 Hz, 2H, C_7H_5),
6.63 (ps.t, 4H, C_7H_5),
7.74 (s, 2H, N*H*).

^{1}H NMR (300 MHz, C_6D_6): δ (ppm)
1.13 (d, $^{3}J_{HH}$ = 6.3 Hz, 12H, CH-C*H*$_3$),
2.10 (quint, ^{3}J = 6.9 Hz, 2H, C*H*$_2$),
3.35 (t, $^{3}J_{HH}$ = 6.9 Hz, 4H, NC*H*$_2$),
3.60 (sept, $^{3}J_{HH}$ = 6.3 Hz, 2H, C*H*-CH$_3$),
6.17 (t, $^{3}J_{HH}$ = 9.3 Hz, 4H, C_7H_5),
6.36 (d, $^{3}J_{HH}$ = 11.3 Hz, 2H, C_7H_5),
6.71 (ps.t, 4H C_7H_5),
8.00 (s, 2H, N*H*).

^{1}H NMR (300 MHz, dioxane d_8): δ (ppm)
1.12 (d, $^{3}J_{HH}$ = 6.3 Hz, 12H, CH-C*H*$_3$),
2.01 (quint, $^{3}J_{HH}$ = 6.9 Hz, 2H, C*H*$_2$),
3.34 (t, $^{3}J_{HH}$ = 6.9 Hz, 4H, NC*H*$_2$),
3.73 (sept, $^{3}J_{HH}$ = 6.3 Hz, 2H, C*H*-CH$_3$),
5.97 (t, $^{3}J_{HH}$ = 9.3 Hz, 2H, C_7H_5),
6.16 (d, $^{3}J_{HH}$ = 10.9 Hz, 2H, C_7H_5),
6.25 (d, $^{3}J_{HH}$ = 11.2 Hz, 2H, C_7H_5),
6.55-6.65 (m, 4H, C_7H_5),
7.65 (s, 2H, N*H*).

^{13}C {^{1}H} NMR (75 MHz, $CDCl_3$): δ (ppm)
22.84 (CH-*C*H$_3$),
31.14 (*C*H$_2$),
45.18 (*C*H-CH$_3$),
45.47 (N-*C*H$_2$),
108.07 and 112.21 ($C_{3,7}$),
117.44 (C_5),
132.63 and 133.12 ($C_{4,6}$),
151.27 and 153.56 ($C_{2,8}$).

^{13}C {^{1}H} NMR (75 MHz, THF d8): δ (ppm)
22.17 (CH-*C*H$_3$),
31.02 (*C*H$_2$),
44.59 (N-*C*H$_2$),
45.09 (*C*H-CH$_2$),
108.33 and 110.98 ($C_{3,7}$),
116.99 (C_5),
132.42 and 132.79 ($C_{4,6}$),
151.23 and 153.12 ($C_{2,8}$).

^{13}C {^{1}H} NMR (75 MHz, C_6D_6): δ (ppm)

23.60 (CH-*C*H_3),
32.21 (*C*H_2),
46.11 (N-*C*H_2),
46.23 (*C*H-CH_3),
109.70 and 112.71 ($C_{3,7}$),
118.52 (C_5),
133.83 and 134.20 ($C_{4,6}$),
152.60 and 154.60 ($C_{2,8}$).

^{13}C {^{1}H} NMR (75 MHz, dioxane d_8): δ (ppm)

22.29 (CH-*C*H_3),
30.78 (*C*H_2),
44.74 (N-*C*H_2),
45.10 (*C*H-CH_3),
108.42 and 111.19 ($C_{3,7}$),
116.97 (C_5),
132.50 and 132.85 ($C_{4,6}$),
151.17 and 153.56 ($C_{2,8}$).

Synthesis of ligand 34

A two neck 50 ml round-bottom flask was charged with 2-(tosy1oxy)tropone (2.50 g, 9.05 mmol), Et_3N (1.05 g, 10.40 mmol), 1,3-diaminopropane (1.19 g, 16.00 mmol) and ethanol (25 ml) and refluxed for 6 h. Concentration in vacuo gave a sticky residue, which was dissolved in $CHCl_3$, washed with saturated aqueous sodium bicarbonate, dried over magnesium sulfate and concentrated to give an oil. This material was chromatographed (silica gel, chloroform:ether 5:1) (0.64 g, 50 %).

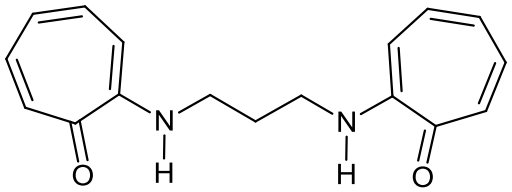

^{1}H NMR (300 MHz, $CDCl_3$): δ (ppm)

2.11 (quint, $^{3}J_{HH}$ = 6.7 Hz, 2H, C*H*$_2$),
3.40 (t, $^{3}J_{HH}$ = 6.7 Hz, 4H, N-C*H*$_2$),
6.44 (d, $^{3}J_{HH}$ = 10.7 Hz, 2H, C_7H_5),
6.61 (t, $^{3}J_{HH}$ = 9.0 Hz, 2H, C_7H_5),
7.05 (t, $^{3}J_{HH}$ = 10.1 Hz, 2H, C_7H_5),
7.12-7.23 (m, 4H, C_7H_5).

^{13}C {^{1}H} NMR (75 MHz, $CDCl_3$): δ (ppm)

27.30 (*C*H_2),
40.11 (N-*C*H_2),
108.70 (C_3),
122.52 (C_5),
128.80 (C_7),

136.22 (C_4),
137.31 (C_6),
155.30 (C_2),
176.64 (C_8).

Synthesis of dilithiated ligand salt 35

A solution of **32** (0.20 g, 0.57 mmol) in Et_2O (10 ml) was cooled at 0 °C and treated dropwise with *n*BuLi (0.72 ml of 1.6 M solution, 0.60 mmol). After 0.5 h of stirring, the volume of the solvent was then reduced to half and the clear solution was placed at -30 °C to obtain yellow crystals in almost quantitative yield.

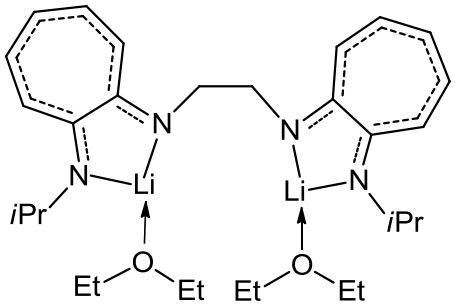

^{7}Li NMR (155 MHz, THF d8): δ (ppm) 1.64.

^{1}H NMR (300 MHz, THF d8): δ (ppm)
1.07 (t, $^{3}J_{HH}$ = 6.9 Hz, 6H, (CH_3CH$_2$)$_2$O),
1.08 (d, $^{3}J_{HH}$ = 6.2 Hz, 12H, CH-CH_3),
3.34 (q, $^{3}J_{HH}$ = 7.0 Hz, 4H, (CH$_3$CH_2)$_2$O),
3.47 (s, 4H, NCH_2),
3.69 (sept, $^{3}J_{HH}$ = 5.7 Hz, 2H, CH-CH$_3$),
5.45 (t, $^{3}J_{HH}$ = 8.9 Hz, 2H, C$_7$H$_5$),
5.90 (d, $^{3}J_{HH}$ = 11.2 Hz, 2H, C$_7$H$_5$),
5.97 (d, $^{3}J_{HH}$ = 11.6 Hz, 2H, C$_7$H$_5$),
6.42 (ps.t, 4H, C$_7$H$_5$).

^{1}H NMR (400 MHz, THF d8): δ (ppm)
1.07 (t, $^{3}J_{HH}$ = 6.9 Hz, 6H, (CH_3CH$_2$)$_2$O),
1.07 (d, $^{3}J_{HH}$ = 6.2 Hz, 12H, CH-CH_3),
3.33 (quart, $^{3}J_{HH}$ = 7.0 Hz, 4H, (CH$_3$CH_2)$_2$O),
3.47 (s, 4H, NCH_2),
3.71 (sept, $^{3}J_{HH}$ = 6.2 Hz, 2H, CH-CH$_3$),
5.45 (t, $^{3}J_{HH}$ = 8.9 Hz, 2H, C$_7$H$_5$),
5.89 (d, $^{3}J_{HH}$ = 11.4 Hz, 2H, C$_7$H$_5$),
5.97 (d, $^{3}J_{HH}$ = 11.4 Hz, 2H, C$_7$H$_5$),
6.42 (ps.t, 4H, C$_7$H$_5$).

^{13}C {^{1}H} NMR (75 MHz, THF d8): δ (ppm)
12.60 (*C*H$_3$CH$_2$)$_2$O),
21.11 (CH-*C*H$_3$),
45.67 (N-*C*H$_2$),
51.31 (*C*H-CH$_3$),
63.23 (CH$_3$*C*H$_2$)$_2$O),

104.31 and 103.89 ($C_{3,7}$),
105.23 (C_5),
129.62 and 129.22 ($C_{4,6}$),
160.77 and 162.00 ($C_{2,8}$).

Synthesis of dilithiated ligand salt 36

A solution of **33** (0.10 g, 0.27 mmol) in Et_2O (2 ml) was cooled at 0 °C and treated dropwise with *n*BuLi (0.38 ml of 1.6 M solution, 0.60 mmol). After 30 min of stirring the clear solution was placed at -30 °C. A fast crystallization from this solution affords X-ray-quality yellow crystals in nearly quantitative yield.

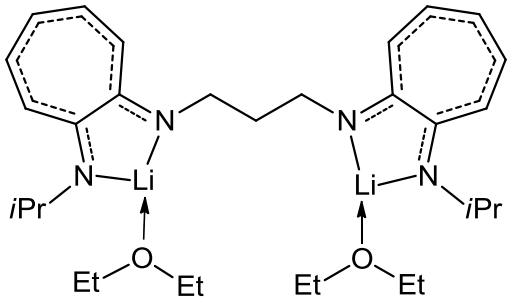

^{7}Li NMR (155 MHz, THF d8): δ (ppm) 1.66.
^{1}H NMR (300 MHz, THF d8): δ (ppm)
1.11 (t, $^3J_{HH}$ = 7.0 Hz, 6H, $(CH_3CH_2)_2O$),
1.12 (d, $^3J_{HH}$ = 6.2 Hz, 12H, $CH\text{-}CH_3$),
1.99 (quint, $^3J_{HH}$ = 7.4 Hz, 2H, CH_2),
3.27-3.43 (m, 8H, $(CH_3CH_2)_2O$ and NCH_2),
3.74 (sept, $^3J_{HH}$ = 5.7 Hz, 2H, $CH\text{-}CH_3$),
5.42 (t, $^3J_{HH}$ = 8.9 Hz, 2H, C_7H_5),
5.89 (d, $^3J_{HH}$ = 11.3 Hz, 2H, C_7H_5),
5.93 (d, $^3J_{HH}$ = 11.3 Hz, 2H, C_7H_5),
6.42 (ps.t, 4H, C_7H_5).
^{1}H NMR (400 MHz, THF d8): δ (ppm)
1.16 (t, $^3J_{HH}$ = 7.0 Hz, 6H, $(CH_3CH_2)_2O$),
1.18 (d, $^3J_{HH}$ = 6.2 Hz, 12H, $CH\text{-}CH_3$),
2.04 (quint, $^3J_{HH}$ = 7.5 Hz, 2H, CH_2),
3.43 (q, $^3J_{HH}$ = 7.0 Hz, 4H, $(CH_3CH_2)_2O$),
3.50 (t, $^3J_{HH}$ = 7.0 Hz, 4H, NCH_2),
3.80 (sept, $^3J_{HH}$ = 6.2 Hz, 2H, $CH\text{-}CH_3$),
5.56 (t, $^3J_{HH}$ = 8.8 Hz, 2H, C_7H_5),
5.95 (d, $^3J_{HH}$ = 11.2 Hz, 2H, C_7H_5),
6.03 (d, $^3J_{HH}$ = 11.3 Hz, 2H, C_7H_5),
6.50 (ps.t, 4H, C_7H_5).
^{13}C {^{1}H} NMR (75 MHz, THF d8): δ (ppm)
16.01($CH_3CH_2)_2O$),
23.32 ($CH\text{-}CH_3$),
32.69 (CH_2),
49.49 ($N\text{-}CH_2$),

47.70 (*C*H-CH_3),
63.22 (CH_3CH_2)$_2$O),
105.96 and 106.19 ($C_{3,7}$),
107.22 (C_5),
131.25 and 131.60 ($C_{4,6}$),
162.90 and 164.11 ($C_{2,8}$).

Synthesis of 37

To a mixture of **32** (0.30 g, 0.86 mmol) and Et_3N (0.19 g, 1.90 mmol) in toluene (10 ml) was slowly added PCl_3 (0.26 g, 1.90 mmol) in toluene (1 ml) at -78 °C. After 1 h the mixture was allowed to warm to ambient temperature and stirred for additional 4 h. After filtration, the precipitate was washed with toluene (3 × 10 ml) and dried under reduced pressure to yield a yellow powder. It was not possible to eliminate Et_3N·HCl whatever the solvent used.

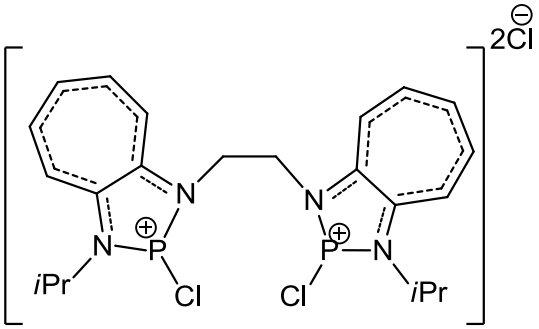

^{31}P {^{1}H} NMR (121 MHz, $CDCl_3$): δ (ppm) 133.80.
^{1}H NMR (300 MHz, $CDCl_3$): δ (ppm)
1.72 (d, $^3J_{HH}$ = 6.4 Hz, 12H, CH-C*H*$_3$),
4.47-4.60 (m, 2H, C*H*-CH_3),
4.95-4.99 (m, 4H, N-C*H*$_2$),
7.75 (t, $^3J_{HH}$ = 9.7 Hz, 2H, C_7H_5),
7.90 (d, $^3J_{HH}$ = 11.3 Hz, 2H, C_7H_5),
8.12 (ps.t, 2H, C_7H_5),
8.30 (ps.t, 2H, C_7H_5),
9.23 (d, $^3J_{HH}$ = 10.6 Hz, 2H, C_7H_5).
^{13}C {^{1}H} NMR (75 MHz, $CDCl_3$): δ (ppm)
21.43 (d, $^3J_{CP}$ = 12.2 Hz, CH-*C*H_3),
43.22 (d, $^2J_{CP}$ = 25.9 Hz, N-*C*H_2),
50.74 (d, $^2J_{CP}$ = 12.6 Hz, *C*H-CH_3),
125.60 and 128.20 ($C_{3,7}$),
135.98 (C_5),
143.09 and 144.64 ($C_{4,6}$),
155.32 and 156.34 ($C_{2,8}$).
^{31}P {^{1}H} NMR (121 MHz, CD_2Cl_2): δ (ppm) 134.62.
^{1}H NMR (300 MHz, CD_2Cl_2): δ (ppm)
1.70 (d, $^3J_{HH}$ = 6.4 Hz, 12H, CH-C*H*$_3$),
4.55-4.68 (m, 2H, C*H*-CH_3),
4.90-4.94 (m, 4H, N-C*H*$_2$),
7.85 (ps.t, 2H, C_7H_5),

8.07 (d, $^{3}J_{HH}$ = 11.3 Hz, 2H, C_7H_5),
8.22-8.30 (m, 4H, C_7H_5),
9.14 (d, $^{3}J_{HH}$ = 10.6 Hz, 2H, C_7H_5).

^{13}C {^{1}H} NMR (75 MHz, CD_2Cl_2): δ (ppm)
21.24 (d, $^{3}J_{CP}$ = 12.2 Hz, CH-*C*H_3),
43.22 (d, $^{2}J_{CP}$ = 25.3 Hz, N-*C*H_2),
50.74 (d, $^{2}J_{CP}$ = 12.6 Hz, *C*H-CH_3),
125.97 and 128.20 ($C_{3,7}$),
136.27 (C_5),
143.52 and 144.53 ($C_{4,6}$),
155.40 and 156.38 ($C_{2,8}$).

Synthesis of 38

- by nucleophilic substitution reaction using an aminolithiated derivative

A solution of **32** (0.25 g, 0.71 mmol) in Et_2O (10 ml) was treated dropwise at 0 °C with *n*BuLi (0.98 ml of 1.6 M solution, 1.56 mmol). After 0.5 h of stirring, the mixture was gradually added to a solution of $AsCl_3$ (0.28 g, 1.56 mmol) in Et_2O (3 ml) at -75 °C. The cold bath was removed, and the turbid yellow solution obtained was warmed to room temperature and stirred for another 4 h. The solution was filtered, washed twice with Et_2O (20 ml) leading to the precipitation of a yellow fine powder. The ^{1}H NMR analysis shows the formation of **38** (55 %) and another unidentified products (45 %).

^{1}H NMR (300 MHz, $CDCl_3$): δ (ppm)
1.75 (d, $^{3}J_{HH}$ = 6.5 Hz, 12H, CH-C*H*$_3$),
4.21-4.33 (m, 4H, NC*H*$_2$),
4.43 (sept, $^{3}J_{HH}$ = 6.5 Hz, 2H, C*H*-CH_3),
7.52 (t, $^{3}J_{HH}$ = 10.3 Hz, 2H, C_7H_5),
7.62 (d, $^{3}J_{HH}$ = 10.5 Hz, 2H, C_7H_5),
7.77 (t, $^{3}J_{HH}$ = 10.3 Hz, 2H, C_7H_5),
8.00 (t, $^{3}J_{HH}$ = 10.4 Hz, 2H, C_7H_5),
8.34 (d, $^{3}J_{HH}$ = 10.9 Hz, 2H, C_7H_5).

- by dehydrohalogenation coupling reaction

A 50 ml Schlenk flask, equipped with a magnetic bar, was charged with **32** (0.25 g, 0.71 mmol), Et_3N (0.16 g, 1.56 mmol) and toluene (5 ml), the resulting clear yellow solution was cooled to at -78 °C. Then, $AsCl_3$ (0.28g, 1.56 mmol) was syringed dropwise into the cooled solution. After 10 minutes, the mixture was allowed to warm to ambient temperature and stirred for additional 4 h. After filtration, volatiles were removed from the precipitate under reduced pressure to yield a yellow powder. It was not possible to eliminate $Et_3N{\cdot}HCl$ whatever the solvent used.

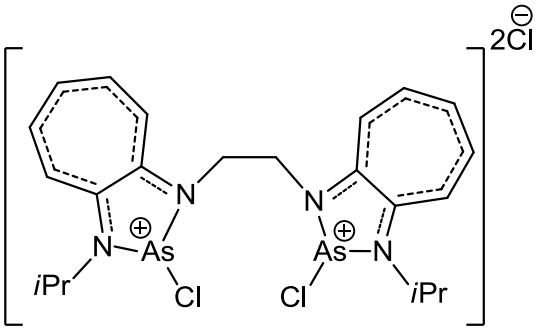

^{1}H NMR (300 MHz, DMSO): δ (ppm)

1.59 (d, $^{3}J_{HH}$ = 5.8 Hz, 12H, CH-CH_3),
4.45-4.60 (m, 6H, NCH_2, CH-CH_3),
7.48 (t, $^{3}J_{HH}$ = 9.1 Hz, 2H, C_7H_5),
7.66-7.86 (m, 4H, C_7H_5),
7.93 (ps.t, 2H, C_7H_5),
8.10 (ps.d, 2H, C_7H_5).

^{13}C {^{1}H} NMR (75 MHz, DMSO): δ (ppm)

21.40 (CH-CH$_3$),
43.46 (N-CH$_2$),
49.83 (CH-CH$_3$),
121.67 and 123.05 ($C_{3,7}$),
136.80 (C_5),
140.67 and 141.06 ($C_{4,6}$),
156.66 and 158.38 ($C_{2,8}$).

Synthesis of 39

- by dehydrohalogenation coupling reaction

To a mixture of **32** (0.25 g, 0.71 mmol) and Et_3N (0.14 g, 1.42 mmol) in toluene (10 ml) was slowly added $SbCl_3$ (0.33 g, 1.42 mmol) in toluene (1 ml) at -78 °C. After 1 h the mixture was allowed to warm to ambient temperature and stirred for additional 4 h. After filtration, the precipitate was washed with toluene (3 × 10 ml), pentane and THF and volatiles were removed under reduced pressure to yield a mixture of **39**, the ammonium salt and another unidentified impurity.

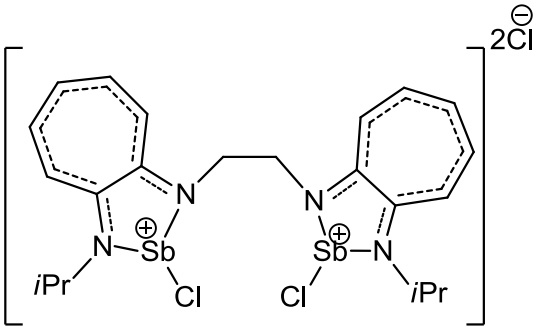

^{1}H NMR (300 MHz, DMSO): δ (ppm)

1.49 (d, $^{3}J_{HH}$ = 6.4 Hz, 12H, CH-CH_3),
3.96-4.07 (m, 2H, CH-CH_3),
4.08-4.15 (m, 4H, NCH_2),
7.47-7.59 (m, 4H, C_7H_5),
7.86 (ps.t, 2H, C_7H_5),
8.35 (ps.d, 2H, C_7H_5),
8.95-9.01 (m, 2H, C_7H_5).

EI-MS: m/z 504 [M^+ - (3Cl, Sb) + H, 3 %], 468 [M^+ - (4Cl, Sb) + H, 12 %], 425 [M^+ - (4Cl, Sb, *i*Pr) + H, 3 %].

- *by nucleophilic substitution reaction using an aminolithiated derivative*

A solution of **32** (0.25 g, 0.71 mmol) in Et_2O (10 ml) was treated dropwise at 0 °C with *n*BuLi (0.98 ml of 1.6 M solution, 1.56 mmol). After 0.5 h of stirring the mixture was gradually added to a solution of $SbCl_3$ (0.33 g, 1.42 mmol) in Et_2O (3 ml) at -75 °C. The cold bath was removed, and the turbid yellow solution obtained was warmed to room temperature and stirred for another 4 h. The solution was filtered, washed twice with Et_2O (20 ml) leading to the precipitation of a yellow fine powder. The ^{1}H NMR analysis indicates the presence of **39**, (50 %) and another unidentified product.

Synthesis of 40

- *by dehydrohalogenation coupling reaction*

To a mixture of **33** (0.20 g, 0.55 mmol) and Et_3N (0.14 g, 1.43 mmol) in toluene (5 ml) was slowly added PCl_3 (0.20 g, 1.43 mmol) in toluene (1 ml) at -78 °C. After 1 h the mixture was allowed to warm to ambient temperature and stirred for additional 4 h. After filtration, the precipitate was dried under reduced pressure yielding a yellow powder. As previously observed for compound **37**, it was not possible to eliminate $Et_3N{\cdot}HCl$ whatever the solvent used.

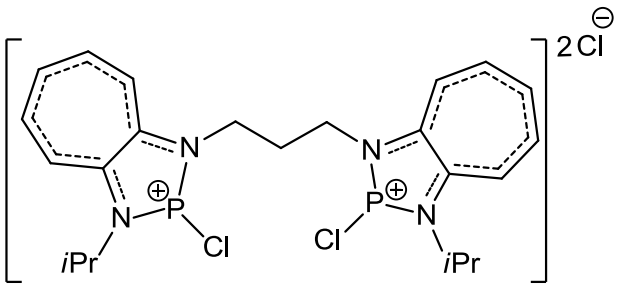

^{31}P {^{1}H} NMR (121 MHz, $CDCl_3$): δ (ppm) 137.22.

^{1}H NMR (300 MHz, $CDCl_3$): δ (ppm)

1.71 (d.d, $^{3}J_{HH}$ = 6.6 Hz, $^{4}J_{HP}$ = 1.5 Hz, 12H, CH-CH_3),
2.75 (quint, $^{3}J_{HH}$ = 7.0 Hz, 2H, CH_2),

4.40-4.60 (m, 2H, C*H*-CH_3),
4.68 (t.d, $^3J_{HH}$ = 7.6 Hz, $^3J_{HP}$ = 12.3 Hz, 4H, NCH_2),
7.73 (t.d, $^3J_{HH}$ = 9.8 Hz, J_{HP} = 2.9 Hz, 2H, C_7H_5),
7.87 (d, $^3J_{HH}$ = 11.0 Hz, 2H, C_7H_5),
8.08 (d, $^3J_{HH}$ = 10.0 Hz, 2H, C_7H_5),
8.33 (t, $^3J_{HH}$ = 9.9 Hz, 2H, C_7H_5),
9.60 (d.d, $^3J_{HH}$ = 10.9 Hz, J_{HP} = 2.1 Hz, 2H, C_7H_5).

^{13}C {^{1}H} NMR (75 MHz, $CDCl_3$): δ (ppm)
21.68 (d, $^3J_{CP}$ = 12.4 Hz, CH-*C*H_3),
27.33 (*C*H_2),
43.33 (d, $^2J_{CP}$ = 18.9 Hz, N-*C*H_2),
50.58 (d, $^2J_{CP}$ = 12.6 Hz, *C*H-CH_3),
125.43 (d, $^3J_{CP}$ = 5.2 Hz) and 128.89 (d, $^3J_{CP}$ = 5.1 Hz) ($C_{3,7}$),
135.99 (C_5),
142.93 and 144.90 (d, $^4J_{CP}$ = 4.2 Hz) ($C_{4,6}$),
154.99 (d, $^2J_{CP}$ = 12.8 Hz) and 157.21 (d, $^2J_{CP}$ = 12.6 Hz) ($C_{2,8}$).

^{31}P {^{1}H} NMR (202 MHz, $CDCl_3$): δ (ppm) 137.23.

^{1}H NMR (500 MHz, $CDCl_3$): δ (ppm)
1.72 (d.d, $^3J_{HH}$ = 6.6 Hz, $^4J_{HP}$ = 1.4 Hz, 12H, CH-C*H*$_3$),
2.74 (quint, $^3J_{HH}$ = 7.0 Hz, 2H, C*H*$_2$),
4.60 (sept.d, $^3J_{HH}$ = 9.7 Hz, $^3J_{HP}$ = 3.0 Hz, 2H, C*H*-CH_3),
4.68 (t.d, $^3J_{HH}$ = 7.7 Hz, $^3J_{HP}$ = 12.3 Hz, 4H, NCH_2),
7.80 (t.d, $^3J_{HH}$ = 9.8 Hz, $^6J_{HP}$ = 2.9 Hz, 2H, H_5),
8.05 (d.d, $^3J_{HH}$ = 10.9 Hz, J_{HP} = 2.1 Hz, 2H, C_7H_5),
8.19 (t, $^3J_{HH}$ = 9.9 Hz, 2H, C_7H_5),
8.35 (t, $^3J_{HH}$ = 10.0 Hz, 2H, C_7H_5),
9.58 (d.d, $^3J_{HH}$ = 10.9 Hz, J_{HP} = 2.0 Hz, 2H, C_7H_5).

^{13}C {^{1}H} NMR (125.75 MHz, $CDCl_3$): δ (ppm)
21.69 (d, $^3J_{CP}$ = 12.4 Hz, CH-*C*H_3),
27.33 (*C*H_2),
43.33 (d, $^2J_{CP}$ = 18.9 Hz, N-*C*H_2),
50.59 (d, $^2J_{CP}$ = 12.6 Hz, *C*H-CH_3),
125.67 (d, $^3J_{CP}$ = 5.1 Hz) and 128.94 (d, $^3J_{CP}$ = 5.2 Hz) ($C_{3,7}$),
136.09 (d, $^5J_{CP}$ = 4.6 Hz, C_5),
143.09 (d, $^4J_{CP}$ = 4.3 Hz), and 144.86 (d, $^4J_{CP}$ = 4.1 Hz) ($C_{4,6}$),
154.95 (d, $^2J_{CP}$ = 12.8 Hz) and 157.14 (d, $^2J_{CP}$ = 12.6 Hz) ($C_{2,8}$).

^{13}C {^{1}H} {^{31}P} NMR (125.75 MHz, $CDCl_3$): δ (ppm)
21.69 (CH-*C*H_3),
27.33 (*C*H_2),
43.33 (N-*C*H_2),
50.59 (*C*H-CH_3),
125.67 and 128.94 ($C_{3,7}$),
136.09 (C_5),
143.09 and 144.84 ($C_{4,6}$),
154.93 and 157.13 ($C_{2,8}$).

EI-MS: m/z 493 [M^+ - 2Cl - H, 7 %].

- by nucleophilic substitution reaction using a potassium derivative

To a suspension of KH (0.07 g, 1.64 mmol) in THF (3 ml) was slowly added **33** (0.30 g, 0.82 mmol) dissolved in THF (4.5 ml) at room temperature and the resulting solution was stirred for 16 h. The KH in excess was then filtered off and the filtrate was concentrated under vacuum. The yellow residue was washed with pentane and dried under vacuum. The resulting powder was dissolved in THF (8 ml) and cooled at -78 °C then PCl_3 was slowly added (0.23 g, 1.64 mmol). After 1 h, the reaction mixture was allowed to heat to ambient temperature and stirred for 14 h. The volatiles were removed under reduced pressure and the resulting solid was washed with toluene (25 ml) to give **40** identified by ^{1}H and ^{31}P NMR. Beside the target compounds the ligand salt **44** was detected in the ^{1}H NMR

- by nucleophilic substitution reaction using an aminolithiated derivative

A 1.6 M solution of *n*BuLi in hexanes (0.86 ml, 1.38 mmol) was slowly added to a cooled (0°C) solution of **33** (0.25 g, 0.69 mmol) in diethyl ether (10 ml). The suspension was warmed to room temperature and stirred for 30 min, and it was slowly added to a cooled (-78 °C) solution of PCl_3 (0.01 g, 0.69 mmol) in diethyl ether (10 ml). The mixture was allowed to reach room temperature and stirred overnight. After filtration, the remaining solid was washed with diethyl ether and dried under vacuum, leading to a yellow powder. The ^{31}P spectrum of the crude product indicated the presence of **40** and two other products non-identified.

Synthesis of 41

- by dehydrohalogenation coupling reaction

Following the same procedure described for **40**, **33** (0.42 g, 1.15 mmol) and Et_3N (0.30 g, 3.00 mmol) in toluene (15 ml) and $AsCl_3$ (0.54 g, 3.00 mmol) in toluene (2 ml) gave a mixture of **41** and $Et_3N{\cdot}HCl$.

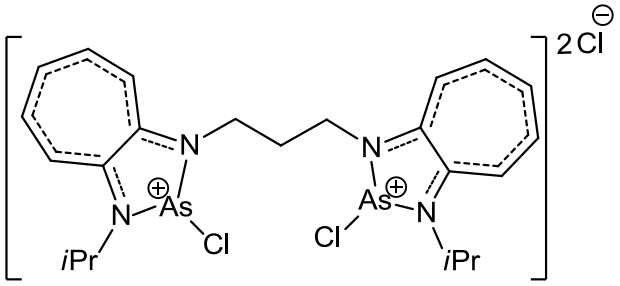

^{1}H NMR (300 MHz, $CDCl_3$): δ (ppm)

1.75 (d, $^3J_{HH}$ = 6.4 Hz, 12H, CH-CH_3),
2.86 (quint, $^3J_{HH}$ = 7.1 Hz, 2H, CH_2),
4.29 (t, $^3J_{HH}$ = 7.2 Hz, 4H, NCH_2),

4.42 (sept, $^{3}J_{HH}$ = 6.5 Hz, 2H, C*H*-CH_3),
7.25-7.35 (m, 4H, C_7H_5),
7.70-7.90 (m, 6H, C_7H_5).

^{13}C {^{1}H} NMR (75 MHz, $CDCl_3$): δ (ppm)
21.98 (CH-*C*H_3),
27.15 (*C*H_2),
44.80 (N-*C*H_2),
50.91 (*C*H-CH_3),
122.41 and 123.68 ($C_{3,7}$),
131.59 (C_5),
140.42 and 141.48 ($C_{4,6}$),
157.35 and 159.71 ($C_{2,8}$).

^{1}H NMR (500 MHz, $CDCl_3$): δ (ppm)
1.82 (d, $^{3}J_{HH}$ = 6.4 Hz, 12H, CH-C*H*$_3$),
2.82 (quint, $^{3}J_{HH}$ = 7.1 Hz, 2H, C*H*$_2$),
4.31 (t, $^{3}J_{HH}$ = 7.2 Hz, 4H, NC*H*$_2$),
4.40 (sept, $^{3}J_{HH}$ = 6.5 Hz, 2H, C*H*-CH_3),
7.30 (t, $^{3}J_{HH}$ = 9.5 Hz, 2H, C_7H_5),
7.35 (d, $^{3}J_{HH}$ = 11.2 Hz, 2H, C_7H_5),
7.71 (t, $^{3}J_{HH}$ = 10.3 Hz, 2H, C_7H_5),
7.78 (ps.t, 2H, C_7H_5),
7.88 (t, $^{3}J_{HH}$ = 11.0 Hz, 2H, C_7H_5).

^{13}C {^{1}H} NMR (125 MHz, $CDCl_3$): δ (ppm)
21.93 (CH-*C*H_3),
27.03 (*C*H_2),
44.80 (N-*C*H_2),
50.90 (*C*H-CH_3),
121.41 and 123.59 ($C_{3,7}$),
131.48 (C_5),
140.40 and 141.38 ($C_{4,6}$),
157.36 and 159.71 ($C_{2,8}$).

EI-MS: m/z 394 [M^+ - (4Cl, As, *i*Pr), 3 %].
CI:NH_3 m/z: 617 [M^+ - Cl, 10 %],.473 [M^+ - (3Cl, As, +1), 100 %].

- by nucleophilic substitution reaction using an aminolithiated derivative

A solution of **33** (0.20 g, 0.55 mmol) in Et_2O (10 ml) was cooled at 0 °C and treated dropwise with *n*BuLi (0.75 ml of 1.6 M solution, 1.20 mmol). After 0.5 h of stirring the clear solution was added drop wise to a solution of $AsCl_3$ (0.20 g, 1.10 mmol) in Et_2O (5 ml) at -75 °C. The ethanol cold bath was removed, and the cloudy yellow solution obtained was warmed to room temperature and stirred for another 4 h. The solution was filtered. The precipitate was washed with Et_2O (2 × 10 ml) and then was extracted with CH_2Cl_2 (2 × 10 ml). After filtration, evaporation of the solvent leads to a yellow powder identified as **41** by ^{1}H NMR.

Synthesis of 42

- by nucleophilic substitution reaction using an aminolithiated derivative

Following same experimental procedure as for the synthesis of **40**, **33** (0.22 g, 0.60 mmol), *n*BuLi (0.75 ml of 1.6 M solution, 1.20 mmol) and $SbCl_3$ (0.28 g, 1.20 mmol) in Et_2O (15 ml) gave **42** in a quantitative yield, mp 101-105 °C (dec.).

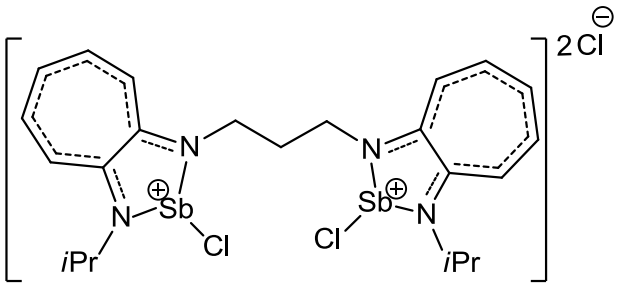

^{1}H NMR (300 MHz, $CDCl_3$): δ (ppm)

1.76 (d, $^3J_{HH}$ = 6.4 Hz, 12H, CH-CH_3),
2.87 (quint, $^3J_{HH}$ = 7.1 Hz, 2H, CH_2),
4.29 (t, $^3J_{HH}$ = 7.2 Hz, 4H, NCH_2),
4.42 (sept, $^3J_{HH}$ = 6.5 Hz, 2H, C*H*-CH_3),
7.27-7.34 (m, 4H, C_7H_5),
7.67-7.89 (m, 6H, C_7H_5).

^{13}C {^{1}H} NMR (75 MHz, $CDCl_3$): δ (ppm)

21.62 (CH-*C*H_3),
25.11 (*C*H_2),
42.02 (N-*C*H_2),
47.73 (*C*H-CH_3),
117.18 and 118.96 ($C_{3,7}$),
127.31 (C_5),
139.88 and 141.06 ($C_{4,6}$),
150.92 and 151.67 ($C_{2,8}$).

CI:NH_3 m/z: 711 [M^+ - Cl, 2 %], 617 [M^+ - 4Cl - Sb, 57 %].

- by dehydrohalogenation coupling reaction

A 50 ml round-bottom flask was charged with 0.27 g of **33** (0.74 mmol), 0.34 g of $SbCl_3$ (1.50 mmol) and 10 ml toluene. To this mixture 0.04 g of Et_3N (1.50 mmol) was added. The turbid orange solution was filtered and washed with toluene (2 × 10 ml) after 4 h of stirring, leading to the precipitation of a yellow powder, corresponding to the desired compound **42** identified by ^{1}H NMR. It was not possible to eliminate Et_3N·HCl.

Synthesis of the salt ligand 43

HCl (35 %, 0.023 g, 0.63 mmol) was gently added to a solution of **32** (0.100 g, 0.28 mmol) in CH_2Cl_2 (5 ml). The turbid orange solution was stirred for 20 minutes at room temperature. The solvent was removed in vacuo, and the NMR spectrum showed a total conversion of the starting product (0.118 g, 98 %, mp 121-124 °C).

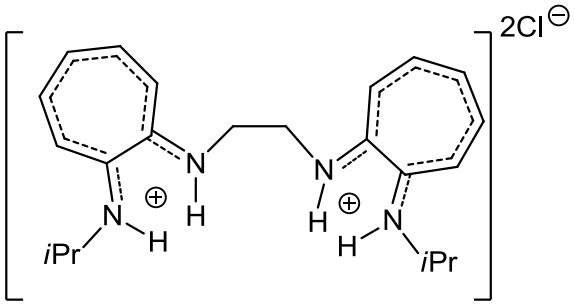

^{1}H NMR (300 MHz, $CDCl_3$): δ (ppm)

1.50 (d, $^3J_{HH}$ = 6.4 Hz, 12H, CH-C*H*$_3$),
3.98 (sept, $^3J_{HH}$ = 6.2 Hz, 2H, C*H*-CH$_3$),
4.12 (s, 4H, N-C*H*$_2$),
6.92-7.07 (m, 4H, C_7H_5),
7.48 (ps.t, 2H, C_7H_5),
7.62-7.75 (m, 4H, C_7H_5),
8.90-9.20 (m, 2H, N*H*),
10.00-10.40 (m, 2H, N*H*).

^{13}C {^{1}H} NMR (75 MHz, $CDCl_3$): δ (ppm)

21.36 (CH-*C*H$_3$),
42.04 (N-*C*H$_2$),
47.48 (*C*H-CH$_2$),
117.16 and 118.59 ($C_{3,7}$),
127.09 (C_5),
139.77 and 140.68 ($C_{4,6}$),
150.77 and 151.36 ($C_{2,8}$).

Synthesis of ligand salt 44

To a solution of **33** (0.100 g, 0.27 mmol) in CH_2Cl_2 (5 ml), HCl (35 %, 0.022 g, 0.59 mmol) was added dropwise. The cloudy orange mixture was stirred for 20 minutes at room temperature. The solvent was removed in vacuo, and the NMR spectrum showed a total conversion of the starting product (0.117 g, 98 %, mp 132-134 °C).

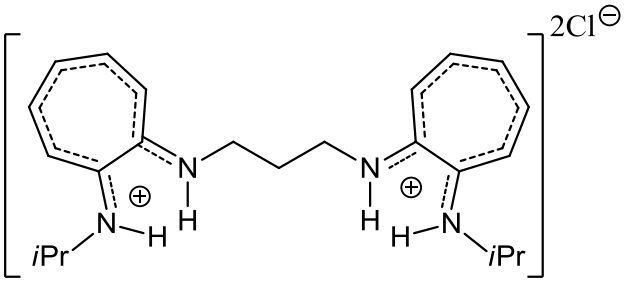

^{1}H NMR (300 MHz, $CDCl_3$): δ (ppm)

1.49 (d, $^{3}J_{HH}$ = 6.3 Hz, 12H, CH-CH_3),
2.58 (ps.q, 2H, CH_2),
3.77 (ps.t, $^{3}J_{HH}$ = 6.9 Hz, 4H, N-CH_2),
3.96 (sept, $^{3}J_{HH}$ = 6.3 Hz, 2H, CH-CH_3),
6.85-7.00 (m, 4H, C_7H_5),
7.29 (d, $^{3}J_{HH}$ = 11.1 Hz, 2H, C_7H_5),
7.45 (t, $^{3}J_{HH}$ = 10.3 Hz, 2H, C_7H_5),
7.59 (t, $^{3}J_{HH}$ = 10.2 Hz, 2H, C_7H_5).

^{13}C {^{1}H} NMR (75 MHz, $CDCl_3$): δ (ppm)

20.87 (CH-$C$$H_3$),
34.70 ($C$$H_2$),
42.18 (N-$C$$H_2$),
47.07 (CH-CH_3),
116.91 and 117.87 ($C_{3,7}$),
126.56 (C_5),
139.62 and 139.89 ($C_{4,6}$),
150.34 and 150.90 ($C_{2,8}$).

Synthesis of 45

To a mixture of **34** (0.21 g, 0.74 mmol) and Et_3N (0.19 g, 1.92 mmol) in dichloromethane (6 ml) was added dropwise PCl_3 (0.26 g, 1.92 mmol) in dichloromethane (1 ml) at -78 °C. After 1 h the ethanol cold bath was removed and the cloudy orange solution obtained was warmed to room temperature and stirred for another 4 h. After filtration, the solvent was pumped out from the precipitate to yield a yellow powder. The product has a very low solubility in $CDCl_3$. The ^{31}P NMR spectrum revealed the presence of two products, one at 157.57 and another at 176.70 ppm (about 50/50).

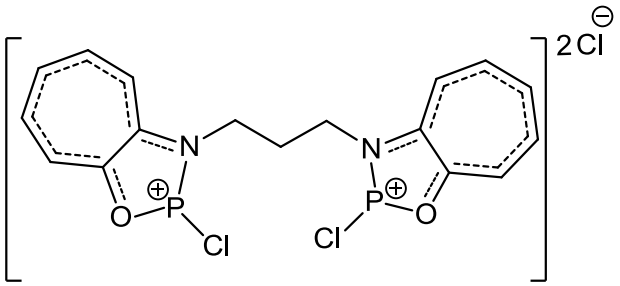

^{1}H NMR (300 MHz, $CDCl_3$): δ (ppm)

2.31-2.38 (m, 2H, CH_2),
3.45-3.64 (m, 4H, NCH_2),
7.55-8.64 (m, 10H, C_7H_5).

The product is oxidized in DMSO

^{31}P {^{1}H} NMR (121 MHz, DMSO): δ (ppm) 5.62.

^{1}H NMR (300 MHz, DMSO): δ (ppm)

2.21 (ps.quint, 2H, CH_2),
3.99 (ps.quart, 4H, NCH_2),
7.70 (ps.t, 2H, C_7H_5),
7.87-7.97 (m, 4H, C_7H_5),
8.07-8.23 (m, 4H, C_7H_5).

Synthesis of 46

To a mixture of **34** (0.21 g, 0.74 mmol) and Et_3N (0.19 g, 1.92 mmol) in dichloromethane (6 ml) was slowly added $AsCl_3$ (0.35 g, 1.92 mmol) in dichloromethane (1 ml) at -78 °C. After 1 h the mixture was allowed to warm to ambient temperature and stirred for additional 4 h. After filtration, volatiles were removed from the precipitate under vacuo to yield a yellow powder. The product has a very low solubility in $CDCl_3$.

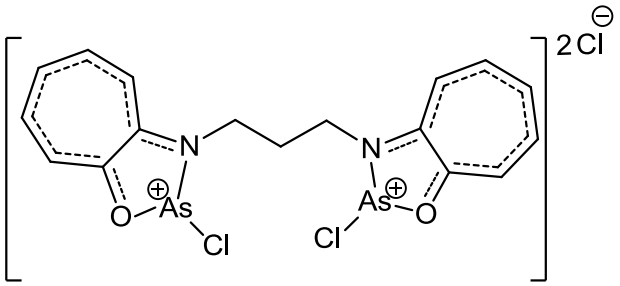

^{1}H NMR (300 MHz, $CDCl_3$): δ (ppm)

2.82 (quint, $^{3}J_{HH}$ = 6.4 Hz, 2H, CH_2),
4.17 (quart, $^{3}J_{HH}$ = 7.1 Hz, 4H, NCH_2),
7.40-8.00 (m, 10H, C_7H_5).

Synthesis of Cl_2Ge·1,4-dioxane

Tetramethyldisiloxane (14.20 g, 106 mmol) was added to germanium(IV) chloride (21.00 g, 98 mmol) in diethyl ether (45 ml) at 40 - 50 °C for 3 h. The hot bath was removed and stirring continued until two separated phases appear. Then the upper colourless phase is removed and 1,4-dioxane (14.10 g, 160 mmol) is gently added leading to a white precipitate. This was filtered off, washed with pentane (3 × 20 ml), and identified as the essentially pure Cl_2Ge·1,4-dioxane (17.54 g, 77 %). In repeat experiments, the yield was found to be somewhat variable,

but not less than 75 %.

Synthesis of bis-germylene 47

A solution of **32** (0.30 g, 0.86 mmol) in diethyl ether (10 ml) was treated with *n*BuLi (1.18 ml, 1.6 M hexane solution, 1.89 mmol) at 0 °C. This mixture was then stirred for 0.5 h and dropwise added to a diethyl ether (10 ml) suspension of $Cl_2Ge{\cdot}$1,4-dioxane (0.40 g, 1.71 mmol) at -78 °C. The mixture immediately became red–brown. After an hour, the mixture was allowed to warm to room temperature and stirred for 14 h. The resulting reddish solution was dried under reduced pressure and washed with toluene (3 × 15 ml) at 50 °C. The resulting solution was dried and the residue washed one more time with pentane (2 × 10 ml). The volatile materials were removed from the residue under vacuo to obtain **47** as an orange solid (0.20 g, 42 %, mp 70-72 °C (dec.)).

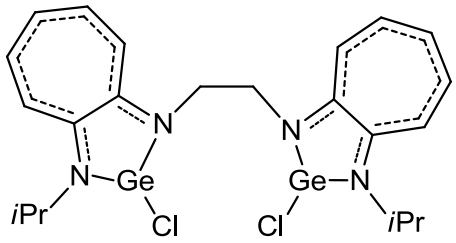

^{1}H NMR (300 MHz, $CDCl_3$): δ (ppm)
1.55 (d, $^3J_{HH}$ = 4.9 Hz, 12H, CH-CH_3),
4.10-4.30 (m, 2H, C*H*-CH_3),
4.19 (s, 4H, NCH_2),
6.74 (t, $^3J_{HH}$ = 9.3 Hz, 2H, C_7H_5),
6.89 (d, $^3J_{HH}$ = 10.3 Hz, 2H, C_7H_5),
7.05 (d, $^3J_{HH}$ = 9.3 Hz, 2H, C_7H_5),
7.27-7.37 (m, 4H, C_7H_5).

^{13}C {^{1}H} NMR (75 MHz, $CDCl_3$): δ (ppm)
23.67 (CH-*C*H_3),
45.82 (N-*C*H_2),
49.38 (*C*H-CH_3),
116.57 and 116.61 ($C_{3,7}$),
124.29 (C_5),
137.40 and 137.54 ($C_{4,6}$),
160.18 and 161.13 ($C_{2,8}$).

EI-MS: m/z 564 [M^+, 21 %], 529 [M^+ - Cl, 19 %], 422 [M^+ - 2Cl, - Ge, 17 %], 379 [M^+ - 2Cl - Ge - *i*Pr, 17 %], 457 [M^+ - Cl – Ge, 4 %], 337 [M^+ - 2Cl - Ge - 2*i*Pr, 3 %].

Synthesis of bis-germylene 48

A solution of **33** (0.40 g, 1.10 mmol) in diethyl ether (15 ml) was treated with *n*BuLi (1.56 ml, 1.6 M hexane solution, 2.20 mmol) at 0 °C. This mixture was then stirred for 0.5 h and dropwise added to a diethyl ether (12 ml) suspension of $Cl_2Ge{\cdot}$1,4-dioxane (0.51 g, 2.20 mmol) at -78 °C. The mixture immediately became deep – red. After an hour, the mixture was allowed to warm to room temperature and stirred for 14 h. The resulting reddish solution was dried under reduced pressure and washed with toluene (2 × 20 ml) at 55 °C. After filtration, the resulting solution was dried and the residue washed one more time with pentane (2 × 10 ml). The volatile materials were removed from the residue under vacuum to obtain the product as an orange – yellow solid (0.35 g, 56 % yield, mp 89 °C (dec.)).

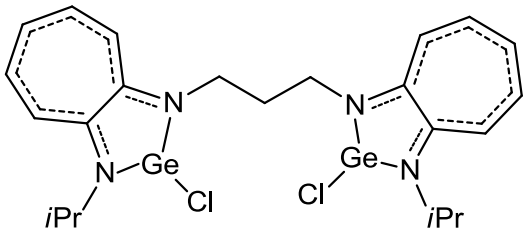

^{1}H NMR (300 MHz, $CDCl_3$): δ (ppm)
1.60 (d, $^3J_{HH}$ = 6.5 Hz, 12H, CH-CH_3),
2.53 (quint, $^3J_{HH}$ = 7.4 Hz, 2H, CH_2),
3.89 (t, $^3J_{HH}$ = 7.4 Hz, 4H, NCH_2),
4.29 (sept, $^3J_{HH}$ = 6.5 Hz, 2H, CH-CH_3),
6.70 (t, $^3J_{HH}$ = 9.4 Hz, 2H, C_7H_5),
6.81-6.91 (m, 4H, C_7H_5),
7.25-7.30 (m, 4H, C_7H_5).

^{13}C {^{1}H} NMR (75 MHz, $CDCl_3$): δ (ppm)
23.55 (CH-CH$_3$),
27.94 (CH$_2$),
44.37 (N-CH$_2$),
49.26 (CH-CH$_3$),
116.09 and 116.33 ($C_{3,7}$),
123.69 (C_5),
137.13 and 137.19 ($C_{4,6}$),
159.97 and 160.99 ($C_{2,8}$).

CI:CH_4 m/z: 578 [M^+, 12 %], 543 [M^+ - Cl, 94 %].
HRMS ($C_{23}H_{30}Cl_2Ge_2N_4$) calcd. 578.0281 amu;
found 578.0307 amu.

Preparation of germylene 49

A diethyl ether solution (35 ml) of [(*i*Pr)$_2$ATI]H (1.00 g, 4.9 mmol) was treated with *n*BuLi (3.06 ml, 1.6M hexane solution) at 0 °C. This mixture was then stirred for 0.5 h and slowly added to $Cl_2Ge{\cdot}$1,4-dioxane (1.14 g, 4.9 mmol) in diethyl ether (20 ml) at -78 °C. The mixture immediately became cloudy. After one hour, the mixture was allowed to warm to room

temperature and stirred overnight. The resulting reddish solution was filtered and the volatiles were removed from the filtrate under reduced pressure to obtain **49** as an orange red solid (1.25 g, 82 %, mp 108-110 °C).

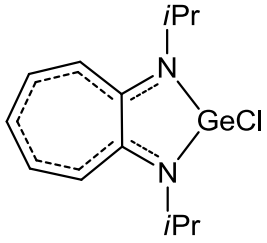

^{1}H NMR (300 MHz, $CDCl_3$): δ (ppm)
1.55 (d, $^{3}J_{HH}$ = 6.3 Hz, 12H, CH-CH_3),
4.18 (sept, $^{3}J_{HH}$ = 6.3 Hz, 2H, CH-CH_3),
6.66 (t, $^{3}J_{HH}$ = 9.3 Hz, 1H, H_5),
6.84 (d, $^{3}J_{HH}$ = 11.2 Hz, 2H, $H_{3,7}$),
7.23 (t, $^{3}J_{HH}$ = 10.4 Hz, 2H, $H_{4,6}$).

^{1}H NMR (300 MHz, C_6D_6): δ (ppm)
1.32 (d, $^{3}J_{HH}$ = 6.3 Hz, 12H, CH-CH_3),
1.55 (d, $^{3}J_{HH}$ = 6.3 Hz, 12H, CH-CH_3),
3.64 (sept, $^{3}J_{HH}$ = 6.3 Hz, 2H, CH-CH_3),
6.25 (t, $^{3}J_{HH}$ = 9.3 Hz, 1H, H_5),
6.69 (d, $^{3}J_{HH}$ = 11.2 Hz, 2H, $H_{3,7}$),
6.72 (t, $^{3}J_{HH}$ = 10.4 Hz, 2H, $H_{4,6}$).

^{13}C {^{1}H} NMR (75 MHz, $CDCl_3$): δ (ppm)
23.80 (CH-CH$_3$),
49.30 (CH-CH$_3$),
115.70 ($C_{3,7}$),
123.00 (C_5),
136.80 ($C_{4,6}$),
160.50 ($C_{2,8}$).

^{13}C {^{1}H} NMR (75 MHz, C_6D_6): δ (ppm)
22.70 and 23.70 (CH-CH$_3$),
49.30 (CH-CH$_3$),
115.50 ($C_{3,7}$),
122.00 (C_5),
136.60 ($C_{4,6}$),
160.60 ($C_{2,8}$).

Preparation of germylene 50

A diethyl ether solution (30 ml) of 2-(isopropy1amino) tropone (0.80 g, 4.91 mmol) was treated over a period of 2 minutes with *n*BuLi (3.60 ml, 1.6 M hexane solution) at 0 °C. This mixture was then stirred for 0.5 h and slowly added to Cl_2Ge·1,4-dioxane (1.16 g, 5.00 mmol) in diethyl ether (20 ml) at -78 °C. The solution immediately turned dark yellow. After an hour, the mixture was allowed to warm to room temperature and stirred for another 12 h. The solvents were evaporated and toluene (3 × 10 ml) was added. After filtration, the volatiles

were removed under reduced pressure to obtain **50** as an yellow solid (0.39 g, 84 %, mp 90 °C).

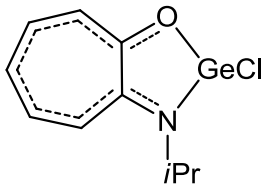

^{1}H NMR (300 MHz, $CDCl_3$): δ (ppm)

1.60 (d, $^{3}J_{HH}$ = 6.4 Hz, 6H, CH-CH_3),
4.20 (sept, $^{3}J_{HH}$ = 6.4 Hz, 1H, CH-CH_3),
7.01 (t.d, $^{3}J_{HH}$ = 9.0 Hz, $^{4}J_{HH}$ = 2.0 Hz, 1H, C_7H_5),
7.12 (d, $^{3}J_{HH}$ = 11.7 Hz, 1H, C_7H_5),
7.24-7.37 (m, 2H, C_7H_5).
7.42-7.51 (m, 1H, C_7H_5).

^{13}C {^{1}H} NMR (75 MHz, $CDCl_3$): δ (ppm)

21.86 (CH-$C$$H_3$),
49.43 (CH-CH_3),
120.41(C_3),
123.54 (C_5),
127.55 (C_7),
138.12 and 139.12 ($C_{4,6}$),
160.27 (C_2),
175.26 (C_8).

^{1}H NMR (300 MHz, C_6D_6): δ (ppm)

1.10 (s.l, 3H, CH-CH_3),
1.34 (s.l, 3H, CH-CH_3),
3.39 (sept, $^{3}J_{HH}$ = 6.5 Hz, 1H, CH-CH_3),
6.23 (t, $^{3}J_{HH}$ = 9.9 Hz, 1H, H_5),
6.29 (d, $^{3}J_{HH}$ = 11.6 Hz, 1H, H_3),
6.53 (t.d, $^{3}J_{HH}$ = 10.1 Hz, $^{4}J_{HH}$ = 1.1 Hz, 1H, H_6),
6.65 (d.d.d, $^{3}J_{HH}$ = 11.6 Hz, $^{3}J_{HH}$ = 9.9 Hz, $^{4}J_{HH}$ = 1.1 Hz, 1H, H_4),
6.94 (d.d, $^{3}J_{HH}$ = 10.3 Hz, $^{4}J_{HH}$ = 0.8 Hz, 1H, H_7).

^{13}C {^{1}H} NMR (75 MHz, C_6D_6): δ (ppm)

20.75 (CH-$C$$H_3$),
48.99 (CH-CH_3),
119.62(C_3),
122.90 (C_7),
126.08 (C_5),
137.55 (C_6),
138.04 (C_4),
159.87 (C_2),
175.62 (C_8).

EI-MS: m/z 271 [M^+, 33 %], 236 [M^+ - Cl, 80 %].

Synthesis of bis-germylene 51

A diethyl ether solution (10 ml) of **34** (0.32 g, 1.13 mmol) was treated with *n*BuLi (1.58 ml, 1.6 M hexane solution) at 0 °C. This mixture was then stirred for 0.5 h and slowly added to Cl_2Ge·1,4-dioxane (0.52 g, 2.26 mmol) in diethyl ether (10 ml) at - 78 °C. The mixture immediately became cloudy. After an hour, the mixture was allowed to warm to room temperature and stirred overnight. The solvents were evaporated and 10 ml of toluene was added. The resulting mixture was filtered and the volatiles were removed from the filtrate under reduced pressure to obtain the product as a yellow solid (0.32 g, 57 %, mp 100 °C (dec.)).

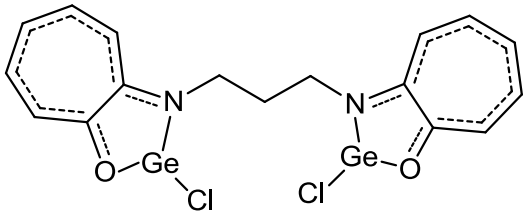

^{1}H NMR (300 MHz, $CDCl_3$): δ (ppm)
2.56 (quint, $^3J_{HH}$ = 7.3 Hz, 2H, CH_2),
3.88 (t, $^3J_{HH}$ = 7.3 Hz, 4H, NCH_2),
7.05-7.40 (m, 10H, C_7H_5).

^{13}C {^{1}H} NMR (75 MHz, $CDCl_3$): δ (ppm)
29.70 (*C*H_2),
44.10 (N-*C*H_2),
120.67 (C_3),
124.12 (C_5),
128.39 (C_7),
138.74 (C_4),
139.74 (C_6),
163.50 (C_2),
176.80 (C_8).

CI:NH_3 m/z 461 [M^+ - HCl, 100 %].

Synthesis of germanethioacid chloride 52

To a solution of **49** (150 mg, 0.48 mmol) in $CHCl_3$ (10 ml) solid sulfur was added (15 mg, 0.48 mmol). The reaction mixture was stirred at 60 °C for 2 h. Evaporation of the solvent yields **52** as a yellow solid (152 mg, 92 %, mp 140-142 °C (dec.)).

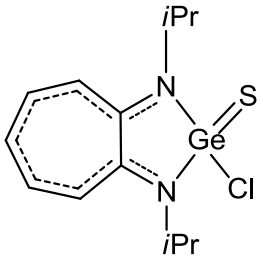

^{1}H NMR (300 MHz, $CDCl_3$): δ (ppm)
1.60 (d, $^{3}J_{HH}$ = 6.6 Hz, 6H, CH-CH_3),
1.75 (d, $^{3}J_{HH}$ = 6.6 Hz, 6H, CH-CH_3),
4.30 (sept, $^{3}J_{HH}$ = 6.6 Hz, 2H, CH-CH_3),
6.96 (t, $^{3}J_{HH}$ = 9.4 Hz, 1H, H_5),
7.04 (d, $^{3}J_{HH}$ = 11.4 Hz, 2H, $H_{4,6}$),
7.48 (t, $^{3}J_{HH}$ = 10.5 Hz, 2H, $H_{3,7}$).

^{13}C {^{1}H} NMR (75 MHz, $CDCl_3$): δ (ppm)
21.92 (CH-$C$$H_3$),
22.14 (CH-$C$$H_3$),
50.12 (CH-CH_3),
117.24 ($C_{3,7}$),
126.63 (C_5),
139.13 ($C_{4,6}$),
150.60 ($C_{2,8}$).

EI-MS: m/z 344 [M^+, 31 %], 311 [M^+ - SH, 53 %], 309 [M^+ - Cl, 46 %].

Synthesis of germaneselenoacid chloride 53

To a solution of **49** (31 mg, 0.10 mmol) in $CDCl_3$ (0.6 ml) solid selenium was added (8 mg, 0.10 mmol). The reaction mixture was stirred at 60 °C for 4.5 h. After evaporation of the solvent, the compound **53** was obtained in nearly quantitative yield (mp 144-146 °C (dec.)).

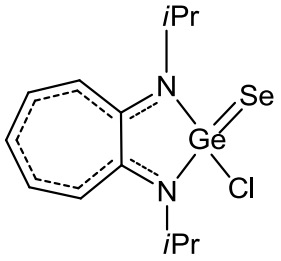

^{77}Se NMR (76 MHz, $CDCl_3$): δ (ppm) –44.91.

^{1}H NMR (300 MHz, $CDCl_3$): δ (ppm)
1.61 (d, $^{3}J_{HH}$ = 6.6 Hz, 6H, CH-CH_3),
1.79 (d, $^{3}J_{HH}$ = 6.6 Hz, 6H, CH-CH_3),
4.37 (sept, $^{3}J_{HH}$ = 6.6 Hz, 2H, CH-CH_3),
6.94 (t, $^{3}J_{HH}$ = 9.4 Hz, 1H, H_5),
7.03 (d, $^{3}J_{HH}$ = 11.6 Hz, 2H, $H_{4,6}$),
7.49 (ps.t, 2H, $H_{3,7}$).

^{1}H NMR (400 MHz, $CDCl_3$): δ (ppm)
1.62 (d, $^{3}J_{HH}$ = 6.6 Hz, 6H, CH-CH_3),
1.80 (d, $^{3}J_{HH}$ = 6.6 Hz, 6H, CH-CH_3),
4.37 (sept, $^{3}J_{HH}$ = 6.6 Hz, 2H, CH-CH_3),
6.94 (t, $^{3}J_{HH}$ = 9.4 Hz, 1H, H_5),
7.02 (d, $^{3}J_{HH}$ = 11.5 Hz, 2H, $H_{4,6}$),
7.48 (ps.t, 2H, $H_{3,7}$).

^{13}C {^{1}H} NMR (75 MHz, $CDCl_3$): δ (ppm)
22.09 (CH-$C$$H_3$),
50.26 (CH-CH_3),
117.35 ($C_{3,7}$),

126.80 (C_5),
138.92 ($C_{4,6}$),
155.70 ($C_{2,8}$).

EI-MS: m/z 390 [M^+, 10 %], 311 [M^+ - Cl, 5 %], 309 [M^+ - Se, 35 %].
Anal. $C_{13}H_{19}ClN_2GeSe$ (390.21): calc. C 40.00, H 4.91, N 7.18;
found C 39.37, H 4.66, N 6.52.

Synthesis of cycloadduct 54

A solution of **49** (0.20 g, 0.64 mmol) in THF (5 ml) was combined with a solution of 3,5 -di-*tert*-butyl-1,2-benzoquinone (0.20 g, 0.64 mmol) in THF (5 ml) and the mixture stirred for 0.5 h at room temperature. The yellow solution was concentrated in vacuo to obtain **54** (0.26 g, 76 %, mp 72-74 °C (dec.)).

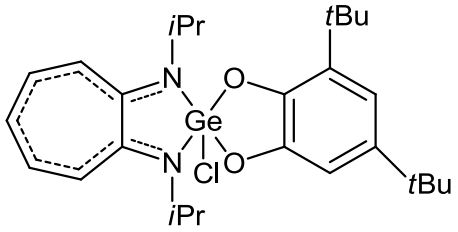

^{1}H NMR (300 MHz, $CDCl_3$): δ (ppm)
1.26 (s, 9H, C(CH_3)$_3$),
1.39 (s, 9H, C(CH_3)$_3$),
1.53 (d, $^3J_{HH}$ = 6.9 Hz, 6H, CH-CH_3),
1.71 (d, $^3J_{HH}$ = 6.9 Hz, 6H, CH-CH_3),
4.78 (sept, $^3J_{HH}$ = 7.0 Hz, 2H, CH-CH_3),
6.68 (d, $^3J_{HH}$ = 2.2 Hz, 1H, C_6H_2),
6.85 (d, $^3J_{HH}$ = 2.1 Hz, 1H, C_6H_2),
6.82 (t, $^3J_{HH}$ = 9.1 Hz, 1H, H_5),
7.22 (d, $^3J_{HH}$ = 11.0 Hz, 2H, $H_{3,7}$),
7.31-7.68 (m, 2H, $H_{4,6}$).

^{13}C {^{1}H} NMR (75 MHz, $CDCl_3$): δ (ppm)
20.14 and 20.80 ((*C*H_3)$_2$CH),
29.71 and 31.87 (C(*C*H_3)$_3$),
34.49 (*C*(CH$_3$)$_3$),
49.99 (*C*H(CH$_3$)$_2$),
107.29 and 112.54 (*C*$_6$H$_2$),
116.29 ($C_{3,7}$),
124.69 (C_5),
137.16 ($C_{4,6}$),
132.69, 140.21, 147.23, 152.72 (C_6H_2, quat.),
163.36 ($C_{2,8}$).

EI-MS: m/z 532 [M^+, 100 %], 517 [M^+ - CH_3, 35 %], 497 [M^+ - Cl, 7 %], 312 [M^+ - benzoquinone, 39 %], 277 [M^+ - Cl - benzoquinone, 67 %].
Anal. $C_{27}H_{39}N_2GeClO_2$ (534.20): calc. C 60.76, H 7.74, N 5.25;
found C 57.79, H 8.04, N 5.07.

Synthesis of cycloadduct 55

A Schlenk tube was charged with 0.10 g (0.37 mmol) of **50**, 0.08 g (0.37 mmol) of 3,5 -di-*tert*-butyl-1,2-benzoquinone and THF (10 ml). After 0.5 h of stirring at room temperature, the volatiles were removed under vacuo leading to a yellow solid identified as **55** (0.19 g, 64 %, mp 106 °C).

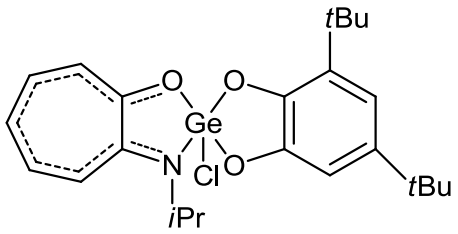

^{1}H NMR (300 MHz, $CDCl_3$): δ (ppm)

1.32 (s, 9H, C(CH_3)$_3$),
1.49 (s, 9H, C(CH_3)$_3$),
1.72 (s, 6H, CH-CH_3),
4.88 (sept, $^{3}J_{HH}$ = 6.9 Hz, 1H, CH-CH_3),
6.79 (d, $^{3}J_{HH}$ = 2.1 Hz, 1H, C_6H_2),
7.02 (d, $^{3}J_{HH}$ = 2.1 Hz, 1H, C_6H_2),
7.16-7.30 (m, 3H, C_7H_5),
7.56-7.70 (m, 2H, C_7H_5).

^{13}C {^{1}H} NMR (75 MHz, $CDCl_3$): δ (ppm)

21.47 and 21.67 ((*C*H_3)$_2$CH),
29.75 and 31.77 (C(*C*H_3)$_3$),
34.51 and 34.56 (C(*C*H_3)$_3$),
50.05 (CH(*C*H_3)$_2$),
107.76 and 113.17 (*C*$_6H_2$),
123.12 (C_3),
128.42 (C_5),
129.05 (C_7),
133.15, 140.95, 142.50, 146.62 (C_6H_2),
139.90 (C_4),
140.21 (C_6),
157.26 (C_2),
165.67 (C_8).

EI-MS: m/z 491 [M^+, 80 %], 476 [M^+ - CH_3, 100 %].

Anal. $C_{24}H_{34}N_2GeClO_3$ (493.14): calc. C 58.51, H 6.96, N 2.84;
found C 54.59, H 7.10, N 2.78.

Synthesis of bis-germylene cycloadduct 56

A solution of **47** (0.25 g, 0.44 mmol) in THF (12 ml) was combined with a solution of 3,5 -di-*tert*-butyl-1,2-benzoquinone (0.19 g, 0.88 mmol) in THF (10 ml) and the mixture stirred for 1.5 h at room temperature. After filtration, the solvent was removed from the precipitate leaving to **56**, a yellow powder (0.27 g, 61 %, mp 138-140 °C (dec.)).

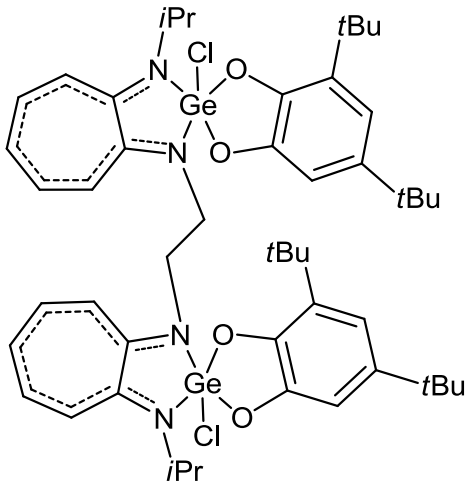

^{1}H NMR (300 MHz, $CDCl_3$): δ (ppm)

1.25 (s, 18H, C(CH_3)$_3$),
1.38 (s, 18H, C(CH_3)$_3$),
1.56 (d, $^{3}J_{HH}$ = 6.7 Hz, 6H, CH-CH_3),
1.72 (d, $^{3}J_{HH}$ = 6.7 Hz, 6H, CH-CH_3),
4.35-4.40 (m, 4H, CH_2-N),
4.89 (sept, $^{3}J_{HH}$ = 7.1 Hz, 2H, CH-CH_3),
6.74 (br.s, 2H, C_6H_2),
6.89-7.03 (m, 6H, C_7H_5),
7.31-7.50 (m, 6H, C_6H_2 and C_7H_5),
7.64-7.74 (m, 2H, C_7H_5).

^{13}C {^{1}H} NMR (75 MHz, $CDCl_3$): δ (ppm)

19.67 and 20.52 ((CH_3)$_2$CH),
29.70 and 31.85 (C(CH_3)$_3$),
34.52 (C(CH_3)$_3$),
43.76 and 43.94 (CH_2-N),
49.60 (CH(CH_3)$_2$),
107.11, 112.83 and 112.96 (C_6H_2),
117.70 (C_7),
118.95 and 119.07 (C_3),
125.98 (C_5),
133.36 (C-C(CH_3)$_3$),
137.64 (C_4),
138.85 and 139.01 (C_6),

140.40 and 140.49 (*C*-C(*C*H_3)$_3$),
142.65, 142.77 and 147.18 (*C*-O),
153.61 and 154.11 ($C_{2,8}$).

CI:NH_3 m/z 950 [M^+ - HCl - H - CH_3, 1 %].

Synthesis of bis-germylene cycloadduct 57

A solution of **48** (0.25 g, 0.43 mmol) in THF (12 ml) was combined with a solution of 3,5 -di-*tert*-butyl-1,2 –benzoquinone (0.19 g, 0.86 mmol) in THF (10 ml) and the mixture stirred for 1.5 h at room temperature. The solvent was evaporated under vacuo and the residue washed with pentane (15 ml). After filtration, the solvent was removed from the precipitate leaving to a yellow powder identified as **57** (0.29 g, 67 %, mp 154 °C (dec.)).

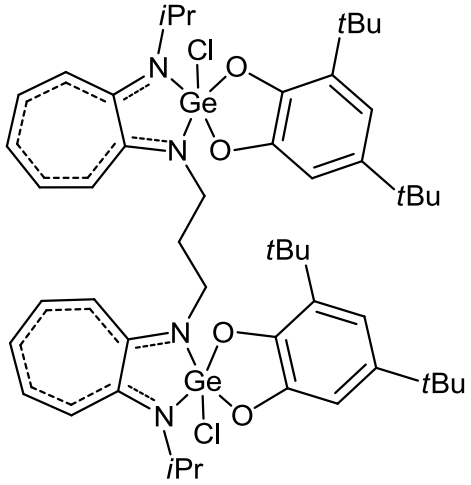

^{1}H NMR (300 MHz, $CDCl_3$): δ (ppm)

1.26 (s, 18H, C(C*H*$_3$)$_3$),
1.42 (s, 18H, C(C*H*$_3$)$_3$),
1.61 (d, $^3J_{HH}$ = 6.7 Hz, 6H, CH-C*H*$_3$),
1.73 (d, $^3J_{HH}$ = 6.7 Hz, 6H, CH-C*H*$_3$),
2.25 (m, 2H, C*H*$_2$),
4.20 (m, 4H, C*H*$_2$-N),
4.76 (sept, $^3J_{HH}$ = 7.0 Hz, 2H, C*H*-CH_3),
6.79 (d, $^3J_{HH}$ = 1.5 Hz, 2H, C_6H_2),
6.97 (d, $^3J_{HH}$ = 1.5 Hz, 2H, C_6H_2),
6.72-6.90 (m, 2H, C_7H_5),
7.18-7.43 (m, 8H, C_7H_5).

^{13}C {^{1}H} NMR (75 MHz, $CDCl_3$): δ (ppm)

19.74 and 20.29 ((*C*H_3)$_2$CH),
25.62 (*C*H_2),
29.76 and 31.89 (C(*C*H_3)$_3$),
34.53 and 34.57 (C(*C*H_3)$_3$),
44.28 (*C*H_2-N),

49.50 ($CH(CH_3)_2$),
107.41 and 112.78 (C_6H_2),
116.26 (C_7),
118.54 (C_3),
125.37 (C_5),
133.02 (C-$C(CH_3)_3$),
137.65 (C_4),
138.35 (C_6),
140.39 (C-$C(CH_3)_3$),
147.21 and 150.97 (C-O),
153.42 and 153.72 ($C_{2,8}$).

CI:NH_3 m/z 983 [M^+ - HCl, 90 %].

Synthesis of bis-germylene tungsten complex 58

A solution of $W(CO)_5THF$ (1.10 mmol), freshly prepared by irradiation of $W(CO)_6$, in THF (20 ml), was added to a stirred suspension of **48** (0.30 g, 0.52 mmol) in THF (6 ml). The solution immediately turned orange (but after stirring 10 min turned deep red). The reaction mixture was stirred at 40 °C for 1 h. After filtration, the solvent was removed from the precipitate leaving a yellow powder identified as **58** (0.48 g, 80 %, mp 200-202 °C).

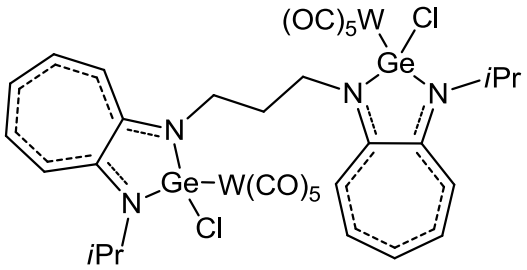

^{1}H NMR (300 MHz, $CDCl_3$): δ (ppm)

1.57 (d, $^3J_{HH}$ = 6.5 Hz, 3H, CH-CH_3),
and 1.59 (d, $^3J_{HH}$ = 6.5 Hz, 3H, CH-CH_3),
1.75 (d, $^3J_{HH}$ = 6.5 Hz, 3H, CH-CH_3),
and 1.77 (d, $^3J_{HH}$ = 6.6 Hz, 3H, CH-CH_3),
2.46 (quint, $^3J_{HH}$ = 7.8 Hz, 2H, CH_2),
4.03-4.18 (m, 4H, NCH_2),
4.35 (sept, $^3J_{HH}$ = 6.7 Hz, 2H, CH-CH_3),
6.92 (t.d, $^3J_{HH}$ = 9.4 Hz, $^4J_{HH}$ = 2.4 Hz, 2H, C_7H_5),
6.93 (t, $^3J_{HH}$ = 9.4 Hz, 1H, C_7H_5),
7.08-7.18 (m, 4H, C_7H_5),
7.39-7.51 (m, 4H, C_7H_5).

^{13}C {^{1}H} NMR (75 MHz, $CDCl_3$): δ (ppm)

21.88, 20.05, 22.83 (CH-CH_3),
25.84, 26.16 (CH_2),
42.67 and 42.74 (N-CH_2),

49.61 (*C*H-CH_3),
117.50 and 117.65, 117.82 ($C_{3,7}$),
126.42 (C_5),
138.34 and 138.97, 139.14 ($C_{4,6}$),
158.02 and 158.05, 158.08, 158.24 ($C_{2,8}$),
197.24 and 197.29 (C_{eq}),
199.57 and 199.65 (C_{ax}).

^{1}H NMR (300 MHz, THF d8): δ (ppm)
1.65 (d, $^3J_{HH}$ = 5.0 Hz, 3H, CH-C*H*$_3$),
and 1.67 (d, $^3J_{HH}$ = 5.1 Hz, 3H, CH-C*H*$_3$),
1.78 (d, $^3J_{HH}$ = 5.0 Hz, 3H, CH-C*H*$_3$),
and 1.80 (d, $^3J_{HH}$ = 4.9 Hz, 3H, CH-C*H*$_3$),
2.40-2.55 (m, 2H, C*H*$_2$),
4.03-4.14 (m, 4H, NC*H*$_2$),
4.54 (sept, $^3J_{HH}$ = 6.6 Hz, 2H, C*H*-CH_3),
7.06 (t, $^3J_{HH}$ = 9.4 Hz, 2H, C_7H_5),
7.22 (ps.t, 2H, C_7H_5),
7.32 (d, $^3J_{HH}$ = 11.3 Hz, 2H, C_7H_5),
7.50-7.66 (m, 4H, C_7H_5).

^{13}C {^{1}H} NMR (75 MHz, THF d8): δ (ppm)
21.29, 21.52, 22.20 (CH-*C*H_3),
25.78, 26.04 (*C*H_2),
42.45 and 42.55 (N-*C*H_2),
49.53 (*C*H-CH_3),
117.61 and 117.79, 118.21 ($C_{3,7}$),
126.61 (C_5),
138.64 and 138.74, 138.88 ($C_{4,6}$),
157.89 and 158.11, 158.14, 158.19 ($C_{2,8}$),
197.32 and 197.35 (C_{eq}),
199.77 and 199.88 (C_{ax}).

CI:NH_3 m/z 867 [M^+ - $W(CO)_5$ - Cl, 1 %].
IR: $\nu_{(CO)}$ = 1936, 1979 and 2070 cm^{-1}.

Synthesis of bis-germylene molybdenum complex 59

In glove box, a Schlenk flask was charged with **48** (0.18 g, 0.31 mmol), a stir bar, and $Mo(CO)_4COD$ (0.10 g, 0.34 mmol). THF (12 ml) was added and the resulting mixture stirred for 16 h at room temperature. The solution was concentrated in vacuo and the residue washed with hexane (5 ml) to yield a mixture of **59** and unidentified products.

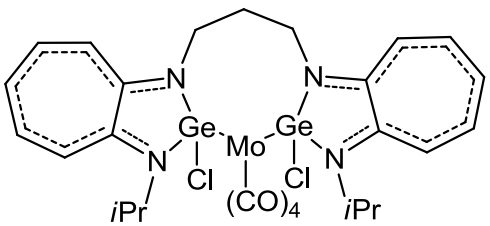

^{1}H NMR (300 MHz, THF): δ (ppm)

1.55 (d, $^3J_{HH}$ = 6.7 Hz, 3H, CH-CH_3),
and 1.58 (d, $^3J_{HH}$ = 6.8 Hz, 3H, CH-CH_3),
1.74 (d, $^3J_{HH}$ = 6.8 Hz, 3H, CH-CH_3),
and 1.81 (d, $^3J_{HH}$ = 6.7 Hz, 3H, CH-CH_3),
2.08-2.17 (m, 2H, CH_2),
3.73-3.81 (m, 2H, NCH_2),
4.14-4.27 (m, 2H, NCH_2),
4.48-4.63 (m, 2H, CH-CH_3),
6.85 (ps.t, 2H, C_7H_5),
7.04 (ps.t, 2H, C_7H_5),
7.21 (ps.t, 2H, C_7H_5),
7.37-7.47 (m, 4H, C_7H_5).

IR: $\nu_{(CO)}$ = 1879 and 2045 cm^{-1}.

Synthesis of bis-germylene tungsten complex 60

In glove box, a Schlenk flask was charged with **48** (0.190 g, 0.327 mmol) and $W(CO)_4COD$ (0.143 g, 0.327 mmol). THF (12 ml) was added and the solution immediately turned bright brown, the resulting mixture stirred for 24 h at room temperature and 2.5 h at 25 °C. The solvent was pumped out and the residue washed with hexane (5 ml) to yield mixture of **60** and unidentified products.

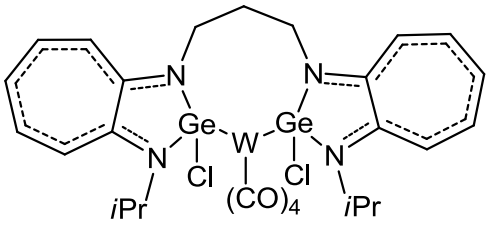

^{1}H NMR (300 MHz, $CDCl_3$): δ (ppm)

1.62 (d, $^3J_{HH}$ = 6.8 Hz, 3H, CH-CH_3),
and 1.65 (d, $^3J_{HH}$ = 6.8 Hz, 3H, CH-CH_3),
1.83 (d, $^3J_{HH}$ = 6.8 Hz, 3H, CH-CH_3),
and 1.90 (d, $^3J_{HH}$ = 6.8 Hz, 3H, CH-CH_3),
2.09-2.18 (m, 2H, CH_2),
3.68-3.83 (m, 2H, NCH_2),
4.15-4.29 (m, 2H, NCH_2),
4.50-4.60 (m, 2H, CH-CH_3),
6.82-6.92 (m, 5H, C_7H_5),
7.34-7.46 (m, 5H, C_7H_5).

IR: $\nu_{(CO)}$ = 1893, 1919 and 2018 cm^{-1}.

X-ray Structural Determination

Structural data were collected at low temperature (193 K) using an oil-coated shock-cooled crystal on a Bruker-AXS CCD 1000 diffractometer with Mo-K_α radiation (λ = 0.71073 Å). Structures were solved by direct methods[93] and all non-hydrogen atoms were refined anisotropically using the least-squares method on F^2 (SHELXL-97)[94] .

Structural data of **36, 53** and **56** are given in tables 9 and 10.

Table 9: Structural refinement data for **36** and **53**

	36	**53**
Empirical formula	$C_{23}H_{30}Li_2N_4$, $2Et_2O$	$C_{13}H_{19}ClGeN_2Se$, CH_2Cl_2
Formula weight	524.63	475.23
Temperature (K)	193(2)	193(2)
Crystal system	Orthorhombic	Orthorhombic
Space group	Pbca	Pbca
a (Å)	14.2311(4)	14.3094(9)
b (Å)	18.9502(4)	15.4620(10)
c (Å)	24.0453(5)	17.2181(10)
α (°)	90	90
β (°)	90	90
γ (°)	90	90
Volume ($Å^3$)	6484.6(3)	3809.5(4)
Z	8	8
Density (calculated)(Mg/m^3)	1.075	1.657
Absorption coefficient (mm^{-1})	0.066	3.935
Reflections collected	72472	39104
Independent reflections	6583 [R(int) = 0.0446]	3484 [R(int) = 0.1627]
Absorption correction	Semi-empirical from equivalents	Full-matrix least-squares
Max. and min. transmission	0.9614 and 0.9490	
Final R indices [I>2sigma(I)]	R1 = 0.0512, wR2 = 0.1231	R1 = 0.0445, wR2 = 0.0841
R indices (all data)	R1 = 0.0844, wR2 = 0.1521	R1 = 0.0980, wR2 = 0.1055
Larg. diff. peak and hole ($eÅ^{-3}$)	0.238 and -0.222	0.644 and -0.527

with $R_1 = \Sigma||F_o|-|F_c||/\Sigma|F_o|$ and $wR_2 = (\Sigma w (F_o^2-F_c^2)^2/\Sigma w(F_o^2)^2)^{0.5}$.

Table 10: Structural refinement data for **58**

	58
Empirical formula	$C_{35}H_{32}Cl_6Ge_2N_4O_{10}W_2$
Formula weight	1394.23
Temperature (K)	193(2)
Crystal system	Monoclinic
Space group	C2/c
a (Å)	16.1886(4)
b (Å)	18.9338(4)
c (Å)	17.1363(4)
α (°)	90
β (°)	114.6850(10)
γ (°)	90
Volume ($Å^3$)	4772.49(19)
Z	4
Density (calculated)(Mg/m^3)	1.940
Absorption coefficient (mm^{-1})	6.441
Reflections collected	30659
Independent reflections	4852 [R(int) = 0.0552]
Absorption correction	Semi-empirical from equivalents
Max. and min. transmission	0.7827 and 0.3590
Final R indices [I>2sigma(I)]	R1 = 0.0344, wR2 = 0.0742
R indices (all data)	R1 = 0.0565, wR2 = 0.0832
Largest diff. peak and hole ($eÅ^{-3}$)	1.616 and -0.767

References

[1] H. V. R. Dias, W. Jin, Z. Wang, *Coord. Chem. Rev.* **1998**, *176*, 67.

[2] M. R. Bürgstein, H. Berberich, P. W. Roesky, *Organometallics* **1998**, *17*, 1452.

[3] P. W. Roesky, *Eur. J. Inorg. Chem.* **1998**, 593.

[4] P. W. Roesky, *Chem. Ber.* **1997**, *130*, 859.

[5] H. V. R. Dias, W. Jin, Z. Wang, *Inorg. Chem.* **1996**, *35*, 6074.

[6] H. V. R. Dias, W. Jin, R. E. Ratcliff, *Inorg. Chem.* **1995**, *34*, 6100.

[7] P. W. Roesky, *Chem. Soc. Rev.* **2000**, *29*, 335.

[8] P. W. Roesky, *Inorg. Chem.* **1998**, *37*, 4507.

[9] P. W. Roesky, M. R. Bürgstein, *Inorg. Chem.* **1999**, *38*, 5629.

[10] P. W. Roesky, *J. Organomet. Chem.* **2000**, *603*, 161.

[11] M. R. Bürgstein, W. Roesky, *Organometallics* **2003**, *22*, 1372.

[12] N. Meyer, A. Zulys, P. W. Roesky, *Organometallics* **2006**, *25*, 4179.

[13] M. R. Bürgstein, E. P. Euringer, P. W. Roesky, *J. Chem. Soc. Dalton. Trans* **2000**, 1045.

[14] S. Schulz, M. Nieger, H. Hupfer, P. W. Roesky, *Eur. J. Inorg. Chem.* **2000**, 1623.

[15] A. Zask, N. Gonnella, K. Nakanishi, C. J. Turner, S. Imajo, T. Nozoe, *Inorg. Chem.* **1986**, *25*, 3400.

[16] P. W. Roesky, *Inorg. Chem.* **1998**, *37*, 4507.

[17] G. R. Fulmer, A. J. M. Miller, N. H. Sherden, H. E. Gottlieb, A. Nudelman, B. M. Stoltz, J. E. Bercaw, K. I. Goldberg, *Organometallics* **2010**, *29*, 2176.

[18] I. Fernandez, E. M. Viviente, F. Breher, P. S. Pregosin, *Chem. Eur. J.* **2005**, *11*, 1495.

[19] D. M. Grant, R. K. Harris, *Encyclopedia of Nuclear Magnetic Resonance, John Wiley & Sons* **1996**.

[20] N. Meyer, P. W. Roesky, *Dalton Trans.* **2007**, 2652.

[21] P. Jutzi, A. Becker, H. G. Stammler, B. Neumann, *Organometallics* **1991**, *10*, 1647.

[22] W. Petz, *Chem. Rev.* **1986**, *86*, 1019.

[23] M. F. Lappert, R. S. Rowe, *Coord. Chem. Rev.* **1990**, *100*, 267.

[24] J. Barrau, J. Escudié, J. Satgé, *Chem. Rev.* **1990**, *90*, 283.

[25] G. L. Wegner, R. J. F. Berger, A. Schier, H. Schmidbaur, *Organometallics* **2001**, *20*, 418.

[26] M. Weidenbruch, *Eur. J. Inorg. Chem.* **1999**, 373.

[27] J. Barrau, G. Rima, *Coord. Chem. Rev.* **1998**, *178-180*, 593.

[28] W. P. Neumann, *Chem. Rev.* **1991**, *91*, 311.

[29] P. T. Matsunaga , J. Kouvetakis, T. L. Groy, *Inorg. Chem.* **1995**, *34*, 5103.

[30] T. Fjeldberg, A. Haaland, B. E. R. Schilling, M. F. Lappert, A. J. Thorne, *J. Chem. Soc., Dalton Trans.* **1986**, 1551.

[31] T. Sasamori, N. Tokitoh, R. B. King, *Encyclopedia of Inorganic Chemistry II, Ed. John Wiley & Sons: Chichester, U.K.* **2005**.

[32] T. Fueno, *The Transition State: A Theoretical Approach, Ed. Gordon and Breach Science Publishers: Langhorne, PA* **1999**.

[33] Y. Mizuhata, T. Sasamori, N. Tokitoh, *Chem. Rev.* **2009**, *109*, 3479.

[34] R. A. Bartlett, P. P. Power, *J. Am. Chem. Soc.* **1990**, *112*, 3660.

[35] S. Kobayashi, S. Cao, *Chem. Lett.* **1994**, *25*, 941.

[36] J. Rouzaud, A. Castel, P. Rivière, H. Gornitzka, J. M. Manriquez, *Organometallics* **2000**, *19*, 4678.

[37] A. V. Zabula, F. E. Hahn, T. Pape, A. Hepp, *Organometallics* **2007**, *26*, 1972.

[38] F. E. Hahn, A. V. Zabula, T. Pape, F. Hupka, *Z. Anorg. Allg. Chem.* **2009**, *635*, 1341.

[39] F. E. Hahn, A. V. Zabula, T. Pape, A. Hepp, *Z. Anorg. Allg. Chem.* **2008**, *634*, 2397.

[40] H. V. R. Dias, Z. Wang, *J. Am. Chem. Soc.* **1997**, *119*, 4650.

[41] A. E. Ayers, H. V. R. Dias, *Inorg. Chem.* **2002**, *41*, 3259.

[42] T. Nozoe, K. Imafuku, B.-Z. Yin, M. Honda, Y. Hara, T. Anoloh, H. Yamamoto, *Bull. Chem. Soc. Jpn* **1988**, *61*, 2531.

[43] *Gaussian 98, Revision A.11.3; Gaussian, Inc.: Pittsburgh, PA* **2002**.

[44] Y. Moreno, Y. Nakamura, T. J. Iijima, *Chem. Phys.* **1960**, *32*, 643.

[45] J. E. Drake, J. L. Hencher, Q. Shen, *Can. J. Chem.* **1977**, *55*, 1104.

[46] L. Walz, D. Thiery, E. M. Peters, H. Wendel, E. Schonher, M. Wojnowski, *Z. Kristallogr.* **1993**, *208*, 207.

[47] L. Pu, M. M. Olmstead, P. P. Power, B. Schiemenz, *Organometallics* **1998**, *17*, 5602.

[48] A. C. Filippou, P. Portius, A. I. Philippopoulos, *Organometallics* **2002**, *21*, 653.

[49] I. Saur, K. Miqueu, G. Rima, J. Barrau, V. Lemierre, A. Chrostowska, J.-M. Sotiropoulos, G. Pfister-Guillouzo, *Organometallics* **2003**, *22*, 3143.

[50] Y. Ding, Q. Ma, I. Uson, H. W. Roesky, M. Noltemeyer, H. G. Schmidt, *J. Am. Chem. Soc.* **2002**, *124*, 8542.

[51] P. Arya, J. Boyer, F. Carre, R. Corriu, G. Lanneau, J. Lapasset, M. Perrot, C. Priou, *Angew. Chem., Int. Ed. Engl.* **1989**, *28*, 1016.

[52] H. Suzuki, N. Tokitoh, S. Nagase, R. Okazaki, *J. Am. Chem. Soc.* **1994**, *116*, 11578.

[53] M. Veith, S. Becker, V. Huch, *Angew. Chem., Int. Ed. Engl.* **1989**, *28*, 1237.

[54] M. C. Kuchta, G. Parkin, *J. Chem. Soc., Chem. Commun.* **1994**, 1351.

[55] T. Matsumoto, N. Tokitoh, R. Okazaki, *Angew. Chem., Int. Ed. Engl.* **1994**, *33*, 2316.

[56] N. Tokitoh, T. Matsumoto, R. Okazaki, *J. Am. Chem. Soc.* **1997**, *119*, 2337.

[57] S. R. Foley, C. Bensimon, D. S. Richeson, *J. Am. Chem. Soc.* **1997**, *119*, 10359.

[58] G. Ossig, A. Meller, C. Bronneke, O. Muller, M. Schafer, R. Herbst-Irmer, *Organometallics* **1997**, *16*, 2116.

[59] T. Matsumoto, N. Tokitoh, R. Okazaki, *J. Am. Chem. Soc.* **1999**, *121*, 8811.

[60] R. Guilard, C. Ratti, J.-M. Barbe, D. Dubois, K. M. Kadish, *Inorg. Chem. Ber.* **1991**, *30*, 1537.

[61] Y. Matsuhashi, N. Tokitoh, R. Okazaki, *Organometallics* **1993**, *12*, 2573.

[62] M. C. Kuchta, G. Parkin, *J. Am. Chem. Soc.* **1994**, *116*, 8372.

[63] Y. Zhou, D. S. Richeson, *J. Am. Chem. Soc.* **1996**, *118*, 10850.

[64] W.-P. Leung, W.-H. Kwok, L. T. C. Law, Z.-Y. Zhou, T. C. W. Mak, *J. Chem. Soc., Chem. Commun.* **1996**, 505.

[65] M. Saito, N. Tokitoh, R. Okazaki, *J. Am. Chem. Soc.* **1997**, *119*, 11124.

[66] W. P. Leung, K. H. Chong, Y. S. Wu, C. W. So, H. S. Chan, T. C. W. Mak, *Eur. J. Inorg. Chem.* **2006**, 808.

[67] H. C. E. McFahrlane, W. McFarlane, *In Multinuclear NMR; Mason, J., Ed.; Plenum Press: New York* **1987**, 417.

[68] Y. Ding, Q. Ma, H. W. Roesky, I. Usón, M. Noltemeyer, H.-G. Schmidt, *Dalton Trans.* **2003**, 1094.

[69] T. Matsumoto, N. Tokitoh, R. Okazaki, *J. Am. Chem. Soc.* **1999**, *121*, 8811.

[70] P. B. Hitchcock, E. Jang, M. F. Lappert, *J. Chem. Soc., Dalton Trans.* **1995**, 3179.

[71] T. Matsumoto, N. Tokitoh, R. Okazaki, *Angew. Chem. Int. Ed. Engl.* **1994**, *33*, 2316.

[72] http://www.sisweb.com/mstools/isotope.htm.

[73] http://fluorine.ch.man.ac.uk/research/mstool.php.

[74] Y. Ding, Q. Ma, H. W. Roesky, R. Herbst-Irmer, I. Uson, M. Noltemeyer, H.-G. Schmidt, *Organometallics* **2002**, *21*, 5216.

[75] I. Saur, S. G. Alonso, J. Barrau, *Appl. Organometal. Chem.* **2005**, *19*, 414.

[76] H. Duddeck, *Progress in NMR Spectroscopy* **1995**, *27*, 1.

[77] M. Sanchez, M. R. Mazières, L. Lamandé, R. Wolf, *Multiple Bonds and Low Coordination Chemistry in Phosphorous Chemistry, (Eds: M. Regitz, O. Scherer), Georg Thieme Verlag, Stuttgart* **1990**, 129.

[78] A. D. McNaught, A. Wilkinson, *IUPAC. Compendium of Chemical Terminology, 2nd ed. Blackwell Scientific Publications, Oxford* **1997**.

[79] O. Kuhl, *Coord. Chem. Rev.* **2004**, *248*, 411.

[80] C. Bibal, S. Mazière, H. Gornitzka, C. Couret, *Organometallics* **2002**, *21*, 2940.

[81] I. Saur, G. Rima, K. Miqueu, H. Gornitzka, J. Barrau, *J. Organomet. Chem.* **2003**, *672*, 77.

[82] P. Jutzi, B. Hampel, K. Stroppel, C. Kruger, K. Angermund, P.Hofman, *Chem. Ber.* **1985**, *118*, 2789.

[83] A. C. Filippou, P. Portius, G. Winter, G. Kociok-Kohn, *J. Organomet. Chem.* **2001**, *11*, 628.

[84] A. C. Filippou, G. Winter, M. Feist, G. Kociok-Kohn, I. Hinz, *Polyhedron* **1998**, *17*, 1103.

[85] A.C. Filippou, G. Winter, G. Kociok-Kohn, C. Troll, I. Hinz, *Organometallics* **1999**, *18*, 2649.

[86] N. Tokitoh, K. Manmaru, R. Okazaki, *Organometallics* **1994**, *13*, 167.

[87] H. Lang, M. Wienmann, W. Fresch, M. Buchner, B. Schiemenz, *Chem. Commun.* **1996**, 1299.

[88] H. Tobita, K. Ishiyama, Y. Kawano, S. Inomata, H. Ogino, *Organometallics* **1998**, *17*, 789.

[89] K. Ueno, K. Yamaguchi, H. Ogino, *Organometallics* **1999**, *18*, 4468.

[90] P. Jutzi, B. Hampel, B.M. Hursthouse, A.J. Howes, *J. Organomet. Chem.* **1986**, *19*, 289.

[91] G. Renner, P. Kircher, G. Huttner, P. Rutsch, K. Heinze, *Eur. J. Inorg. Chem.* **2000**, 879.

[92] W. W. Du Mont, L. Lange, S. Pohl, W. Saak, *Organometallics* **1990**, *9*, 1395.

[93] G. M. Sheldrick, *Acta Cryst.* **1990**, *A46*, 467.

[94] G. M. Sheldrick, *SHELXL-97 Program for Crystal Structure Refinement; University of Göttingen* **1997**.

Conclusion générale/ General conclusions

Conclusion générale

Ce travail a porté sur l'étude de nouveaux pnictogenium (phosphenium, arsénium et stibénium) cations et germylènes stabilisés par complexation intramoléculaire. Notre choix s'est porté sur des substituents N,N' et N,O chélatants comportant un système π-conjugué comme les aminotroponiminate et aminotroponate.

Deux voies de synthèse ont été utilisées à partir du trichloropnictogène (ECl_3, E = P, As, Sb): une réaction de déshydrochloration en présence d'une amine et une réaction de substitution nucléophile par le composé aminolithié. Ces réactions conduisent à la formation de composés dichlorés ou de chloropnictogénium cations par rupture spontanée d'une liaison élément-chlore dans des pourcentages variables suivant la voie utilisée. Ce caractère dissociatif de la liaison E-Cl dépend également de la nature du ligand et de l'élément du groupe 15. Il faut également noter que la stabilité des pnictogenium cations diminue dans le sens phosphore → antimoine.

L'étude par RMN multinoyaux (^{1}H, ^{13}C et ^{31}P) a montré une bonne délocalisation de la charge positive sur le cycle insaturé à 7 chaînons ce qui a été confirmé par l'étude de leur structure par diffraction des rayons X et des calculs quantiques.

Ces premiers résultats semblent indiquer un certain caractère ambivalent surtout dans le cas du phosphénium cation avec un doublet libre situé dans l'orbitale HOMO-1 et un ligand cationique.

Dans le but d'obtenir plus d'information sur leur structure, nous avons réalisé des réactions caractéristiques comme des réactions d'oxydation avec le DMSO, le soufre et le sélénium. Les phosphénium cations se sont révélés les plus réactifs et conduisent très facilement aux composés hydroxylés correspondants stables et isolables dans le cas du soufre et du selenium.

Une réaction inattendue d'élimination de HCl en présence de triéthylamine a conduit à des dioxo- et thiooxo-phosphoranes qui constituent les premiers exemples d'aminométaphosphonate et de son équivalent soufré stabilisés par complexation intramoléculaire.

Les réactions de cycloaddition avec la 3,5-di-*tert*-butyl-*o*-quinone ont permis d'accéder à de nouveaux cycloadduits. Nous avons pu montrer l'existence d'un équilibre entre

l'hydroxyphosphorane obtenu après hydrolyse d'une liaison phosphore-chlore et sa forme ester. La structure de cette dernière a pu être confirmée par diffraction des rayons X.

La dernière partie de ce chapitre porte sur l'aptitude de ces phosphéniums cations à former des complexes avec les métaux de transition. Nous avons pu ainsi isoler un hydroxyphosphénium stabilisé par complexation avec le tungstène.

Nous avons développé l'étude de nouveaux systèmes chélatants: les di-amonitroponimines et di-aminotropones pontées qui offrent deux types de coordination: tétrachélation d'un seul métal central ou complexation de deux métaux dans une structure pontée. En fait, quelle que soit la méthode utilisée ou la longueur de la chaîne carbonée entre les deux fragments chélatants, seuls les bis(pnictogenium)cations pontés ont été obtenus.

Nous avons ensuite réalisée une extension de ces réactions au germanium et pu ainsi accéder à de nouveaux bis-germylènes. Dans ce cas également, nous avons obtenu les formes pontées qui ont pu être isolées et caractérisés. Des calculs DFT ont montré que la forme pseudo-*Trans* était légèrement plus stable que la forme pseudo-*Cis*.

Une étude de leur réactivité a été menée en comparaison avec celle des monogermylènes. Ces espèces bien que tri-coordinnées conservent leur caractère divalent comme le montrent leurs réactions de cycloaddition avec une *o*-quinone. Par contre, ces bis-germylènes se sont montrés peu réactifs vis-à-vis d'agents oxydants comme le soufre ou le sélénium alors que les monogermylènes donnent facilement les germa-thiones ou sélénones correspondantes. Enfin, un bis-germylène complexé par le tungstène a pu être isolé et sa structure déterminée par diffraction des rayons X. Il présente une conformation de type *trans* avec les deux unités germaniés de part et d'autre de la chaîne carbonée.

Ce travail constitue une contribution importante à la chimie des espèces di-coordinnées du groupe 15 (P, As et Sb) et des germylènes. De nombreux composés ont été décrits et certains d'entre eux pour la première fois. Nous envisageons par la suite d'utiliser ces ligands aminotroponiminates pour la stabilisation de phosphinidènes (RP) composés d'un grand intérêt qui n'existent pas pour l'instant à l'état libre.

General conclusions

This work has been focused on the study of new pnictogenium (phosphenium, arsenium and stibenium) cations and of germylenes stabilized by intramolecular complexation. We chose chelating N,N'- and N,O-substituents containing a π-conjugated system like aminotroponiminate and aminotroponate ligands.

Two different routes were envisaged starting from the trichloropnictogene compounds ($E_{15}Cl_3$, E_{15} = P, As, Sb): a base-induced dehydrochlorination coupling reaction and a nucleophilic substitution reaction by an aminolithiated compound. These reactions led to the formation of dichloride compounds or chloropnictogenium cations by autoionisation of an E_{15}-Cl bond with varying ratios according to the synthetic pathway used. The dissociative nature of the bond also depends on the nature of the ligand and the element of group 15. Note that the stability of pnictogenium cations decreases from phosphorus to antimony.

The multinuclear NMR (^{1}H, ^{13}C and ^{31}P) studies showed a high delocalization of the positive charge on the unsaturated 7-membered ring which was confirmed by X-ray diffraction data and quantum chemical calculations.

These preliminary results suggest an ambivalent behaviour, especially in the case of the phosphenium cation, with both an accessible lone pair located in the HOMO-1 and a cationic ligand.

In order to gain more insight about their structure, we performed some characteristic reactions such as oxidation reactions with DMSO, sulfur and selenium. The phosphenium cations are the most reactive and easily led to the corresponding hydroxylated compounds, stable and isolated in the case of sulfur and selenium. An unexpected base-induced dehydrochlorination reaction gave dioxo- and thiooxo-phosphoranes which are the first examples of aminometaphosphonate (and of its sulfur equivalent) stabilized by intramolecular complexation.

Cycloaddition reactions with 3,5-di-*tert*-butyl-*o*-quinone led to new cycloadducts. After hydrolysis of a phosphorus-chlorine bond, we observed the formation of a hydroxyphosphorane in equilibrium with a phosphate ester. The structure of the latter was confirmed by an X-ray diffraction study.

Then, the σ-donor character of these phosphenium cations was highlighted by their complexation with transition-metal complexes. For the first time, a hydroxyphosphenium cation stabilized by complexation with pentacarbonyltungsten was prepared and its structure elucidated by an X-ray single-crystal diffraction study.

In the last part, we developed the study of new chelating systems: bridged di-amonitroponimines and di-aminotropones. These ligands offer two types of coordination: tetradentate chelation of one metal or complexation of two metals in a bridged structure. In fact, whatever the method used or the length of the methylene chain between the two chelating fragments, only the bridged bis(pnictogenium) cations have been obtained.

We then performed an extension of these reactions to germanium. A new type of bridged bis-germylenes was synthesized and fully characterized by various spectroscopic methods. DFT calculations showed a slight stabilization of the pseudo-*Trans* form compared to the pseudo-*Cis* form.

A study of their reactivity was conducted in comparison with that of monogermylenes. These tricoordinated species preserve their divalent character as was shown in the cycloaddition reactions with an *o*-quinone. On the other side, these bis-germylenes did not react with oxidative reagents such as sulfur or selenium while monogermylenes easily give the germane-thiones or -selenones. Finally, a bis-germylene tungsten complex has been isolated and its structure determined by X-ray diffraction. It has a *trans* conformation with germanium unities on both sides of the methylene chain.

This work represents an important contribution to the chemistry of di-coordinated species of 15 group elements (P, As and Sb) and of germylenes. Many compounds are reported, some of them for the first time. We plan to use these aminotroponiminates ligands for the stabilization of phosphinidenes (RP), compounds of great interest with a high synthetic potential that do not yet exist in the free state.

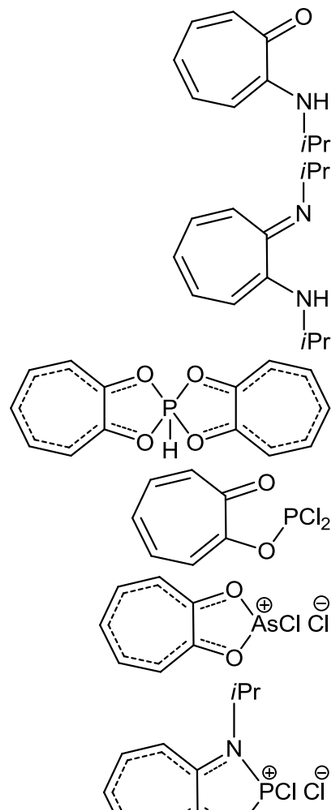

1

2

3

4

5

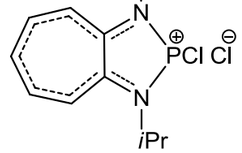

6a

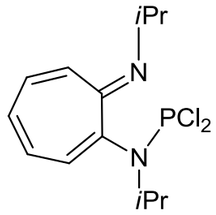

6b

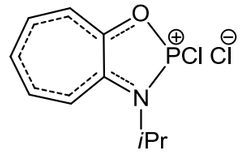

7a

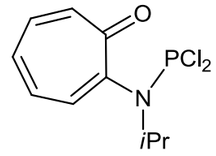

7b

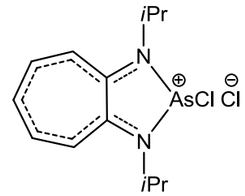

8

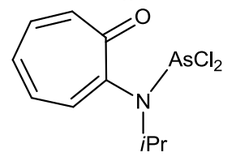

9

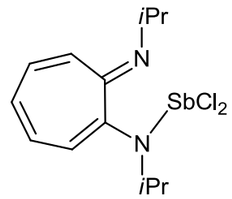

10

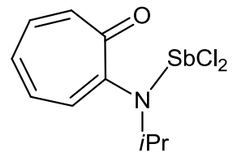

11

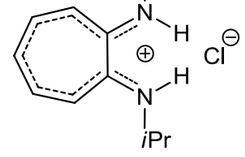

12

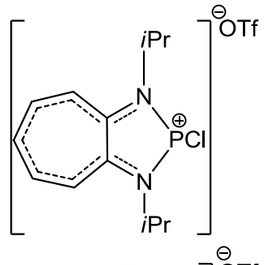

13

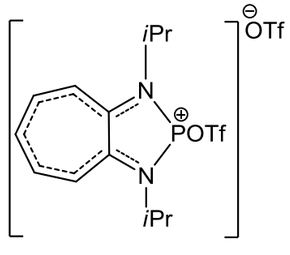

14

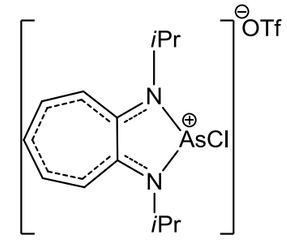

15

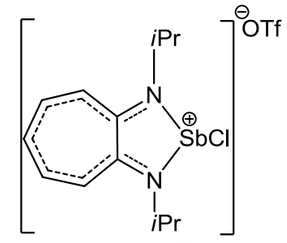

16

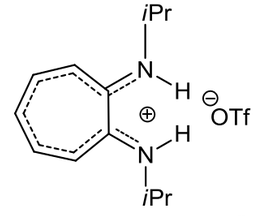

17

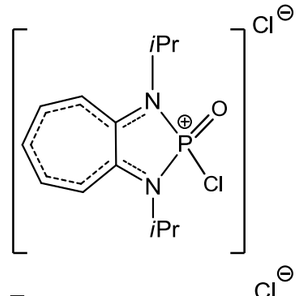

18

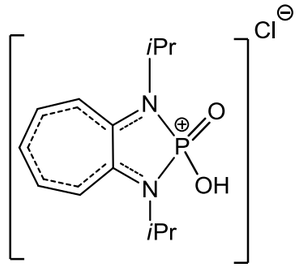

19

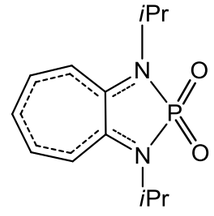

20

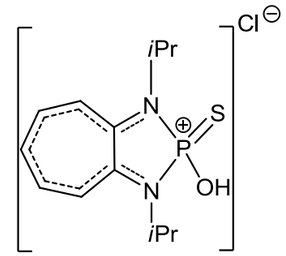

21

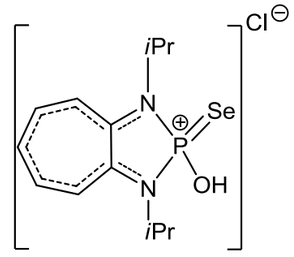

22

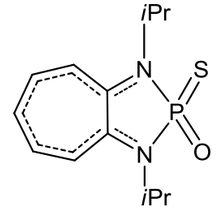

23

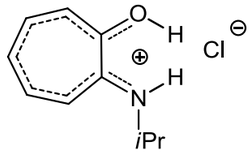

24

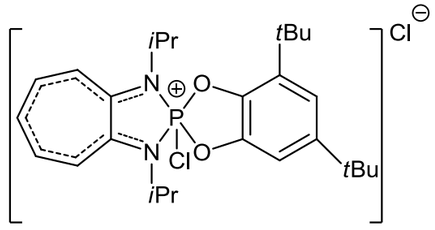

25

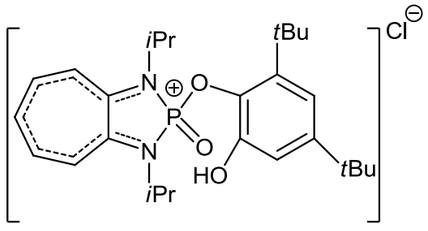

26B

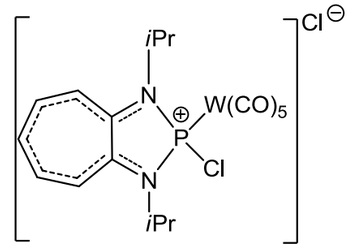

27

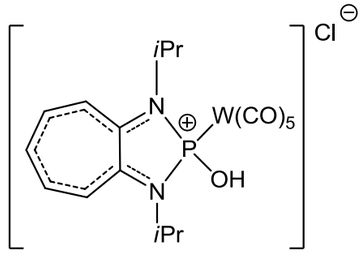

28

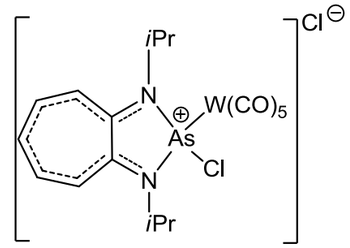

29

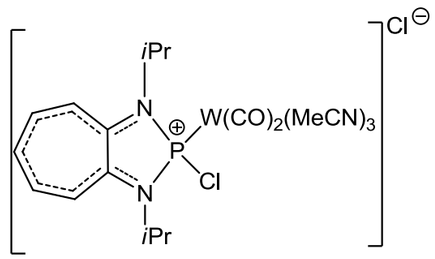

30

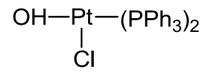

31

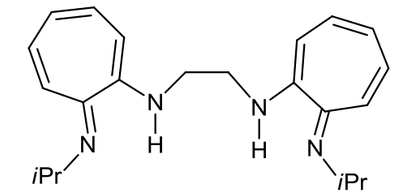

32

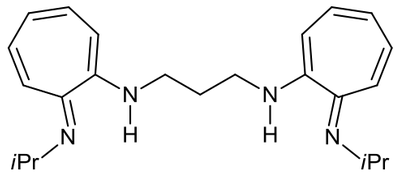

33

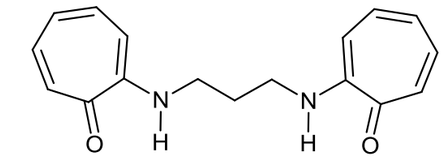

34

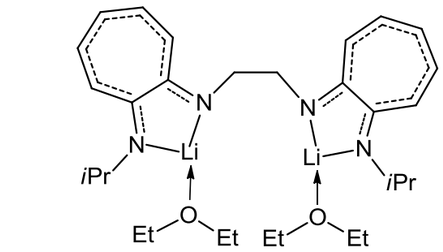

35

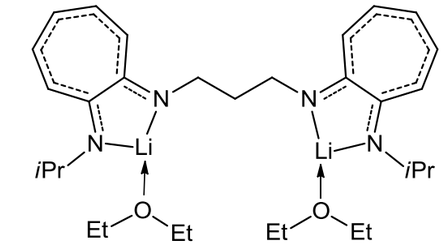

36

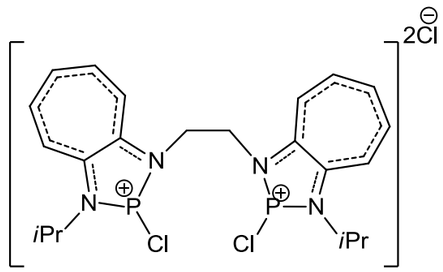

37

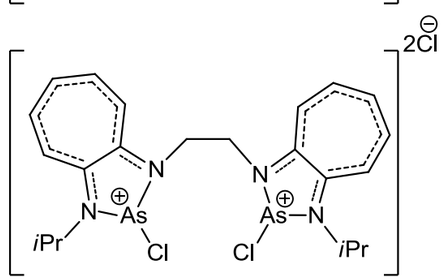

38

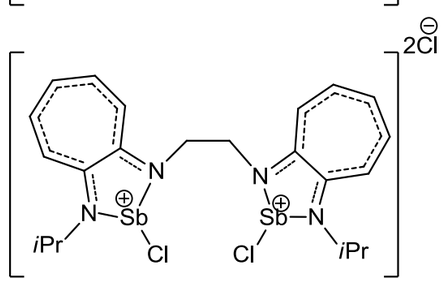

39

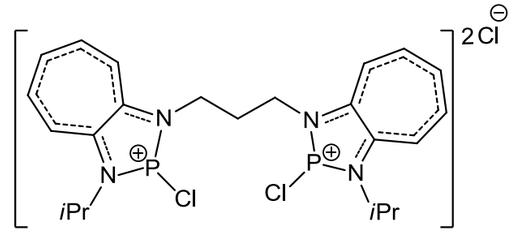

40

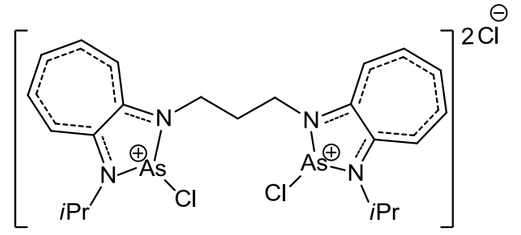

41

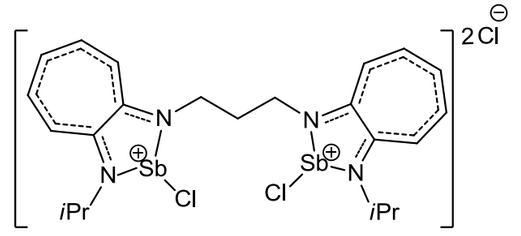

42

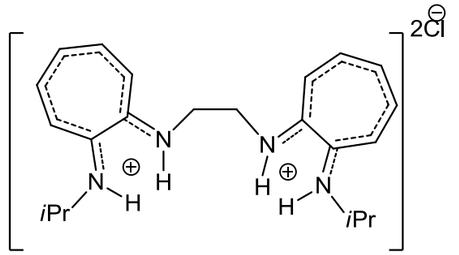

43

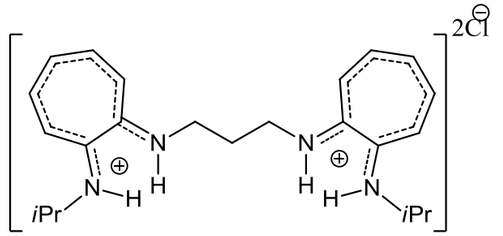

44

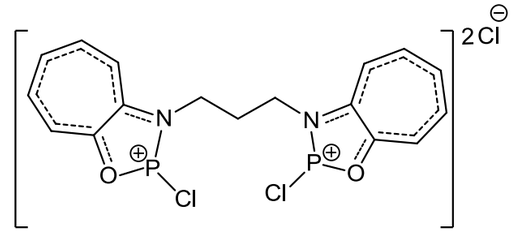

45

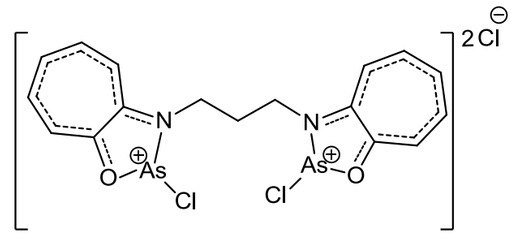

46

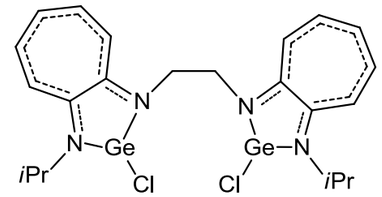

47

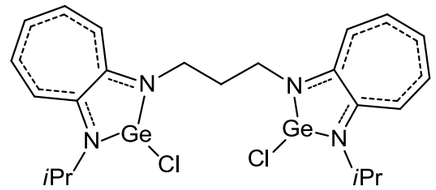

48

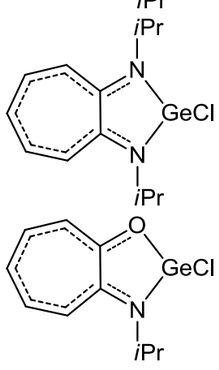

49

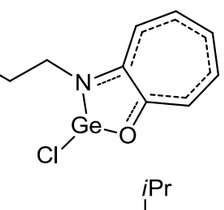

50

51

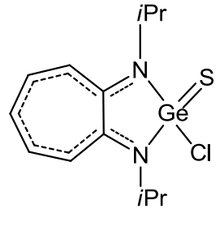

52

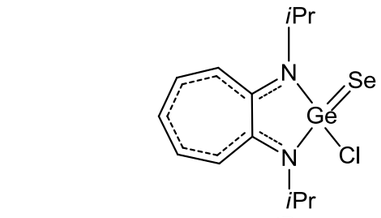
iPr
N
Se
Ge
Cl
N
iPr

53

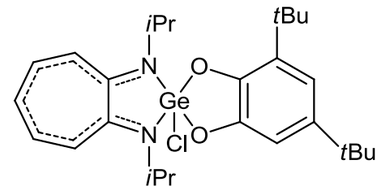
iPr
tBu
N
O
Ge
N
Cl
O
tBu
iPr

54

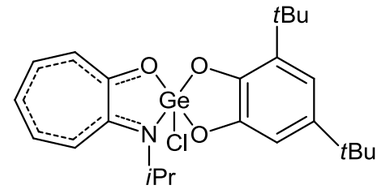
tBu
O
O
Ge
N
Cl
O
tBu
iPr

55

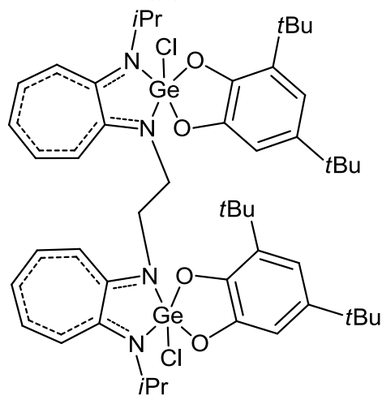
iPr
Cl
tBu
N
O
Ge
N
O
tBu
tBu
N
O
Ge
N
Cl
O
tBu
iPr

56

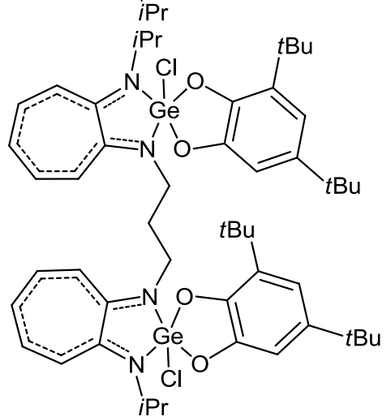
iPr
Cl
tBu
N
O
Ge
N
O
tBu
tBu
N
O
Ge
N
Cl
O
tBu
iPr

57

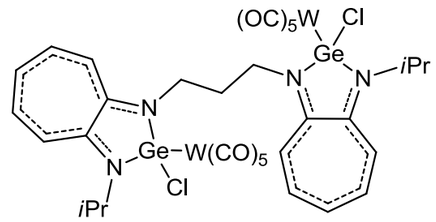

58

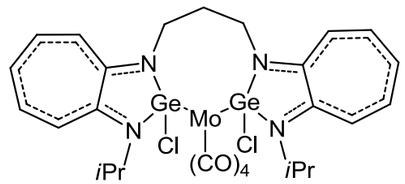

59

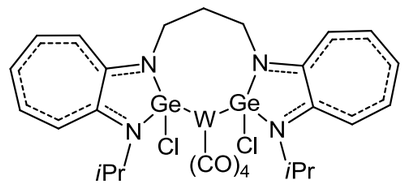

60

N - new product

Abstract

This thesis entitled “N,N'- and N,O-chelated pnictogenium cations (P, As, Sb) and germylenes: syntheses, structural studies and reactivity” is structured in three chapters.

In the first chapter an easy and direct route to the first phosphenium and arsenium cations supported by N,N’ or N,O-chelation derived from a tropolone scaffold was presented. These new compounds were fully characterized by various spectroscopic methods, X-ray analyses and DFT calculations. The expected Lewis amphoterism which is illustrated on the one hand, by the high-lying phosphorus lone-pair orbital (HOMO-1), and on the other hand, by the delocalized positive charge opens up new perspectives for the involvement of these ambiphilic species as valuable ligands for new catalysts.

The second chapter concerns the reactivity of these new pnictogenium cations. A variety of reactions including oxidation (with dimethylsulfoxide, sulfur or selenium), cycloaddition and halide ion extraction were studied. The first example of an aminometaphosphonate (and its sulfur equivalent) stabilized by intramolecular complexation was reported. For the first time, a hydroxyphosphenium cation stabilized by complexation with pentacarbonyltungsten was prepared and its structure elucidated by X-ray single-crystal diffraction study.

The last chapter refers to the synthesis and characterization of bridged bis(pnictogenium) cations with an extension to divalent germanium compounds. Among the most noteworthy result is the stable bis-germylene pentacarbonyl tungsten complex.

Résumé de thèse

Ce travail concerne la stabilisation d'espèces à basse coordinence du groupe 15 (P, As et Sb) et du germanium par des substituents N,N' et N,O chélatants comportant un système π-conjugué comme les aminotroponiminate et aminotroponate.

Le premier chapitre porte sur la mise au point des voies de synthèse de composés dichlorés ou de chloropnictogénium cations. L'étude par RMN multinoyaux (^{1}H, ^{13}C et ^{31}P) des pnictogénium cations a montré une bonne délocalisation de la charge positive sur le cycle insaturé à 7 chaînons ce qui a été confirmé par l'étude de leur structure par diffraction des rayons X et des calculs DFT.

Dans le deuxième chapitre, nous avons réalisé des réactions caractéristiques comme des réactions d'oxydation. Les phosphénium cations conduisent très facilement aux composés hydroxylés correspondants. Une réaction inattendue d'élimination de HCl a conduit à des dioxo- et thiooxo-phosphoranes qui constituent les premiers exemples d'aminométa phosphonate (et de son équivalent soufré) stabilisés par complexation intramoléculaire. Les réactions de cycloaddition avec une *o*-quinone ont également permis d'accéder à de nouveaux cycloadduits. La dernière partie de ce chapitre porte sur l'aptitude de ces phosphéniums cations à former des complexes avec les métaux de transition. Nous avons pu ainsi isoler le premier hydroxyphosphénium stabilisé par complexation avec le tungstène.

Dans le troisième chapitre, nous avons développé l'étude de nouveaux systèmes chélatants: les di-amonitroponimines et di-aminotropones pontées. Nous avons ensuite réalisée une extension de ces réactions au germanium et pu ainsi accéder à de nouveaux bis-germylènes. Ces espèces bien que tri-coordinnées conservent leur caractère divalent comme le montrent leurs réactions de cycloaddition avec une *o*-quinone. Enfin, un bis-germylène complexé par le tungstène a pu être isolé et sa structure déterminée par diffraction des rayons X.

Key words: phosphenium, arsenium, germylene, O,O’ ligand N,O ligand N,N’ ligand, chelates